



<https://theses.gla.ac.uk/>

Theses Digitisation:

<https://www.gla.ac.uk/myglasgow/research/enlighten/theses/digitisation/>

This is a digitised version of the original print thesis.

Copyright and moral rights for this work are retained by the author

A copy can be downloaded for personal non-commercial research or study,
without prior permission or charge

This work cannot be reproduced or quoted extensively from without first
obtaining permission in writing from the author

The content must not be changed in any way or sold commercially in any
format or medium without the formal permission of the author

When referring to this work, full bibliographic details including the author,
title, awarding institution and date of the thesis must be given

Enlighten: Theses

<https://theses.gla.ac.uk/>
research-enlighten@glasgow.ac.uk

THE
HETEROGENEOUS CATALYTIC DECOMPOSITION
O F
AQUEOUS HYDROGEN PEROXIDE
B Y
P-TYPE SEMICONDUCTING METAL OXIDES
AND
ANION EXCHANGE RESINS

B Y

DAVID S. WEIR

A Thesis submitted in accordance with the
regulations governing the award of
the Degree of Doctor of Philosophy in
the Faculty of Science of the University of Glasgow.

October 1958

ProQuest Number: 10656382

All rights reserved

INFORMATION TO ALL USERS

The quality of this reproduction is dependent upon the quality of the copy submitted.

In the unlikely event that the author did not send a complete manuscript and there are missing pages, these will be noted. Also, if material had to be removed, a note will indicate the deletion.



ProQuest 10656382

Published by ProQuest LLC (2017). Copyright of the Dissertation is held by the Author.

All rights reserved.

This work is protected against unauthorized copying under Title 17, United States Code
Microform Edition © ProQuest LLC.

ProQuest LLC.
789 East Eisenhower Parkway
P.O. Box 1346
Ann Arbor, MI 48106 – 1346

ACKNOWLEDGMENTS

The Author wishes to express his appreciation to Professor F. S. Spring, F.R.S., for the privilege of working in his Department and also to Dr. A. B. Hart for his many stimulating and constructive suggestions.

Thanks are also extended to The Department of Scientific and Industrial Research for the provision of a Research Studentship receipt of which is gratefully acknowledged.

5. Surface Area Apparatus and Measurement Technique	59.
(a) Apparatus	59.
(b) Experimental Technique	60.
6. Spectrophotometric Determination of Rate of Solution of Copper During Catalysis	61.
(a) General Considerations	61.
(b) Preparation of Solutions for Analysis	65.
7. Polarographic Detection of Stannate in H_2O_2	68.

MATERIALS

1. Hydrogen Peroxide	72.
2. Catalysts	72.
(a) Cuprous Oxide	72.
(b) Nickelous Oxide	75.
(c) Cobaltous Oxide	76.

RESULTS

Cu_2O/H_2O_2 System

1. General	77.
2. Stability of Catalyst and the Degree of Reproducibility Obtainable	80.
3. Scope of Experimental Investigations	83.
4. The Effect of $[H_2O_2]$ on the Catalyst Efficiency ..	84.
(a) 2 M to 0.25 M	84.
(b) 0.25 M to 0.025 M	87.
5. The Effect of Ionic Strength on the Catalyst Efficiency	88.
(a) 2 M to 0.25 M	88.
(b) 0.25 M to 0.025 M	89.
6. The Effect of Temperature on the Catalyst Efficiency	89.
(a) 2 M to 0.25 M	89.
(b) 0.25 M to 0.025 M	92.
7. The Effect of pH on the Catalyst Efficiency	92.
(a) 2 M to 0.25 M	92.
(b) 0.25 M to 0.025 M	93.

8. The Rate of Copper Dissolution	94.
(a) 2 M to 0.25 M	95.
(b) 0.25 M to 0.025 M	97.
9. Characterisation of Possible Surface Composition	99.
(a) 2 M to 0.25 M	100.
(b) 0.25 M to 0.025 M	102.
(c) Effect of $[H_2O_2]$ on Steady Potential Values of Cu_2O/H_2O_2 Half-cell	102.
(d) Potential Decline Following the Change H_2O_2 to H_2O	103.
10. Surface Area Determination	105.

DISCUSSION

1. Introduction	109.
(a) Object	109.
(b) Origin of Recorded Temperature Differences	109.
(c) Diffusion Control	110.
(d) Temperature Coefficient	110.
2. Efficiency Changes with Cu_2O	112.
(a) 2 M to 0.25 M	112.
(b) 0.25 M to 0.025 M	122.
(c) General Mechanistic Treatment of Results ..	122.
3. Initial Efficiency Changes on Cu_2O Considered as a Catalytic Surface Process	124.
(a) Characteristics	124.
(b) Proposed Reaction Mechanism	125.
(c) Kinetic Interpretation of Proposed Mechanism	129.
(d) Evaluation of Constants in the Rate Equations	134.
(e) Discussion of Proposed Mechanism	138.
(f) Rejected Reaction Schemes	148.
4. The Final Efficiency Growth on Cu_2O Considered as a Bulk Solid Process	156.
5. Potential Measurements from Cu_2O During Reaction	163.
6. Comparison of the NiO/H_2O_2 and CoO/H_2O_2 Systems with the Cu_2O/H_2O_2 System	171.
(a) Results	171.
(b) Discussion	174.
7. The Importance of Isotopic Tracer Studies ..	178.

S E C T I O N I I .I N T R O D U C T I O N

1. Introduction...	180.
--------------------	------

E X P E R I M E N T A L

1. Exchange Material	182.
2. Preparation of Resin in OH form	182.
3. Sampling and Estimation of Resin	183.
4. Resin-Peroxide Equilibrium	184.
5. Decomposition Rate Experiments	186.
(a) Decomposition Apparatus	186.
(b) Steady $[H_2O_2]$ Procedure	187.
(c) Reproducibility of Rate Measurements	188.

R E S U L T S A N D D I S C U S S I O N

1. Attainment of Equilibrium	189.
2. Efficiency of Exchanged Resin as a Catalyst	190.
3. Rate and $[H_2O_2]$	192.
4. Mechanism	196.

C O N C L U S I O N S

Conclusions	200.
-------------	------

G E N E R A L C O N C L U S I O N S F R O M S E C T I O N S I A N D I I

General Conclusions	201.
---------------------	------

F U T U R E L I N E S O F R E S E A R C H

Future Lines of Research	206.
--------------------------	------

R E F E R E N C E S

References	207.
------------	------

§§§§§§§§§§§§

S U M M A R Y

A detailed study is made, by a sensitive flow method, of the changes in catalytic efficiency which occur with time during the decomposition of aqueous H_2O_2 by Cu_2O and CoO . The results form the basis of a discussion of this process.

The experimental technique consists in passing a constant flow of pure, stabiliser-free H_2O_2 over the catalyst and measuring the variations in heat liberated during the decomposition of the H_2O_2 by a two-thermistor system immersed in a thermostatted water bath. The system allows temperature differences of $\pm 0.001^\circ C$ to be rapidly measured.

The catalysts which are prepared by the alternate oxidation and reduction of 20 gauge 'specpure' metal wire are used in the form of a shallow bed of 5 mm. diameter rings which permits free release of evolved O_2 . Excellent reproducibility is obtained.

The above technique is employed in a detailed examination of the Cu_2O/H_2O_2 system with variations of $[H_2O_2]$, pH, ionic strength, temperature and involving observation of the extent of catalyst dissolution. The results show that on exposure of Cu_2O to H_2O_2 a definite sequence of efficiency changes takes place viz:-

- (a) a rapid increase to a peak efficiency
- (b) a relatively slow decline to a minimum efficiency

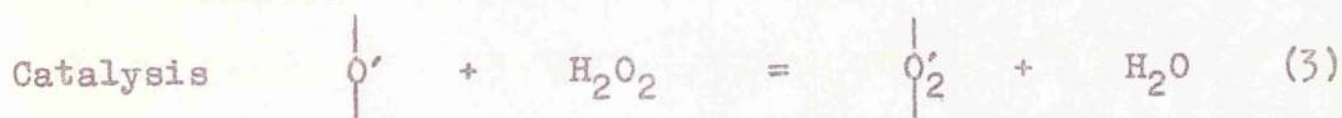
(c) a slow recovery to a final steady value.

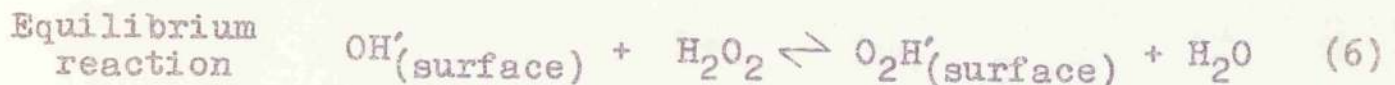
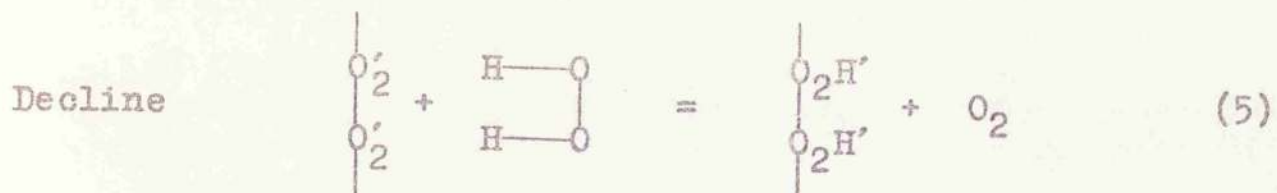
Two successive processes are postulated to describe the above efficiency behaviour, i.e.

- (i) a surface process rapidly growing in rate - (a) - then being poisoned - (b).
- (ii) a slower bulk solid process causing a partial restoration of catalytic efficiency as in (c)

To explain the surface process (i) a mechanism is proposed in which catalysis takes place at surface anchored radicals O_2' and O' . These radicals are envisaged as mainly created by the H_2O_2 although some will be present on any p-type semiconducting surface which has been exposed to oxygen. At the same time there begins a poisoning process which is slower than catalysis and is explained as a dual site conversion of the radical ions (O_2' and O') to stable ions (HO_2' or OH'). This poisoning does not go to completion because of a dual site recovery in which the active radicals are again produced thus providing the possibility of a surface equilibrium.

The reaction scheme is summarised as follows:-





Application of the steady state treatment to the minimum efficiency condition and a limited interpretation of the efficiency decline curves on the basis of the above mechanism allows a kinetic examination from which the overall rate of decomposition at the minimum is given by

$$\text{Rate} = \frac{2 \cdot \sqrt{\frac{k_7 \cdot K}{k_5}} \cdot [\text{H}_2\text{O}_2]}{1 + K [\text{H}_2\text{O}_2]} \left[k_4 + \frac{k_5 \sqrt{\frac{k_7 \cdot K}{k_5}}}{1 + K [\text{H}_2\text{O}_2]} \right]$$

which simplifies to

$$\text{Rate} = A + \frac{B}{[\text{H}_2\text{O}_2]} \quad \text{at high } [\text{H}_2\text{O}_2]$$

$$\text{and Rate} = D \cdot [\text{H}_2\text{O}_2] \quad \text{at low } [\text{H}_2\text{O}_2]$$

These equations fit in exactly with experimental results. Comparison of the constants with experiment together with information drawn from the efficiency changes

with time permit evaluation of the constants k_7 , K and the group $\frac{k_4}{k_5}$.

The recovery process is shown to have the characteristics of a recrystallisation, annealing or solid diffusion process and the kinetics of the change are shown to fall in with this classification.

E.m.f. measurements under identical experimental conditions indicate potential variations similar in form to those taking place in the efficiency of the catalyst. Interpretation of these results is used to sustain the surface mechanism proposed for the efficiency measurements.

Shorter investigations of the systems H_2O_2 and two other p-type oxides NiO and CoO are also described. Under the experimental conditions used for examination of the Cu_2O/H_2O_2 system, NiO does not exhibit catalytic activity but the results for the CoO system suggest that a similar surface process controls catalysis on CoO and therefore possibly on all p-type semiconducting metal oxides. The final slow recovery in efficiency, so prominent in Cu_2O , does not occur in CoO under the experimental conditions used.

A detailed examination of the equilibrium reaction (6), on a different type of surface, is also described. Measurement of the exchange between the OH form of an anion exchange resin and H_2O_2 at low $[H_2O_2]$ is possible without appreciable interference from catalytic decomposition. The

results show that the exchange is rapid, strongly favouring the HO_2 rather than OH .

In addition the results obtained from a brief study of the catalytic properties of the OH form of the anion exchange resin for the decomposition of H_2O_2 are given and a tentative reaction mechanism suggested.

The results with the resin, though of relatively narrow scope, give support to the general picture of H_2O_2 decomposition at solid surfaces derived from the oxide work.

FORM OF THESIS

The thesis deals with the catalytic effect of semi-conducting metal oxides on the decomposition of aqueous H_2O_2 . The major portion concerns a very detailed examination of the heterogeneous catalytic system Cu_2O/H_2O_2 together with a less full account of results obtained from NiO/H_2O_2 and CoO/H_2O_2 . The main purpose of the inclusion of the latter two systems was to test the general applicability of the conclusions reached for the Cu_2O/H_2O_2 system.

In the introduction the historical background associated with homogeneous and heterogeneous catalysis of H_2O_2 in solution is reviewed. Attention is directed to the rather ill-defined treatment of metal oxides as H_2O_2 catalysts and also to the bearing of the modern views on the bulk and surface structure of oxides on their catalytic properties in general. A brief account is given of oxides as nonstoichiometric compounds and semiconductors. The experimental section describes the apparatus, technique and materials used for the investigation of the oxide systems but the results section deals only with the Cu_2O/H_2O_2 system. The discussion is composed of an exhaustive treatment of the Cu_2O/H_2O_2 system culminating in the results obtained from NiO/H_2O_2 and CoO/H_2O_2 and their relation to the Cu_2O/H_2O_2 system.

The thesis ends with a small but important section on the catalytic effect of the hydroxide form of an anion

exchange resin for the decomposition of aqueous H_2O_2 . This work which was suggested by the results obtained from the oxide systems examines an important aspect of the mechanism proposed for oxide catalysts and includes a mechanism proposed for the resin/ H_2O_2 decomposition. It also enables a conclusion to be drawn concerning the relation between oxides and the enzyme catalase as catalysts for H_2O_2 .

SECTION I

I N T R O D U C T I O N

1. General

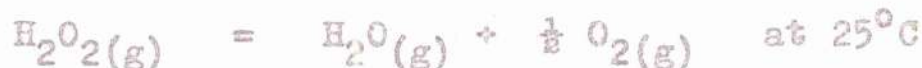
The elucidation of the physical and chemical properties of H_2O_2 has stimulated the interest of a great number of investigators since 1818 when Louis-Jacques Thenard¹ reported the discovery and preparation of the first "oxygenated acid". Such is the practical importance of H_2O_2 e.g.

- (1) an oxidising agent
- (2) a source of energy
- (3) a source of free radicals
- (4) a parent compound for the production of organic and inorganic peroxy compounds

that a great deal of effort has been devoted to its study.

For the present discussion the most important aspect in the development of the chemistry of H_2O_2 has been that associated with the kinetics of decomposition.

Thermodynamically H_2O_2 is an unstable molecule with reference to H_2O and O_2 . Data collected by Schumb, Satterfield and Wentworth² based on work carried out by Giguère³ on the reaction



gives $\Delta G = -29.39 \text{ kcal./mole}$ ($\log K_p = 21.55$)

and $\Delta S = 13.86 \text{ cal./deg.}$

In practice however the pure compound, free from homogeneous and heterogeneous catalysis, is relatively stable since decomposition must initially be associated with the rupture of either the HO----OH or the H----OOH bond. These bonds do not break easily. According to Evans, Hush and Uri⁴ $D_{\text{HO----OH}}$ and $D_{\text{H----O}_2\text{H}}$ for the gas phase dissociation is 55.6 kcal. and 102 kcal. respectively. The presence of a catalyst however allows considerable decomposition to take place under convenient experimental conditions, appearing to penetrate the high energy barrier in a series of small energy steps.

The rupture of these bonds and the subsequent reactions which add up to decomposition of H_2O_2 have been studied in the solution and vapour phase and in the presence of homogeneous and heterogeneous catalysts and in the photochemically initiated case. The results of, and discussions prompted by, these investigations, have yielded important information not only on H_2O_2 reactions but on the mechanisms of chemical catalysis in general.

2. Early Investigations of H_2O_2 Decomposition.

During the years following its discovery Thenard⁵ published many papers on what he now recognised as oxidised water. A great deal of his work was devoted to the preparation of a pure stable compound and such were the standards of his experimental techniques that he produced a stable

anhydrous compound, a feat unattainable by many later workers who considered the compound inherently unstable.

With such a pure material Thenard was able to make many fundamental observations of the physical properties of solutions of H_2O_2 , but his investigations of its chemical activity form perhaps his greatest contribution. He examined the decomposing action on H_2O_2 solutions of many compounds such as Ag, Ag_2O , Pt and iron and he was the first to note that certain substances decomposed the H_2O_2 without undergoing any chemical alterations themselves. Although he made no suggestions as to the mechanism of such action he carried out many detailed observations of this phenomenon e.g. decomposition by Ag_2O^6 , and his results provided valuable information for later workers.

In the years following Thenard's work many speculations were advanced as to the mechanism of his observed phenomena but no new experimental data was obtained. The theory most strongly held during this period was that proposed by Schönbein⁷ who postulated the existence of three forms of oxygen. Two of these forms, named ozone and antozone, were supposed opposite as positive is to negative and reaction consisted in the mutual neutralisation of these two forms producing a third compound and liberating the third form - normal oxygen.

Between 1850 and 1860 Brodie^{8,9} published a series of papers on the decomposition of H_2O_2 by many oxides such as

Ag₂O, MnO₂, BaO, and Cr₂O₃. He proposed that
 "... the element oxygen was formed according
 to a molecular law, identical with that
 according to which compound substances are
 formed."

He also pointed out that the differences in reaction of many
 oxides with H₂O₂ could not be explained simply in terms of
 three forms of oxygen because of the widely different rates
 of catalysis obtained with different oxides and since the
 efficiency of each oxide varied according to its method of
 preparation.

In 1897 Bredig¹⁰ made a considerable contribution to
 existing knowledge by examining the decomposition of H₂O₂ by
 metal sols which he treated as homogeneous systems and which
 he considered as analogues of catalase. In his experiments
 with Au he observed:-

1. that the activity depended on the alkali
 concentration
2. that the specific activity increased with
 increasing sol concentration
3. that the reaction was first order at low [H₂O₂].

These results were later confirmed by Teletof¹¹ in 1940.

The work of Brodie and Bredig and co-workers
 represented the first systematic attempt to understand the
 mechanism of decomposition.

Later workers used both homogeneous and heterogeneous systems but it was mainly from homogeneous systems that the first fruitful results were obtained, results which were later applied with considerable success to the more complex heterogeneous systems.

3. Homogeneous Catalytic Decomposition of H₂O₂

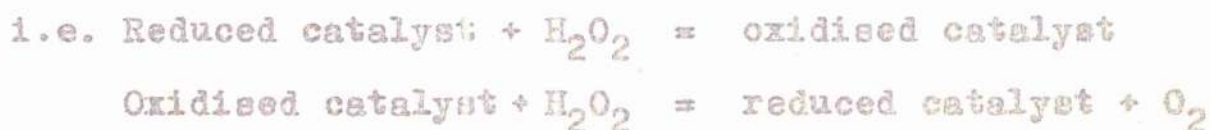
Many systems involving the homogeneous decomposition of H₂O₂ received early investigation. Two main mechanistic approaches were generally adopted to explain the experimental results, viz:-

1. Catalysis was postulated as proceeding through the formation of an active intermediate which subsequently decomposed liberating O₂ and regenerating the catalyst



where C represents the catalyst and C(H₂O₂)₂ the active intermediate.

2. The H₂O₂ was regarded as alternatively acting as an oxidising and reducing agent



Although each of these mechanisms satisfied some aspect of the experimental results neither was able to give a

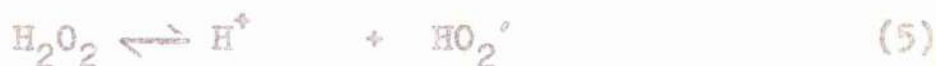
comprehensive explanation of any one system.

In 1934 Haber and Weiss¹² published their classical paper on the homogeneous decomposition of aqueous H_2O_2 solutions by Fe^{++} and Fe^{+++} salts. This paper following similar work by Haber and Willstätter¹³ marks one of the most important advances in chemical kinetics.

For catalysis by Fe^{++} the proposed mechanism was



and for Fe^{+++} catalysis



The main features of this scheme were the postulation of a radical chain mechanism and the identification of the radicals as OH and HO_2 . Initiation, step (1), involved a single electron transfer process which was also considered applicable to electrochemical and photochemical processes. It produced the radicals OH or HO_2 which formed H_2O and O_2 on reacting again with H_2O_2 . Reaction with H_2O_2 propagated a chain reaction and the propagating species were reproduced

according to (2) and (3) the original Haber-Willstätter equations.

The radical mechanism proposed by Haber and Weiss gained important confirmation from the work of Baxendale, Evans and Parks¹⁴ on the initiation of polymerisation reactions. Previous investigations had shown that in vinyl polymerisation reactions the initiation reaction required the production of free radicals. Using the $\text{Fe}^{++}/\text{H}_2\text{O}_2$ system Baxendale, Evans and Parks suggested that polymerisation reactions initiated by it depended on the formation of OH radicals in (1) which they proposed reacted according to the scheme:-



where M represents the monomer.

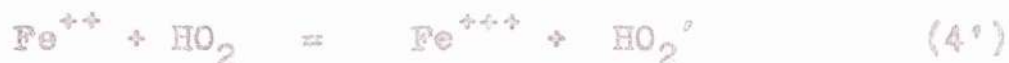
By infra-red analysis of the polymer they were able to identify the OH as the initiating radical and to relate its amount to the polymerisation kinetics.

Evidence for the occurrence of the HO_2 radical (and its ionised form O_2^-) has not been so easy to obtain in a direct form but its participation seems beyond doubt in photochemically and radiochemically initiated decomposition of very pure H_2O_2 solution. Thus Dainton and Rowbottom¹⁵ are able to assign a half-life to the HO_2 radical in very pure H_2O_2 solution irradiated with γ -rays.

The original Haber-Weiss mechanism for $\text{Fe}^{++}/\text{Fe}^{+++}$ catalysis contained no terms in H^+ or OH° implying that the reaction velocity and chain length were independent of acidity. The reaction velocity proved to be pH independent for Fe^{++} but not for Fe^{+++} . It was found, however, that the chain length for the $\text{Fe}^{++}/\text{H}_2\text{O}_2$ reaction was dependent on acidity. The possibility that the H_2O_2 in equation (2) appeared as the anion HO_2° which reacted according to



was dismissed because this step did not account for the acidity variation. A series of chain breaking mechanisms was therefore introduced in addition to equation (4) to explain the pH dependence i.e.



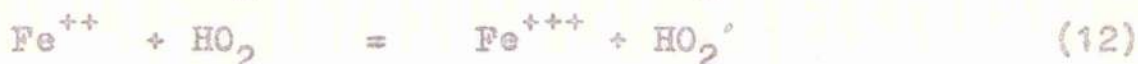
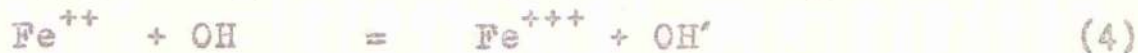
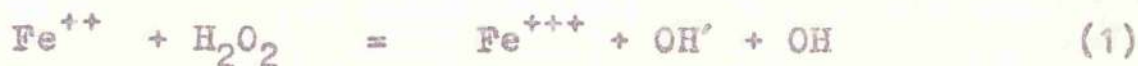
From the reaction scheme (5), (6), (3), (4) and (7) proposed for Fe^{+++} catalysis, kinetic analysis indicated that the rate was dependent on the $[\text{H}_2\text{O}_2]^2$ but experimental results gave a first order dependence. To account for this discrepancy an additional chain terminating reaction



was incorporated into the scheme.

Although this work represented a considerable step forward many experimental details were left unanswered e.g.

the variation of chain length with H^+ . Weiss¹⁶ improved the mechanism with a reaction scheme which combined the mechanisms relating to Fe^{++} and Fe^{+++} catalysis i.e.



Fe^{++} catalysis was explained by equations (1), (2), (3) and (4) and the variation of chain length with H^+ by either

- (a) participation of HO_2' or O_2' in the chain mechanism
- (b) an increase in the chain breaking mechanism due to participation of $H_2O_2^+$ instead of HO_2 or H_2O^+ instead of OH .

Catalysis by Fe^{+++} was represented by equations (3), (4), (6) and (12) in addition to the equilibrium



A still further refinement in this mechanism was made by Barb, Baxendale, George and Hargrave^{17,18} who proposed that the reaction producing O_2 was not

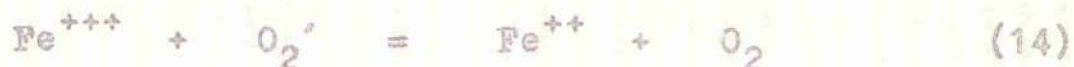


which seemed mechanistically an improbable rearrangement to occur in one step. They proposed instead



which explained satisfactorily their experimental results for both Fe^{++} and Fe^{+++} decomposition of H_2O_2 .

Weiss and Humphrey¹⁹ supported this new development proposed by Baxendale et al. but suggested that the anion O_2' entered into the reaction rather than the undissociated HO_2 i.e.



Although these results have tended to disregard the contribution of



it is still accepted as of considerable importance in the photolysis of dilute aqueous solutions of H_2O_2 ²⁰ and in the decomposition by ionising radiation²¹.

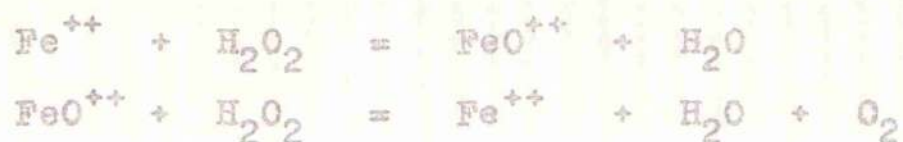
Investigations of this one homogeneous system introduced many postulates which were of general applicability to homogeneously catalysed H_2O_2 decomposition reactions viz.,

- (a) the participation of the radicals OH and HO_2 . These radicals were considered free i.e. unattached to iron ions
- (b) these radicals which were produced by single electron exchange between the catalyst and H_2O_2 propagated chain reactions causing H_2O_2 decomposition.

Although the species H_2O_2^+ and H_2O^+ were introduced to explain various results it seems unlikely that they are in sufficient concentration to appreciably affect the reaction. As a

result of the interest stimulated in solution phase free radical reactions, Evans, Hush and Uri²² formulated energetic and thermodynamic data for many of the proposed primary steps which allowed an assessment of their thermodynamic probability.

An alternative reaction scheme was proposed by Bray and Gorin²³ for the $\text{Fe}^{++}/\text{H}_2\text{O}_2$ reaction. This scheme i.e.



differed considerably from the Haber-Weiss mechanism in that decomposition took place between a catalyst - H_2O_2 intermediate and the H_2O_2 . This mechanism introduces the postulation of a localised reactive intermediate as opposed to the free radicals contained in the Haber-Weiss mechanism.

4. Heterogeneous Catalytic Decomposition of H_2O_2

(a) General Considerations

The essential principle of heterogeneous catalysis is that the reaction cycle is anchored at the solid surface i.e. it occurs within the field of the chemisorption forces. Thus, any catalyst radicals are surface ions, ionic lattice positions or adsorbed radicals. There is also the possibility that the catalyst surface initiates chains which can diffuse into the solution bulk.

A truly heterogeneous catalytic reaction can be analysed into five steps viz.:-

1. Diffusion of reactants to the surface of the catalyst
2. Adsorption of reactants on catalyst surface
3. Reaction on the surface
4. Desorption of products from the surface
5. Diffusion of products from the surface

the slowest of which controls the overall rate of reaction. Since steps 2, 3 and 4 are intimately connected with the surface processes, catalysis at the interface of a solid and fluid is necessarily very complex involving a number of solid parameters whose influence is only of recent years beginning to be qualitatively understood.

These parameters have sometimes been divided into two groups i.e.

1. geometric factors²⁴
2. electronic factors²⁵

and with this division their study has provided a means of comparison between solid properties and catalytic activity.

Much study has been devoted to the correlation of solid activity with the relative dimensions of the solid surface and the reacting molecules. The earlier work of Langmuir^{26,27,28} was based on surface geometry and Burk²⁹ proposed that the surface decreased the activation energy of the reaction by adsorbing the reacting molecules in such a way that the distance between the points of maximum intensity in their

attractive forces was different in the adsorbed state than in the free molecule. Differences in the atomic distances involved in different lattice planes has been used by Beeck, Smith and Wheeler³⁰ and Beeck³¹ to explain differences in the hydrogenation of ethylene on oriented and unoriented condensed metal films, and Twigg and Rideal³² following experimental investigations on exchange between olefines and deuterium on Ni surfaces^{33,34} proposed that interatomic spacing was important in the hydrogenation of a double bond which required two-point contact. Particularly convincing was the work of Balandin³⁵ who dealt with specific reactions of large molecules where the fit with the surface was often very detailed.

Although the most emphasis in early studies had been placed on the geometric factor several workers e.g. Russell²⁵ had attempted to correlate catalytic activity and the catalyst's electronic structure, but it was not until the theories of the solid state were developed that the importance of the electronic factor in the solid could be fully discussed. Catalysis was held to proceed via surface electrovalencies i.e. through the transfer of electrons to and fro between the solid and the adsorbed species. The first worker to make definite measurements on this basis was Schwab³⁶ who varied the electronic structure and therefore, electron availability of many homogeneous and heterogeneous metal alloys by incorporating metals of different electronic structure.

Following Schwab many workers examined the importance of electronic structure in catalysis. Important contributions were made by Dowden and Reynolds³⁷ who on the basis of initiation involving electron exchange, successfully linked activity with electron availability for many reactions. For example, anomalous results obtained by Beeck and co-workers on ethylene hydrogenation over Cu, Ag and Au and Group VIII metals were successfully explained by Dowden and Reynolds as due to holes in the 3d, 4d and 5d bands of the Group VIII metals. Similar effects were observed by Couper and Eley³⁸ who showed that the inclusion of Au into Pd decreased the activity of Pd for the conversion of para hydrogen despite the similarity in atomic radii of Au and Pd. Further work by Dowden and Reynolds³⁹ on the decomposition of H₂O₂ on Ni-Cu alloys supported their earlier theories. They showed that the rate of decomposition decreased as the electron availability decreased, a result in harmony with a Haber-Weiss initiation reaction of the form



The early studies of Langmuir assumed that the surface was composed of a geometric array of sites on which adsorption and reaction took place with equal probability. Calorimetric studies by e.g. Garner⁴⁰ and Taylor⁴¹ have established in many cases that the heats of adsorption vary with the fraction of the surface covered. This observation was interpreted by Taylor⁴² as due to the existence of 'active sites' on which

preferential adsorption and reaction took place depending on the energy barriers involved.

Whether catalysis is preceded by adsorption involving covalent bonding of the adsorbed molecule or electron transfer between the metal atom and the adsorbed molecule, the work function of the metal as a whole or the degree of completion of the metal atom d-band are clearly the important factors determining catalytic activity.

Catalysis involving metal oxides is however more complex and the interaction of the adsorbed molecules with electrons or electron defects associated with the oxide lattice is recognised as the important consideration. Thus Gray and Darby⁴³ postulated that adsorption of O_2 on NiO occurred preferentially on metal ions involving electron transfer from the metal ion to the O_2 forming O' . This would be of vital importance in the catalysis by NiO of oxidation reactions e.g. CO/O_2 to CO_2 or hydrocarbon oxidations.

Volkenshtein⁴⁴ suggested that catalytic activity was associated with the equilibrium of surface micro-defects - a theory later extended by Boudart⁴⁵, - and Taylor and Thon⁴⁶ postulated that only one type of active centre was responsible for a given catalytic reaction. This theory assumed that the active sites consisted of dissociatively chemisorbed reactants.

Each system, particularly in the case of oxides, must

however be considered separately. The catalyst in the absence of the substrate will have a surface consisting of variously saturated ions, unsaturated lattice positions etc. When the substrate is admitted the adsorption will alter this situation in a specific way giving rise to a range of 'active sites' consisting of condensed radicals of various kinds each perhaps capable of reaction with the unadsorbed substrate constituents.

(b) Early Heterogeneous Studies

It was to be expected that the theories which had been so successful in understanding homogeneous reactions should be applied to the interpretation of heterogeneous systems.

From his observations on the decomposition of H_2O_2 by Pt, Au, Pd, Ag and Zn, Weiss⁴⁷ proposed that the initiating action of the surface metal atoms was similar to that exerted by dissolved metal ions i.e. an electron from the metal split the adsorbed H_2O_2 producing the radical OH i.e.

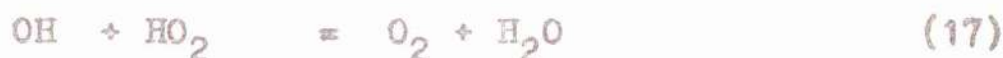


or in alkaline solution



The removal of an electron from a metal is governed by the potential barrier at the surface which in turn is

controlled by the work function. Using a method proposed by Garney⁴⁸, Weiss decreased the work function of many metals by applying a negative potential and found that the catalytic activity was increased, an effect in agreement with the electron transfer theory if (15) was the rate controlling step. In his interpretation of the results Weiss ignored the influence of a layer of oxide stating that such a layer would be transparent to electrons and that catalysis would be controlled solely by the electronic nature of the underlying metal. He also considered that radical chains took place in a high concentration region adsorbed at the surface of the metal. The short chain lengths found were explained on the proposition of termination by surface removal of the free radicals propagating the chains i.e.



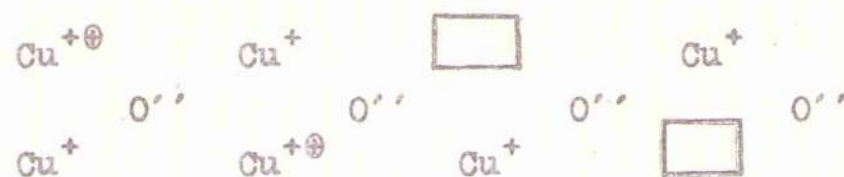
(c) Semiconducting Oxides as Catalysts

An explanation of the properties of oxides as catalysts demands an understanding of their electronic structure and the rôle of ionic lattice defects etc., in their make up.

The most active catalysts for H_2O_2 decomposition^{49,50} are those in which the stable oxide has a tendency to form,

in air, a small amount of a higher valency oxide e.g. Cu_2O , CoO and to a lesser extent NiO . Such oxides are examples of the class of P-type semiconductors. They exhibit non-faradaic conductivity in the solid state and the current carrier is identified as a positive entity - the "electron hole" - which can be thought of when localised as the cation of higher valency e.g. Cu^{++} in Cu_2O .

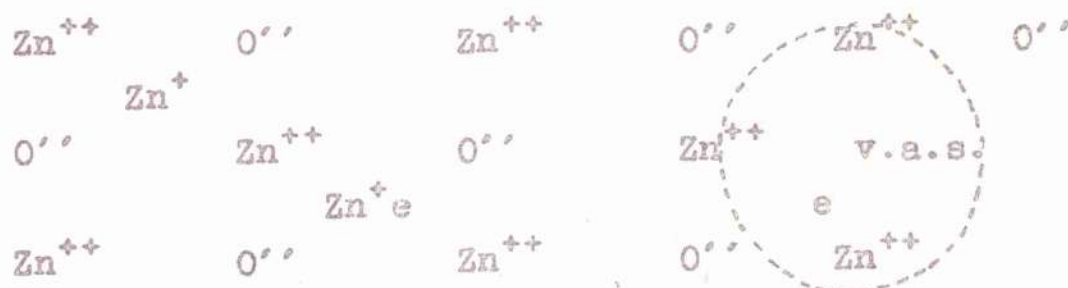
i.e.



where \oplus represents a positive hole

represents a vacant cation site

These oxides are to be distinguished from N-type semiconductors in which current is transported non-faradaically also but now by mobile excess electrons e.g. in ZnO containing a slight excess of Zn atoms held in interstitial positions where they readily ionise. The localised electrons can be considered as a Zn^+ ion which in an array of Zn^{++} is a negative entity e.g.



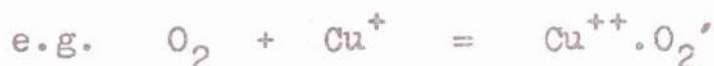
where e represents quasi-free electrons

Zn^+ represents an interstitial zinc ion.

But the oxide structure is more complex than the conduction would imply. There are also lattice ion defects of various kinds, e.g. it is assumed that in any real crystal at any temperature there exists a number of imperfections which are in a state of equilibrium with the perfect lattice. The limiting cases for this type are equal concentrations of vacant anion and cation sites - Schottky defect - and the presence of interstitial atoms or ions - Frenkel defect. Conduction is caused by the migration of the vacant sites or interstitial entities through a series of lattice positions.

Particularly relevant to the consideration of the catalysts as semiconductors has been the work of Garner and co-workers on the oxidation of Cu and the reactions CO/O_2 and N_2O decomposition on Cu_2O . Examination by Garner, Grey and Stone⁵¹ of the oxidation of copper and the adsorption of various gases on Cu_2O produced several interesting observations.

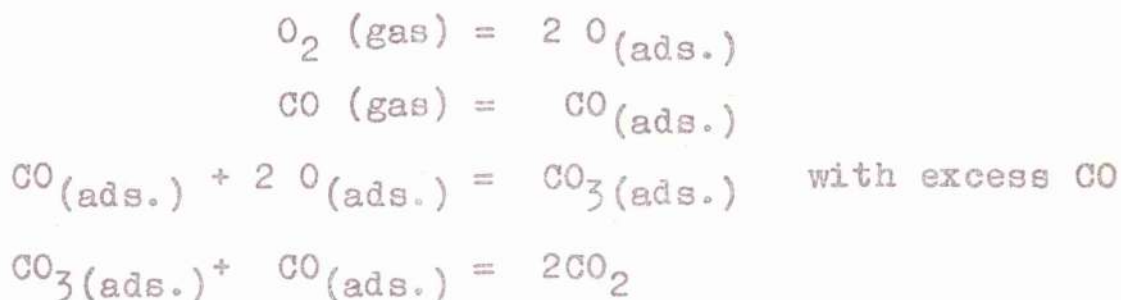
- (i) The oxygen was adsorbed on the Cu_2O in a particularly active form which was associated with the conductance electrons since its adsorption was accompanied by an increase in the conductivity of the Cu_2O . The oxygen was therefore considered adsorbed as O' or O_2' ions inducing the formation of a positive hole



thereby increasing the conductivity

- (ii) They proposed that the O_2 was adsorbed as a molecule since the heat of adsorption did not exceed 30-35 kcal./mole.
- (iii) The activity of the surface was destroyed by CO. From this they concluded that adsorption occurred on exposed Cu atoms lying above the normal lattice. Treatment with CO formed an intermediate complex carbonate which subsequently decomposed liberating O_2 and destroying a vacant cation site.
- (iv) They suggested that the adsorption of O_2 as a negative species was an important step in the CO/O_2 reaction taking place on Cu_2O .

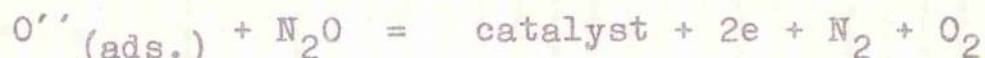
Further work by Garner, Stone and Tiley⁵² established that O_2 was dissociatively adsorbed either as O' or O'' and a reaction mechanism for the CO/O_2 reaction on Cu_2O was proposed involving the establishment of a stationary state between the adsorbed species CO , O and CO_3 i.e.



The adsorption of O_2 was considered the rate controlling step since it involved



Similar catalytic and conductivity measurements carried out by Wagner⁵³ suggested the occurrence of an analogous process during the decomposition of N_2O on ZnO . The proposed mechanism involved a rate determining electron exchange across an adsorbed layer i.e.



Although the decomposition of H_2O_2 represents a more complex picture than either CO/O_2 reaction or N_2O decomposition there are reasons to suggest that the basic mechanisms may be similar. These reasons are

- (i) The relative catalytic efficiencies of various oxides for the CO/O_2 reaction as reported by Stone⁵⁴ is similar to that observed by Giguère⁵⁵ and Ross⁴⁹ for the vapour phase decomposition of H_2O_2 . For CO/O_2 reaction in order of decreasing activity



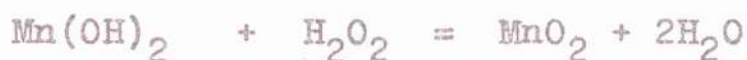
compared to



for the vapour phase decomposition of H_2O_2 . These results suggest that P-type oxides are more active than N-type oxides which are more active than insulators.

- (ii) A similar oxide efficiency relationship for the decomposition of N_2O has been compiled by Dell, Stone and Tiley⁵⁶ following extensive work by Schmid and Keller⁵⁷.

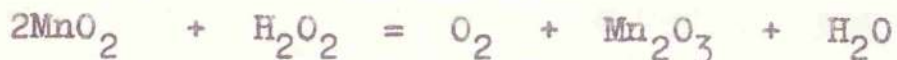
There has not been a great deal of work carried out on the heterogeneous decomposition of aqueous H_2O_2 solutions by oxides. Broughton and Wentworth⁵⁸ and Broughton, Wentworth and Laing⁵⁹ studied the catalysis of H_2O_2 by MnO_2 and showed that Mn^{++} accumulated in solution until the solution was saturated with $Mn(OH)_2$. Alternate oxidation and reduction of the MnO_2 formed the basis of their proposed mechanism which was as follows



This reaction scheme was further supported by radioactive tracer experiments.

Similar measurements on various supported manganese oxides were carried out by Mooi and Selwood⁶⁰ who postulated a different mechanism to that proposed by Broughton and Wentworth. This mechanism, based on relevant free energy data and observations made by Dubois^{61,62} on the composition of manganese oxide, involved simultaneous oxidation and reduction between tri and tetra valent manganese in the form

of a Haber-Weiss one-electron step i.e.



Recent work by Voltz and Weller⁶³ has been directed towards a correlation between catalytic activity and surface oxidation state. The catalysts used were chromia and chromia/alumina which had been pretreated at 500°C in an atmosphere of H₂ or O₂, and it was found that the oxidised catalysts were six to eight times as active as the reduced ones. Also Schwab⁶⁴ observed that the spinel MgO . Fe₂O₃ was a better catalyst for aqueous H₂O₂ decomposition than the spinel ZnO . Fe₂O₃. Replacement of the Mg⁺⁺ by Zn⁺⁺ in the magnesium ferrite improved its efficiency by a considerable amount.

5. Purpose of Present Investigations.

Present theory concerning heterogeneous catalytic decomposition of H₂O₂ is based on one of two main approaches i.e.

(i) A Haber-Weiss type mechanism.

This mechanism which is mainly based on analogy with homogeneous systems identifies the radicals OH and HO₂ (O₂') as the reactive, chain propagating species. The radicals which are produced by electron transfer at the solid surface are considered free to propagate

the reaction in the high concentration region near the surface.

(ii) A Bray and Gorin type mechanism.

This mechanism which has not attracted supporters as has the Haber-Weiss scheme, proposes an active intermediate formed between the catalyst and the H_2O_2 i.e. unlike the free unrestricted radicals contained in the Haber-Weiss scheme this reactive species is localised being permanently linked with the catalyst proper. Although this theory was also developed from homogeneous systems it has been successfully applied to heterogeneous enzyme catalytic systems e.g. the decomposition of H_2O_2 by the enzyme catalase is believed to proceed according to the scheme



where E is the enzyme
S is the H_2O_2
P is the product

The interpretation of results obtained from reaction between H_2O_2 and inorganic solid surfaces is further complicated by possible oxide formation. No metallic surface can be considered free from oxide. Under normal atmospheric conditions such formations may be only a few (say 20 - 100)

angstroms thick but in systems involving the decomposition of H_2O_2 , formation of an appreciable thickness of oxide layer is to be expected. The formation of such an oxide has been dismissed from many kinetic discussions on the assumption that it does not affect the catalytic properties of the bulk catalyst. Dowden and Reynolds³⁹ discussed this added complication but suggested that the short covalent forces present in the metal oxides were dependent only on the oxide layer and therefore changes in catalysis caused by changes in the electronic structure of the metal were explainable only by direct reference to the bulk metal. If however reaction takes place at active sites on the surface i.e. localised free radicals then results must be related to the oxide layer since changes in the electronic nature of the underlying metal would reasonably be expected to alter the reactivity and number of the active positions.

It does not therefore appear valid to interpret the results from heterogeneous H_2O_2 catalysed systems without considering the exact nature of the catalysing surface, with particular reference to oxide formation. A suggestion of a cycle suitable for an oxide surface is contained in the scheme proposed by Bray and Gorin²³ for the $Fe^{++}/Fe^{+++} - H_2O_2$ homogeneous reaction. Uri⁶⁵ considered this scheme was unlikely in solution for two reasons. These were

- (i) A complex rearrangement was required which did not agree with the experimental activation energies of

5 to 10 kcals as found by Baxendale, Evans and Parks¹⁴.

- (ii) No iron atoms in the final polymer were detected by Baxendale, Evans and Parks in the $\text{Fe}^{++}/\text{H}_2\text{O}_2$ initiated polymerisation reactions.

The Bray and Gorin scheme was developed however for the homogeneous $\text{Fe}^{++}/\text{H}_2\text{O}_2$ reaction and the above disadvantages need not necessarily apply to a heterogeneous process where it may be that a Bray and Gorin type mechanism more truly represents the solid surface.

Work carried out in this laboratory by Hart and McFadyen⁶⁶ and Hart and Ross⁶⁷ on the vapour phase decomposition of H_2O_2 , further emphasised the importance of oxidised metal surfaces. Thus, using flow methods Hart and McFadyen examined decomposition on Cu and Ni gauzes which had been exposed to the atmosphere. A series of interesting cyclic efficiency changes were observed which were later repeated by Hart and Ross using bulk oxides.

It was clear from these results that the oxide itself played an important rôle in the catalysis. There was in fact no evidence to suggest that a thin oxide film on a metal surface possessed any noticeably different action than the bulk oxide itself.

The first aim of this work was therefore to test these conclusions with oxide catalysts in the solution phase. In particular it was regarded as important to test for the

presence of the slow cyclic effects obtained in the vapour phase. If these occurred in the solution phase as well, it would substantiate the conclusions that they were due to processes occurring in the oxide or oxide/hydroxide itself. It was hoped also to be able to link the work on oxides with that on enzymes. An oxide might possibly be shown to be a better model than a metal of an enzyme considered as a heterogeneous catalyst rather than as the quasi-homogeneous one it is usually taken to be.

A further aim was to attempt by a detailed study of the kinetics of the catalytic process and of the kinetics of the changes in catalyst efficiency to obtain some insight into the detailed mechanism of H_2O_2 decomposition. The bulk of the work concerned in this approach applied to the one catalyst Cu_2O . It was necessary to extend the examination to one or two similar oxides to show that the effects were not specific to the one substance.

Arising out of the interpretation of the early results, experiments were seen to be necessary on model surfaces consisting of HO' and HO_2' ions held to a relatively inert solid. This led to experiments with anion exchange resins which proved to be most helpful in examining crucial stages in the main conclusions.

EXPERIMENTAL

1. Introduction

The object of the work was to study the decomposition of aqueous H_2O_2 on solid oxides in such a way as to permit special investigation of any efficiency changes which could be ascribed to some alteration in the state of the catalyst during reaction. For this purpose a static system in which the change of $[H_2O_2]$ with time in a volume of solution containing a fixed quantity of the catalyst would have been unsuitable. Such systems involve simple experimental techniques but interpretation of the results would be difficult if catalytic efficiency is affected by such variables as substrate concentration, solution of catalyst, stirring and shaking and the particular problem of gas bubble separation from a particulate catalyst.

A flow system was therefore chosen. This enabled attention to be focused readily on the changes taking place in the efficiency of the catalyst. An apparatus giving constant flow conditions was designed and a technique developed by which the efficiency of the catalyst could be continually observed during the course of the reaction.

2. Efficiency Apparatus and Experimental Technique.

The apparatus and technique is dealt with under two headings:-

- (a) Steady propulsion of standard substrate
- (b) Measurement of changes in catalyst efficiency

(a) Steady Propulsion of Standard Substrate

(a.i) Propulsion of substrate.

A steady uncontaminated stream of reactants was obtained by pumping the substrate to a constant head device by a simple nitrogen lift and using the hydrostatic head to drive the liquids through the apparatus. The nitrogen lift was an adaptation of the air-lift principle used in industry and was preferred over mechanical pumping because of the danger of contamination from pump gland lubricant or diaphragm materials.

The liquid flowed (Fig.1) from reservoir R_1 to reservoir R_2 . An uptake pipe P_1 led from reservoir R_2 to the constant level tanks situated above bench level at a height sufficient to give the hydrostatic pressure required to force the liquids through the experimental assembly at the maximum required velocity. A lead from a nitrogen cylinder was hooked under the uptake pipe P_1 and the flow of nitrogen carried the liquid up to the constant level tank in a series of slugs.

The reactants from the constant head tanks were metered at bench level in previously calibrated liquid flow meters (Fig.2).

When the flow system was coupled to a heating

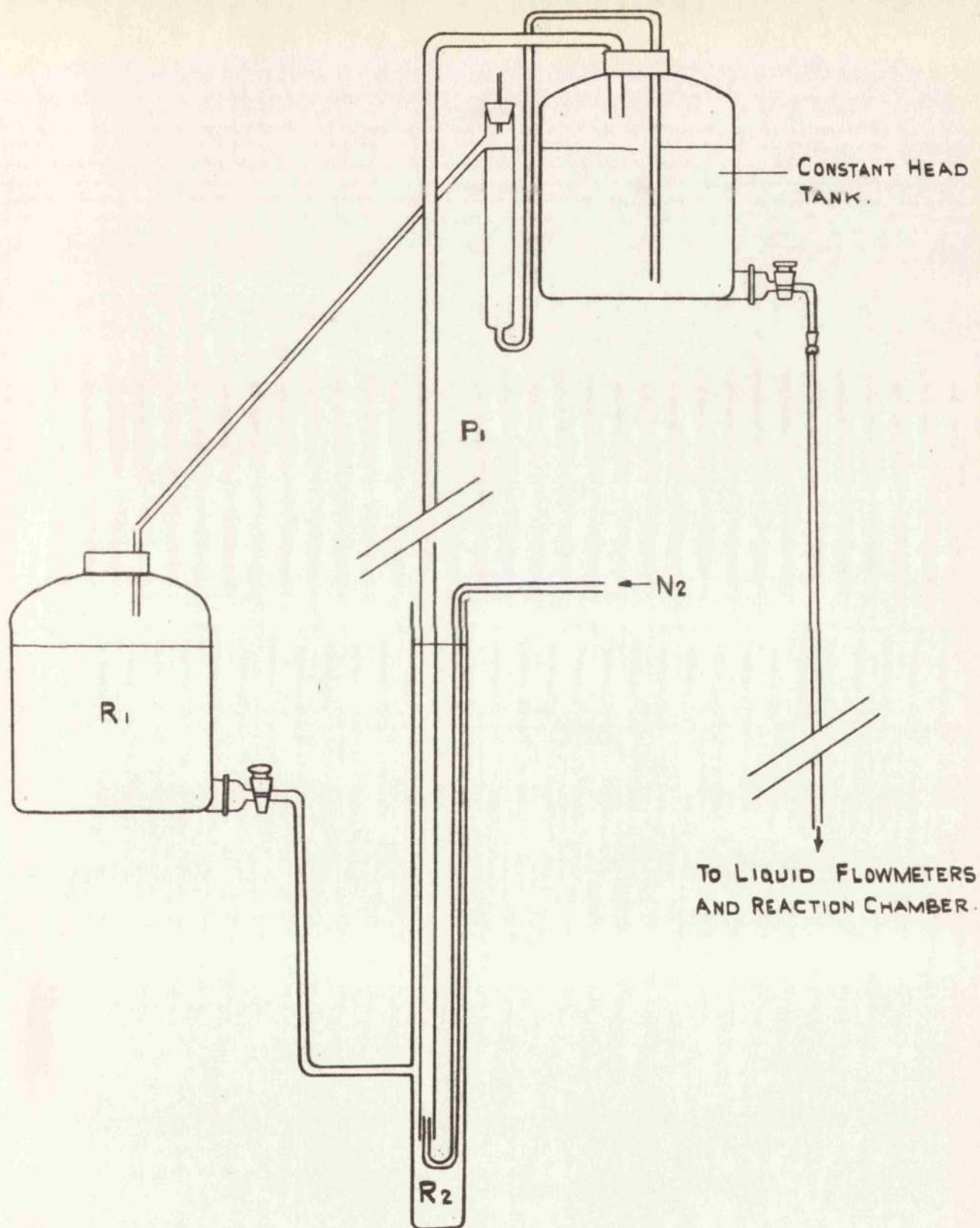


FIG. 1. THE SECTION OF THE EFFICIENCY APPARATUS GIVING CONSTANT FLOW OF REACTANTS.

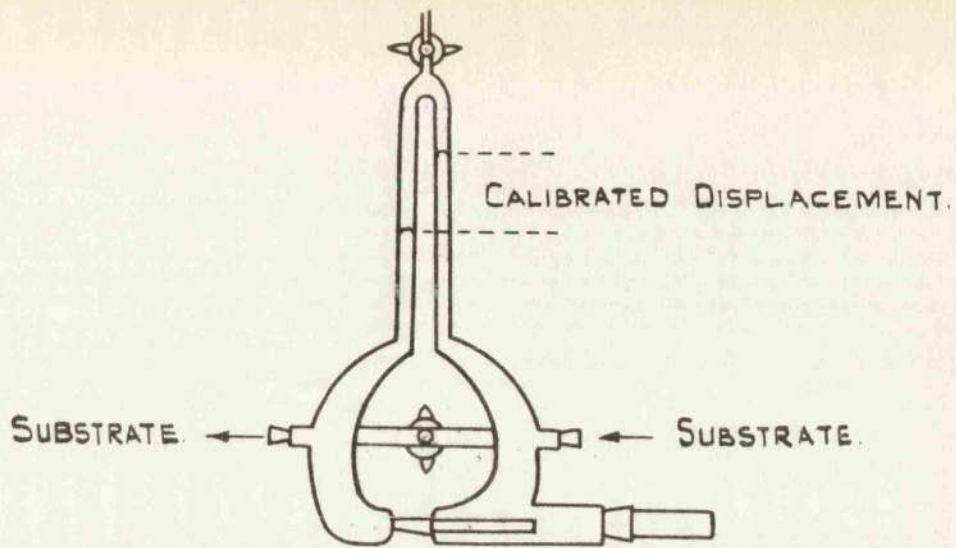


FIG. 2. LIQUID FLOWMETER.

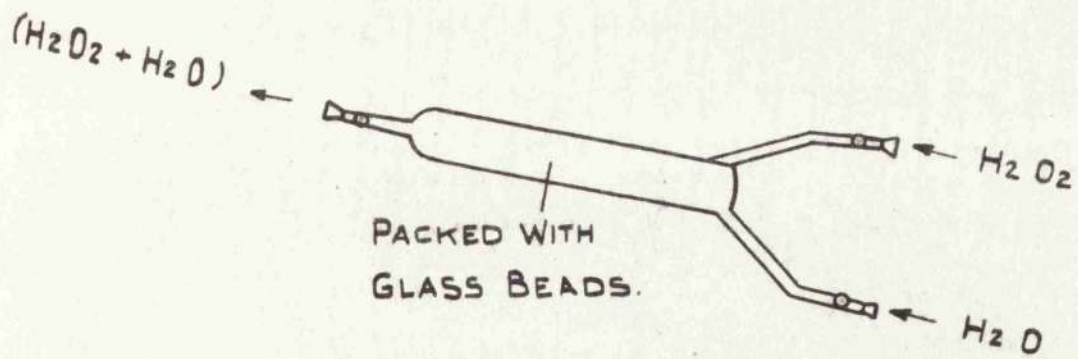


FIG. 3. ORIGINAL MIXING DEVICE.

coil and reaction chamber, decomposition of the H_2O_2 produced slight fluctuations in pressure across the system disturbing slightly the constant rate of flow delivered from the meters. The meters were completely insulated from these small variations in pressure by short sections of capillary tube sealed in between the reaction chamber and flow meters.

(a.ii) Alteration of Substrate Concentration.

Two independent streams of H_2O_2 and H_2O were used to produce variations in the substrate concentration by altering their relative rates of flow. All runs were made at the same total flow rate so as to exclude flow conditions as a variable in the efficiency considerations.

The mixer first used in the apparatus was built in immediately after the flow meters so that only one heating coil was necessary. The mixing chamber (Fig.3) was a cylinder 10 cm. by 2 cm. internal diameter angled upward to reduce the danger of dead spaces and bad mixing. The chamber was packed with glass beads to break up the streams and give added turbulence. Equal flow rates of water and peroxide were set and 25 ml. portions of the resulting mixed stream were collected every minute. At a noted time the peroxide was shut off and a further series of samples collected. The collected effluent was titrated against standard permanganate and the results plotted as shown (Fig.4). From the time the peroxide was switched off 4 minutes elapsed before the

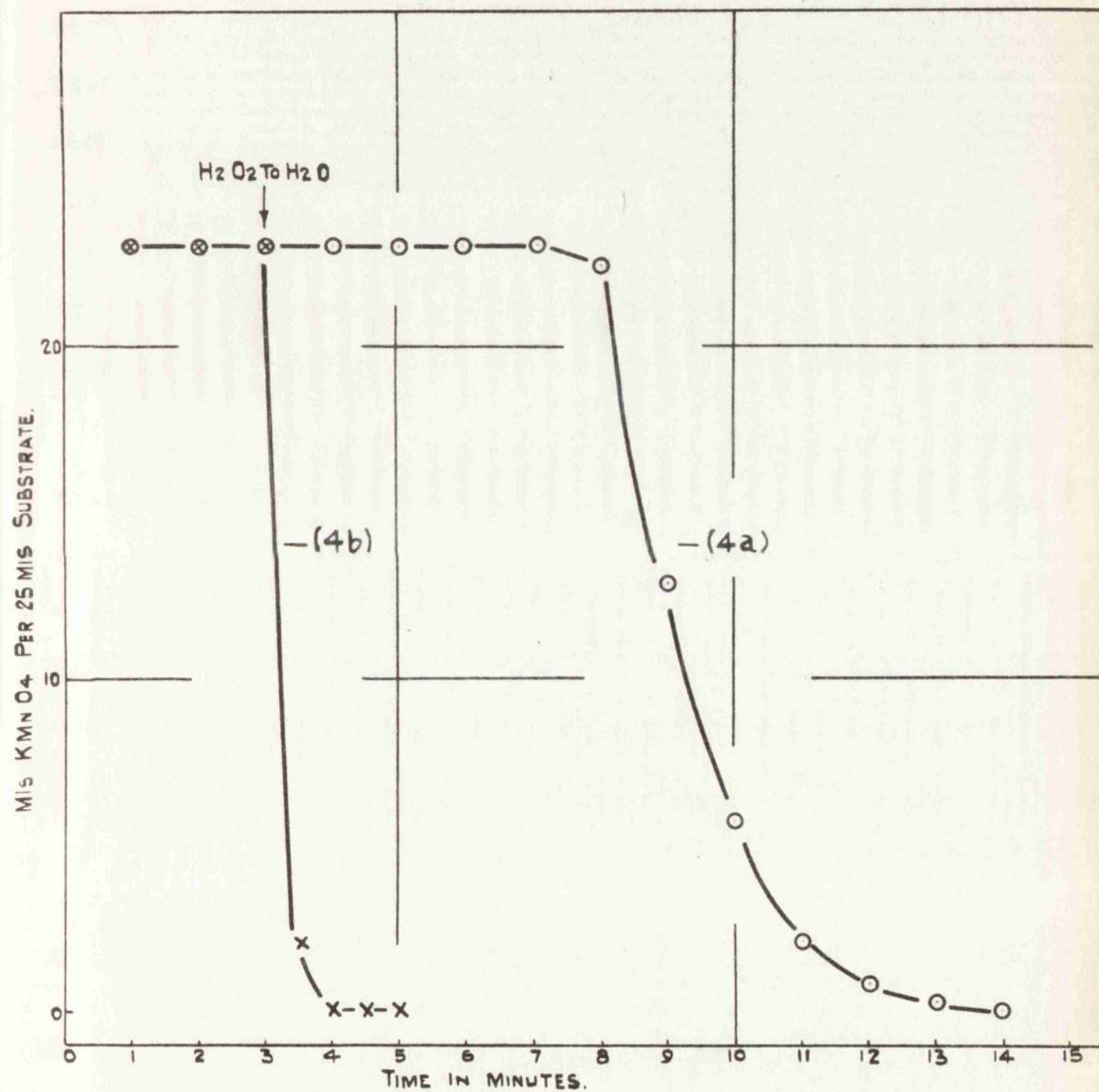


FIG. 4. SHOWING THE TIME TAKEN FOR A CHANGE IN SUBSTRATE CONCENTRATION TO BECOME ESTABLISHED IN THE REACTION CHAMBER USING (a) ORIGINAL MIXER AND (b) IMPROVED MIXING DEVICE.

original mixture was swept clear from the mixing chamber heating coil and reaction tube. A further 7.5 minutes passed before pure water was obtained. Although a sharp change from peroxide to water is more difficult to achieve than a change in H_2O_2 concentration, it is clear from the diffuse character of Fig.4a that the position and design of the mixing chamber did not permit a close and accurate examination of the change-over period.

The system finally adopted is shown in Fig.5. The single heating coil in the original arrangement was replaced by a separate coil for both H_2O and H_2O_2 . The mixing was carried out immediately before the catalyst chamber by simply joining the separate streams. Two stop-cocks immediately before the mixing point enabled either stream to be completely shut off and a three-way stop-cock after the mixer allowed the reaction chamber to be by-passed and the concentration of the substrate entering the chamber determined. With this scheme the change over to new conditions was sharp (Fig.4 b) being almost complete in 30 seconds.

(a.iii) Substrate Heating System.

The solutions were heated to the reaction temperature in a thermostatted water-bath containing the heating coils, mixing point and reaction chamber. The bath was heated by Robertson heating lamps and the temperature controlled by a hot wire vacuum switch and toluene regulator.

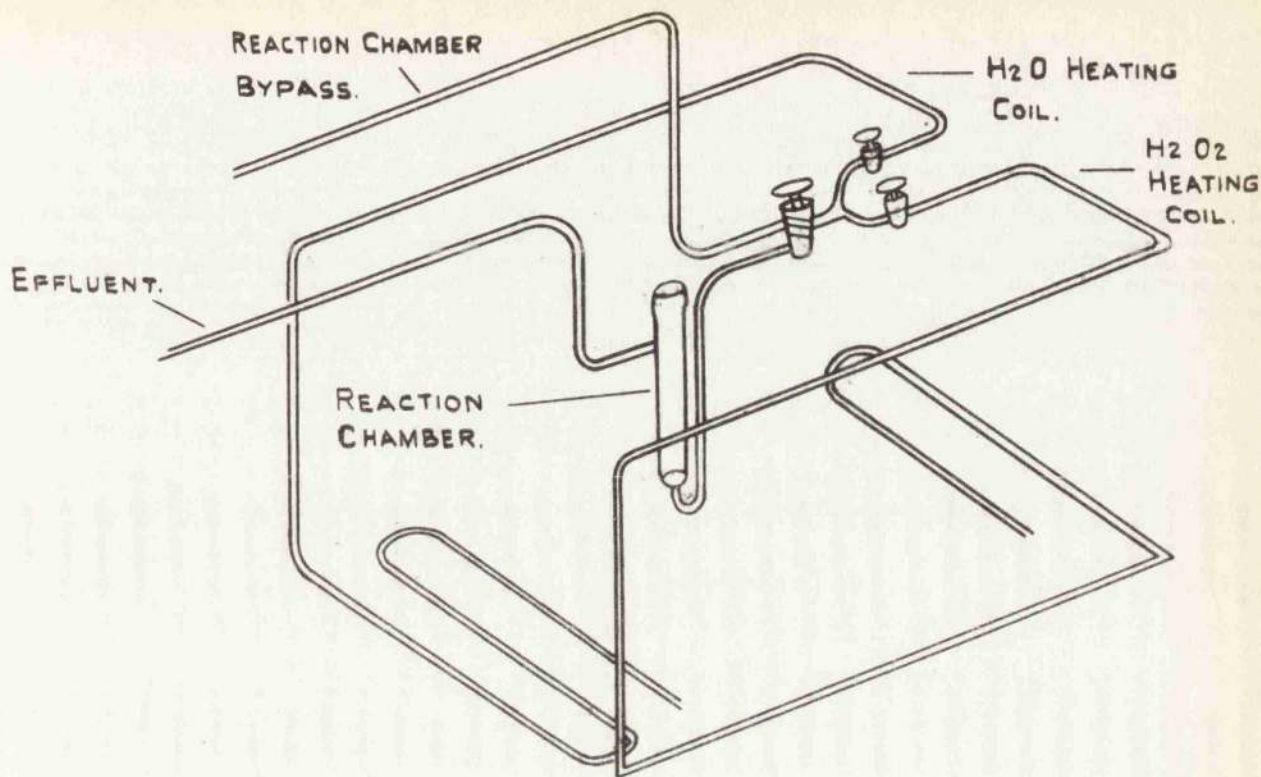


FIG. 5. SECTION OF EFFICIENCY APPARATUS SHOWING THE INDIVIDUAL HEATING COILS FOR H₂O AND H₂O₂ WITH DIRECT MIXING TAKING PLACE IMMEDIATELY BEFORE THE REACTION CHAMBER.

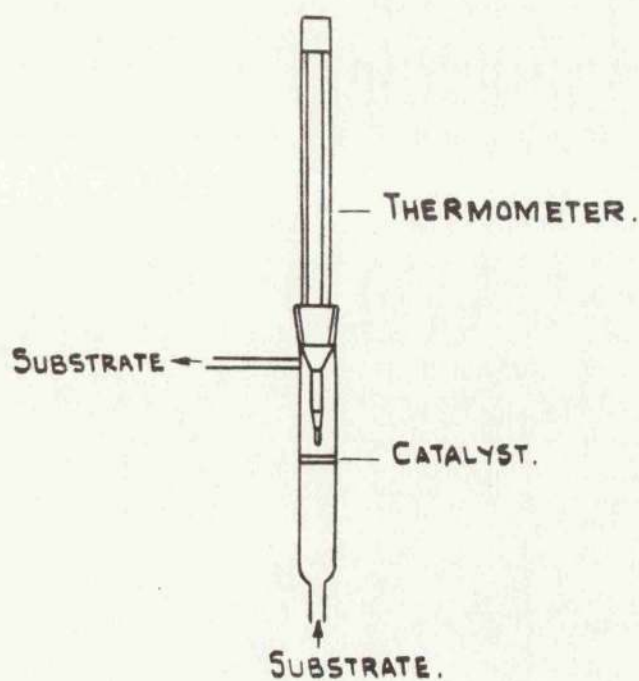


FIG. 6. REACTION CHAMBER IN WHICH % DECOMPOSITION WAS DETERMINED BY KMnO₄ TITRATION.

Three stirrers were necessary to give adequate circulation in the bath. The heating coils were of 5 mm. diameter tubing 5 meters long. This length was sufficient to bring the temperature of the solutions close to that of the bath and to reduce temperature fluctuations to a degree which permitted the sensitive measurement of catalysis by temperature rise which is described below. This was achieved by approaching to within 0.5° of the bath temperature and by ensuring that the stock solutions had been given time to reach equilibrium with room temperature before commencing a run. It was necessary to by-pass the reaction chamber with substrate until temperature equilibrium was attained.

(b) Measurement of Changes in Catalyst Efficiency

In a flow system the measurement of changes in catalyst efficiency can be made by observing:-

- (i) the loss in substrate concentration by sampling and analysis of substrate or product.
- (ii) continuous measurement of change in some physical property of the solution.

The choice of a method was limited by the need to work at as small as possible a decomposition for two reasons:-

- (a) to keep the $[H_2O_2]$ as far as possible constant over the catalyst zone
- (b) the need to keep the O_2 evolution down in order to

reduce the possibility of gas occlusion in the catalyst bed.

In practice the second requirement set an upper limit of 0.005 moles of H_2O_2 per minute or approximately 1 ml of O_2 gas per second, but this was only tolerated at the higher $[\text{H}_2\text{O}_2]$. At 0.025 M a decomposition of 0.0025 M per litre was the maximum permitted. These requirements favoured an estimation of the product rather than the reactants.

Measurement of oxygen evolution is quite a sensitive indication of decomposition. Thus a 0.1% decomposition of 0.5 M H_2O_2 flowing at 100 mls per minute evolves 1.12 mls of O_2 per minute. The method is however difficult to use as a fast continuous method since the evolved oxygen has to be efficiently separated from the liquid streams and this introduces some delay. The liquid must also initially have a standard degree of gas saturation. In the present method the fact that the liquid was saturated with N_2 which came out of solution on warming to the bath temperature created an extra difficulty for this method.

Estimation of the $[\text{H}_2\text{O}_2]$ in samples collected over short periods of time either by colorimetric methods or by direct KMnO_4 titrations is heavily handicapped in the present work by the need to operate at very small fractions of change. Colorimetric methods e.g. titanium dioxide and concentrated H_2SO_4 , iodide (U.V. estimation of straw colour) or iodide and starch (visible estimation of blue colour with standard starch)

are the most sensitive but are only applicable at total concentrations of 10^{-3} and below. No measurements were made at such low $[H_2O_2]$. In an illustrative run titration with 0.1N $KMnO_4$ was used to measure the amount of 0.05 M H_2O_2 decomposed by Cu_2O (oxidised copper gauze) jammed in the reaction chamber (Fig.6). Water at a definite flow rate, pH and ionic strength was passed through the system until thermal equilibrium was attained. The water was then replaced by 0.05 M H_2O_2 at the same flow, pH and ionic strength. Samples of the substrate leaving the reaction chamber were collected at equal time intervals and titrated against the $KMnO_4$. The titration results (Fig.7) show that large percentage decomposition is required to use this method. The amount of O_2 evolved and the concentration gradient across the catalyst are increased by such a rise in percentage decomposition. Tests showed that for measurable concentration changes the rate of O_2 evolution and the concentration gradient become appreciable so that the catalyst surface area and concentration effects are obscured.

The physical method adopted had also to take account of the fractional change limitation mentioned above and to work on a parameter limited to the amount of product formed rather than the amount of H_2O_2 lost. The method used was to measure the heat evolved in the catalysis.

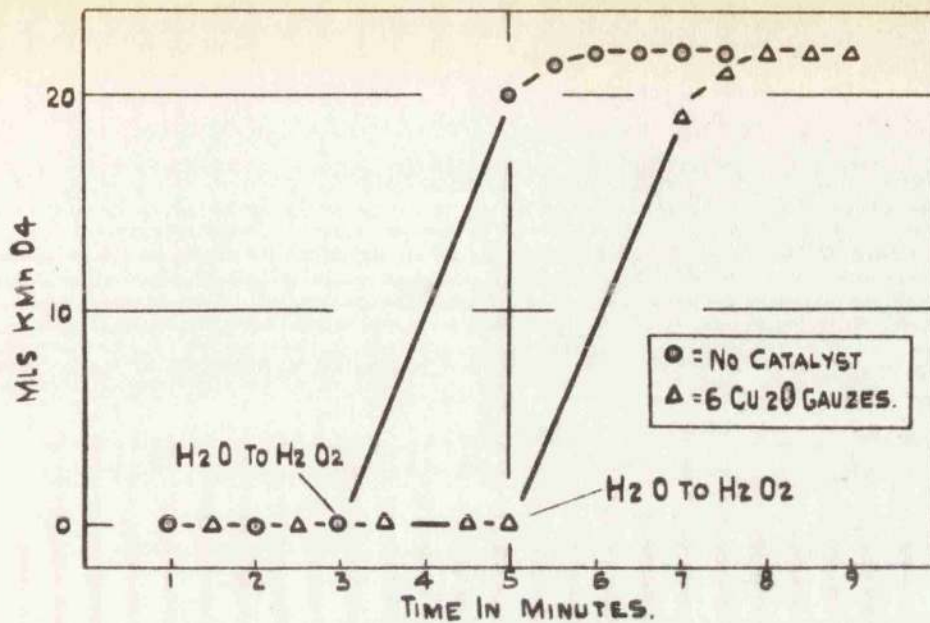


FIG. 7. MLS KMnO₄ REQUIRED TO NEUTRALISE EQUAL VOLUMES OF SUBSTRATE LEAVING THE REACTION CHAMBER.

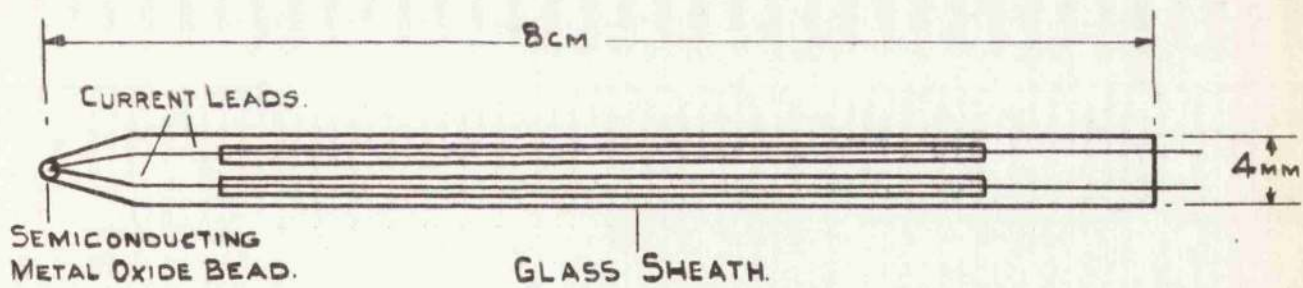


FIG. 8. BEAD TYPE THERMISTOR.

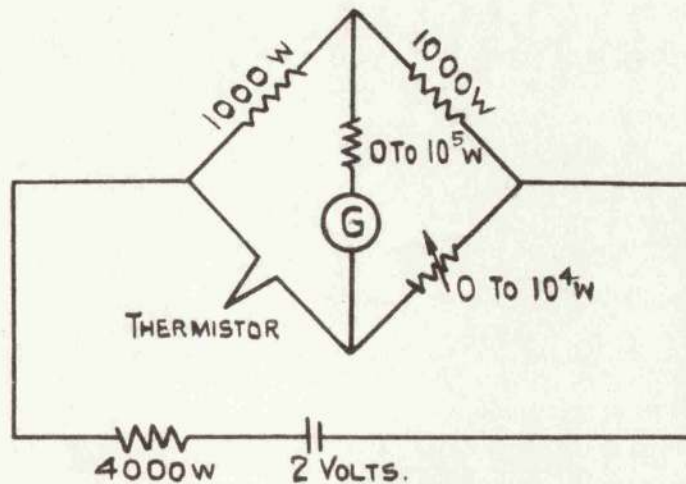


FIG. 9. WHEATSTONE BRIDGE CIRCUIT USED TO MEASURE THE RESISTANCE OF THE THERMISTORS.

(b.i) Thermal Measurement of Decomposition.

The 1% decomposition of 1 litre of a 1 M solution of H_2O_2 to liquid H_2O and O_2 liberates 235 calories⁶⁸ raising the temperature by $0.235^\circ C$ if the process is adiabatic. 1% decomposition of a 0.02 M solution would result in a 0.005° rise.

Adiabatic conditions have been assumed to obtain at the centre of the reaction chamber provided temperature differences of not more than 1.5° are used. It is seen therefore that a sensitive measurement of the temperature before and after the catalyst would give a precise indication of the amount of decomposition under the given conditions and hence of the catalyst efficiency. Furthermore it is possible to make such measurements with negligible delay by having a thermometer element of low heat capacity in direct contact with the fluid.

Two such elements have been successfully used in similar rate/time measurements viz:-

- (a) thermocouples
- (b) thermistors

The measurement of temperature differences as an indication of the rate of small amounts of rapid exothermic reactions was used by Bengough and Melville^{69,70} with a thermocouple. In this way they followed the non-stationary initial rate of photopolymerisation. The rise in temperature

was measured on a single thermo-junction placed at the centre of the reaction vessel. The slight change in e.m.f. had to be amplified by a low impedance D.C. amplifier and automatically recorded. During the short time that readings were taken the reaction at the centre of the vessel was considered adiabatic since the reaction mixture was heated uniformly by chemical reaction and cooling only occurred through the walls.

The sensitivity of such a method depends on the constancy of the ambient temperature and the reproducibility of changes in e.m.f. with temperature. The complete reaction chamber was immersed in a thermostatically controlled bath maintained to within 0.01°C . Tests showed that this slight fluctuation produced changes inside the reaction chamber of the order of 0.001°C which were negligible compared with the temperature changes caused by polymerisation. The relationship between e.m.f. and temperature was obtained by calibration and a high degree of reproducibility obtained.

The thermal measurements carried out by Bengough and Melville were successfully repeated by Miyama⁷¹ and Fujii and Tanaka⁷² using a bead type thermistor (Fig.8) as the temperature sensitive element.

Thermistors are a special type of resistance thermometer consisting of a fragment of a semiconductor sealed in a thin protective glass sheath. They are more sensitive to temperature than a metal (e.g. Pt) resistance thermometer. Many workers have given detailed study to the temperature /

resistance characteristics of semiconductors. Thus Becker, Green and Pearson⁷³ using typical mixed oxide semiconductors (manganese-nickel oxide and manganese-nickel-cobalt oxide) showed that R the resistance varied with the absolute temperature to a first approximation according to the law

$$R = R_0 \cdot e^{\left(\frac{B}{T} - \frac{B}{T_0}\right)}$$

$$\text{i.e. } \log R = \frac{B}{T} - \text{constant}$$

where T = temperature in $^{\circ}\text{K}$.

$R = R_0$ when $T = T_0$

$B =$ a constant $= 2.303 \times$ slope of the $\log R/\frac{1}{T}$ line.

Examination of the plot of $\log R$ against $\frac{1}{T}$ over a large temperature range shows that the slope of the line increases linearly with temperature and a more precise expression is

$$R = A \cdot T^{-c} \cdot e^{\frac{D}{T}}$$

where c is a small positive or negative number or zero.

Over short ranges of temperature however the graph $\log R/\frac{1}{T}$ can be taken as linear and the simple expression used.

The theory of this relationship is well understood following the work of Mott⁷⁴ and others. Current is carried by electrons or positive holes which are contained at concentrations fixed by the composition and pretreatment of the

oxide mixture. The conductivity of the material is then given by

$$\text{Conductivity} = A.e^{-\frac{W}{RT}}$$

where A is a constant depending on the number of charge carriers and their mobility in the particular crystal. W is an energy factor being the height of the potential barrier which impedes the movement of the carrier. It is clear that A would not be expected to remain fixed over a wide temperature range since lattice expansion would affect mobility not to mention possible changes in the number of charge carriers.

The use of thermistors places less exacting requirements in the resistance measurements than a platinum resistance thermometer, requiring only a conventional Wheatstone bridge and sensitive galvanometer. Their use for temperature changes of as little as 0.001° does require considerable care however i.e.

(i) The ultimate accuracy of any temperature sensitive element is the accuracy with which it is calibrated.

Since the linearity between $\log R$ and $\frac{1}{T}$ is only strictly observed over short temperature ranges it is necessary to calibrate the thermistors over short ranges (say 5°) about the temperature of use.

(ii) It has been shown that once calibrated thermistors remain stable over short periods but they may vary slightly over years^{73,75,76,77,78,79}. Although the

precise nature of the effects causing fluctuations in the stability are not entirely understood, Beck⁷⁸ has suggested that exposure to wide temperature differences is an important factor. Although altering the position of the $\log R/\frac{1}{T}$ calibration line relative to the axis, these changes (which alter the value of the constant in the calibration equation) do not affect their use as a differential instrument. If the thermistors are used only in the narrow temperature range over which they have been calibrated these changes, if any, are small and extremely slow and any series of results based on temperature difference measurements are entirely reliable.

(iii) For the accurate measurement of small temperature differences care has to be taken to see that the heat generated by the measuring current in the bead is so small that it raises the bead temperature to an extent negligible compared with the temperature differences being measured. The voltage across the Wheatstone bridge must therefore be kept to a minimum and resistances used in the circuit to reduce the current flowing through the thermistor to a very small value.

This temperature rise of the element is of course dependent not only on the measuring current but on the heat dissipated from the thermistor. This as shown by Becker, Green and Pearson⁷³ (who found $\Delta T_{\text{induced current}} = \text{constant} \times \text{heat dissipated}$) depends on the thermal conductivity of the medium and on the rate of flow which should

therefore be kept constant in a series of comparable runs. By working with very small measuring currents it was possible however to neglect both of these factors.

(b.ii) Resistance Measuring Circuit.

A Wheatstone bridge circuit (Fig.9) was used to measure the resistance of the thermistor. A 2 volt accumulator with a 4000 ohm resistance in series provided current. The thermistor resistance was balanced against a 5-dial Decade resistance box (Muirhead A, 825-N) with a range of 0 - 10^4 ohms in steps of 0.1 and an accuracy of $\pm 0.1\% \pm (0.002 \text{ ohms} \times \text{No. of dials})$ for resistances above 1 ohm and $\pm 0.5\% \pm (0.002 \text{ ohm} \times \text{No. of dials})$ for 0.1 ohm steps. The 1000 ohm resistances in the fixed bridge arms were adjusted to $\pm 0.1\%$ with unifilar windings of eureka wire and balance was observed on a Cambridge galvanometer No.L298469 used in conjunction with a meter scale. A resistance of 1000 ohms in series with the galvanometer gave the best compromise between damping and sensitivity.

The thermistors available for use were known to have a resistance of about 1000 ohms at 40°C . Therefore for the above circuit at 40°C we have

$$\text{Resistance between A and B} = \frac{1}{R_1} + \frac{1}{R_2} = \frac{1}{2000} + \frac{1}{2000} = \frac{1}{1000}$$

$$\text{i.e. } R_{AB} = 1000 \text{ ohms}$$

$$\begin{aligned} \text{Total resistance in circuit} &= (1000 + 4000) \text{ ohms} \\ &= 5000 \text{ ohms} \end{aligned}$$

$$\text{Current flowing through circuit} = \frac{E}{R} = \frac{2}{5000} \text{ amps}$$

$$\begin{aligned} \therefore \text{Current flowing through each arm} &= \frac{1}{5000} \text{ amps} \\ &= 2 \cdot 10^{-4} \text{ amps.} \end{aligned}$$

The potential difference across thermistor with a resistance of 1000 ohms and a current of $2 \cdot 10^{-4}$ amps = $2 \cdot 10^{-4} \cdot 1000$ volts

$$\begin{aligned} \therefore \text{Watts dissipated in thermistor} &= 2 \cdot 10^{-4} \cdot 1000 \cdot 2 \cdot 10^{-4} \text{ watts} \\ &= 0.04 \text{ milliwatts.} \end{aligned}$$

If the ambient temperature is increased to 50°C the resistance of the thermistor drops to 800 ohms and the watts dissipated becomes 0.2 milliwatts.

At both temperatures the dissipation is very small. The dissipation constant was determined by measuring the resistance with a range of battery resistances (from 0 to 8000 ohms) and thus a range of bridge currents, and carrying out the calculation above. Fig.10 shows power dissipation plotted against ΔT . k , the dissipation constant, is found to be 232 degrees per watt. Thus the temperature elevation at 0.04 milliwatt is 0.008° but the effect of small changes in the variable resistance i.e. small temperature changes, is completely negligible.

(b.iii) Calibration of Thermistors.

Measurement of temperature by this method requires an accurate calibration of the thermistors over the temperature

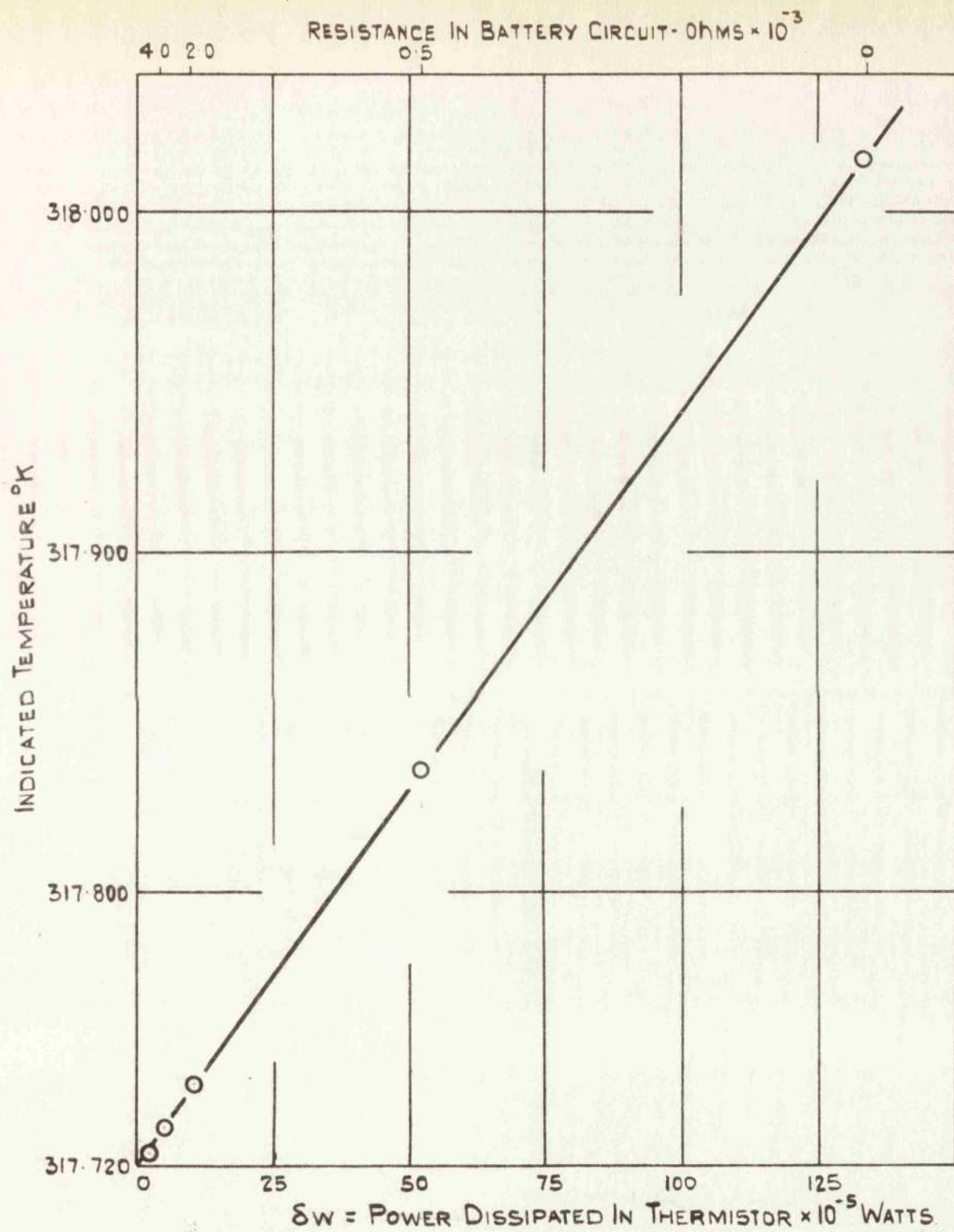


FIG. 10. SHOWING RELATION BETWEEN THERMISTOR BRIDGE CURRENT AND INDICATED TEMPERATURE. LINEAR PLOT OF T/POWER-LOSS AT 45°C GIVES $\Delta T = 232 \times \delta W$. UNDER CONDITIONS OF 100 MLG PER MINUTE FLOW IN APPARATUS.

range considered. Several methods of calibration were tried.

1. The thermistor was placed in a Dewar flask containing stirred water at 50°C. As the temperature dropped the resistance corresponding to various temperatures measured on a 0.1° thermometer were recorded. The plot of $\log R$ against $\frac{1}{T}$ gave a straight line over 30 centigrade degrees with a readable accuracy of 0.02°C. Although not accurate enough - several points were displaced by as much as 0.1 of a degree due it was thought to the insensitivity of the large bulbed thermometer to small temperatures recorded on the thermistor - the method did demonstrate the range of application of the relationship

$$\log R = \frac{B}{T} + \text{constant}$$

2. The thermistor was strapped to the bulb of a 6 degree Beckman thermometer and the arrangement placed in a small water bath which was immersed in the thermostatted bath described above. The water in the flask was agitated with a stirrer and the mouth of the tube packed with cotton wool to reduce heat loss at the surface from evaporation. A telescope focused on the Beckman scale allowed the temperature to be read to $\pm 0.001^\circ\text{C}$ and by varying the temperature of the thermostatted bath the temperature/resistance values were obtained over the range 40°C - 50°C.

The results obtained from this system were still not accurate enough and the ultimate sensitivity of the galvanometer could not be brought into play: each point was associated with an uncertainty of about 0.05° . The deficiencies in the system were:-

- (a) The thermistor fluctuated rapidly over a range of $\pm 0.05^{\circ}$ while the Beckman stayed constant. This was due to micro differences in the temperature of the water which never came to a sufficiently steady temperature throughout. The large Beckman bulb with its slow response smoothed out these temperature eddies. These differences could not be reduced by more vigorous stirring probably because this added to the heat losses at the surface.
 - (b) Temperature control was not adequate. An overall swing upwards of about 0.01° occurred following the "on" period of the heating lamp.
3. The method finally adopted gave adequate accuracy.

The water surrounding the thermistor was replaced by 100 mls of unstirred mercury. A more rapid mixing of heat was thereby obtained and surface evaporation heat losses eliminated. The temperature control in the bath was very much improved by re-designing the heating system. Three stirrers operating at maximum speed gave good circulation. Two were located at

complementary corners of the bath and the third was placed adjacent to the vessel containing the thermistor. Background heat was supplied by two Robertson heating lamps wired in parallel and connected through a Variac adjusted so that the system was just losing heat. A third lamp controlled by a close set toluene regulator and relay switch gave the necessary temperature control. This system when properly settled gave a temperature control of $\pm 0.001^{\circ}\text{C}$ with 1 to 2 second on-off periods. The stoppered vessel containing the thermistor and Beckman thermometer (adjusted for the range $40^{\circ}\text{C} - 45^{\circ}\text{C}$) was immersed in the bath and the system allowed to reach thermal equilibrium at 40°C . The $\pm 0.001^{\circ}$ temperature fluctuations in the bath were recorded sharply on the thermistor and no other fluctuations were manifest. The temperature of the thermostatted bath was increased in 1° steps to 50°C and resistance-temperature measurements carried out as before. From five figure log tables the values of $\log R$ and $\frac{1}{T}$ were calculated and the average values at each degree step determined. The section of the calibration table shown below indicates the constancy with which the thermostatted bath was maintained and the accuracy with which small temperature fluctuations were recorded.

Temp.on Beckman	Resist. ohms	Deflec- tion	Corrected Resistance	Absol. temp.	$\frac{1}{T}$	log R
3.428	906.3	- 2	906.340	318.715	3137598	2.9572787
3.430	906.3	+10	906.229	318.717	3137579	2.9572379
3.432	906.3	+19	906.164	318.719	3137559	2.9572068
3.433	906.3	+24	906.129	318.720	3137550	2.9571900
4.702	872.3	-19	872.418	319.989	3125179	2.9407246
4.700	872.4	- 9	872.456	319.987	3125127	2.9407435
4.700	872.3	-15	872.393	319.987	3125127	2.9407122
4.700	872.3	- 9	872.356	319.987	3125127	2.9406938
4.700	872.4	- 2	872.413	319.987	3125127	2.9407221

The second and third decimal places in the corrected resistance measurements were given by the deflection from absolute balance. A change of 0.1 ohms produced a deflection of 16 mm. The plot of log R against $\frac{1}{T}$ on very large graph paper gave a straight line over the calibration range with a readable accuracy to 0.001°. This calibration was carried out separately for each of the two thermistors used.

(b.iv). Thermistor Arrangement.

A two-thermistor arrangement (Fig.11) was adopted to measure the efficiency changes. The reaction chamber was 12 cm. long by 2 cm. internal diameter with the catalyst bed located at the centre. The thermistors sealed into B.24 and B.19 sockets with polythene, were situated as shown in direct

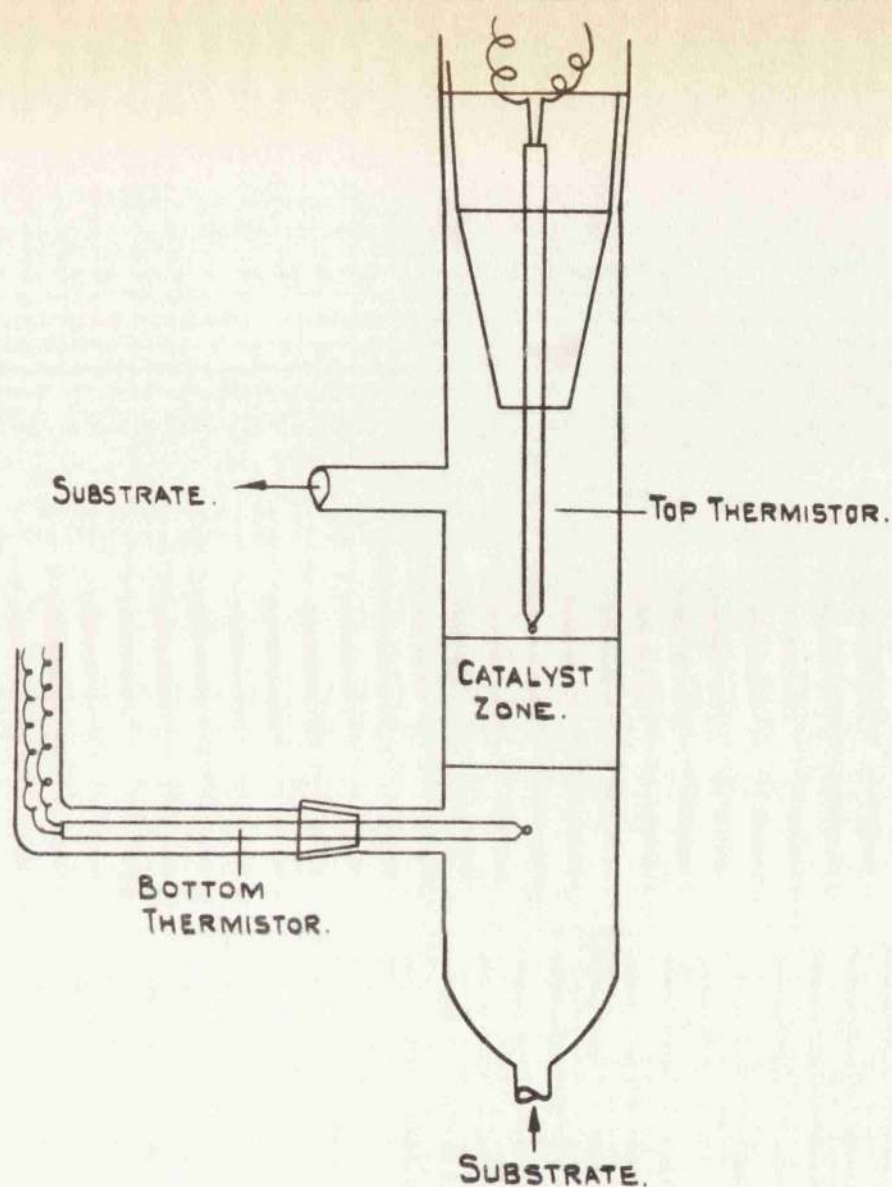


FIG. 11. REACTION CHAMBER WITH A TWO THERMISTOR SYSTEM FOR MEASURING TEMPERATURE DIFFERENCE ACROSS CATALYST BED.

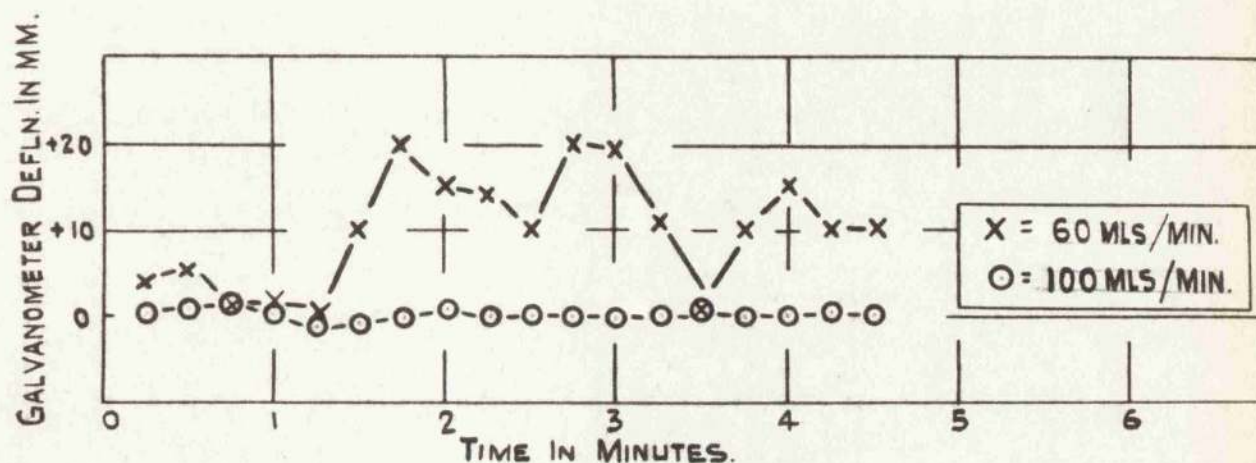


FIG. 12a & 12b. VARIATIONS IN THE RECORDED TEMPERATURE OF THE SUBSTRATE AT DIFFERENT RATES OF FLOW.

line before and immediately after the catalyst bed. Since the reaction chamber was immersed in the bath the leads from the bottom thermistor were encased in a glass sheath.

A two-thermistor system was preferred to a one-thermistor system for several reasons, viz:

1. The one-thermistor system where the element is placed after the catalyst bed assumes that the temperature before the catalyst bed of both H_2O and H_2O_2 streams is the same. This requires that each stream is heated to exactly the same temperature which in fact was not quite achieved.
2. One thermistor does not allow the temperature of the incident stream to be continually checked during decomposition. Temperature difference is therefore based on a pre-decomposition value.
3. It was convenient to have a regular check on the thermistors by comparing them with one another to guard against breakdown of one of them. As mentioned above a variation in the stability of a thermistor need not alter the slope of the calibration line. If therefore thermistors with similar composition are used (i.e. with parallel calibration lines) an alteration in the characteristics of either causes a regular alteration in the temperature differences measured under a given condition. Such checks were carried out regularly. After 18 months a deviation in

resistance had occurred at 45°C and 100 mls a minute flow which amounted to 0.137° expressed as a temperature difference. Since one thermistor read higher and the other lower by approximately the same amount the temperature recorded by each thermistor altered by only 0.068° during that period.

(b.v) Temperature Control of Flowing Substrate.

The temperature control of the flowing substrate was found to vary with rate of flow.

Water at 60 mls/minute was passed through the heating coil and reaction chamber. At thermal equilibrium resistance was established on one of the thermistors and the deflections produced on the scale noted over a considerable period. At this rate of flow the temperature fluctuated with a range of 0.003 degrees (Fig.12a). The fluctuations were decreased ten times when the rate of flow was increased to 100 mls per minute (Fig.12b). Subsequent rate measurements were carried out at this rate of flow since this degree of control was in excess of the temperature differences likely to be measured.

(b.vi) Calibration of Flowmeters.

The flowmeters were calibrated by measuring the volume of water passing through in a given time. The volume was measured at 20°C but the meters were run at room temperature $18^{\circ}\text{C} \pm 2^{\circ}$. The actual volume flow through the catalyst

chamber requires to be adjusted by the density ratio because of the higher temperature in the experiments. This increases the flow at 40°C by 1.0% above the flowmeter indicated volume and by 1.35% at 50°C. The small increase of 0.35% in the flow rate through the bed was allowed for in considering results at the two temperatures. Its effect was in fact unimportant.

(c) Complete Apparatus

The apparatus finally used is shown in Fig.13. The complete assembly was built in Pyrex glass with short sections of polythene tube to give flexibility. Polythene is completely inert to H_2O_2 solutions. The stock of H_2O_2 and H_2O was contained in two 15 litre glass bottles with ground glass stop-cocks. The stock bottles were joined to the nitrogen pump reservoirs by short sections of 7 mm polythene tube welded to the glass to give firm adhesion. The nitrogen pump reservoirs were glass cylinders 1.5 meters high and 3 cm. internal diameter, containing the uptake pipe and link from the nitrogen cylinder. The uptake pipe - a 7 mm. internal diameter pipe with a B.10 joint in the middle - led into the constant level tanks which were supported 2.5 meters above the bench on a Dexion iron frame. The 10 litre constant level tanks were joined to the downtake pipe through a ground glass stop-cock and B.10 joint. The overflow from the overhead tanks led back to the stock bottles. A B.10 joint joined the 5 mm. internal diameter downtake pipe to the liquid

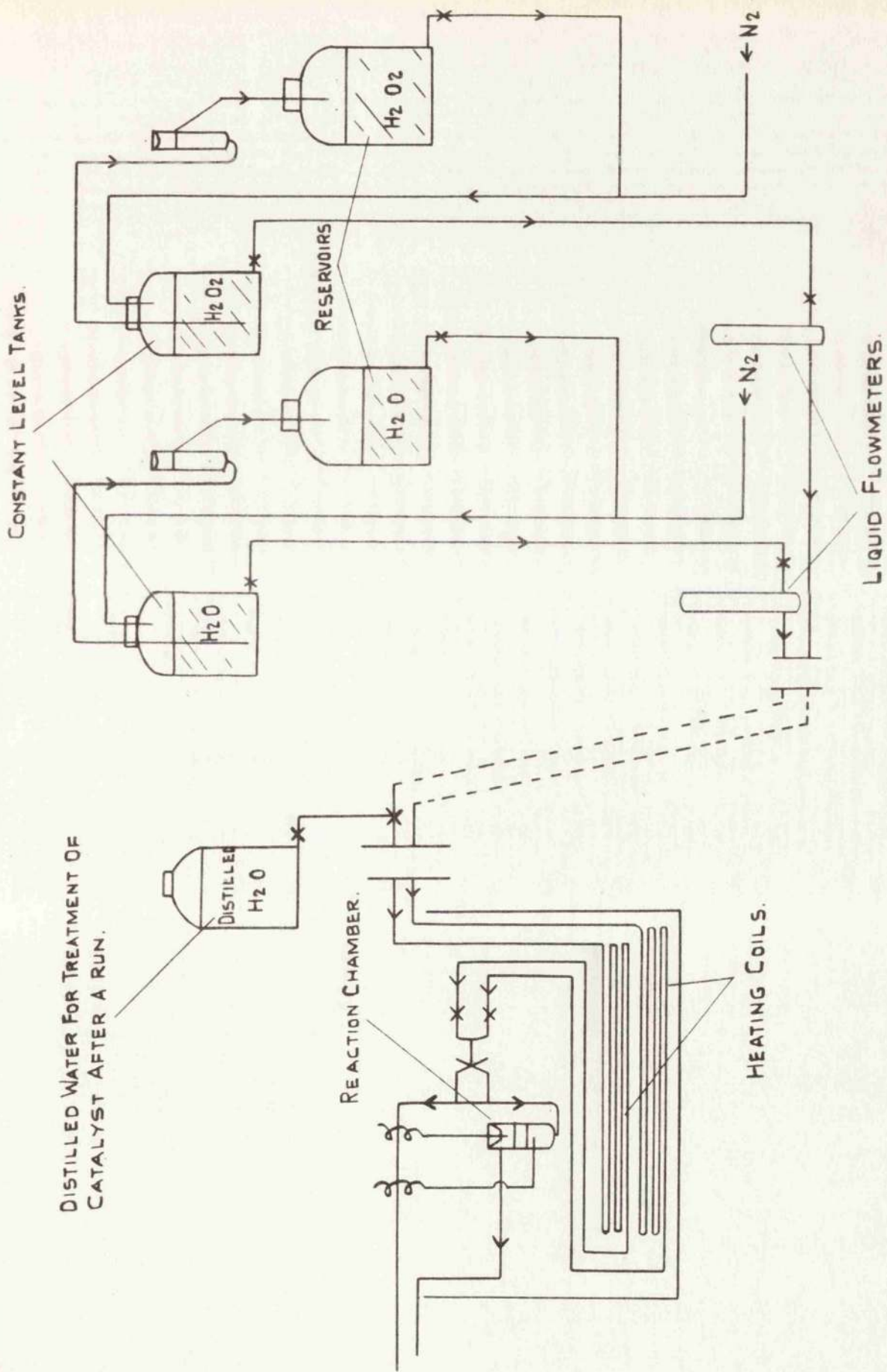


FIG. 13. COMPLETE EFFICIENCY APPARATUS ASSEMBLY.

flowmeters. The sections on either side of the flowmeters were of 5 mm. polythene tube. This gave necessary flexibility at this point and allowed the rate of flow to be controlled by screwclips. The flowmeters were joined to the heating coils by a B.10 cone and socket. On the H_2O line a three-way stop-cock immediately before the heating coil allowed a flow of distilled water to be passed through the reaction chamber at the end of the run. Stop-cocks and joints were entirely free of grease. The heating coils consisted each of 5 meters of 5 mm. internal diameter tube joined to the mixing device by a B.10 cone and socket. The reaction chamber was connected to the mixing device by a B.7 cone and socket.

(d) Experimental Technique.

The apparatus was loaded with H_2O_2 solution and H_2O at the same pH and ionic strength. The rate of circulation was adjusted so that solution could be removed at 100 mls per minute without disturbing the constant level.

H_2O at 100 mls/minute was passed through the reaction chamber and the Variac adjusted to give thermal equilibrium. When this was reached the resistance measurements of both thermistors were noted at regular intervals while H_2O was passing through the system. When the initial temperature difference had been definitely established the H_2O was replaced by H_2O_2 flowing at the same rate. 30 seconds after

the change the resistance variations in the top thermistor were regularly noted at short time intervals. Following the initial rapid efficiency changes the variations become slower and the resistance of each thermistor can be easily recorded. This was continued until a final steady efficiency state was reached. The test was completed by re-passing H_2O to ensure that the catalyst system had returned to its initial state, that the ambient temperature had remained constant and that the thermistors had not undergone any change during reaction.

On completion of the test distilled water was passed through the system for a time to ensure complete removal of reactants adhering to the catalyst surface. The catalyst was allowed to remain in distilled water until the next test.

From this procedure an accurate determination of the variations in temperature difference can be obtained during the whole test except for the period immediately following the change from H_2O to H_2O_2 . Rapid changes occur during this period so that the resistance variations of only one thermistor can be successfully followed. Several manual methods were tried unsuccessfully to improve the measurement of temperature difference during this important period. For example a three-position switch was incorporated into the system so that either element could be quickly brought into the circuit.

Consideration of the temperature differences involved however indicated how this could be successfully accomplished. When H_2O is passing through the system the temperature of both thermistors remains constant and the resistances of the thermistors can be individually measured. Ideally replacement of the H_2O by dilute H_2O_2 under the same conditions should not affect the temperature of the bottom thermistor so that attention can be concentrated at first on the top element and the temperature differences calculated from an assumed constant initial temperature.

In the present apparatus this condition was complicated since individual heating coils were used. As a result the initial H_2O_2 entering the reaction chamber was at a slightly higher temperature than the subsequent solution, since a volume equal to the volume of the H_2O_2 heating coil remained static in the heating bath during the passage of H_2O . In addition the length of the H_2O_2 coil was shorter than the H_2O coil so that the temperature of the H_2O_2 stream was slightly below that of the H_2O . The temperature differences taking place in the bottom thermistor, following the change H_2O to H_2O_2 , should therefore involve a small drop preceded by a slight rise.

Experiment verified this completely (Fig. 14) giving excellent reproducibility and it was justifiable to assume that this pattern occurred in all runs so that immediately following the change H_2O to H_2O_2 attention could be focused

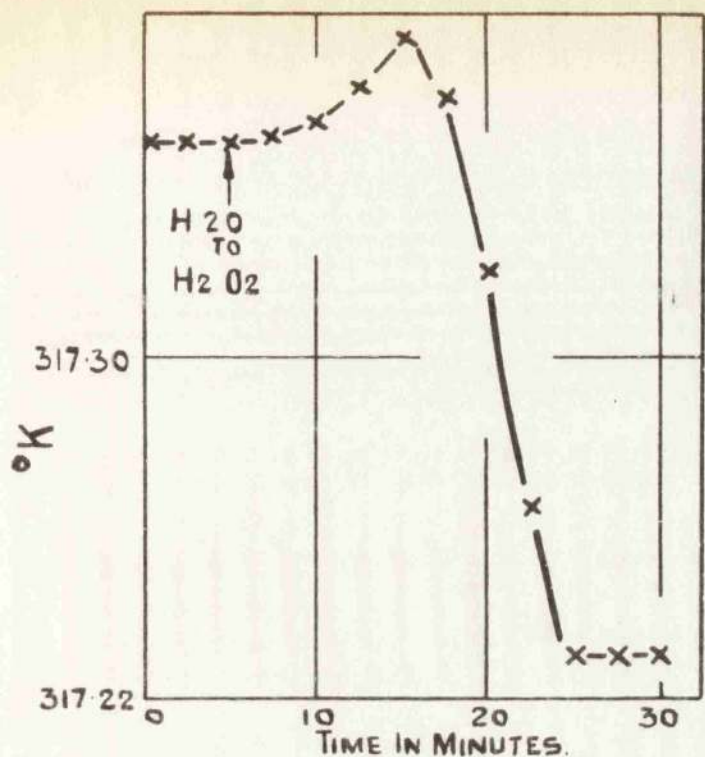


FIG. 14. SHOWING THE SYSTEMATIC TEMPERATURE CHANGES RECORDED BY THE BOTTOM THERMISTOR FOLLOWING THE CHANGE H₂O TO H₂O₂

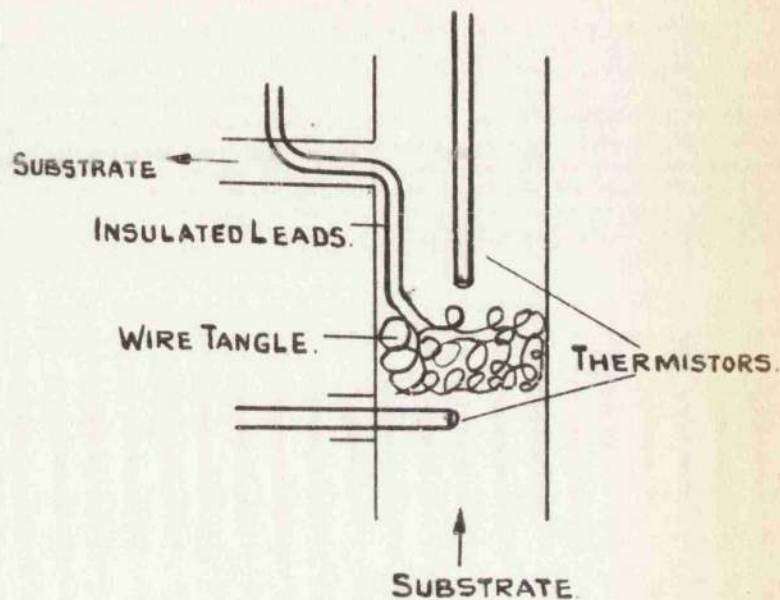


FIG. 15 REACTION CHAMBER ASSEMBLY FOR VERIFICATION OF ADIABATIC BEHAVIOUR IN REACTION CHAMBER.

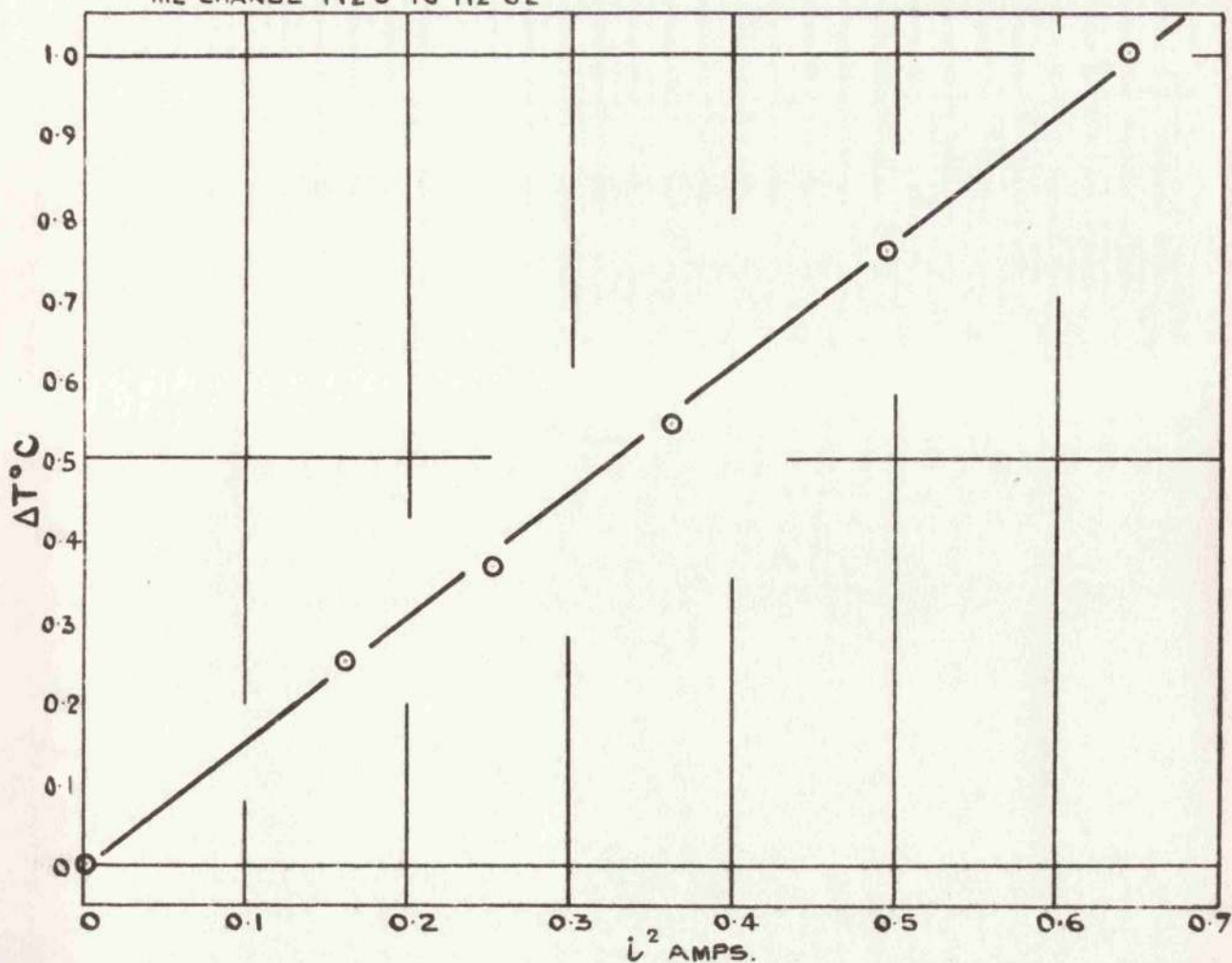


FIG. 16. PLOT OF $\Delta T/i^2$ WHERE ΔT IS TEMPERATURE INCREASE CAUSED BY i AMPS AT FLOW RATE OF 93.7 MLS/MINUTE. SLOPE = $1.541/i^2$

on the top thermistor and the subsequent temperature measurements corrected using the temperature fluctuation curve of the bottom thermistor.

As a result the temperature differences during this important initial period were accurately determined giving complete coverage of the whole reaction period without recourse to electrical recording methods which would have seriously complicated the technique.

(e) Initial Trial of Efficiency Apparatus.

The first test run on the apparatus was made with a silver wire catalyst which was chosen to be free from slow changes with time. The results showed very well the degree of reproducibility achieved. The two runs were carried out on successive days the catalyst being stored in water overnight. The temperature rise on each run was the same $0.675 \pm 0.001^{\circ}$ each being constant within the indicated range for a period of 25 minutes measurement. Data for the tests are $[H_2O_2] = 0.36$ M, temperature = $45^{\circ}C$, ionic strength = 0.001 and flow = 100 mls/minute. These figures demonstrate that changes of efficiency of the order of 1% of that measured could be detected with certainty and precision.

(f) Experimental Verification of Adiabatic Behaviour
in Reaction Chamber.

The validity of the assumption that the temperature rise indicated by the thermistors was a measure of the heat release in the catalyst zone - and hence the amount of reaction - was tested in the following experiment.

In place of the catalyst a tangle of 46 gauge insulated constantin resistance wire (of total resistance 10 ohms) was placed in the reaction chamber. The ends of the wire were soldered to 25 gauge insulated copper wire, the soldered connection being insulated by an adherent coating of wax. The wire leads were brought out of the side arm (Fig.15) and passed through a 40 ohm rheostat and a substandard Sangamo-Weston ammeter to an 18 volt battery. The rheostat could be adjusted to give a range of current up to 1 amp which was calculated as sufficient to dissipate heat in the resistance wire to raise the temperature of the flow of 100 mls per minute by about 1.5°C .

The experiment was carried out by first bringing the apparatus to equilibrium at 45°C . The resistance of the top thermistor was read first with no current in the resistance wire and then with 0.4 to 0.8 amps in 0.1 amp steps. Very steady and reproducible thermistor resistances were obtained at each current setting. Over the range of one degree in temperature rise the graph of ΔT against i^2 ,

where i is the current in amps, was perfectly linear, passing through the origin with a slope almost equal to the theoretical value. Fig.16 shows the line - slope = $1.546 \times i^2$ degrees for a given current i - for a flow of 93.7 mls/minute. The theoretical slope was calculated as follows:-

$$\begin{aligned} \left. \begin{array}{l} \text{Energy dissipated/sec. in} \\ \text{the 10.0 ohm resistance} \end{array} \right\} &= 10.0 \cdot i^2 \text{ joules} \\ &= \frac{10.0 \times i^2}{4.18} \text{ cal.} \\ \text{Flow of water/sec.} &= \frac{93.7}{60} \text{ mls} = \frac{93.7 \times 0.992}{60} \text{ gms.} \\ \text{Temperature rise } \Delta T &= \frac{10.0 \times 60}{4.18 \times 93.7 \times 0.992 \times 0.998} i^2 \\ &= 1.541 \times i^2 \text{ degrees} \end{aligned}$$

where the specific gravity of water at 45°C is 0.992 and the specific heat is 0.998.

The experimental figure of $1.546 \times i^2$ degrees lies very close to the theoretical value. The greatest source of error was the flow where ± 0.5 is all that can be claimed. Another systematic uncertainty in this test experiment was the arrangement of the resistance wire. In earlier tests temperatures above and below the theoretical were obtained because, it was thought, the wire was bunched unevenly. Only when a very uniform spread was achieved was the above result obtained.

During the test the resistance of the bottom thermistor, which was checked at each current setting, remained fairly constant showing that there was no leak back of heat from the decomposition zone.

3. Potential Apparatus and Experimental Technique.

(a) Apparatus.

The apparatus for measurement of electrode potentials of Cu_2O in presence of H_2O_2 under the conditions of catalysis is shown in Fig.17.

As in the efficiency apparatus H_2O_2 and H_2O were contained in flasks F_1 and F_2 . The respective solutions were drawn through the system by a water vacuum pump connected to a side arm on the catalyst chamber, and a three-way stop-cock allowed either solution to be individually selected.

The catalyst chamber (insert, Fig.17) was 15 cm long and 1 cm. internal diameter with a B.19 socket at the top. The vacuum pump was attached to a side arm at the top of the chamber and an internal seal electrically connected the substrate passing through the chamber to a reference electrode. The catalyst in the form of wire was sealed with polythene into an extended B.19 cone so that the tip of the internal seal was adjacent to the catalyst surface.

The potential was measured on a Muirhead potentiometer type D-72-A used in conjunction with a Cambridge spot galvanometer. All potentials were measured against a saturated calomel electrode connected to the catalyst chamber by a sodium perchlorate salt bridge.

The catalyst chamber and solution reservoirs were constructed in Pyrex glass and immersed along with the

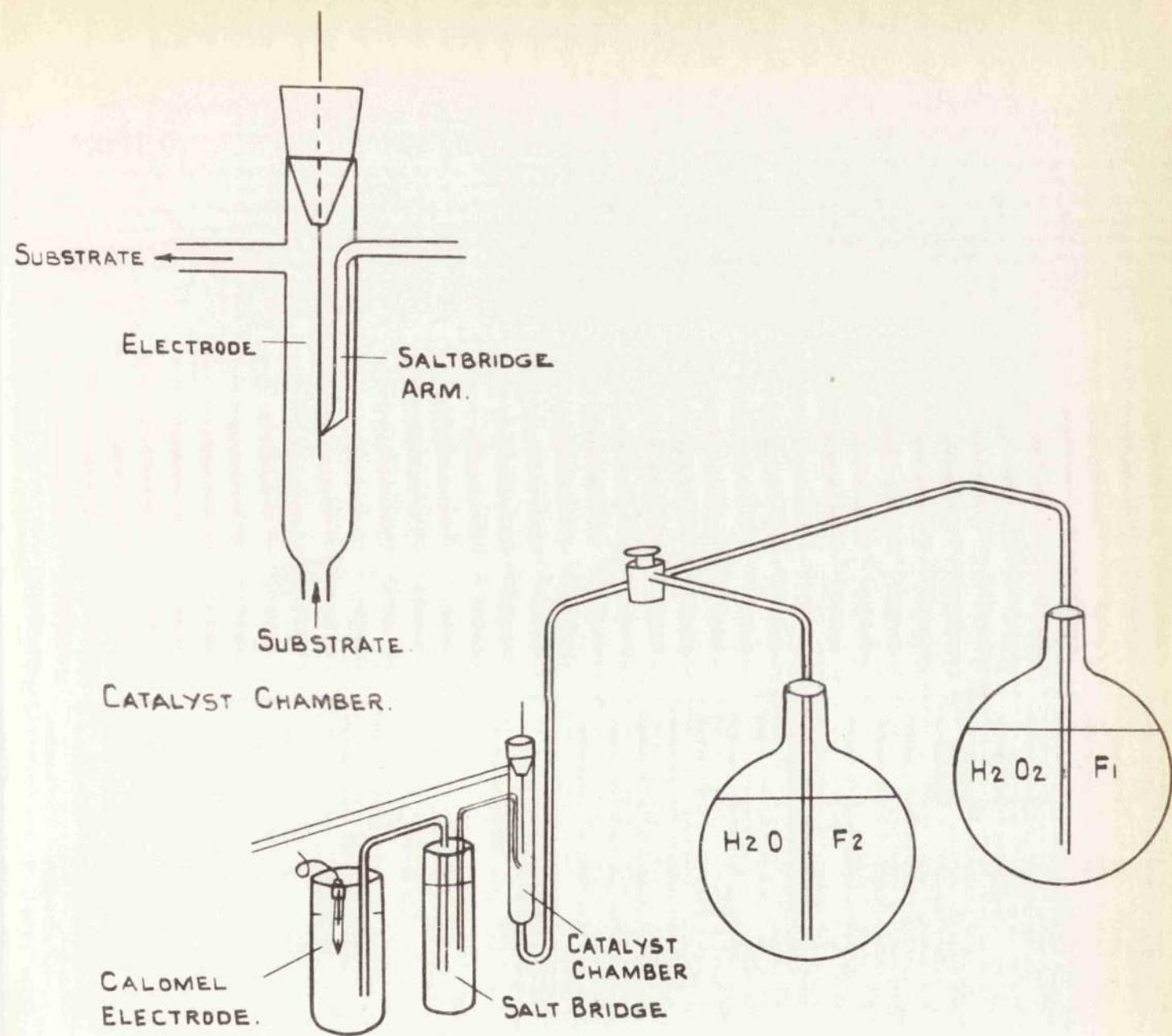


FIG. 17. APPARATUS FOR MEASUREMENT OF ELECTRODE POTENTIALS
 OF Cu_2O IN H_2O AND H_2O_2 UNDER CONDITIONS
 SIMILAR TO KINETIC INVESTIGATIONS.

reference electrode in a thermostatically controlled water bath at 45°C.

(b) Experimental Technique.

The catalyst under examination was placed in position and the assembly allowed to reach thermal equilibrium at the reaction temperature. The salt bridge was checked for air gaps and the potentiometer balanced against a standard Weston cell.

With the three-way stop-cock connected to F₂ water was drawn through the system and the equilibrium potential determined at regular intervals. When a constant potential was reached the stop-cock was connected to F₁ and H₂O₂ drawn through the catalyst chamber. Immediately the change was effected potential measurements were taken until a steady potential had again been attained.

The test was completed by a return to initial conditions.

4. Cleaning of Apparatus.

It was important to avoid the use of chromic acid cleaning mixtures which are known to leave the glass slightly catalytically active.

The method adopted consisted of first rinsing the section with concentrated analar H₂SO₄ and washing thoroughly with water. This effectively removed any grease adhering to

the glass. It was next rinsed with EtOH and a few mls of concentrated analar HNO_3 were added. The resulting vigorous reaction liberated hot nitrous fumes which were allowed to permeate the system. The section was finally washed thoroughly in distilled water.

Glass surfaces thus treated showed no activity to H_2O_2 at 50°C as evidenced by complete absence of bubbles even after some hours standing.

5. Surface Area Apparatus and Measurement Technique.

(a) Apparatus.

The apparatus used (Fig.18) was a modified version of that proposed for ethylene adsorption at -183°C by Duncan⁸⁰ and Wooten and Callaway-Brown⁸¹. The mercury seals used by the above workers were replaced for convenience by vacuum stopcocks and a series of three expansion volumes were introduced. The use of stop-cock grease introduced no difficulties in the range of measurements made and greatly facilitated the procedure.

The apparatus was evacuated by a rotary backed mercury diffusion pump attached to the vacuum manifold through two liquid air traps. The total volume of the apparatus was 2,100 c.c. and it was pumped out for several days with flaming until a pressure of $8.2 \cdot 10^{-6}$ mm. Hg increased to only $7.9 \cdot 10^{-5}$ mm. Hg in 60 hours. Such a small leakage would not interfere with any surface area measurements.

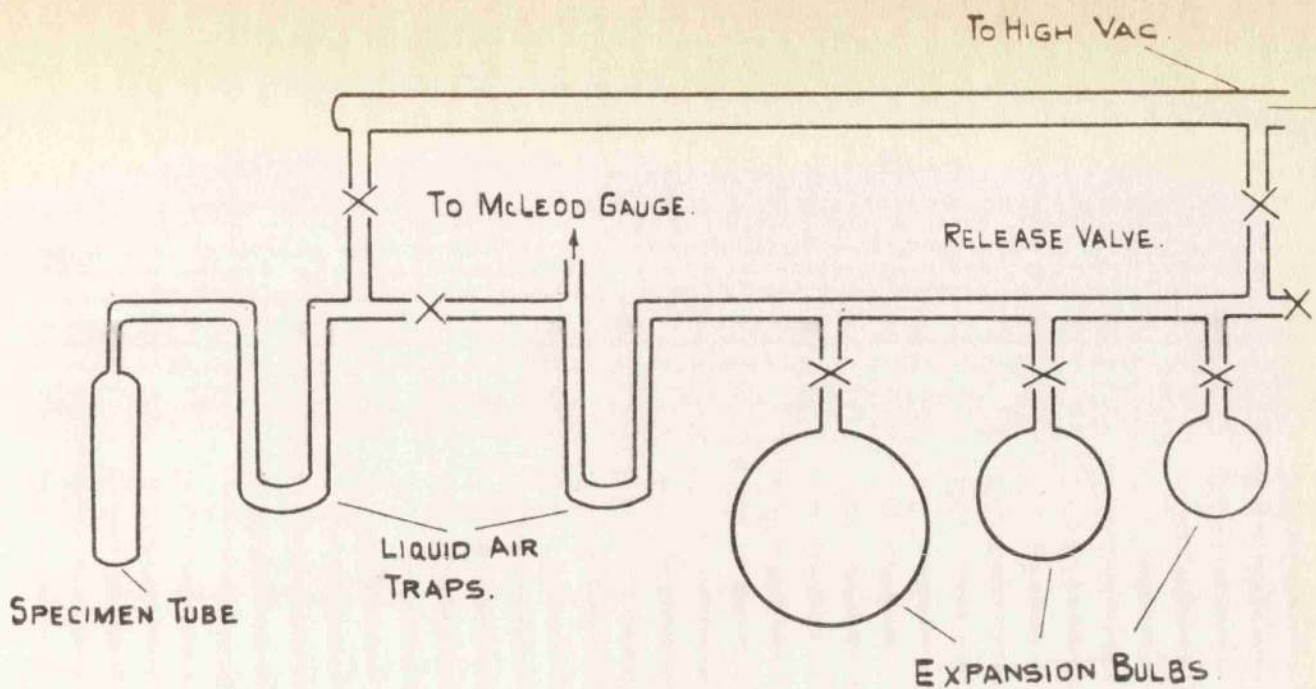


FIG. 18. SURFACE AREA DETERMINATION APPARATUS.

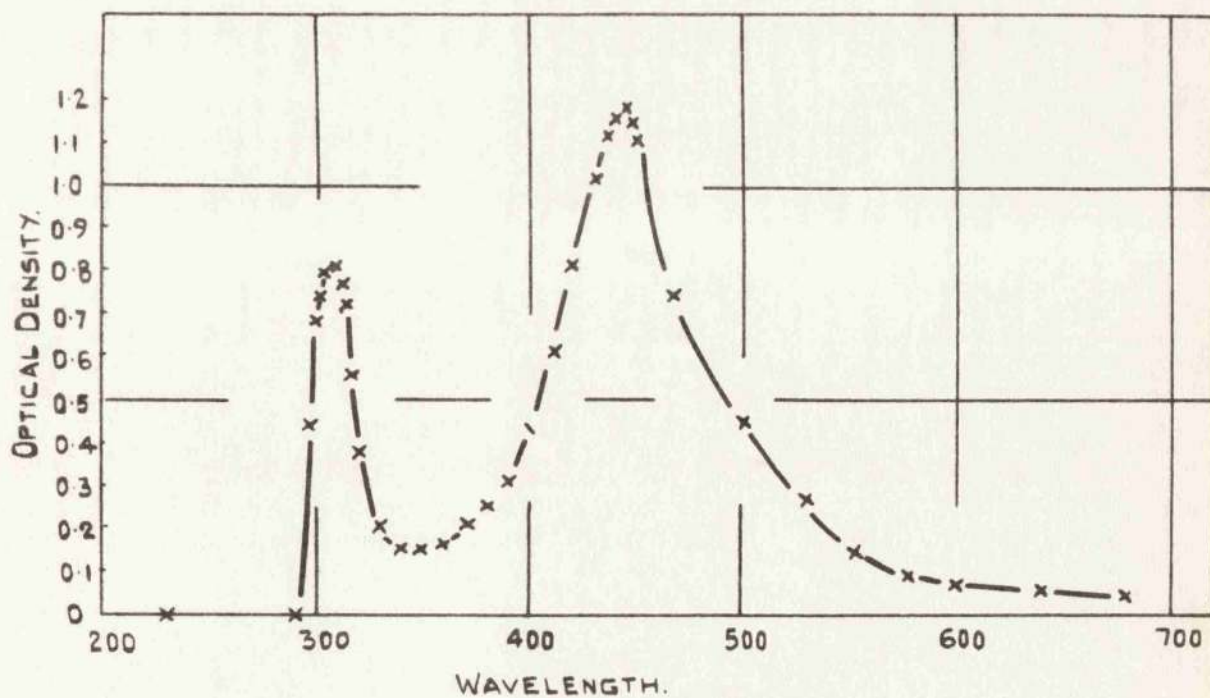


FIG. 19. ABSORPTION CURVE FOR STANDARD Cu^{++} SOLUTION.

The volumes of the various parts of the apparatus were calibrated with dry air (the cold traps being in place) against that of the McLeod gauge bulb used as a gas pipette. The McLeod bulb volume had been calibrated with mercury previous to construction.

(b) Experimental Technique.

When a sufficient vacuum was obtained and held the expansion bulbs were closed to the manifold. A 500 mls flask containing ethylene (99% purity kept dry over P_2O_5) was connected to the manifold via the release tube. The C_2H_4 was allowed into the system and three times successively evaporated, condensed with liquid O_2 and pumped off using the two U-tubes as alternate condensation traps to further ensure purity. Finally the middle fraction was admitted to the larger expansion bulb which was used as a storage vessel. This was then closed to the manifold and the system again pumped out.

With the specimen tube isolated liquid O_2 was placed round the specimen tube and the protective U-tube, to a carefully adjusted height - the same as during calibration. A little C_2H_4 was allowed into the system (giving a pressure of not more than 0.025 mm. i.e. insufficient to reach the condensation pressure when admitted to the specimen) and the pressure measured on the McLeod gauge by a cathetometer reading to 0.001 mm. The specimen tube was then connected

with the system and the pressure measured at regular intervals until the equilibrium pressure was reached. This procedure was repeated several times until the equilibrium pressure was approximately $1.0 \cdot 10^{-2}$ mm. Hg.

The reading of the McLeod gauge was carried out by bringing the mercury meniscus in the capillary arm parallel to the enclosed limb to a position near the top of the closed capillary. The length of the trapped gas space and the height of the open limb mercury above the meniscus in the closed limb were both read accurately with the cathetometer i.e. h_1 and h_2 . For each reading the level was adjusted to give independent sets of heights. The pressure was then calculated from the equation

$$P = \left(\frac{h_1 \times h_2}{2} \right)^2 \times 6.342 \times 10^{-6} \text{ mm.}$$

which had previously been determined from the dimensions of the McLeod bulb and capillary.

6. Spectrophotometric Determination of Rate of Solution of Copper during Catalysis.

(a) General Considerations.

Dissolution of the catalyst accompanies, under certain conditions, H_2O_2 solution phase catalysis. Under flow conditions this does not affect the composition of the solution but it is important that the relation between dissolution and

catalysis be known. A spectrophotometric method was therefore developed for the determination of the micro amounts of copper in the solution leaving the catalyst chamber using sodium diethyldithiocarbamate (NaDDC) which forms a yellow compound with Cu^{++} .

NaDDC dissolves readily in water giving a colourless alkaline solution. This solution decomposes on keeping and for accurate results a freshly prepared 0.1% solution is recommended⁸². The colour complex is formed in acid, neutral or alkaline conditions but is best formed at pH 9 where it is sensitive to 1 part of Cu^{++} in 50 million.

Two methods can be used for the determination of the intensity of the complex i.e.

1. Extraction four times with CCl_4 ⁸³
2. Direct estimation.

Extraction with CCl_4 is the more accurate method and is usually used in the presence of interfering elements. The adsorption curve has maxima at 436, 294 and 272 m/ μ but 436 m/ μ is always chosen for analytical purposes⁸⁴ since interfering effects are at a minimum at this wavelength.

In the absence of interfering ions the direct estimation although less accurate is quicker and less laborious. As shown by Moseley, Rohwer and Moore⁸⁵ clear aqueous solutions may be obtained for such determinations by the addition of a protective colloid which prevents coagulation of the

complex molecules.

As no interfering metal ions were expected the direct method was adopted. The intensity of the colour complex was measured on a Unicam Spectrophotometer S.P.600 which gives accurate colorimetric measurements within the visible and near infra-red regions.

The adsorption of monochromatic plane polarised light in an isotropic medium is given by

1. Lambert's Law

$$- \frac{dI}{dx} \propto I$$

where I is the intensity of the light beam and x is the distance traversed by the light through the solution

2. Beer's Law

$$- \frac{dI}{dc} \propto I$$

where c is the concentration of the adsorbing material.

In the integrated form these two laws can be combined to give light transmitted through distance d = $e^{-\epsilon'cd} = 10^{-\epsilon cd}$ / incident light

where d is distance in cms., c is the concentration in gm. molecules per litre and ϵ is the molar extinction coefficient. The quantity ($\epsilon \cdot c \cdot d$) i.e.

$$\log_{10} \frac{\text{light incident}}{\text{light transmitted}}$$

is called the optical density and is the quantity measured on the spectrophotometer.

If the above treatment applies then optical density in a cell of given length should be linearly dependent on c the concentration. This was first tested.

Three solutions were prepared, viz.,

1. a series of copper solutions containing known amounts of Cu^{++} by dissolving approximately 0.12 gm. of pure CuO in a little concentrated HCl , making up to 250 mls and diluting this tenfold to give a solution containing approximately 0.04 gm. per litre of Cu^{++} ,
2. a 0.1% solution of NaDDC ,
3. a 1% solution of gum acacia prepared according to the method suggested by Zinzade⁸⁵ in which the gum is dissolved in distilled water at 50°C .

The solutions prepared for analysis contained

- (i) 10 mls of Cu^{++} solution
- (ii) 5 mls gum acacia solution
- (iii) 5 mls NaDDC solution
- (iv) NH_4OH until pH was approximately 9 (using a test paper)
- (v) H_2O to make total volume up to 50 mls.

and the analysis was carried out in 1 cm. cells at a wavelength of $443 \text{ m}\mu$ against blank solutions of gum acacia,

NaDDC and ammonia. This wavelength was chosen since examination of a standard Cu^{++} solution over the range 200 m μ to 900 m μ (Fig.19) showed maximum adsorption at 443 m μ .

The results obtained (Table 1) showed strict linearity

Solution	Copper present per 50 mls	Optical Density
1	$0.377 \cdot 10^{-3}$ gms	1.06
2	$0.189 \cdot 10^{-3}$ gms	0.536
3	$0.094 \cdot 10^{-3}$ gms	0.257
4	$0.047 \cdot 10^{-3}$ gms	0.123
5	$0.024 \cdot 10^{-3}$ gms	0.051

Table 1. Optical density figures for a series of Cu^{++} solutions. The results show that optical density varies linearly with $[\text{Cu}^{++}]$.

for the relationship between optical density and concentration and the resulting line was used as a calibration curve. It was found that pH did affect the optical density but this effect was not critical and the rough adjustment to pH 9 was adequate to secure reproducibility.

(b) Preparation of Solutions for Analysis

A series of tests on this subject were carried out and several important conclusions derived from the results (Table 2.). These conclusions are:-

(i) Comparison of tests 1 and 2 show that the presence of

Test	Test solution	Optical density using as a blank	Optical density using as a blank
1.	a) 10mls standard Cu^{++} solution b) 5mls gum acacia c) NH_4OH d) 5mls NaDDC e) H_2O up to 50mls	a) b) 5mls gum acacia c) NH_4OH d) 5mls NaDDC e) H_2O up to 50mls 1.1	a) 10mls 2M H_2O_2 , pH=4.5, $\mu=0.001$ b) 5mls gum acacia c) NH_4OH d) 5mls NaDDC e) H_2O up to 50mls 1.1
2.	a) 10mls standard Cu^{++} solution b) 10mls 2M H_2O_2 , pH=4.5, $\mu=0.001$ c) 5 mls gum acacia d) NH_4OH e) 5 mls NaDDC f) H_2O up to 50mls	0.975	0.98
3.	a) 10mls standard Cu^{++} solution b) conc.HCl evaporate to dryness and take up in dilute HCl c) 5mls gum acacia d) NH_4OH e) 5mls NaDDC f) H_2O up to 50mls	1.1	1.1
4.	a) 10mls standard Cu^{++} solution b) 10mls 2M H_2O_2 , pH=4.5, $\mu=0.001$ c) conc.HCl evaporate to dryness and take up in dilute HCl d) 5mls gum acacia e) NH_4OH f) 5mls NaDDC g) H_2O up to 50mls	1.09	1.09

Table 2.

H_2O_2 prevents the full development of the complex. Although this effect is small at the test $[Cu^{++}]$ it became appreciable in the smaller $[Cu^{++}]$ range expected from catalysis. It was therefore necessary to remove H_2O_2 before testing for Cu^{++} .

(ii) The most successful method for the complete removal of H_2O_2 from the Cu^{++} containing substrate consisted of evaporating the solution to dryness. The method was as follows:-

- (a) A little concentrated HCl was added to the Cu^{++} containing H_2O_2 solution to convert the Cu^{++} to soluble chloride.
- (b) The solution was evaporated to dryness in a Pyrex beaker on a water bath and the residue taken up in a little dilute HCl.
- (c) Gum acacia, NaDDC and NH_4OH were added as in the calibration method and the solution made up to 50 mls.

Comparison of Test 3 with Test 1 shows that the evaporation procedure gives an accurate estimation of Cu^{++} present and Tests 3 and 4 show that the H_2O_2 is completely removed by this procedure giving reproducible results.

(iii) H_2O_2 has no effect on the adsorption of Cu^{++} free solutions which are used for blanks. There was of

course no reason to include H_2O_2 in the blank when following out the procedure of Test 4 which was the one adopted.

7. Polarographic Detection of Stannate in H_2O_2 .

The H_2O_2 used in the kinetic experiments was prepared from 86% w/w material. This material can be stabilised by the addition of small quantities of sodium stannate which when present as colloidal particles adsorbs foreign metal ions.

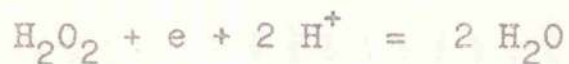
The exact effect of sodium stannate on a catalytic system is not precisely known but it does reduce the activity of the catalyst. This is probably due to the formation of adsorbed stannates on the surface of the catalyst. As a result the H_2O_2 used for kinetic measurements must be free from parts per million of sodium stannate. Although the H_2O_2 used for the present investigations was supplied as unstabilised, it was considered necessary to test each consignment for traces of tin as this was the only impurity which could as a result of an error in consignment appear in the material supplied.

For the polarographic estimation of Sn in H_2O_2 three points were considered viz.,

1. Complete destruction of H_2O_2
2. Composition of suitable supporting electrolyte

3. Preparation of standard Sn solution.

1. Complete destruction of H_2O_2 is essential in polarographic work since at -1.3 v. a rapid increase in potential occurs due to the reduction of H_2O_2 according to the equation



as suggested by Heyrovsky⁸⁷. The method adopted was similar to that employed in the determination of Cu^{++} i.e. the H_2O_2 containing solution was evaporated to dryness and made up to a standard volume.

2. Although the standard potential of the $\text{Sn}^{++++}/\text{Sn}^{++}$ ion couple is -0.1 v. vs. the standard calomel, the Sn^{++++} ion is not easily reduced at the dropping mercury electrode because of its tendency to complex. These complexes are either too stable or are reduced too slowly to permit the occurrence of a wave.

According to Lingane⁸⁸ such complexing takes place in electrolytes such as NaOH, acid neutral or basic tartrate, and in acidic oxalate. Previous experiments by Lingane⁸⁹ showed that a poorly developed wave could be obtained from tin solutions supported by 1 M perchloric acid containing 0.5M NaCl. Since no wave was detected in solutions containing only perchloric acid Lingane suggested that the hexaqua-stannic ions formed in chloride free solutions were replaced by a mixed aquachloro complex e.g. $\text{Sn}(\text{H}_2\text{O})_4\text{Cl}^{+++}$ whose rate

of reduction was faster than that of the hexaquastannic ion. As the concentration of the Cl^- ion was increased from 0.2 M, Lingane⁹⁰ showed that the reduction wave increased in height until at 4 M a well developed doublet of constant height was obtained i.e. the progressive conversion of the hexaqua complex into a series of chloro complexes culminating in SnCl_6^{4-} . Since the height of the first wave of the doublet at chloride concentrations above 4 M was $\frac{1}{2}$ of the total height, the first stage was identified as Sn^{++++} to Sn^{++} followed by Sn^{++} to Sn.

A tin solution containing 4.28 p.p.m. Sn was therefore prepared in a solution containing 4 M NH_4Cl , 1 M HCl and 0.005% gum acacia. From this solution the reduction steps Sn^{++++} to Sn^{++} at half-wave potential of -4.6v vs Hg electrode and Sn^{++} to Sn at half-wave potential of -2.5v vs Hg electrode were easily detected (polarogram 1 Fig.20) and showed no deterioration with time. In addition an H_2O_2 solution containing the same amount of Sn (present as sodium stannate) was subject to the decomposition technique and made up to a standard solution as above. Polarograms from this solution (2, Fig.20) demonstrated that the decomposition technique allowed an accurate estimation of the Sn present since the height of the individual steps in polarograms 1 and 2 were equal.

3. For a quantitative estimation of tin, standard Sn^{++++}

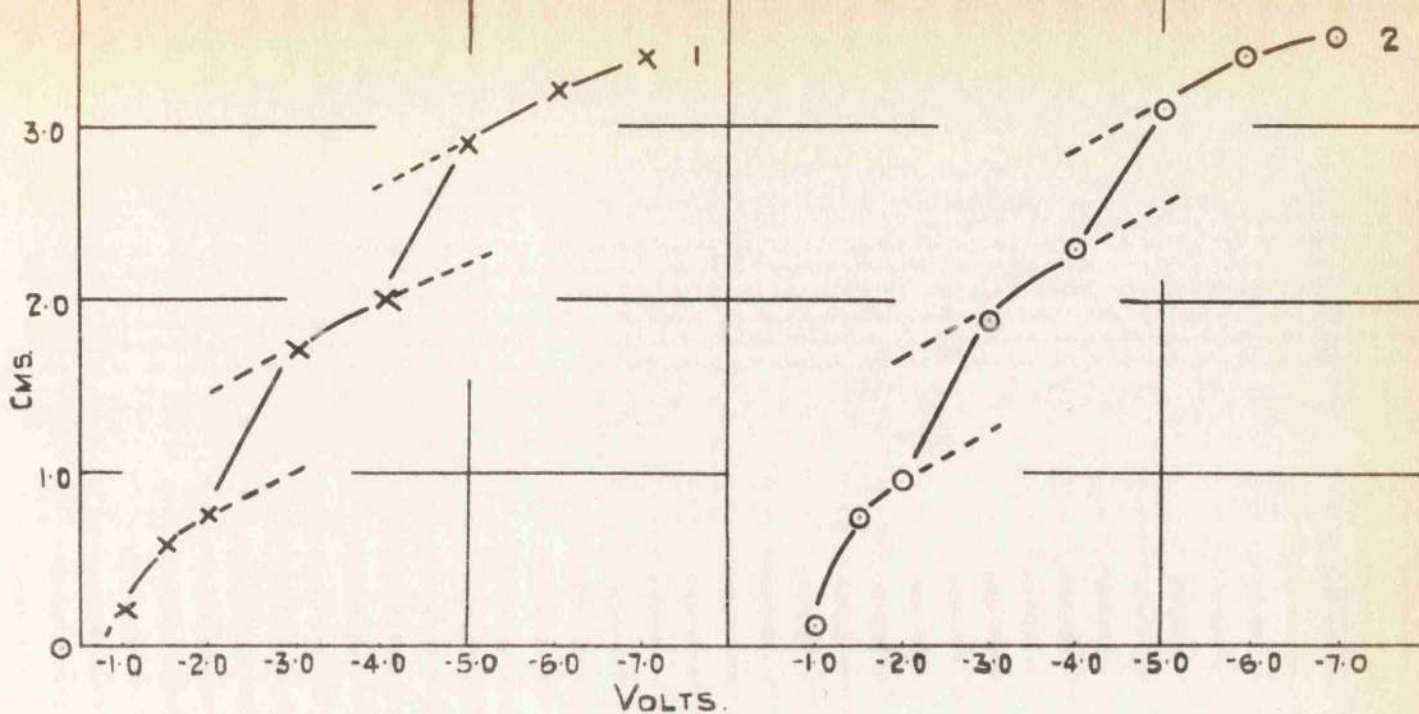


FIG. 20. SHOWING POLAROGRAMS OBTAINED FROM A STANDARD Sn^{+++} SOLUTION (1) AND AN H_2O_2 SOLUTION CONTAINING THE SAME AMOUNT OF Sn^{+++} WHICH HAS BEEN SUBJECT TO THE H_2O_2 DESTRUCTION PROCEDURE (2).

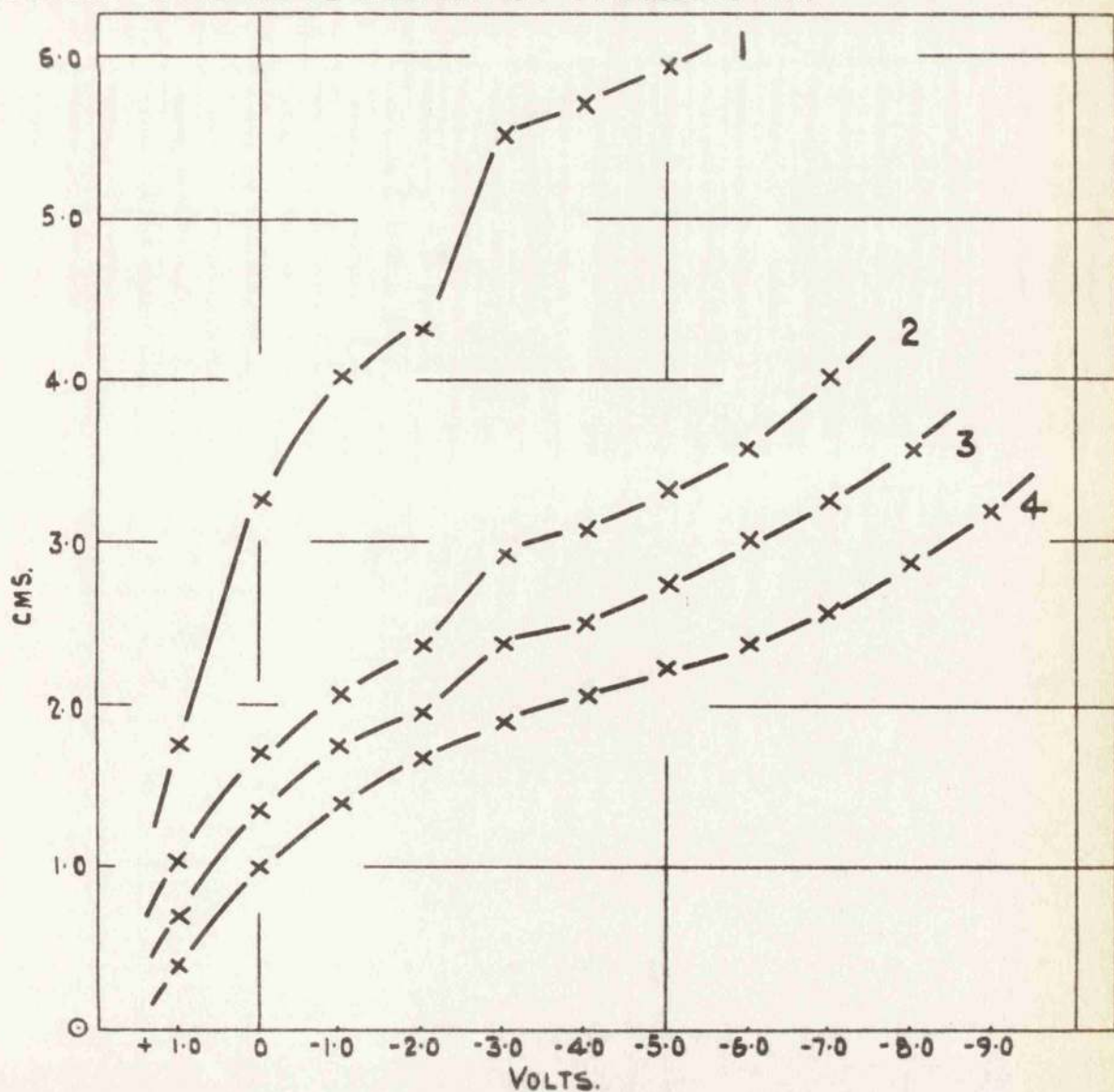


FIG. 21. POLAROGRAMS OBTAINED FROM A STANDARD Sn^{++} SOLUTION SHOWING DECAY OF STEP DUE TO HYDROLYSIS 1 TO 4.

solutions are recommended for calibration rather than Sn^{++} solutions. Polarograms 1,2,3 and 4 Fig.21 show a progressive decrease in the Sn^{++} to Sn step depending on the age of the prepared Sn^{++} solution. It is probable that the Sn^{++} ion is hydrolysed on standing forming a compound which is too stable to be reduced at the dropping mercury electrode.

Applying the procedures detailed above each peroxide solution used for kinetic measurements was tested for the presence of tin. In all cases no tin above approximately 0.1 p.p.m. was detected. This figure represents the ultimate sensitivity of the available polarograph since 4.28 p.p.m. Sn gave a Sn^{++++} to Sn^{++} step of 3.5 cm. at maximum sensitivity.

M A T E R I A L S

1. Hydrogen Peroxide.

The peroxide solutions used were prepared by dilution of 86% w/w high test peroxide obtained pure from Laporte Chemicals Ltd. in one gallon polythene containers in which the material was kept until required. As reported above each consignment was carefully tested for accidental contamination by stannate the commercial stabiliser and a serious inhibitor in catalysed reactions. The concentration of the diluted solutions was estimated by titrating against standard potassium permanganate, and alterations in the pH were made by the addition of standard sodium hydroxide and perchloric acid solutions prepared from analytical grade reagents. The ionic strength of the H_2O_2 solutions and other solutions used were adjusted with sodium perchlorate. Since this reagent could not be obtained analytically pure, several crystallisations were carried out until the main impurity - chloride - had been removed.

2. Catalysts.

(a) Cuprous oxide

The cuprous oxide used for the catalytic decomposition of H_2O_2 was obtained by partially oxidising copper wire. A rigid adherent layer suitable for use under liquid flow conditions was thereby obtained.

Many early conflicting views were expressed on the composition of the oxide film formed by low temperature oxidation (200°C) before agreement was reached. In 1922 Niggli⁹¹ recognised the cubic form of the cuprous system from the diffraction pattern produced from such an oxidised copper foil. A year later Hinshelwood⁹² and Constable⁹³ suggested that the oxide formed in tinted films between 200°C and 300°C were entirely cupric oxide. In 1930 G.P. Thomson⁹⁴ examined the electron diffraction patterns produced from copper and oxidised copper. No rings were observed from a highly polished surface. If the specimen was left in air at atmospheric pressure for about an hour faint rings could be detected which if left for 24 hours under the same conditions became measurable although still blurred. The intensity and clarity of the rings were greatly improved if the specimen was heated gently in an electric furnace until the copper underwent a considerable change in colour. The size of the rings produced from such an oxide were in the ratio $\sqrt{2.99} : \sqrt{4.09} : \sqrt{11.0} : \sqrt{18.8}$ which suggested a face centred cubic structure of side 4.21 Å. This value was in agreement with those previously suggested for the dimensions of the cuprous oxide lattice. When the polished blocks were heated on red hot brass and allowed to cool in air the diffraction pattern indicated an oxide of unknown structure. Later Murison⁹⁵ identified the oxide as a mixture of cuprous and cupric oxide and showed that if a specimen was heated between 300°C and 500°C either Cu₂O or a

Cu_2O - CuO mixture was equally probable. The Cu_2O - CuO mixture was almost exclusively formed if air or O_2 was blown through the furnace during heating.

More evidence for the support of cuprous oxide formation was supplied by Darbyshire⁹⁶ who after cleaning copper foil with fine emery paper heat tinted it in a bunsen flame. The oxide film formed was removed electrolytically⁹⁷ and the electron diffraction pattern examined. The values obtained indicated the cubic Cu_2O system and gave a unit cell dimension of 4.26 Å. The values obtained by Darbyshire were substantiated by Preston and Bircumshaw⁹⁸ who found Cu_2O only in films produced on copper in the air at ordinary temperatures and in the air at 100°C.

It appears therefore that at temperatures below 200°C the oxide formed by heating copper in air is almost exclusively cuprous. If the temperature is increased to between 300°C and 400°C a proportion of CuO is obtained which increases if air or O_2 is blown over the surface. A wholly CuO surface film is never obtained except at temperatures above 600°C but continued heating at lower temperatures will increase the proportion of the cupric form as the thickness of the cuprous film increases.

In a flow system where catalysis is accompanied by the evolution of gas it is essential that the gas be removed immediately from the catalyst surface so that the surface area exposed to the substrate remains constant. A catalyst bed

consisting of several layers of oxidised copper gauze was found unsuitable since gas bubbles were trapped between the gauzes. The form finally adopted consisted of a collection of oxidised copper rings supported on a single oxidised copper gauze. The rings were made from 20 gauge 'Specpure' copper wire bent into circles 5 mm. diameter.

The components of the catalyst bed which were degreased by refluxing in CCl_4 , were oxidised in a furnace at 170°C until the first change in colour took place. The oxide skin was then reduced by heating in an atmosphere of H_2 at 400°C and reoxidising at 170°C . Successive oxidation and reduction produced an active oxide surface.

(b) Nickelous oxide.

As in copper the catalyst was prepared from 20 gauge 'Specpure' wire bent into 5 mm. diameter circles. A black NiO film was formed on the degreased nickel rings by alternate oxidation at 300°C and reduction in H_2 at 400°C . Oxidation below this temperature produced a thin almost invisible oxide layer.

According to Briggs, Jones and Wynne-Jones⁹⁹ a smooth adherent oxide layer of varying thickness can be produced on nickel by electrodeposition on the metal from a solution containing 0.1N NiSO_4 , 0.1N NaAc. , and 0.001N KOH at 25°C . Variations in the anodic-cathodic cycling sequence were shown to affect the thickness and adherence of the deposit.

NiO was initially prepared according to this method but the process was discontinued since even the most strongly deposited film was easily removed. A short section of wire half of which was oxidised in this way was immersed in 1.5 M H_2O_2 at pH 4.6 and 45°C . A vigorous evolution of O_2 accompanied the almost instantaneous removal of the oxide. Subsequent decomposition which was very small came only from the section which had been anodised.

(c) Cobaltous oxide.

The CoO was prepared from degreased 'Specpure' 20 gauge cobalt wire, by alternate oxidation at 300°C and reduction in H_2 at 400°C . The catalyst was employed as above in 5 mm. circles.

R E S U L T S

Cu₂O/H₂O₂ System

1. General.

The amount of H₂O₂ decomposed per litre (ΔC) by the catalyst as measured by the temperature difference (ΔT) between the thermistors has been taken as a direct measurement of the efficiencies of the catalyst under the conditions of the experiment. It is necessary at this point to refer again to the relation between ΔC and ΔT . Using the fact that decomposition of 1 mole of H₂O₂ in 1 litre of aqueous solution will raise the temperature by 23 degrees if the experiment is carried out adiabatically then

$$\Delta C = \frac{\Delta T}{23} \text{ moles per litre}$$

In all the experiments the flow was standardised at 100 mls per minute so that 10 minutes are taken for 1 litre to pass. This is highly relevant to the assignment of a magnitude to "catalyst efficiency" as are such questions as the form of the catalyst surface and the method of bed packing. All these factors were constant throughout the kinetic experiments and it is justifiable therefore to regard ΔC as a measure of efficiency.

In later treatment of mechanism, efficiency has been designated as \underline{r} (or rate of decomposition); \underline{r} should of

course be referred to a well defined zone in the catalyst bed since $[H_2O_2]$ changes along it. Since this concentration change is small however (3% in the low $[H_2O_2]$ zone and 1.5% for 2M H_2O_2) it appears reasonable to regard the whole catalyst as at one uniform condition.

The error in doing so in the low $[H_2O_2]$ region may be demonstrated. First however a relation between efficiency and concentration must be assumed. In this region 1st. order is the obvious assumption. Then at a given point along the bed

$$\text{rate} = k_1 c \quad (1)$$

where c is the $[H_2O_2]$ at this point and

$$\text{rate} = \frac{-dc}{dt} \quad (2)$$

is the fall in concentration when the solution advances an infinitesimal amount farther up the bed in a time dt

$$\text{i.e.} \quad \frac{-dc}{dt} = k_1 c \quad (3)$$

Integration gives

$$-\ln c = k_1 t + \text{constant} \quad (4)$$

and if c_t is the concentration leaving the catalyst bed at time t , then when $t = 0$

$$\text{constant} = -\ln c_0$$

where c_0 is the concentration reaching the catalyst.

$\therefore \ln \frac{c_0}{c_t} = k_1 t = k_2$ since \underline{t} is a constant at constant flow.

This equation may be put in terms of Δc_T

$$\text{i.e. } -\ln\left(1 - \frac{\Delta c_T}{c_0}\right) = k_2$$

where Δc_T is the concentration change over the whole catalyst. This gives, on expanding the left hand side

$$\frac{\Delta c_T}{c_0} + \frac{1}{2} \left(\frac{\Delta c_T}{c_0}\right)^2 + \frac{1}{3} \left(\frac{\Delta c_T}{c_0}\right)^3 + \dots = k_2$$

It is clear that an error of at most only 4% is caused by neglecting all except the first term in the expansion so that

$$\Delta c_T = k_2 c_0$$

or at any point in the bed

$$\Delta c = k_2 c \quad (5)$$

which could have been derived directly from (3) by putting

$$dc = \Delta c$$

$$\text{i.e. } \Delta c = k_1 c \cdot dt = k_2 c$$

The conclusion is the same if other kinetic processes (i.e. zero order or fractional orders) are assumed to connect rate at any point in the bed and concentration.

The results are presented with the efficiency, \underline{r} , in terms of moles per litre per minute i.e. $\frac{\Delta T}{230}$, but in

many of the graphs ΔT is plotted directly as a measure of efficiency. Fig.22 is a typical example of the changes in ΔT with time for Cu_2O catalysts. The process of arriving at ΔT from the thermistor resistance readings is illustrated in Table 3. The log R value in columns 5 or 6 is applied to the very large scale straight line calibration graph to give $\frac{1}{T}$ values (columns 7 and 8).

2. Stability of Catalyst and the Degree of Reproducibility Obtainable.

The kinetic work on Cu_2O catalysis was carried out on one charge of catalyst which was left in the reaction chamber between tests submerged in distilled water. Previous investigations had shown that the catalyst always returned to its initial state after removal of H_2O_2 (i.e. on replacing H_2O_2 solution by the distilled water) an observation fully substantiated during subsequent tests.

The difficulties associated with reproducibility in heterogeneous catalytic systems are notorious. Many of these difficulties were avoided using one charge of catalyst which never underwent any permanent alteration in activity, and a remarkable degree of reproducibility was obtained. Fig.22 and 23 illustrate this achievement. In Fig.22 efficiency results obtained at both high and low H_2O_2 are shown. These results were not obtained on successive runs

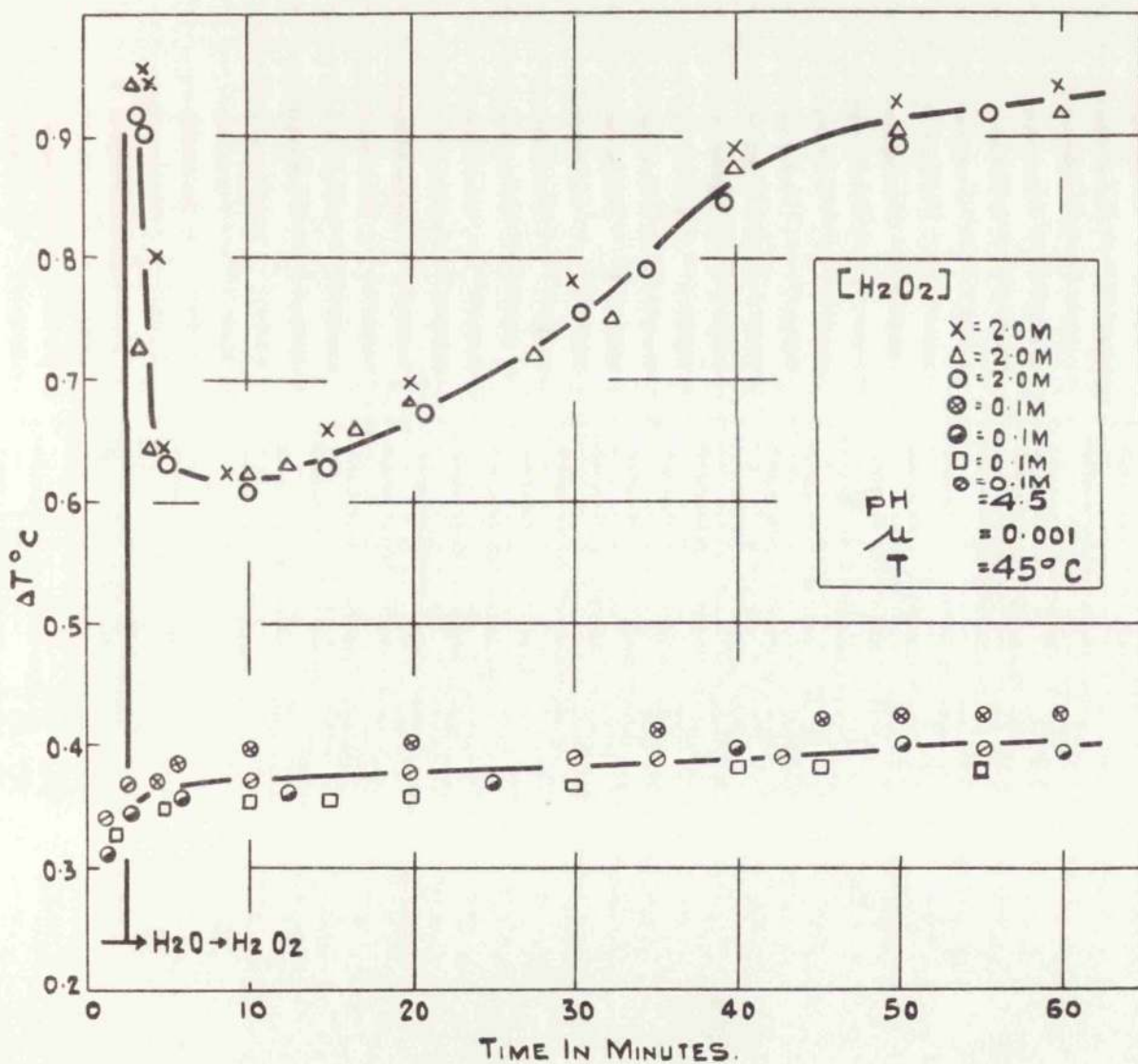


FIG. 22. TYPICAL VARIATIONS IN CATALYTIC EFFICIENCY OF Cu_2O IN BOTH HIGH AND LOW $[H_2O_2]$ ZONES. ALSO DEMONSTRATED IS THE STABILITY OF THE CATALYST AND THE REPRODUCIBILITY OBTAINED OVER A PERIOD OF 2 YRS, SINCE THE RESULTS SHOWN COVER THAT PERIOD.

Col. 1	2	3	4	5	6
Substrate	Rate mls/minute	Corrected resistance ohms			
		Entrance Thermistor R_1	Exit Thermistor R_2	Log R_1	Log R_2
H_2O	100	941.018	778.882	9735979	8914717
		941.018	778.87	9735979	8914650
		940.994	778.74	9735868	8913925
H_2O_2	100		767.82		8852594
			765.52		8839565
			765.4		8838885
			765.49		8839395
			765.94		8841948
			768.21		8854800
		769.94		8864569	

Col. 7	8	9	10	11
$\frac{1}{T_1}$	$\frac{1}{T_2}$	T_1	T_2	ΔT
314999	314679	317.461	317.784	0.323
314999	314679	317.461	317.784	0.323
314999	314673	317.461	317.790	0.329
	314202	317.455	318.267	0.812
	314107	317.465	318.363	0.898
	314100	317.473	318.370	0.897
	314105	317.462	318.365	0.903
	314123	317.428	318.347	0.919
	314220		318.249	
	314295	317.456	318.174	0.718

Table 3.

but were interspersed over a period of 2 years. In Fig.23 variations in catalyst efficiency under identical experimental conditions are shown for two tests separated by a period of 18 months during which extensive studies were carried out on the catalyst under various conditions. The results demonstrate the stability of the catalyst and the high degree of reproducibility obtained in the main features viz.,

- (i) The initial peak efficiencies are 0.600 and 0.600 respectively.
- (ii) The initial peak is followed by a fall in efficiency reaching 0.395 in 10 minutes (Fig.23a) and 0.352 in 9.5 minutes (Fig.23b).
- (iii) After the minimum, efficiency slowly recovers to a higher constant value. In 23a it reaches 0.870 in 55 minutes, a recovery of 0.235, and in 23b it reaches 0.768 in 65 minutes, a recovery of 0.200.

Although the used catalyst exhibited a slight tendency to remain in a less active state (the rate of poisoning was faster and the rate of recovery slower) the effect was so small even over the extended period of 18 months that it can be neglected, and the catalyst regarded as stable and reproducible from one run to the next. Even in the low $[H_2O_2]$ zone where such effects become relatively more important the differences in catalytic efficiency over 2 years were very small. At 0.1 M typical runs gave final efficiencies of 0.19° and 0.165° i.e. a difference of only 0.025° over

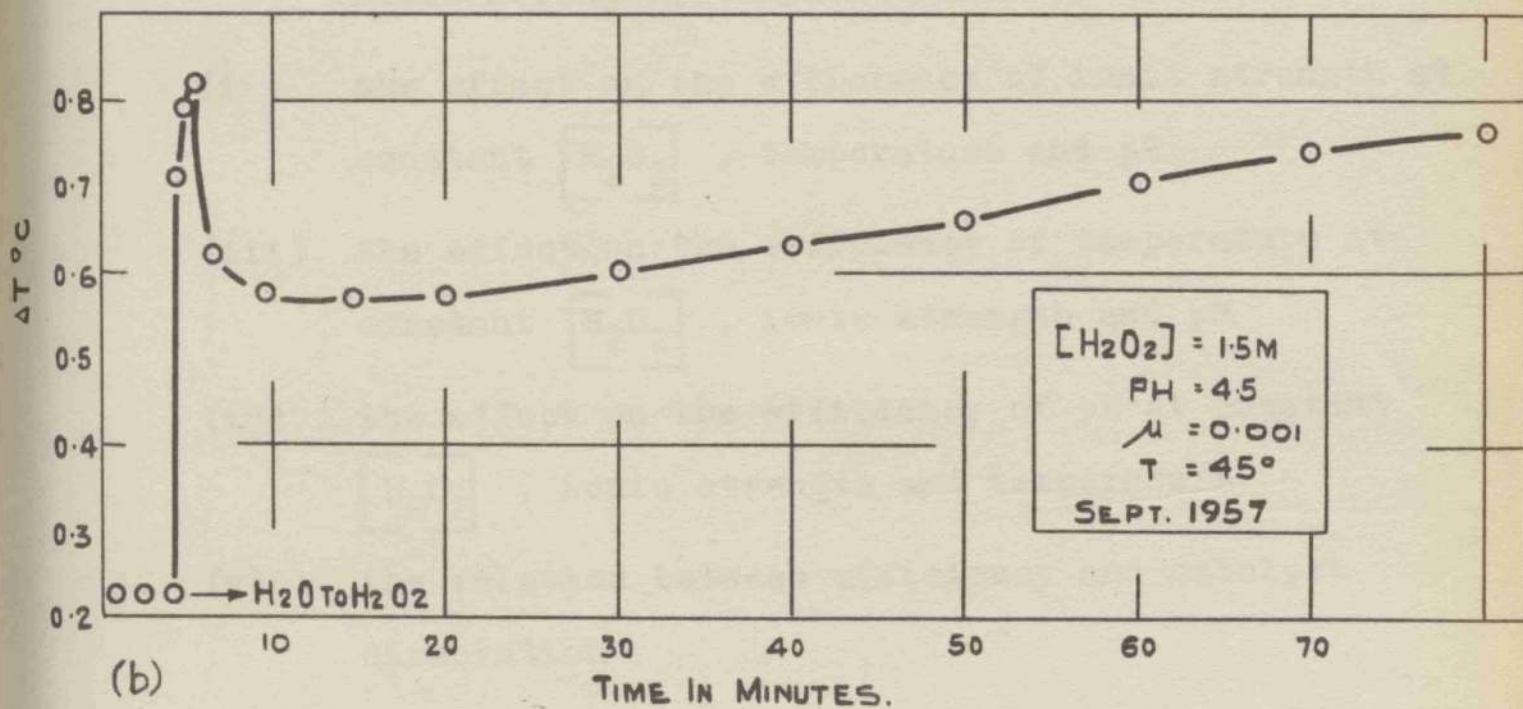
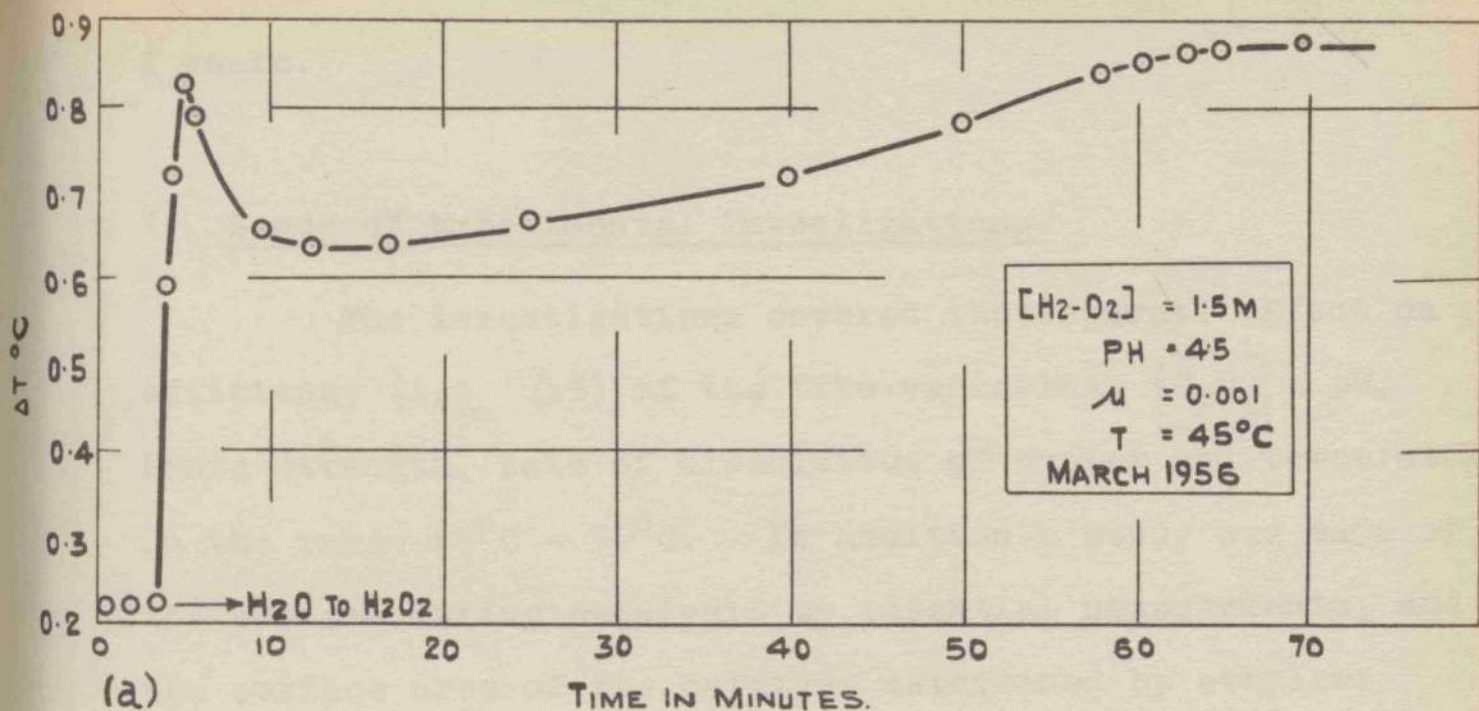


FIG. 23. A COMPARISON OF THE EFFICIENCY CHANGES TAKING PLACE ON THE SAME Cu_2O CATALYST UNDER IDENTICAL CONDITIONS AFTER 18 MONTHS CONTINUOUS USE.

2 years.

3. Scope of Experimental Investigations.

The investigations covered the separate effect on efficiency (i.e. ΔT) of the five variables, $[H_2O_2]$, pH, ionic strength, rate of dissolution of copper and temperature in the range $40^\circ C - 50^\circ C$. In addition a study was made of the surface during catalysis by potential measurements, and the surface area of the catalyst determined by ethylene adsorption. The various studies in this section were thus:-

- (i) the effect on the efficiency of $[H_2O_2]$ at constant ionic strength, temperature and pH
- (ii) the effect on the efficiency of ionic strength at constant $[H_2O_2]$, temperature and pH
- (iii) the effect on the efficiency of temperature at constant $[H_2O_2]$, ionic strength and pH
- (iv) the effect on the efficiency of pH at constant $[H_2O_2]$, ionic strength and temperature
- (v) the relation between efficiency and catalyst dissolution
- (vi) the characterisation of surface composition
- (vii) surface area determination.

The $[H_2O_2]$ effect was studied from 2 M to 0.025 M.

Variations in the $[H_2O_2]$ over this range revealed two distinct zones of behaviour, one operating above and the other below an $[H_2O_2]$ of 0.25 M (Fig.24). Above 0.25 M - which shall be referred to as the "high $[H_2O_2]$ zone" - a regular pattern of efficiency changes were observed, but below 0.25 M - the "low $[H_2O_2]$ zone" - a more or less steady efficiency was maintained from first exposure.

For purposes of presentation the effect of the variables given above will each be dealt with, with reference to these separate zones i.e.

- (a) 2 M to 0.25 M H_2O_2 - high $[H_2O_2]$ zone.
- (b) 0.25 M to 0.025 M H_2O_2 - low $[H_2O_2]$ zone

4. The Effect of $[H_2O_2]$ on the Catalyst Efficiency.

- (a) 2 M to 0.25 M

As mentioned above characteristic changes took place in the efficiency of the catalyst while in prolonged contact with H_2O_2 above a concentration of 0.25 M. These changes were as follows (Fig.24, 2 M curve).

- (i) Immediately the water was replaced by H_2O_2 , point A, the efficiency increased rapidly to a maximum value - section BC.
- (ii) The initial peak value was followed almost immediately by a relatively slow fall in efficiency

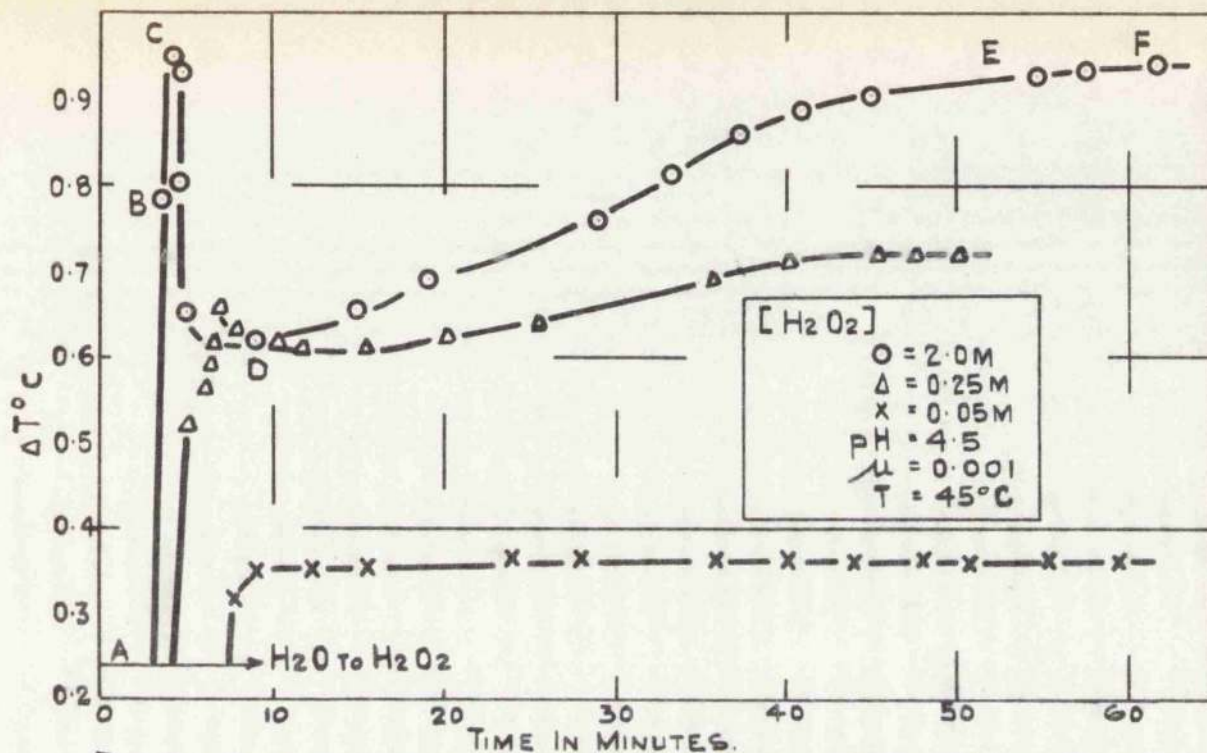


FIG. 24. CHARACTERISTIC VARIATIONS IN EFFICIENCY OF Cu_2O WHICH TAKE PLACE IN THE TWO CONCENTRATION ZONES. I.E. VARIABLE EFFICIENCY ABOVE 0.25M AND CONSTANT EFFICIENCY BELOW 0.25M.

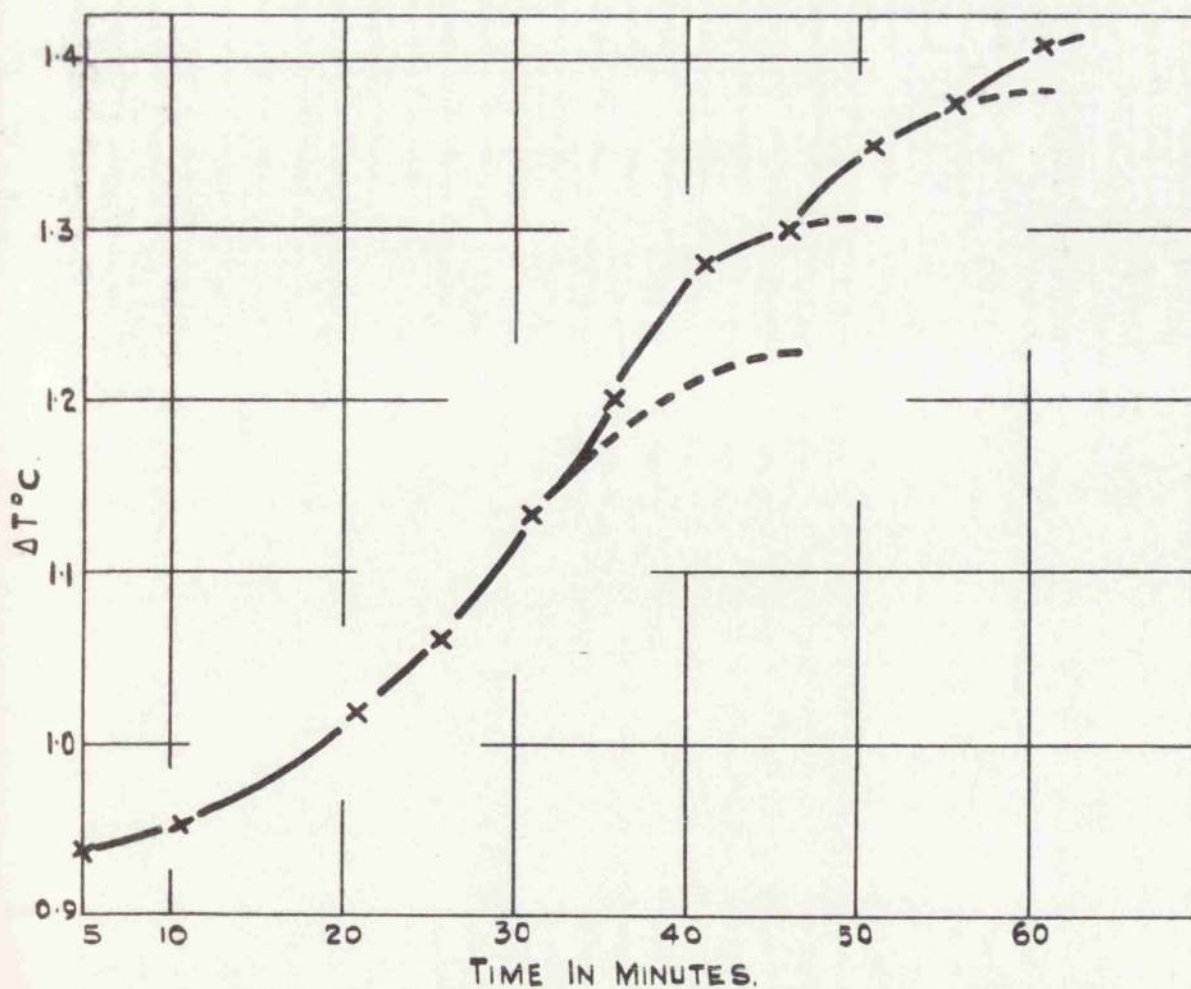


FIG. 25. CHARACTERISTIC RECOVERY PROCESS IN EFFICIENCY OF Cu_2O SHOWING INITIAL SIGMOIDAL BEHAVIOUR FOLLOWED BY INTERMITTENT LEAPS.

to a minimum value - section CD.

- (iii) The minimum value was followed by a slow increase in efficiency which finally reached a second maximum - section DE. A feature of this slow recovery process was the initial sigmoidal shape which at high rates of decomposition was followed by a series of intermittent leaps (Fig.25).
- (iv) This maximum was maintained during further contact - section EF.

The effect of $[H_2O_2]$ on this sequence of efficiency changes is shown in Figs. 26,27,28,29. Variations in the $[H_2O_2]$ although not affecting the pattern of the efficiency changes did affect their extent and rate of change, i.e.,

- (i) The initial increase in efficiency was not observably affected by $[H_2O_2]$ in this range, but the peak efficiency changed linearly with $[H_2O_2]$ (Fig.30).
- (ii) The rate of decline of the efficiency from the peak efficiency value appeared slightly affected by $[H_2O_2]$. Table 4 shows the period of $\frac{1}{2}$ -decay i.e.

Molarity of H_2O_2	2.	1.5	1.0	0.5
$\frac{1}{2}$ - decay in secs.	30	60	120	160

Table 4.

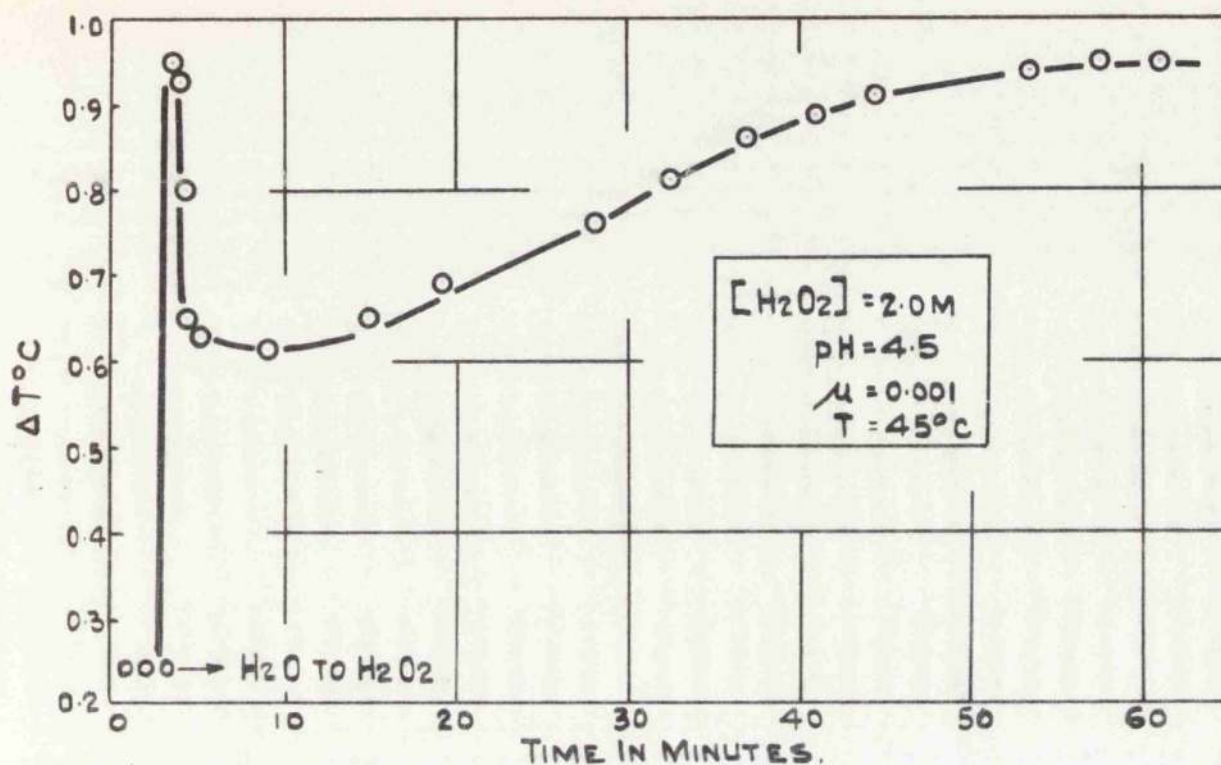


FIG 26. Cu₂O EFFICIENCY CHANGES TAKING PLACE DURING CONTACT WITH 2M. H₂O₂.

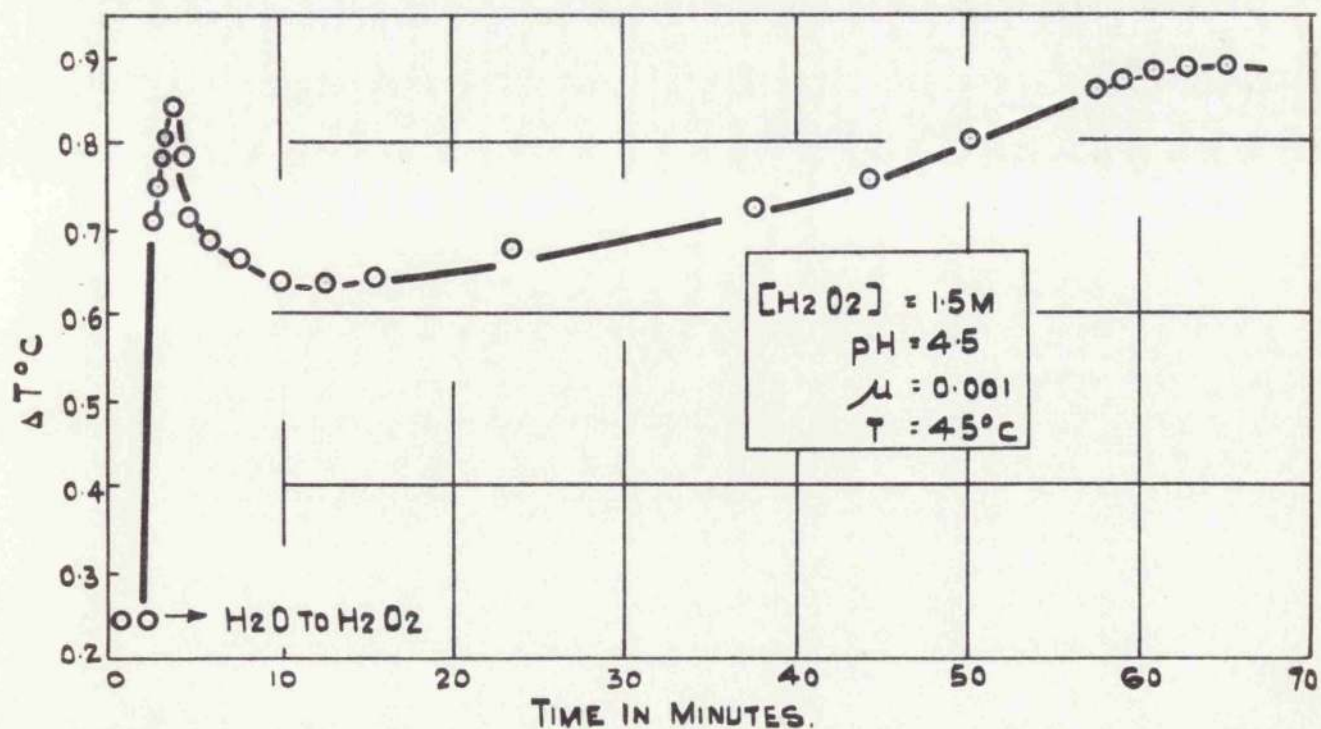


FIG. 27. Cu₂O EFFICIENCY CHANGES TAKING PLACE DURING CONTACT WITH 1.5M. H₂O₂.

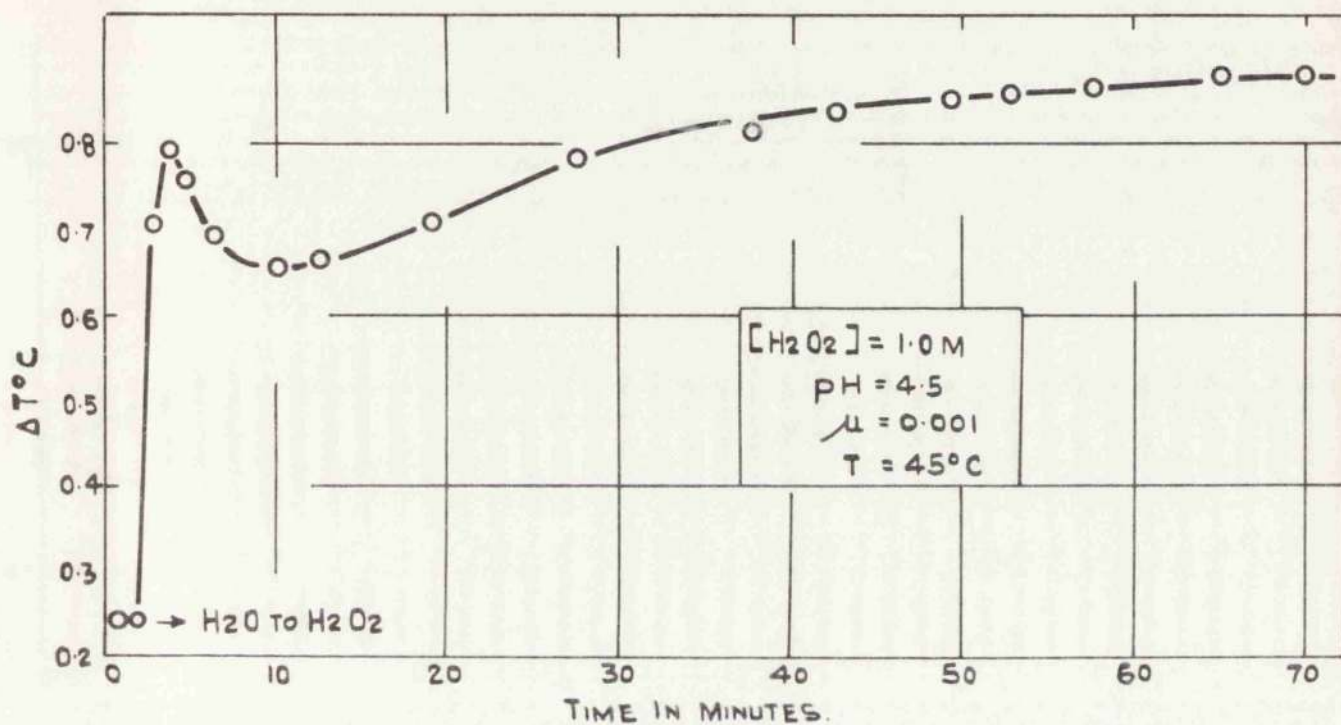


FIG. 28. Cu_2O EFFICIENCY CHANGES TAKING PLACE DURING CONTACT WITH 1.0M. H_2O_2 .

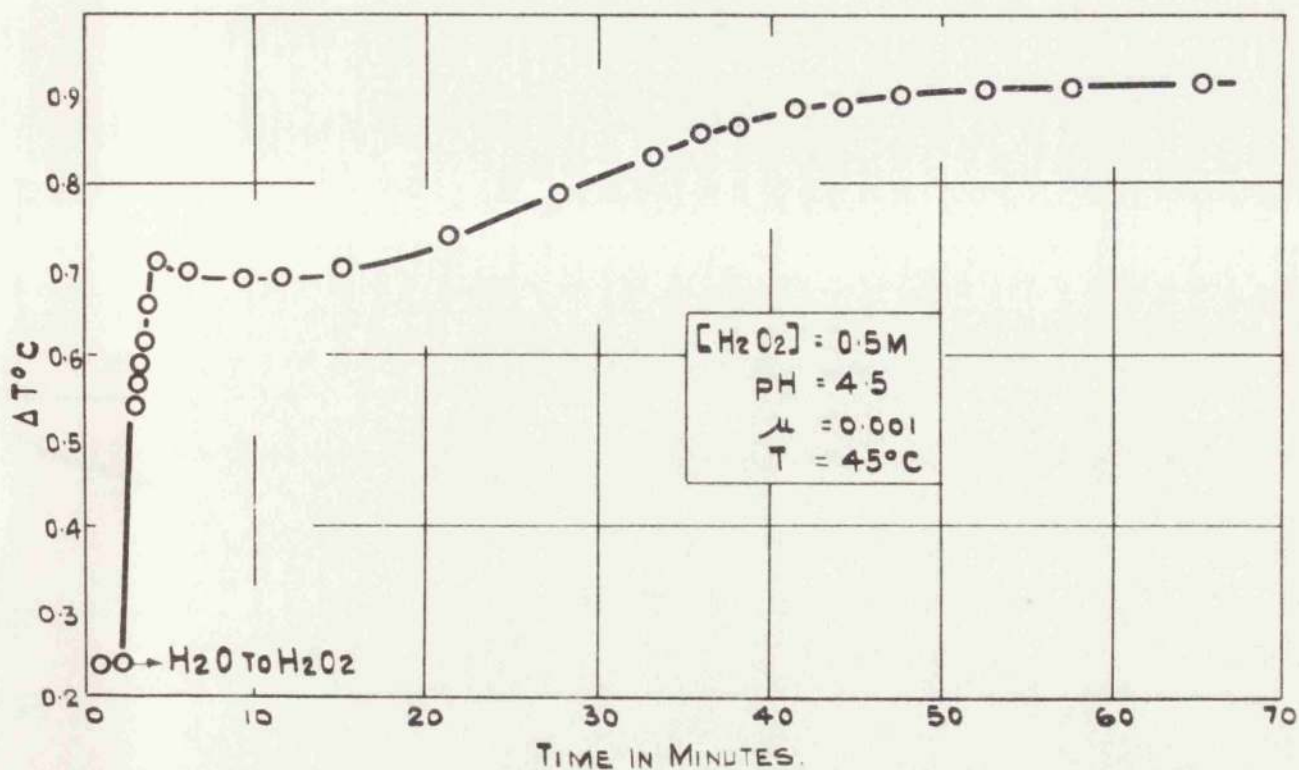


FIG. 29. Cu_2O EFFICIENCY CHANGES TAKING PLACE DURING CONTACT WITH 0.5M H_2O_2 .

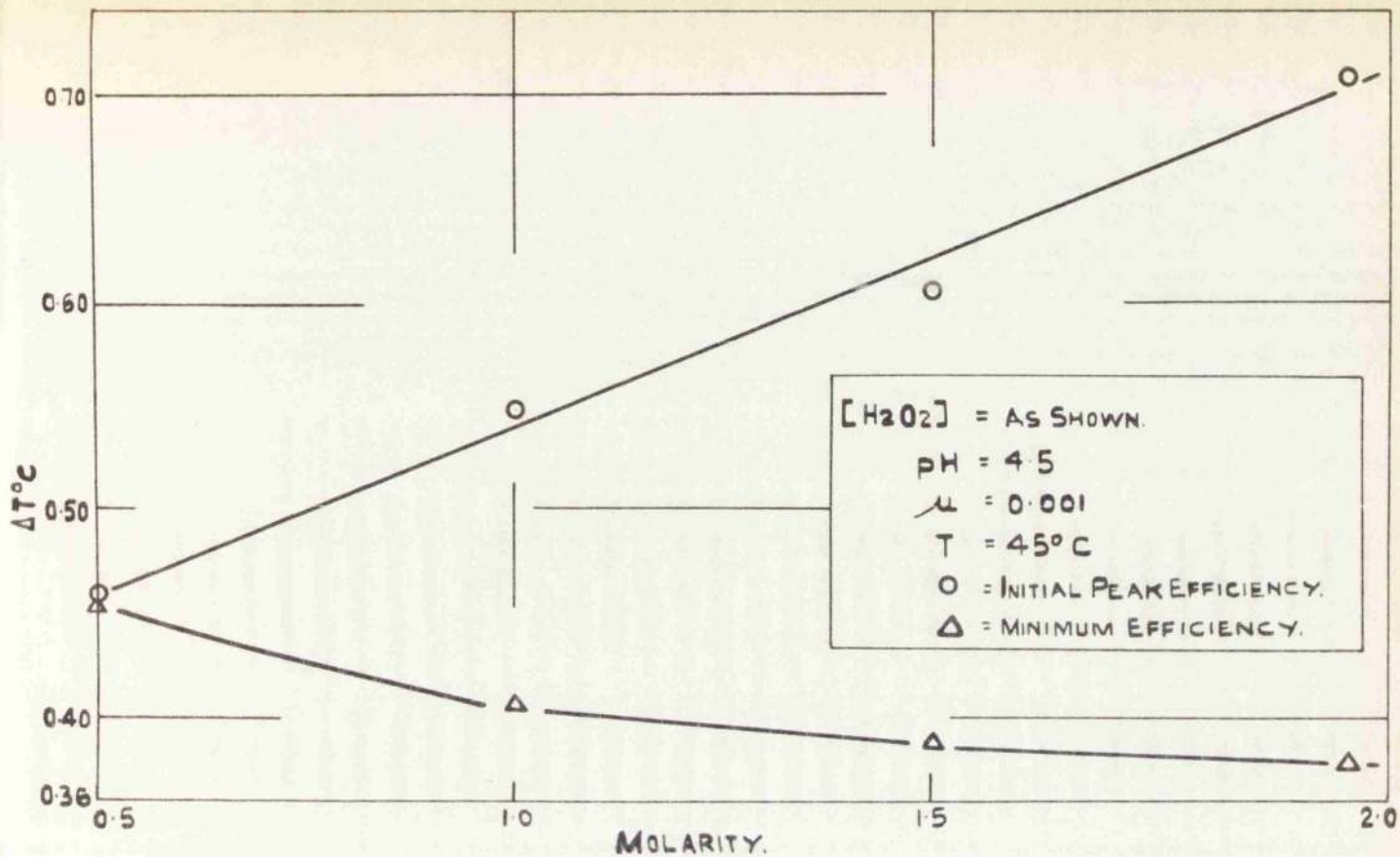


FIG. 30. THE EFFECT OF $[H_2O_2]$ ON (a) THE INITIAL PEAK EFFICIENCY (b) THE SUBSEQUENT MINIMUM EFFICIENCY OF Cu_2O .

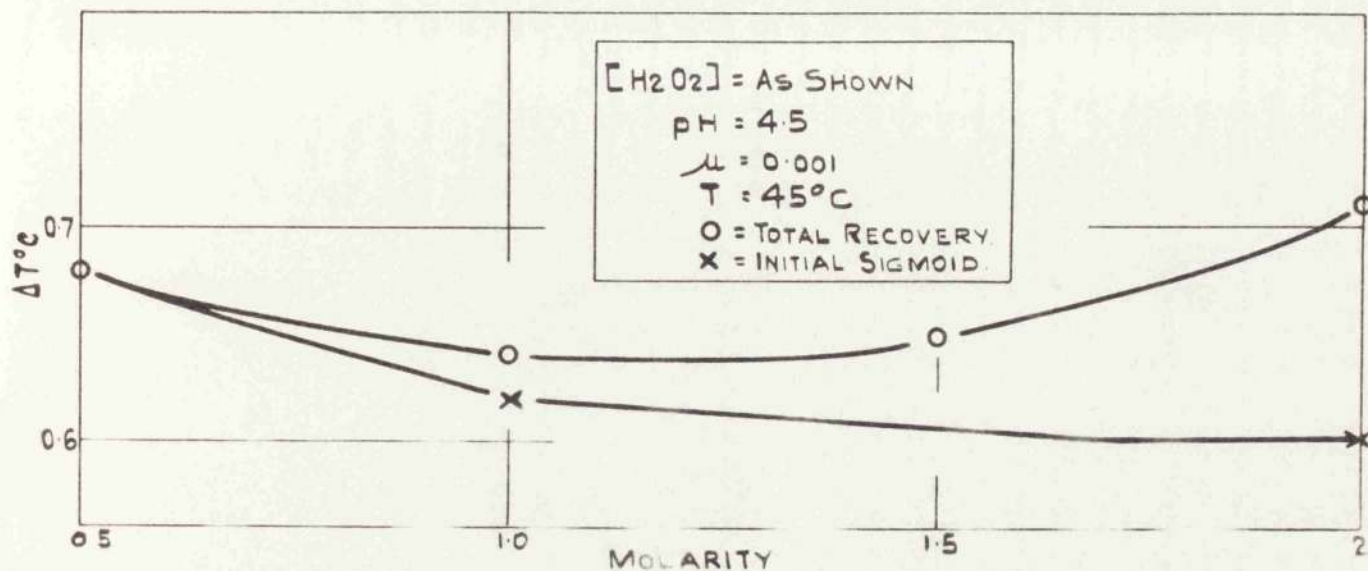


FIG. 31. THE EFFECT OF $[H_2O_2]$ ON (a) FINAL EFFICIENCY VALUE OF TOTAL RECOVERY AND (b) FINAL EFFICIENCY VALUE OF INITIAL SIGMOID, FOR Cu_2O .

the time in seconds for half-completion of the decay at the different concentrations. It must be emphasised that the $\frac{1}{2}$ -decay periods could not be determined with great accuracy but they do suggest a dependence on $[H_2O_2]$.

- (iii) The minimum efficiency value was only slightly - but significantly - affected by $[H_2O_2]$, (Fig.30). As the $[H_2O_2]$ was decreased there was a slight increase in the minimum efficiency value.
- (iv) The final increase in efficiency was unaffected by

Molarity of H_2O_2	2.	1.5	1.	0.5
$\frac{1}{2}$ -recovery in mins.	22	30	20	20

Table 5.

Molarity of H_2O_2	2.	1.5	1.	0.5
$\frac{1}{2}$ -recovery in mins.	21	23	19	20

Table 6.

$[H_2O_2]$. Table 5 and Table 6 show the period of $\frac{1}{2}$ -recovery for the total recovery process (including the intermittent leaps) - Table 5 - and the initial

period of sigmoidal behaviour - Table 6.

- (v) The final steady efficiency (this value includes the final intermittent leaps as well as the initial sigmoid) which was maintained during further contact with H_2O_2 was only slightly affected by $[\text{H}_2\text{O}_2]$ (Fig.31). There was at first a slight fall of efficiency with increasing $[\text{H}_2\text{O}_2]$ - as in (iii) above - followed by a marked rise which contrasts with the behaviour at the minimum.

(b) 0.25 M to 0.025 M

In this region the initial peak entirely disappeared. The efficiency rose rapidly to a level from which it subsequently climbed very slightly to a constant value. This is shown in the curve for 0.05 M (Fig.24). In Fig.37 it will be observed that for 0.1 M at 50°C there is a detectable tendency to return to an initial peak with a subsequent sharper rise to the final steady value.

In this concentration region the efficiency bore a remarkably strict first order relation with the $[\text{H}_2\text{O}_2]$ (Fig.32 and Fig.33).

Although the results obtained at 0.25 M have been interpreted in terms of the low concentration conditions, the 0.25 M case exhibits intermediate effects and must be considered a borderline case between the two zones of behaviour. It does for example exhibit efficiency changes during the

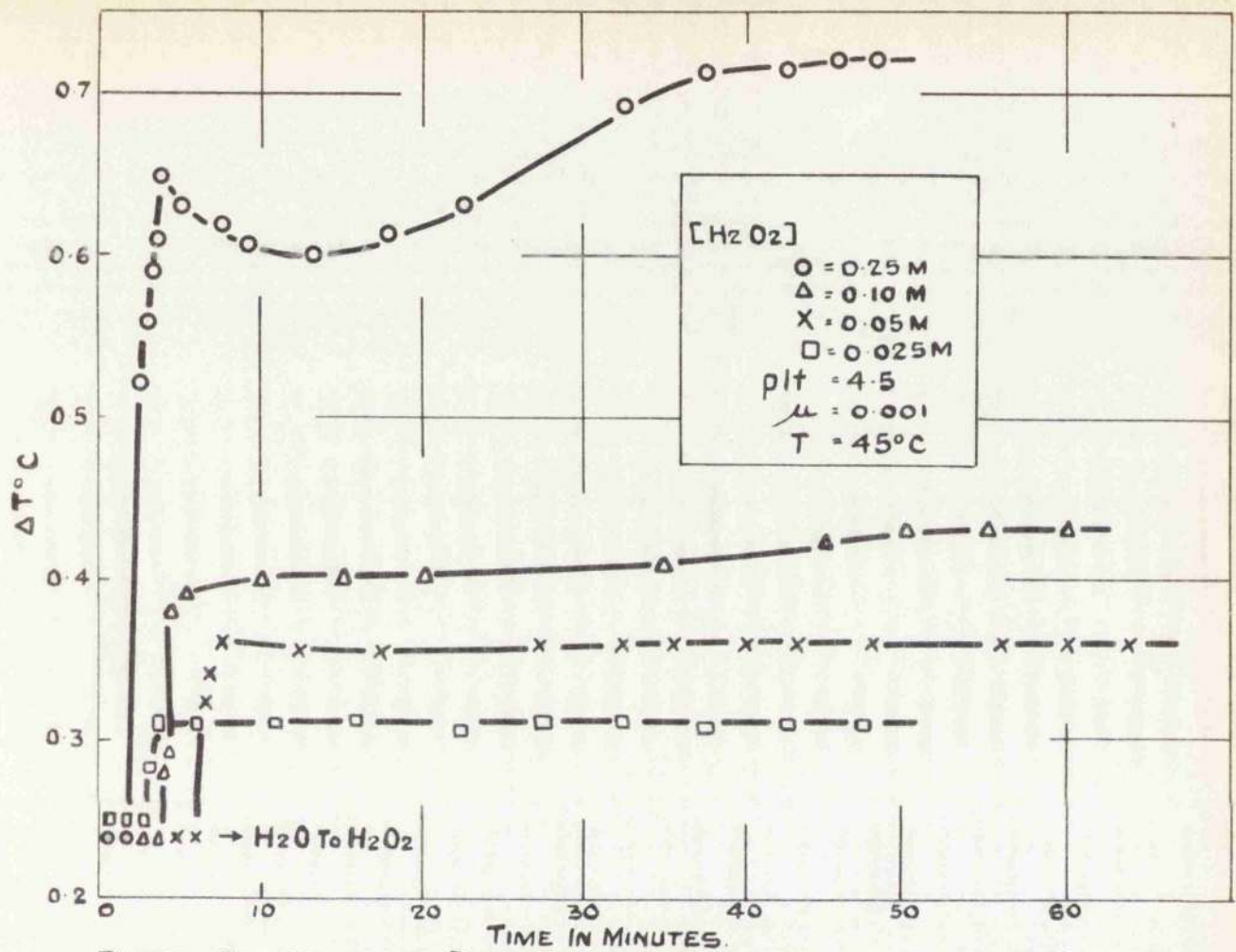


FIG. 32. THE EFFECT OF [H₂O₂] ON THE EFFICIENCY OF THE Cu₂O CATALYST IN THE LOW CONCENTRATION ZONE.

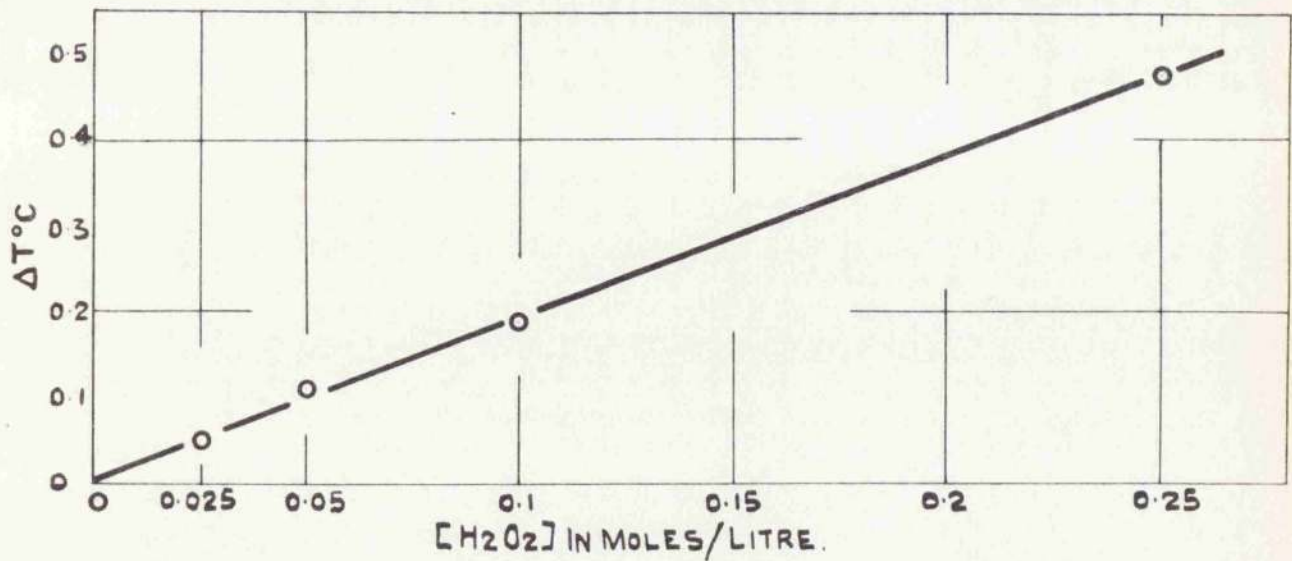


FIG. 33. 1ST ORDER PLOT OF FINAL EFFICIENCY VALUES V. [H₂O₂] FOR THE LOW H₂O₂ CONCENTRATION REGION IN THE SYSTEM Cu₂O/H₂O₂.

presence of H_2O_2 although to a much lesser degree than is encountered at the high concentrations. In addition the final efficiency lies on the first order line connecting $[H_2O_2]$ and ΔT for the low concentration region, at a value well below that usually encountered where normal recovery stages are involved.

5. The Effect of Ionic Strength on the Catalyst Efficiency.

The effect of ionic strength was studied over the range $\mu = 0.0001$ to $\mu = 0.01$ where μ , the ionic strength, is given by:-

$$\mu = \frac{1}{2} \sum c z^2$$

where c = concentration in molalities

z = charge carried by the individual ions

For a single uniunivalent electrolyte like sodium perchlorate

$$\mu = c$$

(a) 2 M to 0.25 M

The results (Fig.34) give no indication of dependence on μ since a hundred-fold increase in the ionic strength produced no significant increase in the efficiency of the catalyst or in the rate of dissolution of the catalyst (copper dissolution is dealt with below).

Although the minimum efficiency appears to decrease

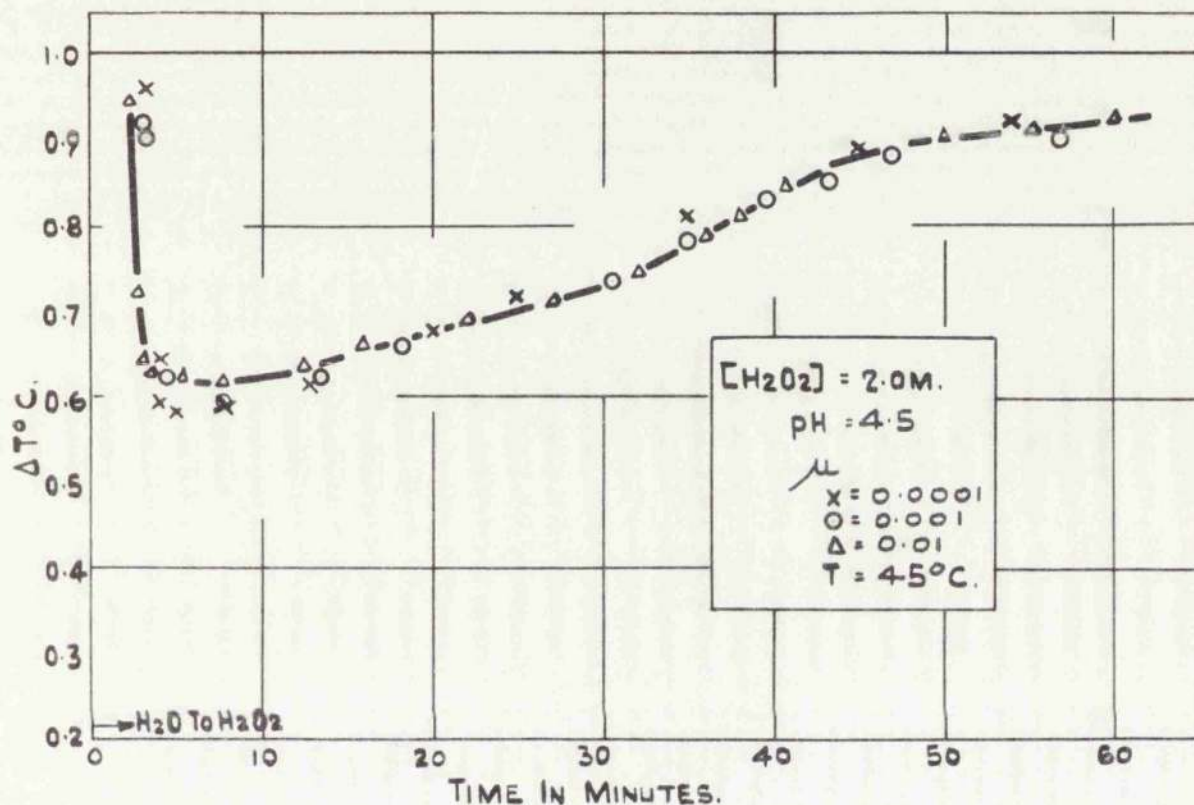


FIG 34. SHOWING THE EFFECT OF IONIC STRENGTH ON THE EFFICIENCY CHANGES OF Cu_2O IN THE HIGH CONCENTRATION ZONE.

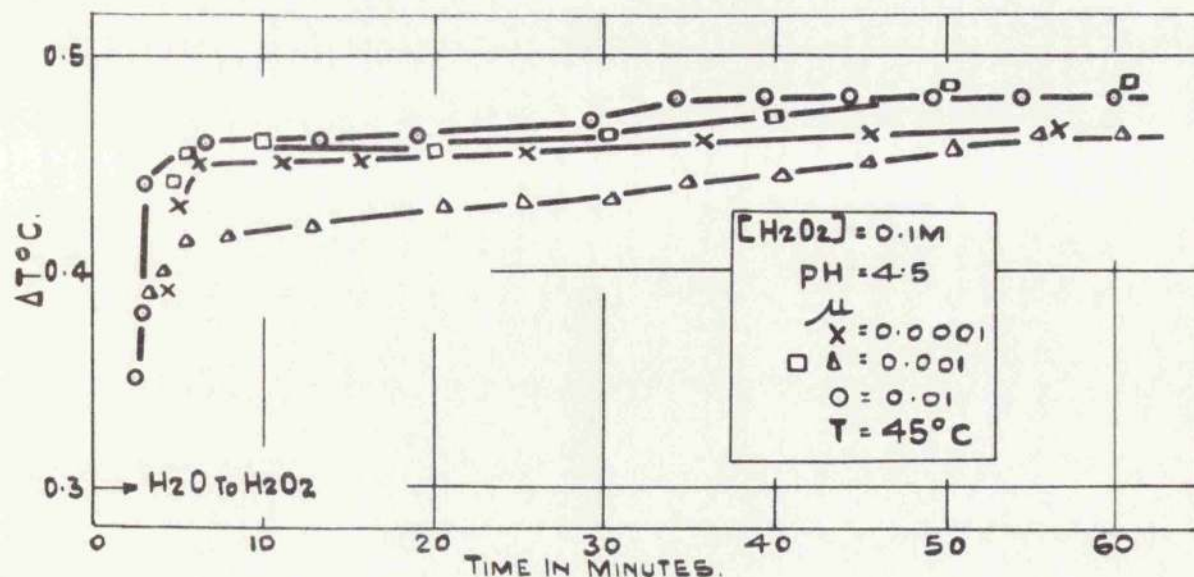


FIG.35. SHOWING THE EFFECT OF IONIC STRENGTH ON THE EFFICIENCY OF Cu_2O DURING CONTACT WITH H_2O_2 IN THE LOW CONCENTRATION ZONE. THE TWO CURVES SHOWN FOR 0.001 WERE OBTAINED TWO YEARS APART.

with decreasing ionic strength the effect is negligible compared with the variation of ionic strength. The effect on the final steady efficiency is also negligible.

(b) 0.25 M to 0.025 M

As in the higher concentration region, ionic strength produced no systematic effect on the efficiency of the catalyst. (Fig.35).

6. The Effect of Temperature on the Catalyst Efficiency.

The effect of temperature on the processes is shown in Figs.36 and 37. In both concentration zones the effect is quite clear both on the efficiency values at the peak, minimum and first steady values and on the rates of the changes in efficiency.

The results are correlated by use of the equation

$$\log_{10}(\text{efficiency}) = \frac{-E_A}{2.3 R.T} + \text{constant}$$

in which E_A is the apparent energy of activation of the process. Its significance will be discussed later.

(a) 2 M to 0.25 M

(i) At the initial peak efficiency, the plot of $\log(\text{efficiency})$ against $\frac{1}{T}$ (Fig.38) is linear and the slope gives an activation energy of 16.5 kcals.

(ii) The decline from the peak efficiency to the minimum

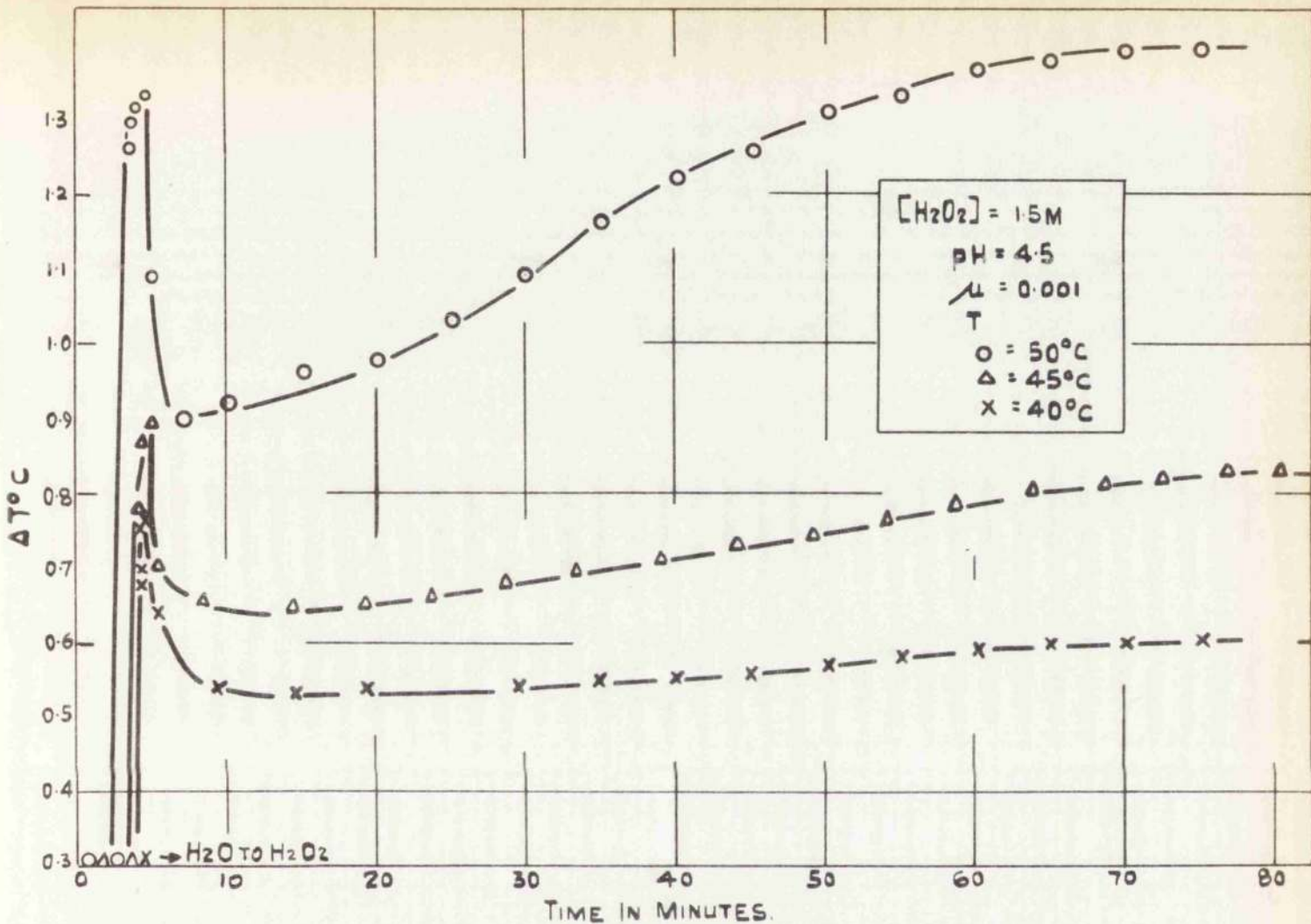


FIG 36. INFLUENCE OF TEMPERATURE ON THE EFFICIENCY CHANGES TAKING PLACE ON Cu_2O DURING PROLONGED CONTACT WITH H_2O_2 IN THE HIGH CONCENTRATION ZONE.

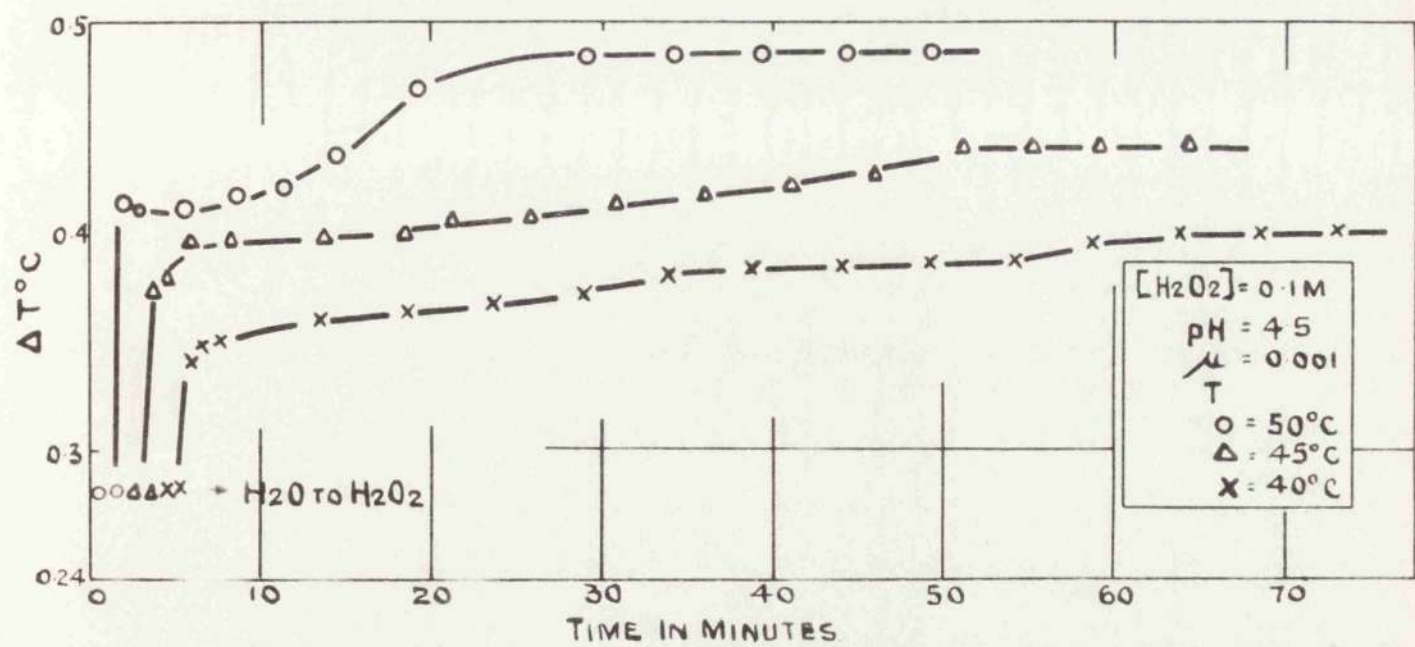


FIG 37 INFLUENCE OF TEMPERATURE ON THE EFFICIENCY CHANGES TAKING PLACE ON Cu_2O DURING PROLONGED CONTACT WITH H_2O_2 IN THE LOW CONCENTRATION ZONE.

efficiency was not significantly affected by temperature. Indeed, if the half-time of the decay is taken as a measure of the rate of this particular process, temperature has practically no effect (Table 7). On the other hand if the tangent to the

Temperature °C	Half-time of Decline secs.	$\frac{d(\text{efficiency})}{dt}$ peak
40	40	1.2
45	30	1.8
50	30	2.2

Table 7.

decay curve at the peak is taken then the figures given in Column 3 (Table 7) are obtained, where the figures are in hundredths of a degree (ΔT) per second. These figures give a rough energy of activation of 12 ± 5 kcals. (Fig.38) which suggests that it is either the same or less than that found for the peak rate.

- (iii) As in (i) an increase in temperature increased the minimum efficiency value such that $\log(\text{efficiency})$ against $\frac{1}{T}$, (Fig.38) gave an activation energy of 19.5 kcals.
- (iv) The final slow increase in efficiency from the minimum value was affected by temperature, both in

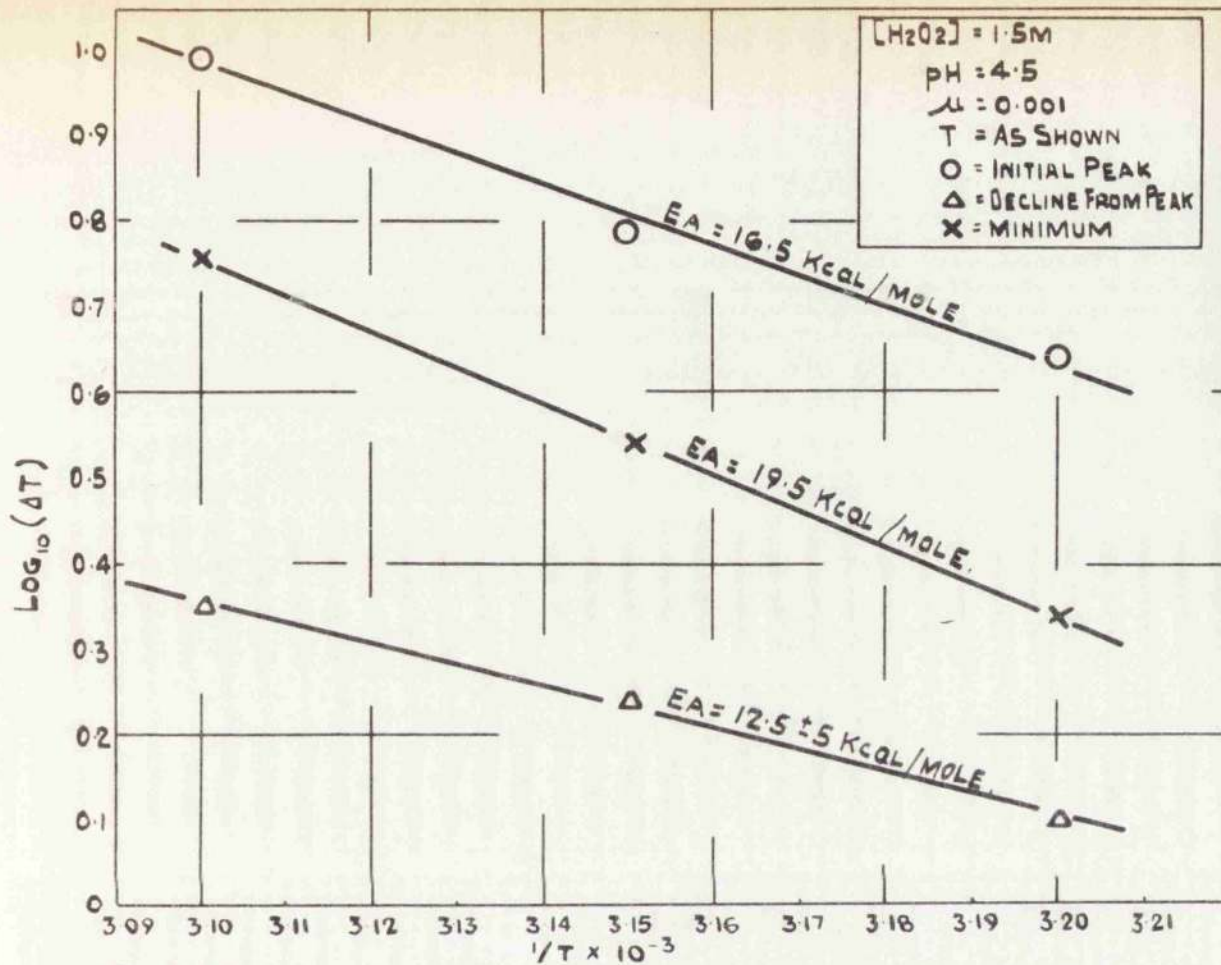


FIG. 38. VARIATION OF PEAK, DECLINE FROM PEAK, AND MINIMUM EFFICIENCY OF Cu_2O WITH TEMPERATURE. SLOPE IS PROPORTIONAL TO EA.

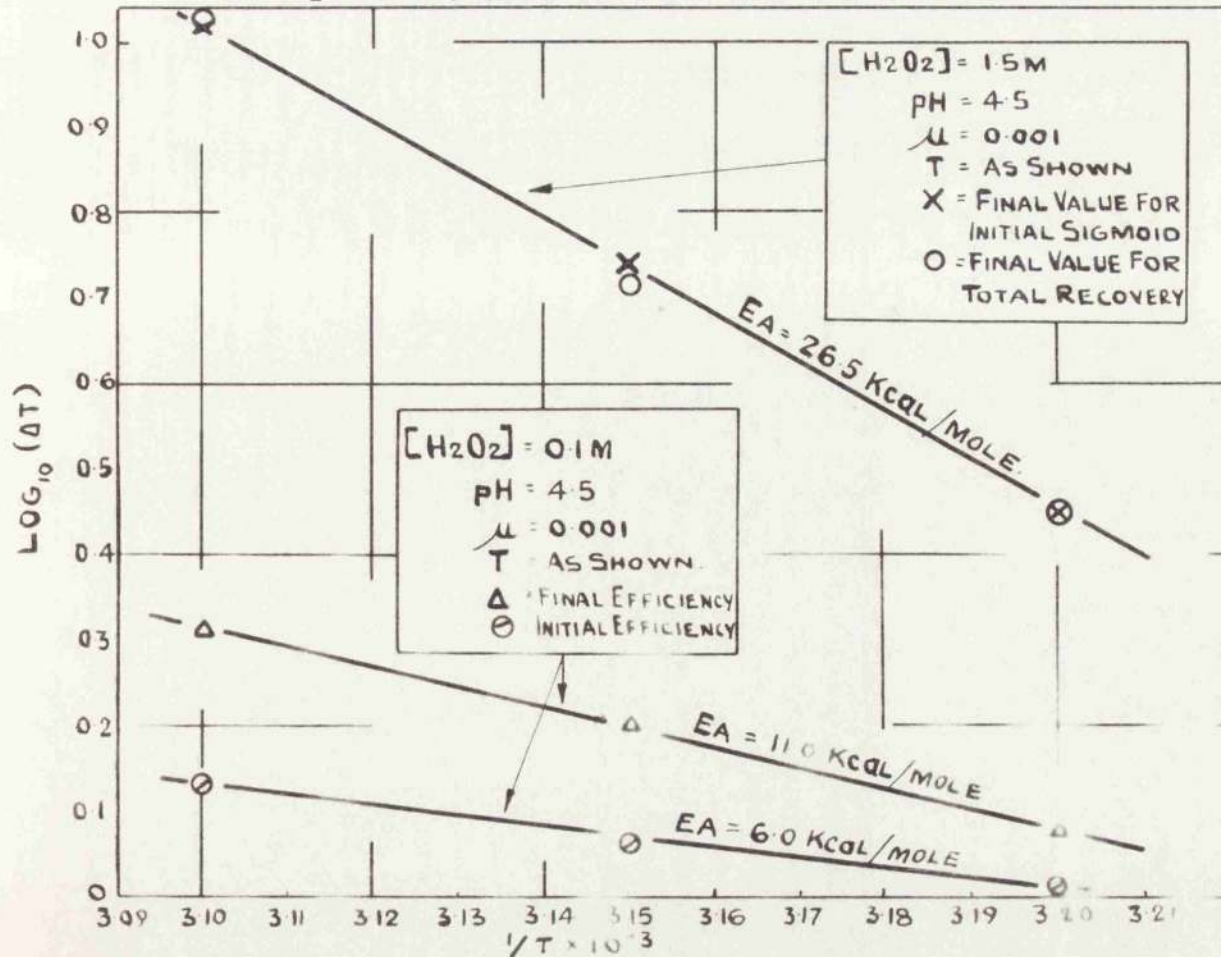


FIG. 39. VARIATION OF Cu_2O EFFICIENCY WITH TEMPERATURE AS SHOWN.

the rate at which it took place and in the final value which it attained. The half-life periods at 40°C, 45°C and 50°C both for the total recovery process (including the intermittent leaps referred to above which became quite marked at 50°C (Fig.25)) and also for the initial sigmoid are shown in Table 8. A value of 26.5 kcals. (Fig.39) was

Temperature °C	Half-life Periods in minutes	
	Total Recovery	Initial Sigmoid
40	40	40
45	35	33
50	27	30

Table 8.

obtained for the energy of activation of the initial sigmoid shaped section of the recovery process. Also included in Fig.39 are the log(efficiency) figures for the overall recovery value which do not differ appreciably from the sigmoid values.

- (v) Another effect of temperature increase which is clearly indicated by Fig.36 is that an increase in temperature decreases the time spent in the minimum efficiency state.

(b) 0.25 M to 0.025 M.

The final efficiency value reached on prolonged contact with H_2O_2 was affected by temperature (Fig.37) giving an activation energy of 11.0 kcal. (Fig.39). The slight increase in efficiency which normally takes place in this region was also affected by temperature and an activation energy of 6 kcal. was found for the state immediately attained on exposure of the catalyst to H_2O_2 (Fig.39).

7. The Effect of pH on the Catalyst Efficiency

The H_2O_2 molecule in aqueous solution is slightly dissociated according to the equilibrium:-



The value of the equilibrium constant

$$K = \frac{[HO_2'] [H^+]}{[H_2O_2]}$$

has been determined independently by Joyner¹⁰⁰ and Kargin¹⁰¹. Joyner found a value of 1.78×10^{-12} gm. moles per litre at 20°C and Kargin 1.55×10^{-12} gm. moles per litre at the same temperature.

(a) 2 M to 0.25 M

The effect of $[H^+]$ on the efficiency was examined at pH 4.5, 5.15, 7.7 and 8.0. The results are shown in

Fig.40. A reduction in the $[H^+]$ increases the overall level of the cyclic efficiency changes, but proportionally the increases involved are small compared with the alterations in the $[H^+]$ taking place. Table 9 shows that a

pH	4.5	5.15	7.7	8.0
H^+ moles/ litre	3162.0×10^{-8}	707.9×10^{-8}	1.995×10^{-8}	1.0×10^{-8}
HO_2 moles/ litre	2.665×10^{-7}	11.93×10^{-7}	423.0×10^{-7}	844.0×10^{-7}
Peak ΔT	0.6	0.91	0.99	1.73
Minimum ΔT	0.35	0.54	0.56	0.99
Final ΔT (total)	0.549	0.778	1.300	1.545
Final ΔT (sigmoid)	0.5	0.74	1.07	1.42

Table 9.

three thousand-fold decrease in the $[H^+]$ causes approximately a three-fold increase in the peak, minimum and final efficiency values.

(b) 0.25 M to 0.025 M.

In the low concentration zone the pH effect was studied at pH 4.5, 5.6, 6.7, 7.6, 8.5, 9.5 and 10.2. The results are given graphically in Fig.41 which is drawn on a large scale to accentuate the pH effect.

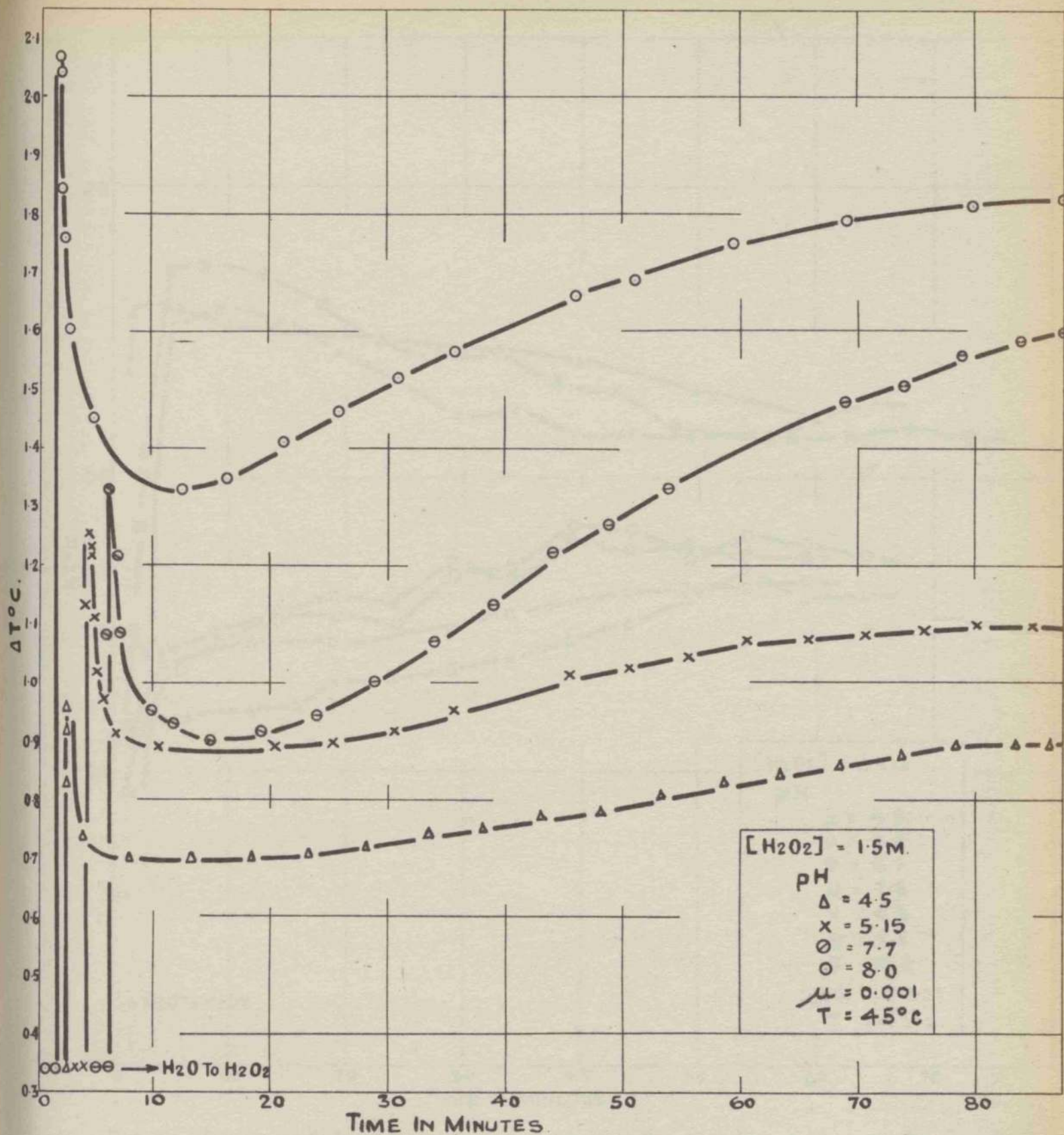


FIG. 40. VARIATION OF Cu_2O EFFICIENCY WITH pH. IN THE HIGH CONCENTRATION ZONE.

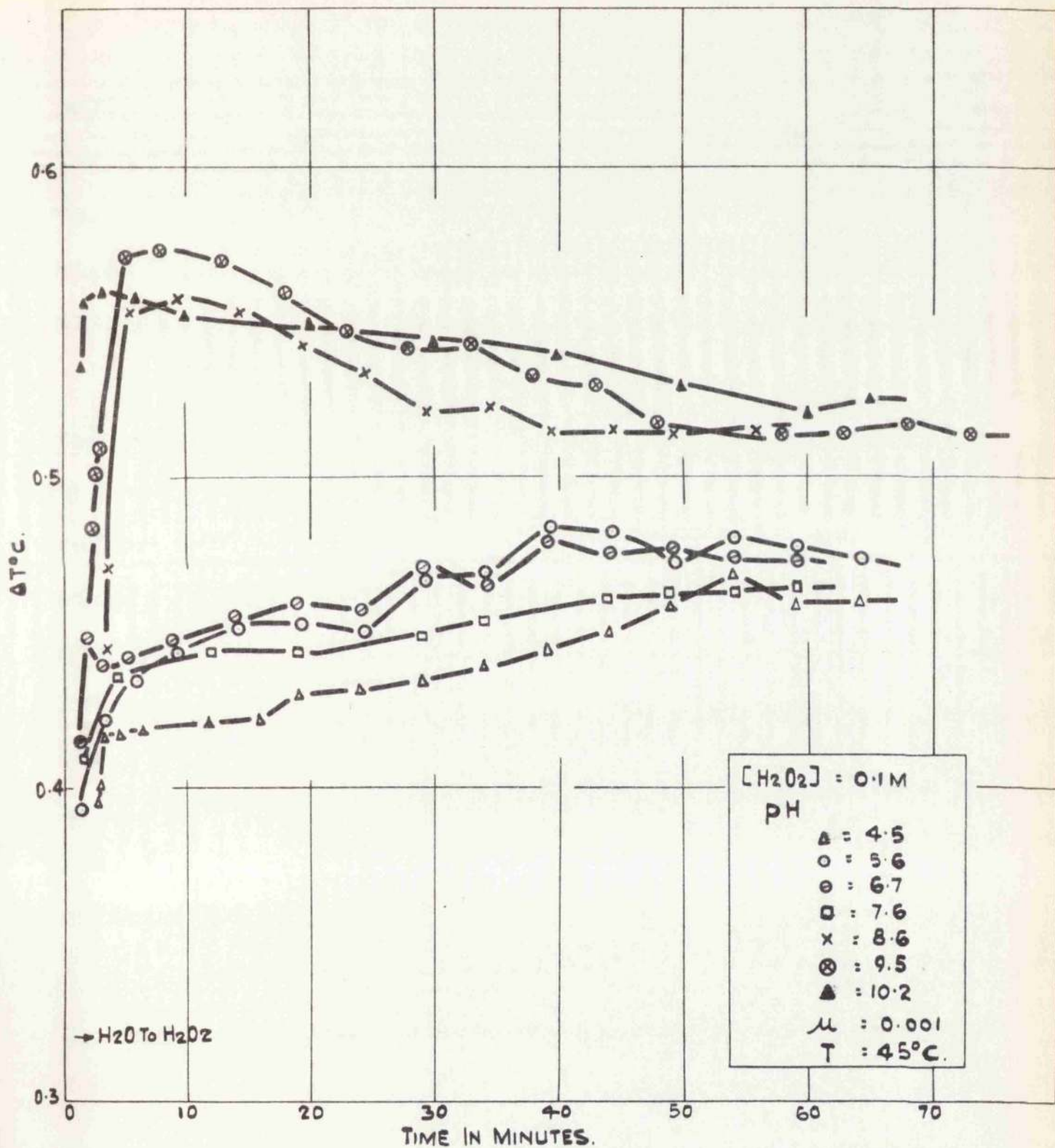


FIG. 41. VARIATION OF Cu_2O EFFICIENCY WITH pH. IN THE LOW CONCENTRATION ZONE.

The effect of pH is small. A distinct efficiency pattern can however be seen. At pH 4.5, 5.6, 6.7 and 7.6 the efficiencies lie in a tight band in which the individual values increase very slightly reaching steady levels after approximately 40 minutes. The steady values finally attained all agree to within 0.01 of a degree.

Above pH 7.6 a second band was obtained containing the results at pH 8.5, 9.5 and 10.2. In this case however the efficiencies decrease slightly before reaching steady values all of which lie approximately 0.05 degrees above the steady values obtained in the lower pH range. A considerable discrepancy arises between the two groups for the efficiency attained shortly after exposure to H_2O_2 . Thus at 10 minutes the efficiency at pH 6.7 is expressed as 0.12 and at pH 8.5 as 0.235. An "iso-pH" point clearly exists at about pH 8 i.e. the pH at which there is neither rise nor fall in efficiency after exposure to H_2O_2 .

8. The Rate of Copper Dissolution.

The rate of dissolution of copper was determined - as moles of copper per litre of effluent - at regular time intervals under each set of conditions. Although the results which are summarised in Figs.42 to 48 suggest that dissolution is not directly connected with efficiency several very interesting effects were observed. No variation in copper

dissolution was observed to parallel the efficiency changes so the time scale in Figs.42 to 48 merely covers the test period.

(a) 2 M to 0.25 M.

(i) $\boxed{H_2O_2}$ effect.

In the presence of H_2O_2 the rate of dissolution decreased with increasing $\boxed{H_2O_2}$ —(Fig.42)—until at 2 M dissolution was entirely suppressed. Since dissolution always took place in the presence of pure water this result suggests that an insoluble layer is formed on the catalyst surface at 2 M.

That dissolution is not simply connected with efficiency can be seen from Table 10 where a decrease in

$\boxed{H_2O_2}$	Rate of Dissolution moles/litre x 10^{-6}	Peak Efficiency	Minimum Efficiency	Final Efficiency	
				Total	Signoid
1.5 M	3	0.60	0.39	0.65	0.57
0.025 M	11	0.06	0.06	0.06	-

Table 10.

$\boxed{H_2O_2}$ from 1.5 M to 0.025 M produced much larger variations in efficiency than in rate of dissolution.

(ii) Ionic Strength Effect.

An increase in the ionic strength from 0.001 to 0.01

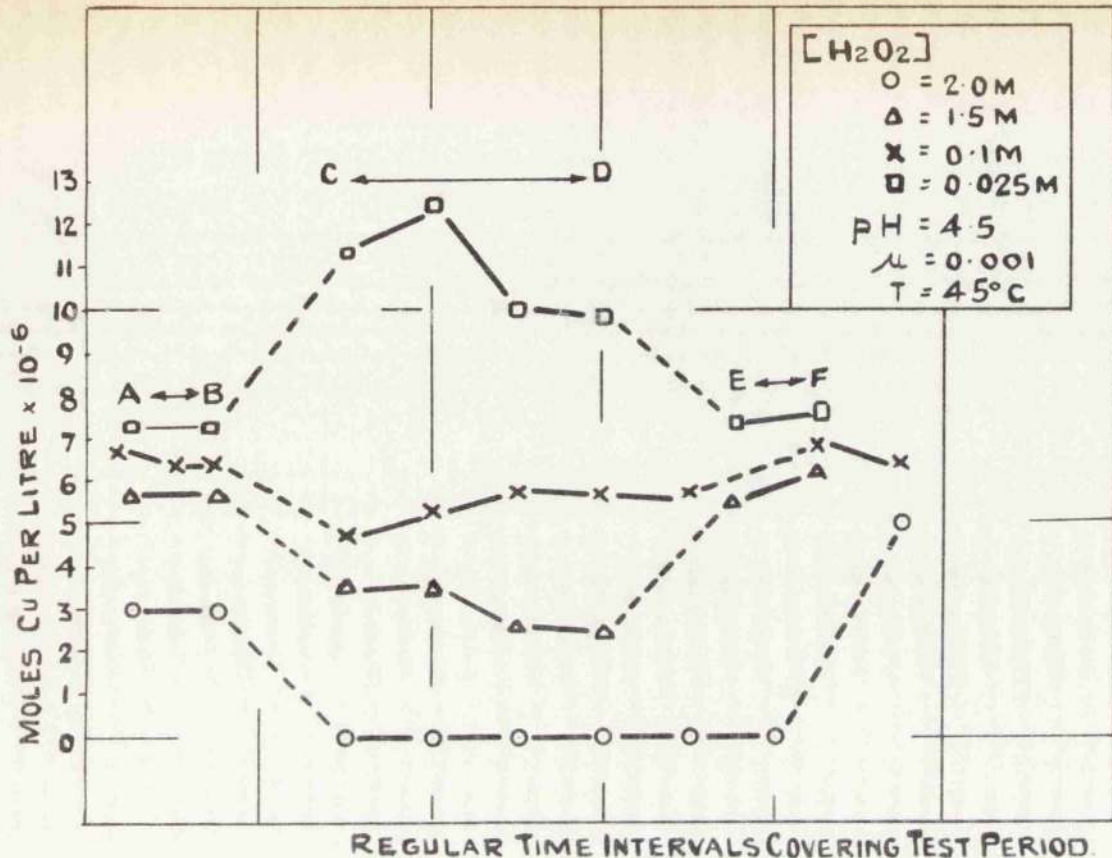


FIG. 42. THE EFFECT OF $[H_2O_2]$ ON THE RATE OF DISSOLUTION OF CU DURING - AB - INITIAL CONTACT WITH WATER. CD - DECOMPOSITION OF H_2O_2 EF - FINAL CONTACT WITH WATER.

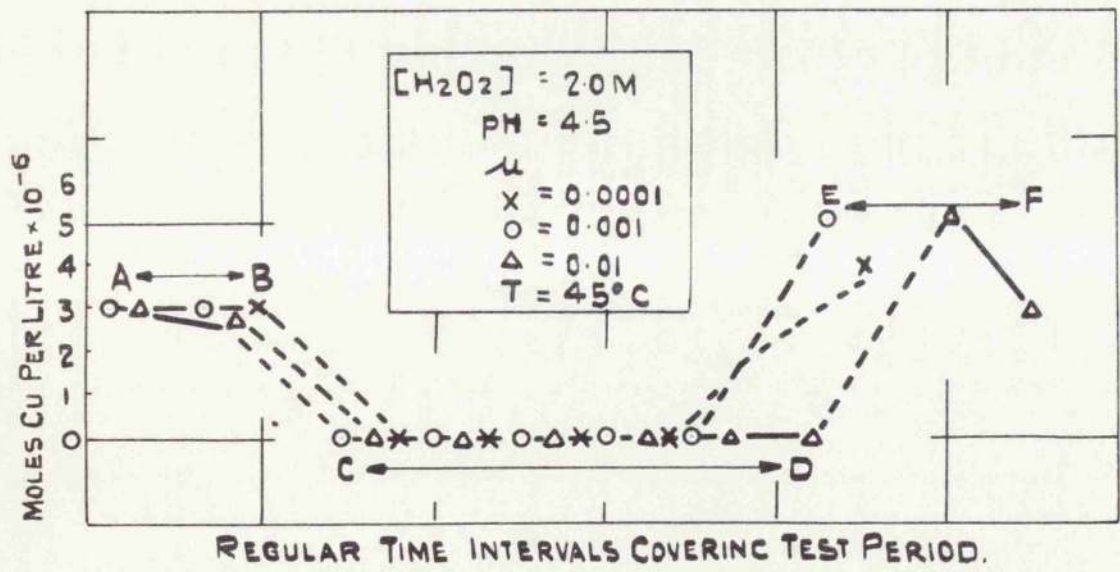


FIG. 43. THE EFFECT OF IONIC STRENGTH ON RATE OF DISSOLUTION OF CU IN THE HIGH $[H_2O_2]$ ZONE.

produced no alteration in the rate of dissolution either in the presence of water or in the presence of H_2O_2 (Fig.43). Efficiency was also unaltered by this change.

(iii) Temperature Effect.

An increase in temperature from $40^\circ C$ to $45^\circ C$ to $50^\circ C$, although producing an increase in efficiency, did not cause any significant alteration in rate of dissolution either in the presence of water or H_2O_2 (Fig.44). The close similarity between the rates obtained before and after treatment with H_2O_2 suggests that chipping of the catalyst surface occurs during catalysis producing the fluctuating results usually obtained.

(iv) pH Effect.

The effect of pH is shown in Fig.45. Between pH 4.5 and 8.0 the rate of dissolution in the presence of H_2O_2 remains fairly constant at about 3.5. In the presence of water however the rate of dissolution drops from 5.5 to 0.5 moles of $Cu \times 10^{-6}$ when the pH is increased from 4.5 to 5.15. Further increase in pH tends to reduce this rate almost to zero.

It appears that above pH 4.5 a fairly stable catalyst surface is formed in the presence of water. This stability however is insufficient to withstand the eroding action of H_2O_2 but is re-established when peroxide is replaced by water.

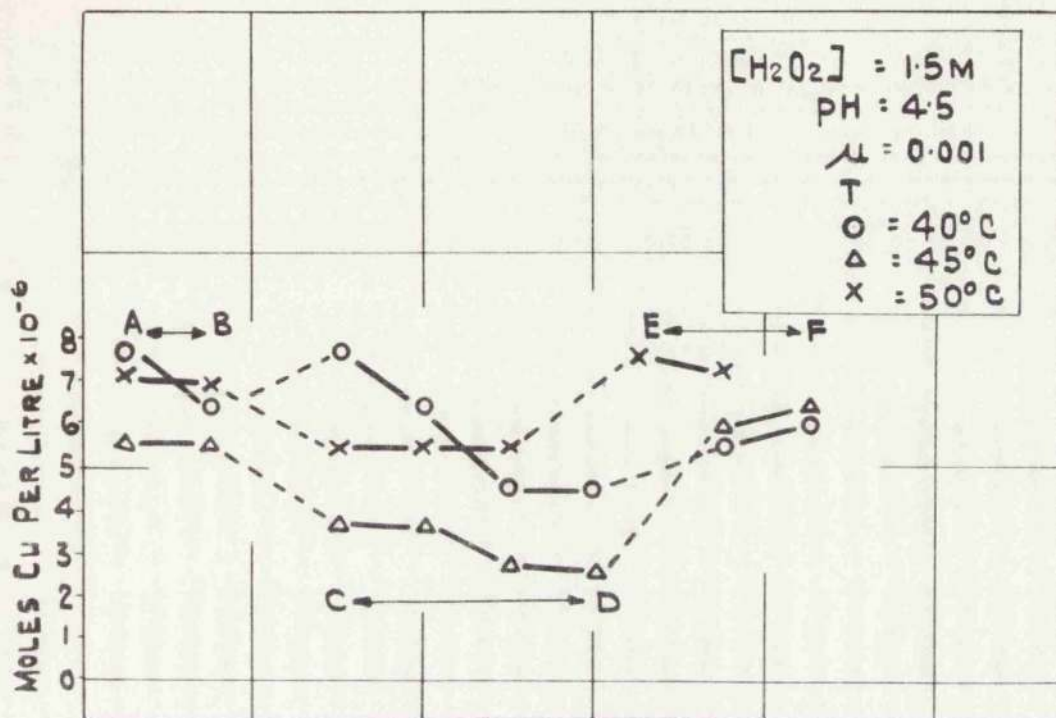


FIG. 44. THE EFFECT OF TEMPERATURE ON THE RATE OF CU DISSOLUTION IN THE HIGH $[H_2O_2]$ ZONE.

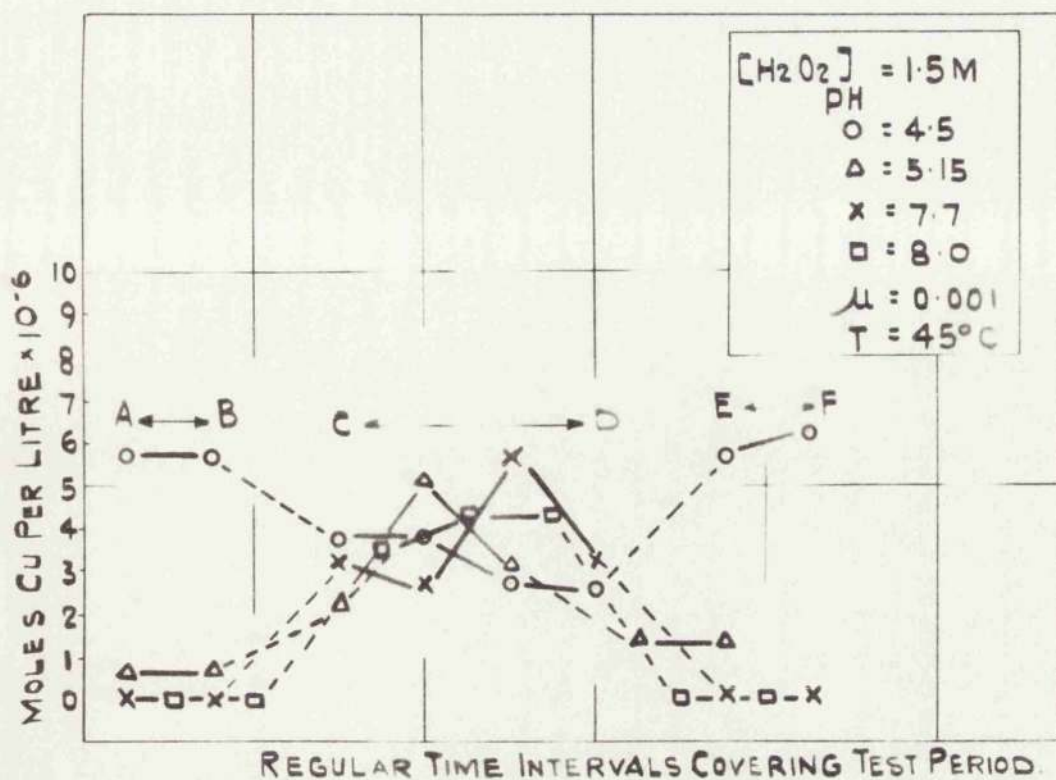


FIG. 45. THE EFFECT OF pH ON THE RATE OF CU DISSOLUTION IN THE HIGH $[H_2O_2]$ ZONE.

(b) 0.25 M to 0.025 M

(i) $[H_2O_2]$ Effect.

As above a decrease in $[H_2O_2]$ increased the rate of dissolution (Fig.42). At 0.025 M the rate actually exceeded by about 30% the rate in pure water, but at higher $[H_2O_2]$ there was always a tendency - increasing with increasing $[H_2O_2]$ - to suppress dissolution.

(ii) Ionic Strength Effect.

The effect of ionic strength in this concentration zone was similar to that encountered in the high concentration region. An increase in ionic strength from 0.0001 to 0.01 produced no increase in rate of dissolution during contact with water or during contact with H_2O_2 solution (Fig.46).

(iii) Temperature Effect.

During contact with water an increase in temperature produced a decrease in the rate of dissolution, a relationship which was re-established after catalysis (Fig.47). During contact with H_2O_2 no significant variation with temperature could be detected although the efficiency increased with increasing temperature.

(iv) pH Effect.

In agreement with results obtained in the high $[H_2O_2]$

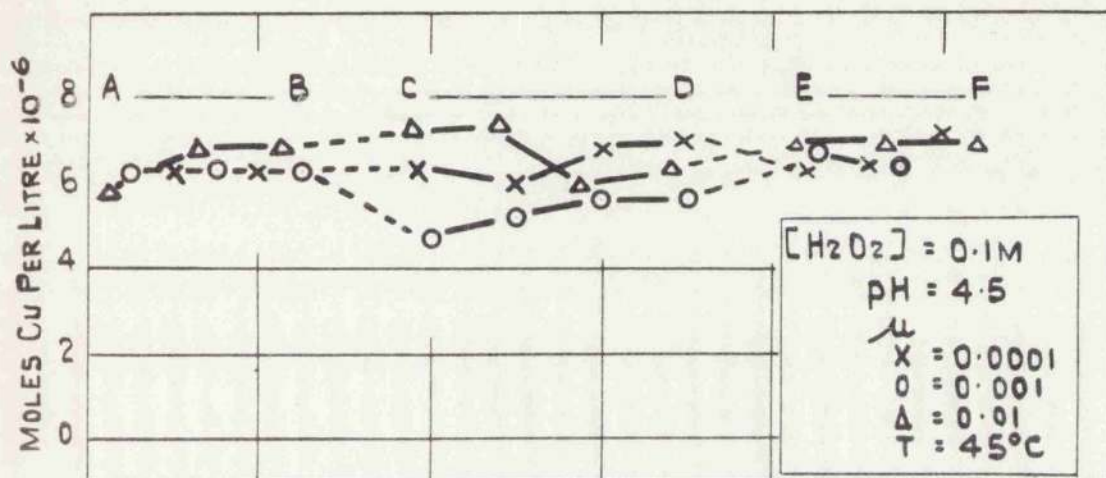


FIG. 46. THE EFFECT OF IONIC STRENGTH ON RATE OF DISSOLUTION OF CU IN THE LOW $[H_2O_2]$ ZONE.

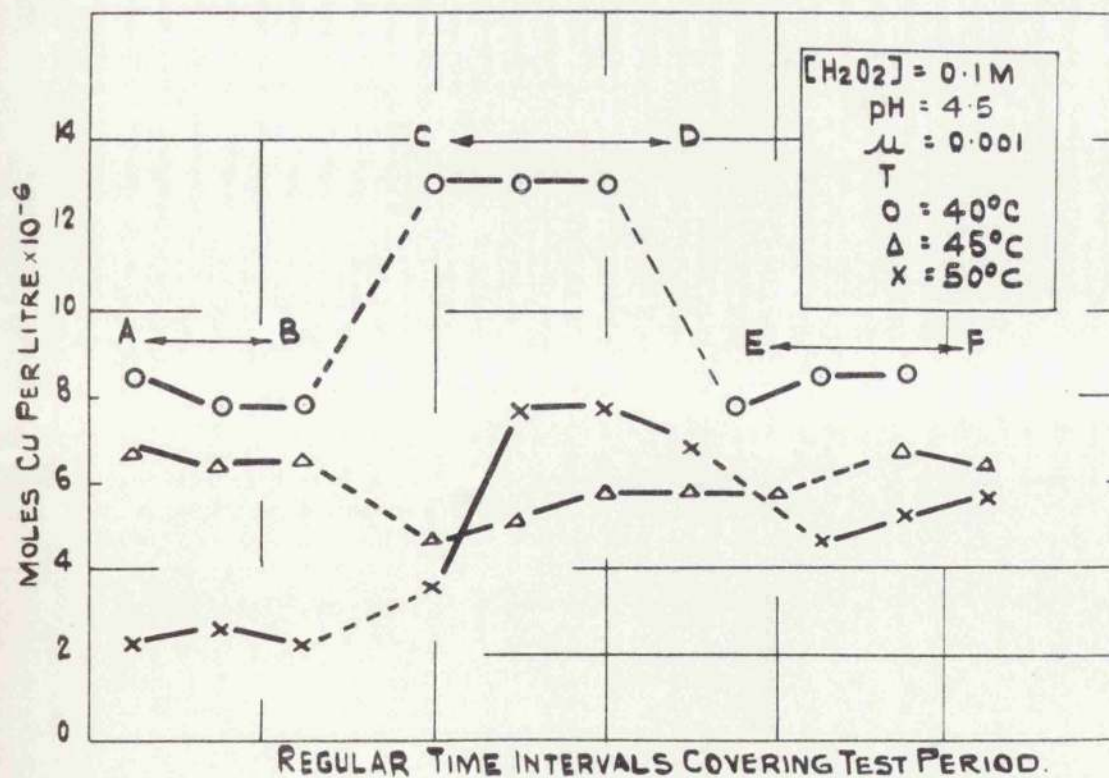


FIG. 47. THE EFFECT OF TEMPERATURE ON THE RATE OF DISSOLUTION OF CU IN THE LOW $[H_2O_2]$ ZONE.

zone, an increase in pH from 4.5 to 5.6 decreased the rate of dissolution during contact with water from $7 \cdot 10^{-6}$ moles per litre to $1 \cdot 10^{-6}$ moles per litre (Fig.48 a and b).

Further increase in pH reduced this value until dissolution had almost ceased at pH 7.

In this $\boxed{H_2O_2}$ zone the amount dissolved during catalysis is relatively high. Contrary to results obtained in the high $\boxed{H_2O_2}$ zone, increase in pH reduced this amount from $6 \cdot 10^{-6}$ at pH 4.5 to $3 \cdot 10^{-6}$ at 5.6. Continued increase in pH did not reduce the amount any further but it is interesting to note that this value is similar to the steady value obtained in the high $\boxed{H_2O_2}$ zone.

From the results detailed above the following general results are inferred.

A. During contact with H_2O_2 .

- (i) Increase in $\boxed{H_2O_2}$ reduces the amount of copper dissolved until none is dissolved at 2 M.
- (ii) Ionic strength does not influence the amount dissolved.
- (iii) Temperature does not affect the rate of dissolution.
- (iv) Increase in pH reduces the amount dissolved to a limit of $3 \cdot 10^{-6}$ moles/litre.

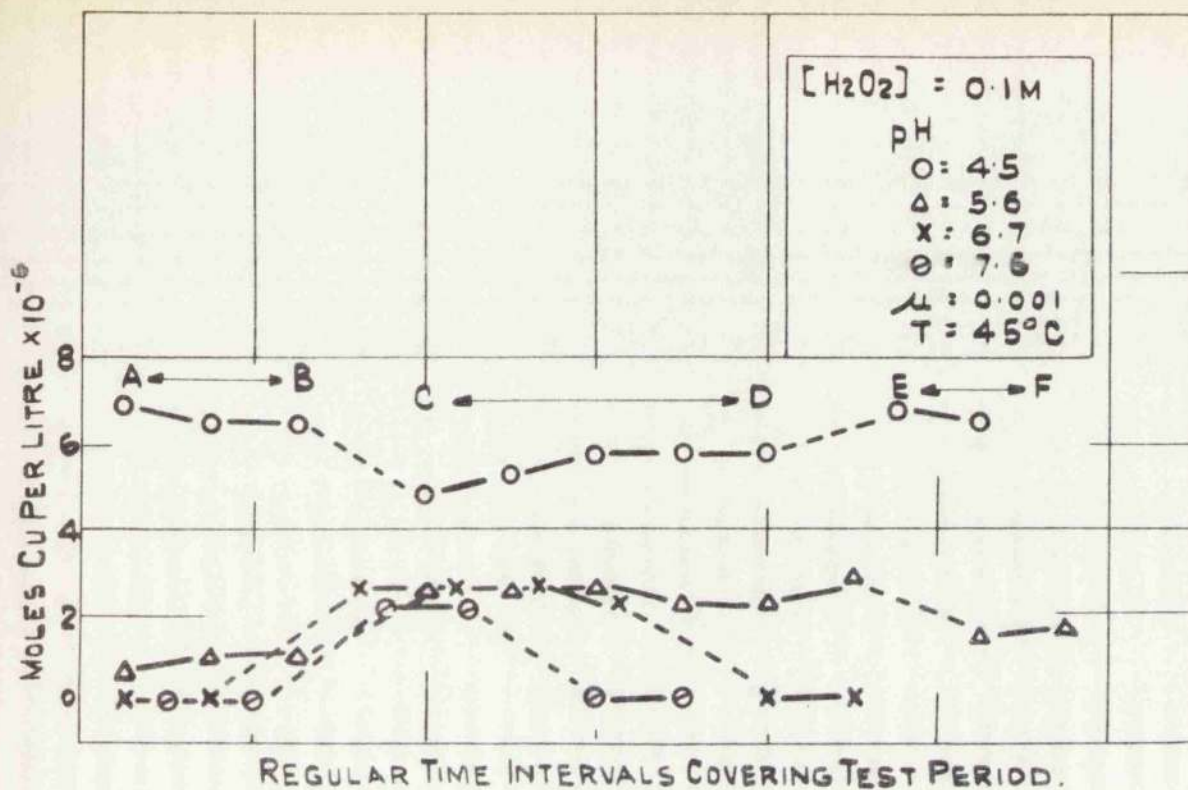


FIG. 48a.

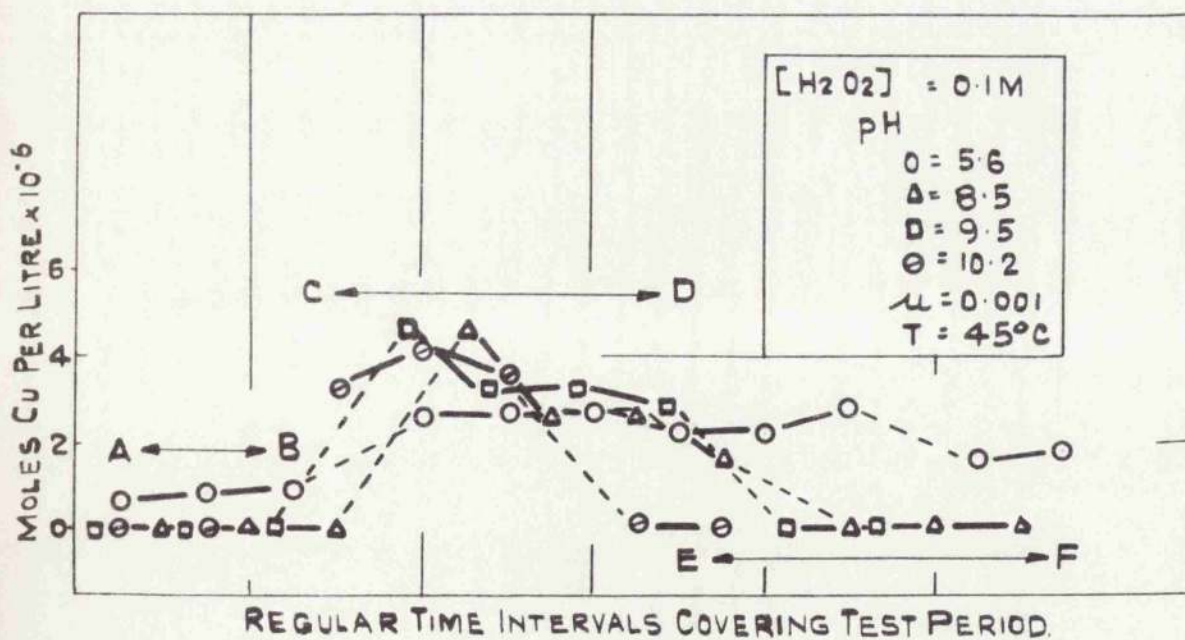


FIG. 48b.

FIG. 48a & b - THE EFFECT OF PH ON THE RATE OF DISSOLUTION OF CU IN THE LOW $[H_2O_2]$ ZONE.

B. During contact with H_2O

- (i) The amount dissolved before or after catalysis is independent of the amount dissolved during catalysis. $[H_2O_2]$ has therefore no permanent effect.
- (ii) Ionic strength has no effect on the amount dissolved.
- (iii) Temperature has a small adverse effect on the rate of dissolution.
- (iv) Increase in pH reduces the amount dissolved from about $6 \cdot 10^{-6}$ moles/litre at pH 5 to zero at about pH 7.

C. In all cases occasional evidence of micro particles of black oxide suggests an explanation for the wide variation in copper dissolved especially with H_2O_2 .

9. Characterisation of Possible Surface Composition.

The variations in efficiency of the catalyst during decomposition of high $[H_2O_2]$ solutions can be explained by the simple supposition that during prolonged contact with H_2O_2 a series of surface species are formed by

- (i) oxidation or reduction to a higher or lower valency state or
- (ii) compound formation e.g. of hydroperoxide or peroxide.

If such a series of surface states existed each being

responsible for a different catalytic efficiency, variations in the surface equilibrium potential might permit identification of the various surfaces in the light of known surface equilibrium potentials.

The potential results are described below.

The cuprous oxide electrodes were prepared by alternate oxidation and reduction of degreased Cu wire in the same manner as for the catalyst. The equilibrium potential of the electrode was determined

- A. in water before and after exposure to H_2O_2 and
- B. throughout the whole of the catalytic period.

A. $\text{Cu}_2\text{O}/\text{H}_2\text{O}$.

The potential of a freshly prepared $\text{Cu}_2\text{O}/\text{H}_2\text{O}$ surface was always found to be -0.06 volts (i.e. negative to the S.C.E.). After contact with H_2O_2 the $\text{Cu}_2\text{O}/\text{H}_2\text{O}$ half-cell returned to a potential lying between $+0.03$ volts and $+0.05$ volts. Even if the exposed electrode was allowed to remain in water for several days or was baked for 1 hour at 120°C , a negative potential could not again be obtained.

B. $\text{Cu}_2\text{O}/\text{H}_2\text{O}_2$.

(a) 2 M to 0.25 M

Immediately the H_2O was replaced by H_2O_2 the potential rose rapidly to a peak value. Following the peak

value a cyclic change occurred which was similar to the variations observed in the measurement of catalyst efficiency during decomposition, i.e a decrease to a minimum followed by an increase to a steady state.

Fig.49 shows the potential changes obtained from successive tests on one Cu_2O electrode. These changes are:-

- (i) A rapid increase in potential immediately following the change from H_2O to H_2O_2 .
- (ii) In each case the potential underwent the above cyclic change. The fall to the minimum was small i.e. approximately 0.015 volts (inset, Fig.49) but definite and similar in form to the efficiency fall to the minimum.
- (iii) A reproducible final steady state, preceded by an increase from the minimum was always obtained. It was independent of $\boxed{\text{H}_2\text{O}_2}$.
- (iv) A slow decrease in potential followed the change back to water.
- (v) Fig.50 shows the results obtained from a fresh Cu_2O electrode and a fresh, degreased, bare Cu electrode. The potential changes are similar in all respects adding weight to the contention that the thin oxide film always present on metals behaves similarly to a definite oxide surface.

EQUILIBRIUM POTENTIAL IN VOLTS VS. STANDARD CALOMEL ELECTRODE.

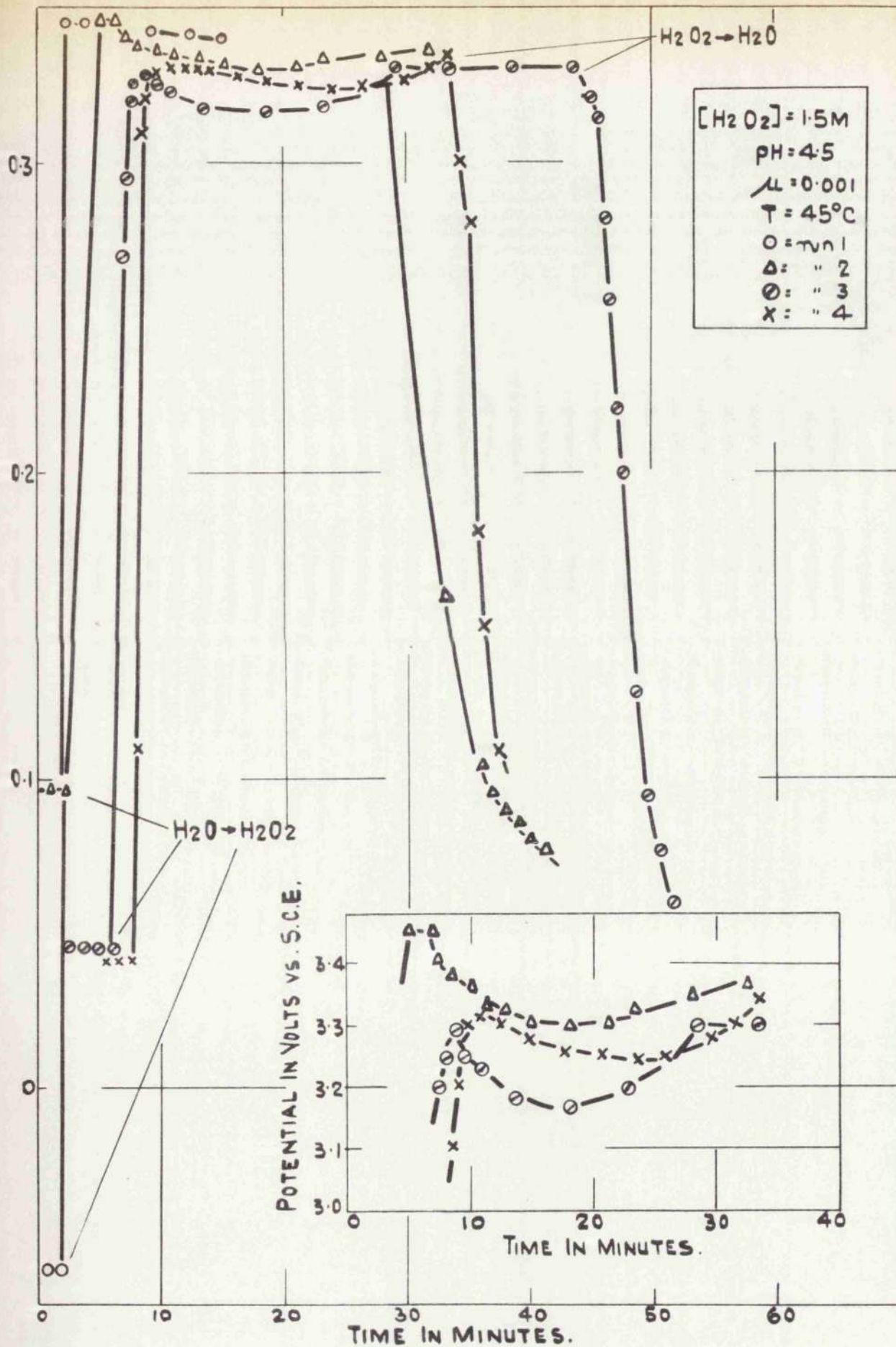


FIG. 49. VARIATIONS IN POTENTIAL OF Cu_2O ELECTRODE (Q) IN WATER BEFORE AND AFTER EXPOSURE TO H_2O_2 (b) THROUGHOUT THE WHOLE CATALYTIC PERIOD.

EQUILIBRIUM POTENTIAL IN VOLTS VS S.C.E.

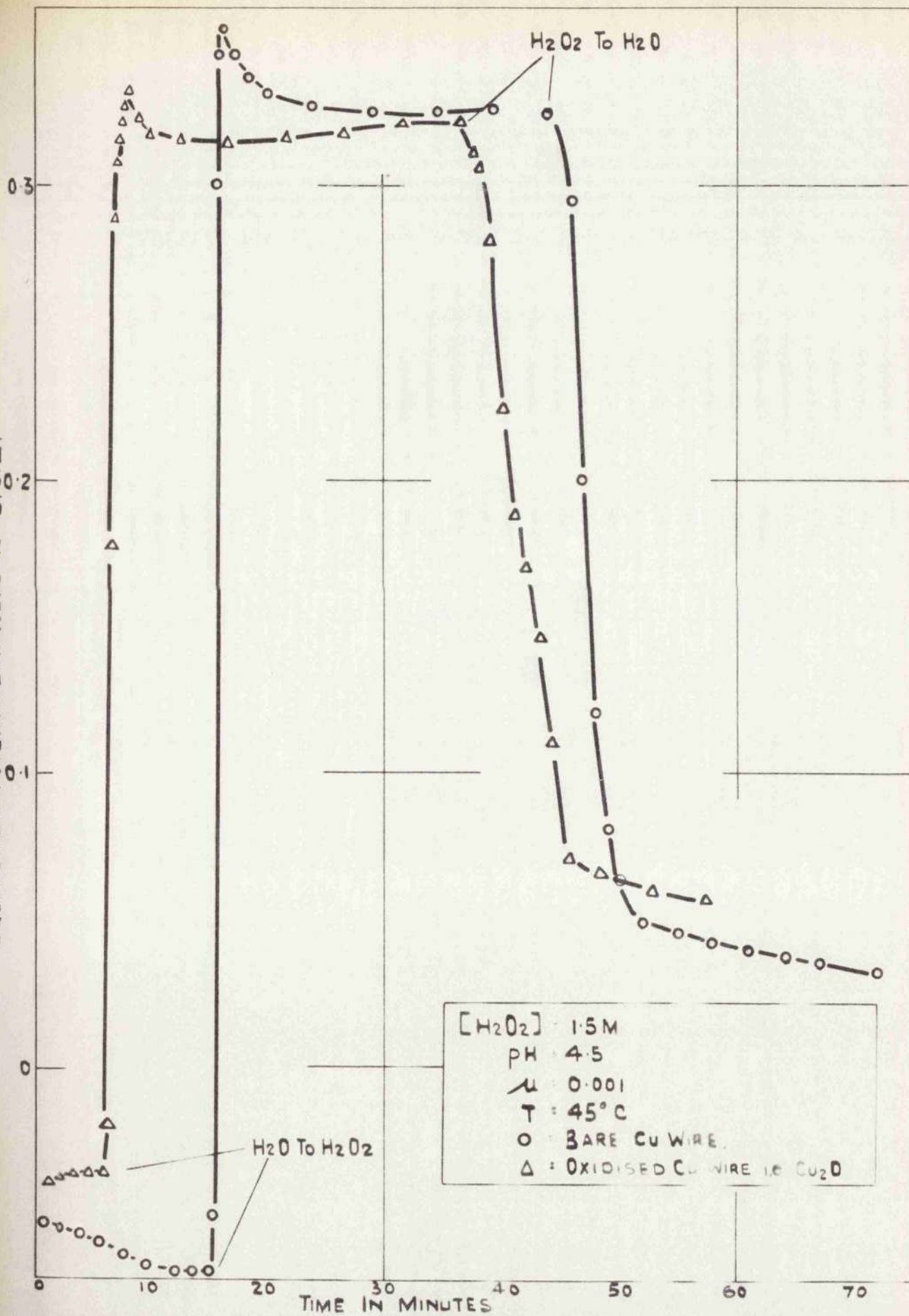


FIG. 50. VARIATIONS IN POTENTIAL OF A CU AND Cu_2O ELECTRODE.

(b) 0.25 M to 0.025 M

In the low concentration zone (Fig.51) the change from H_2O to H_2O_2 was accompanied by an increase in potential to a value which remained constant during prolonged contact with H_2O_2 . No cyclic changes in potential were observed which is in agreement with efficiency results obtained in this $[H_2O_2]$ zone.

The change from H_2O_2 back to H_2O was accompanied by a slow decrease in efficiency as observed in the higher $[H_2O_2]$ region.

(c) Effect of $[H_2O_2]$ on Steady Potential Values of Cu_2O/H_2O_2 Half-cell.

The variation with $[H_2O_2]$ of the final steady potential is shown in Figs.51 and 52.

Above 0.25 M the potential is unaffected by $[H_2O_2]$ and satisfies the relationship

$$e = 0.87 - 0.063 \text{ pH}$$

This equation was found by Bockris and Oldfield¹⁰² to express the variation of potential of gold and platinum electrodes in the $[H_2O_2]$ zone 5 M to 10^{-6} M. A similar relationship was shown by Hart, Aitken and Beaton¹⁰³ to apply to Ag for $[H_2O_2]$ of 0.1 and upwards.

Below 0.5 M the potential is proportional to

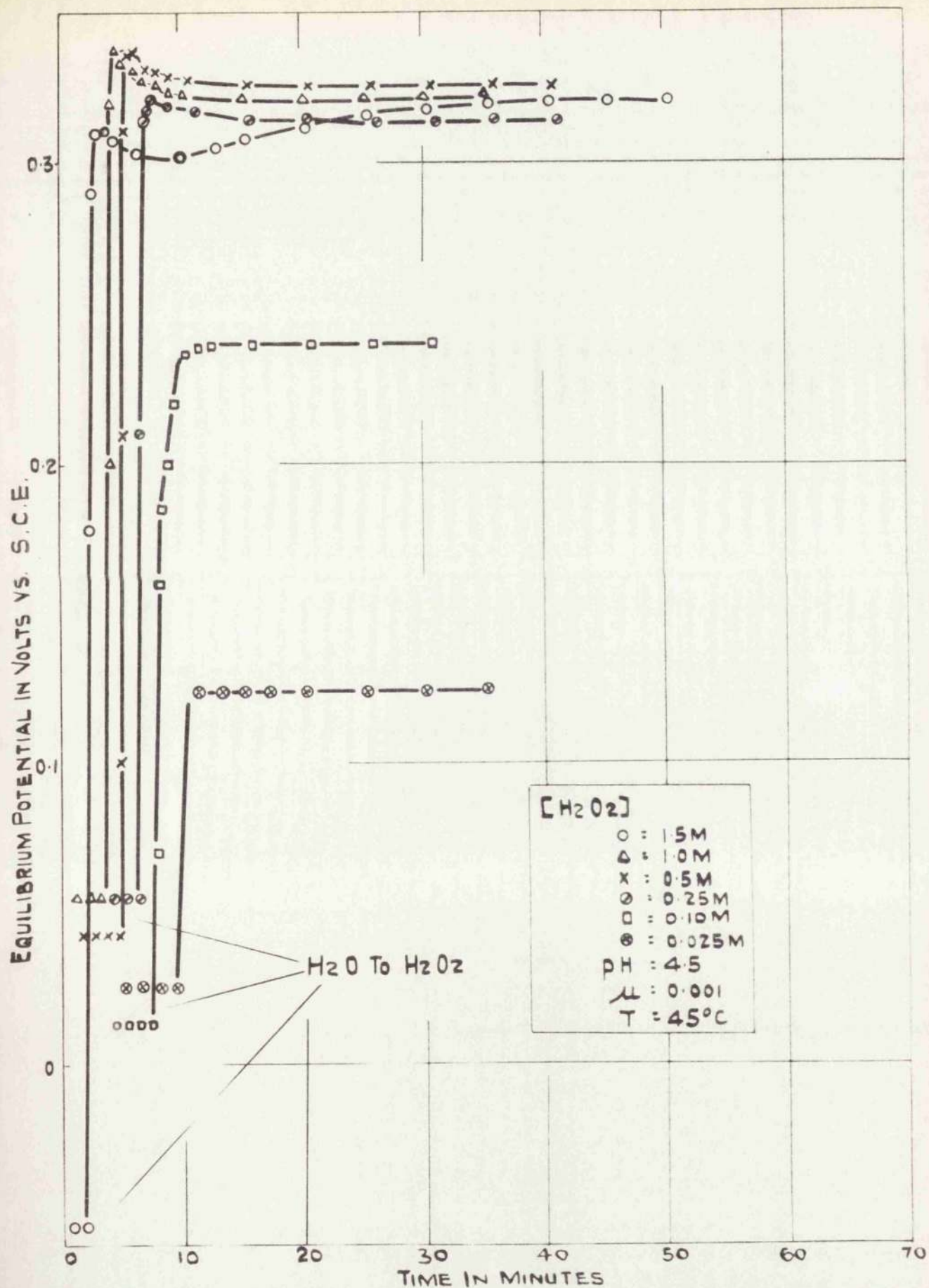


FIG 51. SHOWING (a) THE EFFECT OF [H₂O₂] ON THE FINAL POTENTIAL OF THE HALF-CELL Cu₂O/H₂O₂ (b) THE POTENTIAL VARIATIONS IN THE LOW [H₂O₂] ZONE FOLLOWING THE CHANGE H₂O TO H₂O₂.

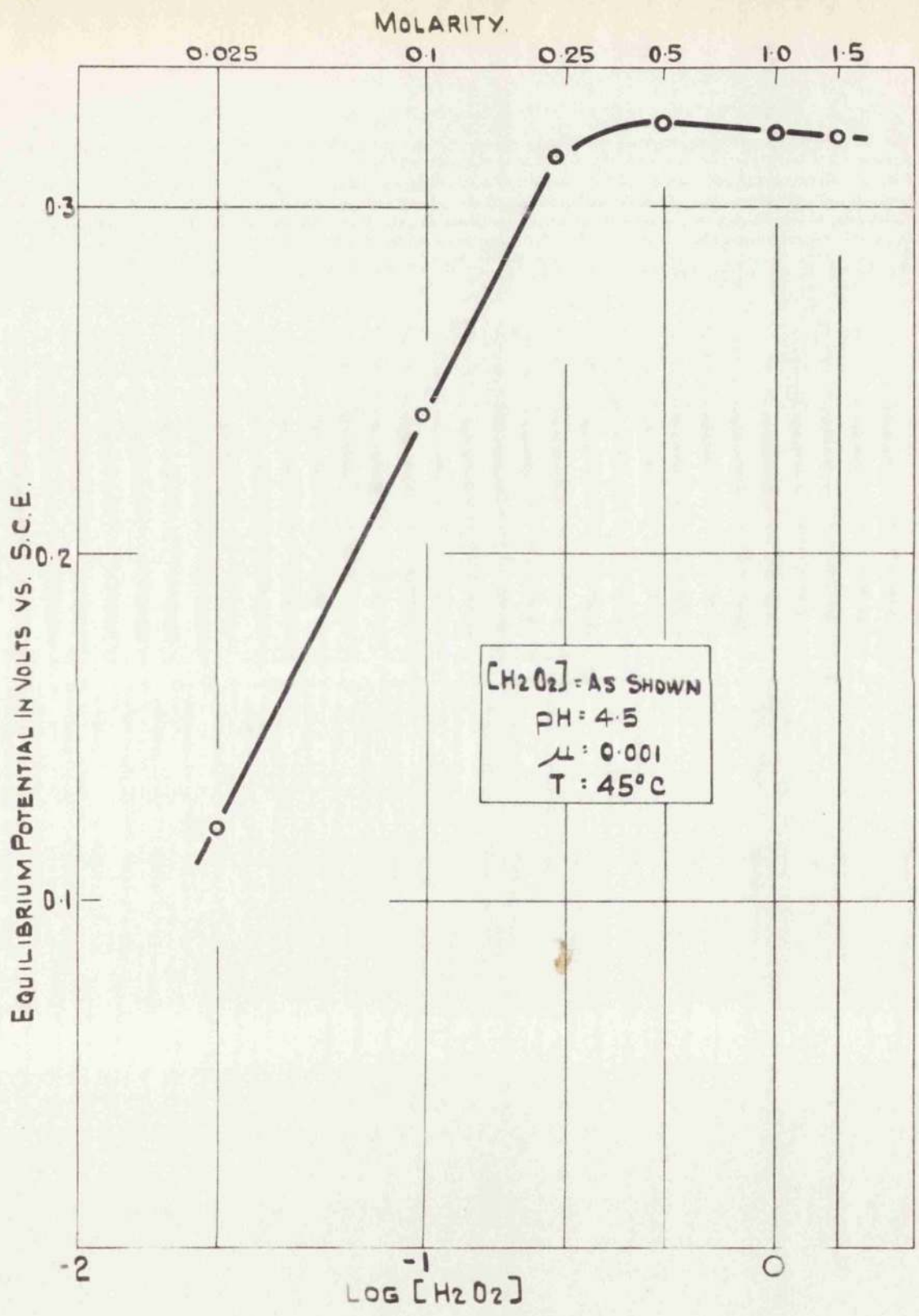


FIG. 52. SHOWING THE VARIATION WITH [H₂O₂] OF THE FINAL POTENTIAL OF THE HALF-CELL Cu₂O/H₂O₂.

$\log_{10} [\text{H}_2\text{O}_2]$. (Fig 52).

(d) Potential Decline Following the Change H_2O_2 to H_2O .

A close examination of the potential was made following the change from H_2O_2 to H_2O . The following points were noted:-

- (i) The potential fell relatively slowly in spite of the rapid replacement of the H_2O_2 by H_2O (Fig.53).
- (ii) Oxygen continued to be evolved even when no H_2O_2 could be detected in the electrode chamber.
- (iii) The potential seemed to be related to the rate of evolution of oxygen. In Fig.53 oxygen continued to be evolved until point B and the increase in potential noted at point A was accompanied by an increase in the rate of evolution of oxygen.

A cessation in oxygen evolution - point B - was accompanied by a decrease in the rate of fall of potential.

- (iv) A brief but rapid evolution of oxygen occurred from the Cu_2O electrode when H_2O was moved across a surface which had been surrounded by still H_2O for 24 hours after treatment with H_2O_2 . In addition traces of H_2O_2 could be detected in the effluent at this point.

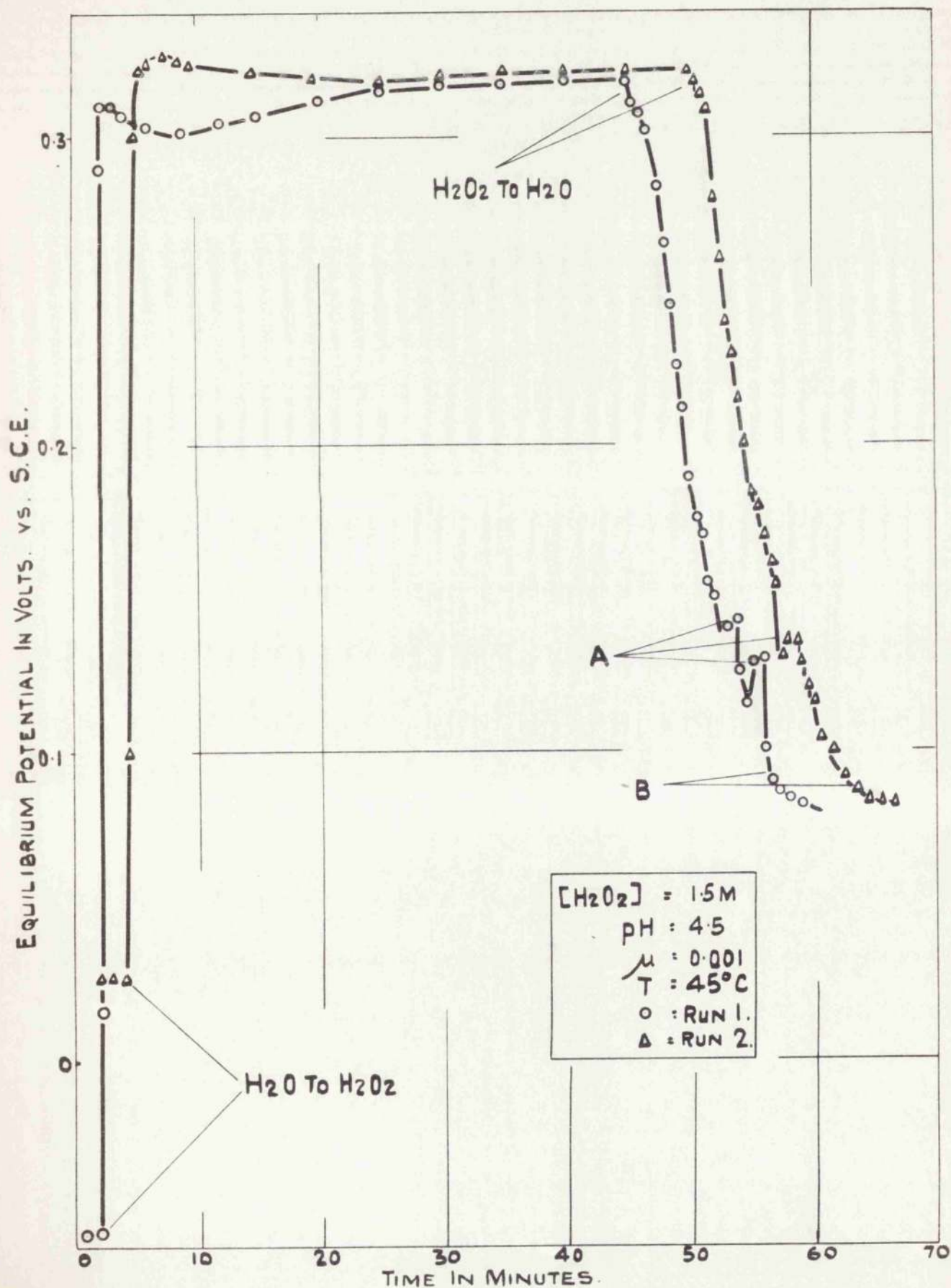


FIG. 53. SHOWING THE FALL IN POTENTIAL ON THE CU ELECTRODE FOLLOWING THE CHANGE H₂O₂ TO H₂O

(i), (ii) and (iii) suggest that H_2O_2 exerts two influences on the electrode surface i.e.

1. Accompanying the change H_2O to H_2O_2 the potential rises rapidly due to the production of a species on the catalyst surface which controls the potential. On removal of H_2O_2 this species slowly reverts to its previous state causing a relatively slow fall in potential.
2. A moderately stable compound is formed on the catalyst surface.

The following figures (Table 11) give the potential of the Cu/Cu_2O electrode under the conditions of the above experiments. The values given are referred to the S.C.E. at $45^\circ C$. This can be corrected if necessary to the standard hydrogen scale by adding 0.230 i.e. the potential of the S.C.E. at $45^\circ C$ relative to H_2 .

Half-cell	Potential	Results	Average Potential		
Fresh Cu_2O in $\text{Cu}_2\text{O}/\text{H}_2\text{O}$	-0.06 :	-0.04 :	-0.07	-0.056	
H_2O_2 treated Cu_2O in $\text{Cu}_2\text{O}/\text{H}_2\text{O}$	+0.04 :	+0.044 :	+0.054 :	+0.054	+0.037
	+0.042 :	+0.026 :	+0.012 :	+0.03	
$\text{Cu}_2\text{O}/\text{H}_2\text{O}_2$					
(a) Peak	+0.345 :	+0.345 :	+0.330 :	+0.332	
	+0.332 :	+0.350 :	+0.338 :	+0.338	+0.333
	+0.310 :	+0.320 :	+0.330		
(b) Minimum	+0.330 :	+0.324 :	+0.318 :	+0.324	
	+0.30 :	+0.31 :	+0.32 :	+0.326	+0.319
(c) Final	+0.330 :	+0.334 :	+0.336 :	+0.326	
	+0.326 :	+0.314 :	+0.320		+0.327

Table 11.

10. Surface Area Determination

The surface area of the Cu_2O catalyst used in the catalytic studies was determined as described above.

After each addition of ethylene the number of moles adsorbed - N_x - and the equilibrium pressure attained - p_x - were determined from the relationships

$$PV = N_xRT$$

where P is the pressure drop due to adsorption

and V is the apparatus volume involved

and

$$p_x = \left(\frac{h_1 + h_2}{2} \right)^2 \times 6.342 \cdot 10^{-6} \text{ m.m. (pp.61 above)}$$

(columns 1 and 2 Table 12).

N_x moles $\times 10^{-7}$	p_x mm $\times 10^{-3}$	$p_0 - p_x$ mm $\times 10^{-3}$	$\frac{p_x}{N_x(p_0 - p_x)} \times 10^3$	$\frac{p_x}{p_0}$
6.3	0.08	30.4	4.3	0.003
21.1	0.16	30.3	2.5	0.0053
36.3	0.32	30.2	2.92	0.0107
55.9	1.0	29.5	6.06	0.033
78.9	2.5	28.0	11.2	0.0834
103.3	4.8	25.7	18.2	0.16
123.0	7.92	22.5	28.7	0.264
138.0	10.02	20.5	35.4	0.33
154.3	13.4	17.1	50.8	0.45

Table 12.

The plot of p_x against N_x (Fig.54) indicated typical multilayer adsorption. No clear indication of the completion of a monolayer - "B point" - could be seen from the isotherm and the Brunauer, Emmett and Teller¹⁰⁴ theoretical treatment of multilayer adsorption was used to calculate

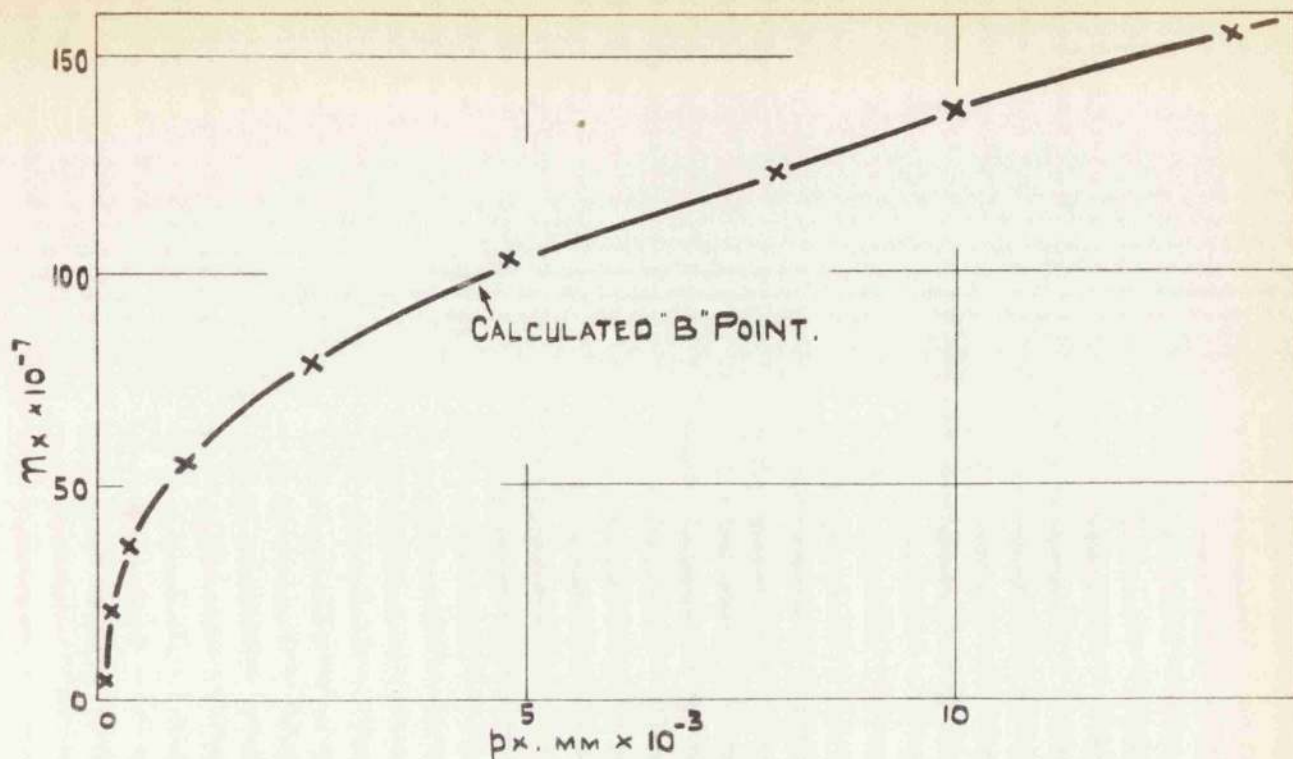


FIG. 54. SURFACE AREA ISOTHERM ($\text{C}_2\text{H}_4: -183$) FOR Cu_2O SHOWING CALCULATED "B" POINT.

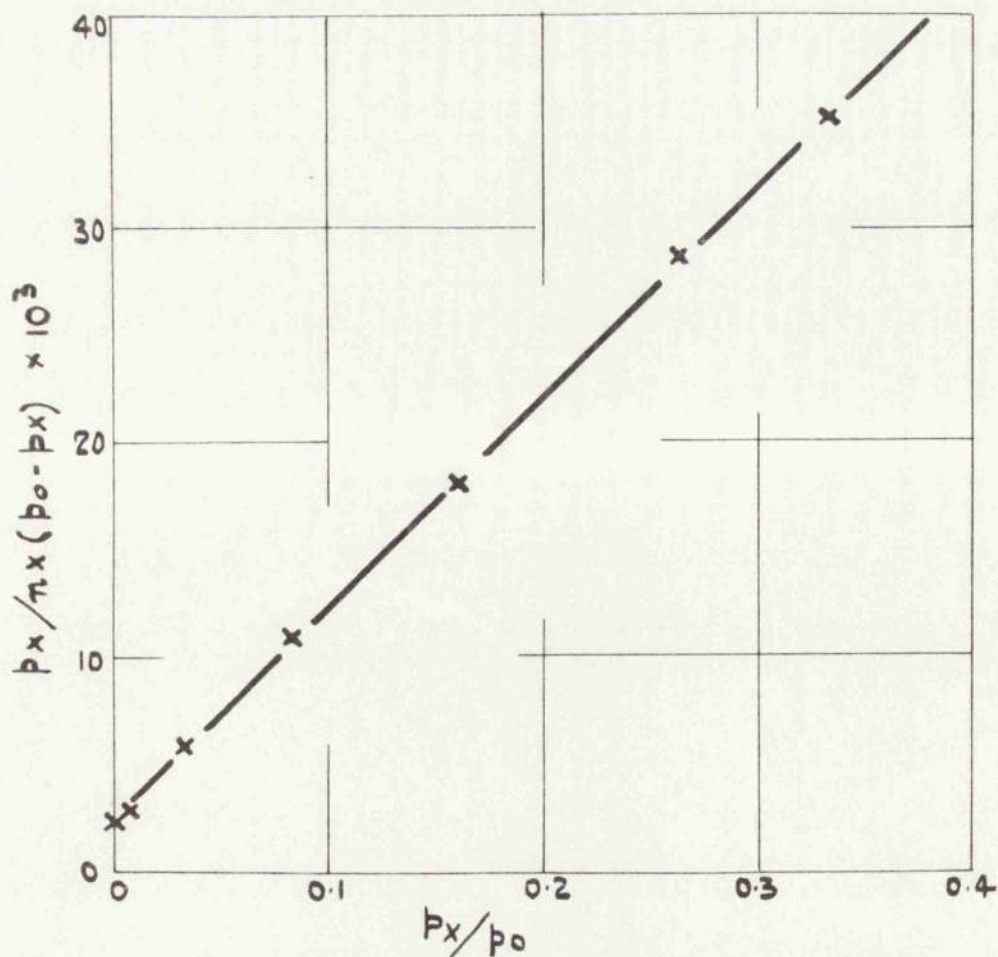


FIG. 55. B.E.T. ESTIMATION OF THE VOLUME OF THE MONOLAYER ADSORBED ON Cu_2O .

the volume of the monolayer.

From the B.E.T. treatment

$$\frac{px}{Nx(po - px)} = \frac{1}{Nm \cdot C} + \frac{C - 1}{Nm \cdot C} \cdot \frac{px}{po}$$

where Nx = number of moles adsorbed at pressure px

Nm = number of moles adsorbed when the entire surface is covered by a unimolecular layer

po = saturated vapour pressure ($30.5 \cdot 10^{-3}$ m.m.Hg for C_2H_4 at $-183^\circ C$)

$C = \exp. (E_1 - E_L)RT$

E_1 = heat of adsorption of 1st layer

E_L = latent heat of vapourisation

According to this equation a plot of $\frac{px}{Nx(po - px)}$ against $\frac{px}{po}$ should give a straight line where

$$\text{slope} = \frac{C - 1}{Nm \cdot C} \quad \text{and intercept} = \frac{1}{Nm \cdot C}$$

from which Nm can be calculated. By plotting Nx against $\frac{px}{po}$, Nm can also be determined from the point of inflection po on this curve.

The values of $(po - px)$, $\frac{px}{Nx(po - px)}$ and $\frac{px}{po}$ were

calculated - columns 3, 4 and 5 Table 12 - and $\frac{px}{Nx(po - px)}$ plotted against $\frac{px}{po}$. A straight line was obtained (Fig.55) from which

$$\text{Slope} = 9.9 \cdot 10^4 = \frac{C - 1}{Nm \cdot C} \quad \text{and Intercept} = 2.7 \cdot 10^3 = \frac{1}{Nm \cdot C}$$

$$\therefore C = 37.7 \quad \text{and} \quad Nm = 9.83 \cdot 10^{-6}$$

Since 1 c.c. m.m. of adsorbed ethylene covers 57.2 cm^2
(Wooten and Callaway-Brown¹⁰⁵) 1 mole covers $1.045 \cdot 10^9 \text{ cm}^2$

$$\begin{aligned} \therefore Nm \text{ moles cover } & 1.045 \cdot 10^9 \cdot 9.83 \cdot 10^{-6} \text{ cm}^2 \\ & = 1.03 \cdot 10^4 \text{ cm}^2 \end{aligned}$$

Since approximately 10% by weight of the total catalyst was used for surface area determination the total surface area was estimated at $1 \cdot 10^5 \text{ cm}^2$.

DISCUSSION1. Introduction.(a) Object.

The object was to study under flow conditions the catalytic decomposition of aqueous H_2O_2 by semiconducting metal oxides and in particular to investigate changes occurring in the catalyst efficiency during the non-steady part of the process. Results from the Cu_2O/H_2O_2 system show that marked and characteristic catalytic efficiency changes take place before a steady rate process is achieved.

(b) Origin of Recorded Temperature Differences.

It is necessary to establish clearly the origin of the recorded temperature differences since it is possible that they are not associated with the efficiency of the catalyst but are caused by some temperature effect of different origin. It is reasonable to neglect (a) a temperature control effect or (b) a heat of decomposition effect, since the temperature of the substrate immediately before the catalyst remains constant and the temperature rise caused by decomposition is so small that there can be no question of it measurably affecting the efficiency.

It can be concluded therefore that the temperature variations do reflect true changes in catalyst efficiency.

(c) Diffusion Control.

Rate processes controlled by diffusion to a surface are common in solid/liquid systems. The step is characterised by first order kinetics and activation energies of between 3 and 5 kcal.

First order dependence on $[H_2O_2]$ occurs in the Cu_2O/H_2O_2 system at the initial peak in the high $[H_2O_2]$ region and at the steady state in the low $[H_2O_2]$ zone, but neither stage can be considered diffusion controlled since they have high temperature coefficients leading to activation energies of 16.5 and 19.5 kcal. respectively.

Rejection of solution phase diffusion as the limiting factor is supported by the widely different rates obtained with Ag_2O , Cu_2O , NiO and CoO under identical experimental conditions. With 0.35 M H_2O_2 a steady efficiency equivalent to $0.675^\circ C$ was quickly attained using 1" length of 0.011" diameter oxidised Ag wire. At this same $[H_2O_2]$ 72" of 0.036" diameter oxidised Cu wire reached a steady state of $0.7^\circ C$, 142" of 0.036" diameter oxidised Ni wire gave no detectable decomposition and 36" of 0.036" diameter oxidised Co wire reached $0.4^\circ C$.

Decomposition is clearly surface controlled and subsequent discussion is based on this conclusion.

(d) Temperature Coefficient.

The temperature coefficient is usually obtained by measuring the steady reaction rate at a series of temperatures

from which a plot of $\log_{10} k$ against $\frac{1}{T}$ should yield a straight line with a slope equal to $-\frac{E_A}{2.3 \cdot R.T.}$

It is a common feature in kinetic data of reactions occurring on solid surfaces that the energy of activation varies with the initial temperature from which the temperature changes are made. It is usual to consider this compensation effect as an entropy of activation which changes proportionally to the activation energy i.e.

$$\text{rate} = k_0 \cdot \exp. \left[\frac{S + \Delta S^\ddagger}{R} \right] \exp. \left[\frac{-E - \Delta E^\ddagger}{RT} \right]$$

with $\Delta S^\ddagger = f \Delta E^\ddagger$

Zwietering and Roukens¹⁰⁶ explained this compensation effect as due to a transition, from the immobile to the mobile state, of the activated complex which accompanied the decrease of adsorption energy and the rise of activation energy with increasing coverage.

Ross⁴⁹ noted this effect in his investigations of the vapour phase decomposition of H_2O_2 by semiconducting metal oxides (Table 13) where he assumed that the surface came to an activity equilibrium when exposed to a constant temperature

Temperature of Change. °C.	Activation Energy. kcal./mole
76 - 58	13.2 ± 0.5
58 - 100	11.8 ± 0.5
100 - 38	13.4 ± 0.5

Table 13.

the level of which determined the level of the activity equilibrium.

A similar explanation has been proposed by Roginskii and Tselinskaya¹⁰⁷ who envisaged a surface composed of sites of varying energy whose influence therefore varied with temperature.

Determination of the temperature coefficient in the present work was confined to the range 40°C to 50°C. At such a level ionic defects can be considered immobile and the variation of activation energy with temperature negligible. Under these circumstances it is to be expected that activation energy remains constant varying only according to a variation of the rate controlling step and the adsorption of a rate changing species.

2. Efficiency Changes with Cu₂O.

As stated above the results may be considered:-

- (a) at high $[H_2O_2]$ - 2 M to 0.25 M
- (b) at low $[H_2O_2]$ - 0.25 M to 0.025 M.

(a) 2 M to 0.25 M

Six stages can be recognised in this zone (Fig.23).

1. An initial rapid increase in efficiency to a peak value.
2. A peak efficiency.
3. A relatively slow fall from the peak efficiency.
4. A minimum efficiency.

5. A slow recovery in efficiency.

6. A final steady efficiency.

1. Initial rapid increase.

There are two possible explanations for the observed initial increase:-

- (i) The values are significant and refer to a real catalyst efficiency increase on contact with H_2O_2
- (ii) The effect is due to the setting up of concentration equilibrium in the solution following the change from H_2O to H_2O_2 .

If (i) then a change affecting the oxide in depth must be ruled out since the process is very rapid. There may be however a surface exchange reaction such as



or one in which some active radical or radical ion is created as discussed below. In any case there is no doubt that (ii) must also be considered and to unravel the details of any process such as (i) with a background of (ii) would be impossible with the present apparatus.

2. Peak efficiency.

The significance of the peak efficiency might be ambiguous if it is considered an arrest; i.e. a condition where a rising efficiency is overtaken by a declining process.

A true initial efficiency could perhaps be obtained by projecting the efficiency decline curve back to zero time, if there was an accurate knowledge of the law governing the decline.

If it is assumed that the steady solution conditions are established linearly with time for all solutions it may follow that the measured peak efficiency will vary in the same manner with $[H_2O_2]$ etc. as would a "true initial peak" value.

The experimental properties of the peak rate are:-

- (i) Peak efficiency = $k + k' [H_2O_2]$
- (ii) It is independent of pH and ionic strength.
- (iii) The activation energy is 16.5 kcal. as calculated

$$\text{from } E = RT^2 \frac{d \ln(\text{peak efficiency})}{dt} \text{ at } 1.5 \text{ M}$$

The activation energy values are regarded as little more than an indication of the size of the temperature effect.

3. Decline from the peak efficiency.

The peak efficiency was slowly poisoned, reaching a minimum value after approximately 10 minutes. The rate of decline was unaffected by ionic strength, temperature and pH, but increased with increasing $[H_2O_2]$.

The following conclusions can be drawn:-

- (a) At constant $[H_2O_2]$ the rate of decomposition falls from the peak according to

$$\frac{1}{\text{rate of decomposition}} \propto \text{time} \quad (1)$$

- see Fig.56.

- (B) Surface area data on the dried oxide gave a roughness factor of 10^3 and an adsorbed monolayer containing $1.0 \cdot 10^5$ moles of ethylene. Since the ethylene molecule is similar in dimensions to the H_2O_2 molecule it is reasonable to assume that this figure is within a factor of 2 of the maximum possible number of sites on the catalyst surface at which an H_2O_2 molecule could be adsorbed. It is possible that H_2O_2 will be adsorbed and decomposed in cracks which must largely compose the surface, but it is likely that the evolved O_2 will be unable to escape freely and will thus seal off the crack surface from further contact with H_2O_2 solution. This suggestion has support in that after catalysis and submersion in H_2O a short-lived evolution of O_2 can be observed when H_2O is passed vigorously over the catalyst surface.

It is therefore very likely that the effective active surface will be very much smaller than the equivalent of $2 \cdot 10^{-5}$ moles. The number of moles of H_2O_2 destroyed in the time required to pass from the peak efficiency to the minimum is, at 1.0 M H_2O_2 ,

$1.2 \cdot 10^{-2}$. Taking the number of active sites as $2.0 \cdot 10^{-5}$, 600 H_2O_2 molecules are destroyed per active site during this period.

Thus the decline is not due to a mechanism whereby each decomposition of an H_2O_2 leads to poisoning of the site involved.

Several alternatives are possible, viz:-

- (i) a slow surface process proportional to the $[H_2O_2]$ but separate from catalysis
- (ii) a slow surface process proportional to decomposition
- (iii) a slow surface rearrangement
- (iv) a reaction in the oxide penetrating into the bulk.

It is convenient at this point to regard the highly active surface species as S-X where it need not be decided yet whether S-X is a property of the original oxide surface or whether it is generated by H_2O_2 during the initial rapid increase to the peak.

For (i) a reaction of the form

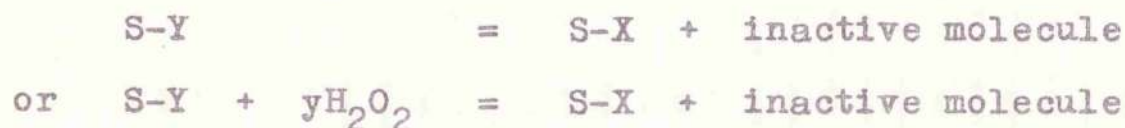


is suggested where S-Y is either

- (a) a less active catalyst centre than S-X
- or (b) a stable surface species unable to cause catalysis.

If (a) the minimum steady state can be either the rate corresponding to complete conversion to S-Y or an

equilibrium reaction involving poisoning and regeneration. Regeneration is necessary to explain the appreciable rate of decomposition at the minimum efficiency. It implies a step of the kind



If (b) the minimum efficiency must be due to an equilibrium as in (a).

For (ii) there is the possible formulation



where Z is HO_2 , HO , O' or O_2' an H_2O_2 derived intermediate. As in (i) S-Y can either be catalytically less active than S-X or completely inert and it is likely that the minimum efficiency would be an equilibrium depending on regeneration of the less active S-Y.

Because of the sensitive dependence of the rate of decline (i.e. the rate of poisoning) on $[\text{H}_2\text{O}_2]$ it seems reasonable to regard the alternatives (iii) and (iv) as the least likely; (iv) perhaps least of all.

Kinetically (i) and (ii) are identical if the $[\text{Z}]$ is proportional to $[\text{H}_2\text{O}_2]$. To analyse (i) the treatment may be simplified by proposing for the peak the two reactions, viz:-

(a) Catalysis:-



$$\text{Rate of catalysis} = r = knc$$

where $[H_2O_2] = c$ and $n =$ the fraction of the oxide surface in the active form $S-X$.

(b) Poisoning:-



$$\text{Rate of poisoning} = k'n^2c$$

Ignoring the regeneration of $S-Y$ which may be justifiable near the peak when the fraction of the surface covered by it should be small i.e. $n \approx 1$, then

$$\frac{-dn}{dt} = k'n^2c \quad \text{and} \quad \left(\frac{dr}{dt}\right)_{\text{peak}} = k \frac{dn \cdot c}{dt}$$

$$\text{i.e.} \quad \left(\frac{dr}{dt}\right)_{\text{peak}} = -k k' n^2 c^2$$

At constant n i.e. at the peak value itself

$$-\left(\frac{dr}{dt}\right)_{\text{peak}} \propto [H_2O_2]^2$$

As will be pointed out below this relationship cannot be verified experimentally since the "true peak efficiency" cannot possibly be measured with the present apparatus.

However r near the peak efficiency may be simply related to time over a short period during which it remains true that regeneration is small i.e.

$$\frac{dr}{dt} = -k k' n^2 c^2 \quad \text{and} \quad r = knc$$

$$\therefore \frac{-dr}{dt} = \frac{k'}{k} r^2$$

which gives on integration the experimental form of equation (1) above, viz:

$$\frac{1}{r} = \frac{k'}{k} \cdot t + \text{constant} \quad (2)$$

Although as was stated above the "true peak efficiency" is not measured it would appear from equation (1) and (2) that at the range measured regeneration is small.

In addition equation (2) gives the variation of rate with time to be independent of $[\text{H}_2\text{O}_2]$. Experimental results (Fig.56) do indeed give this since the plot of $\frac{1}{r}$ /time for 1.5 M H_2O_2 and 1.0 M H_2O_2 are parallel.

The combination of a catalytic reaction which is unimolecular in surface species and a bimolecular surface poisoning step is the only one which accords closely with experimental findings. This will be discussed in further detail later.

4. Minimum efficiency.

The minimum efficiency is unaffected by ionic strength and is only very slightly affected by $[\text{H}^+]$. It has an activation energy of 19.5 kcal. and varies inversely with the $[\text{H}_2\text{O}_2]$. This variation (Fig.57) can be represented in the form

$$\text{efficiency} = k + k' \cdot \frac{1}{[\text{H}_2\text{O}_2]}$$

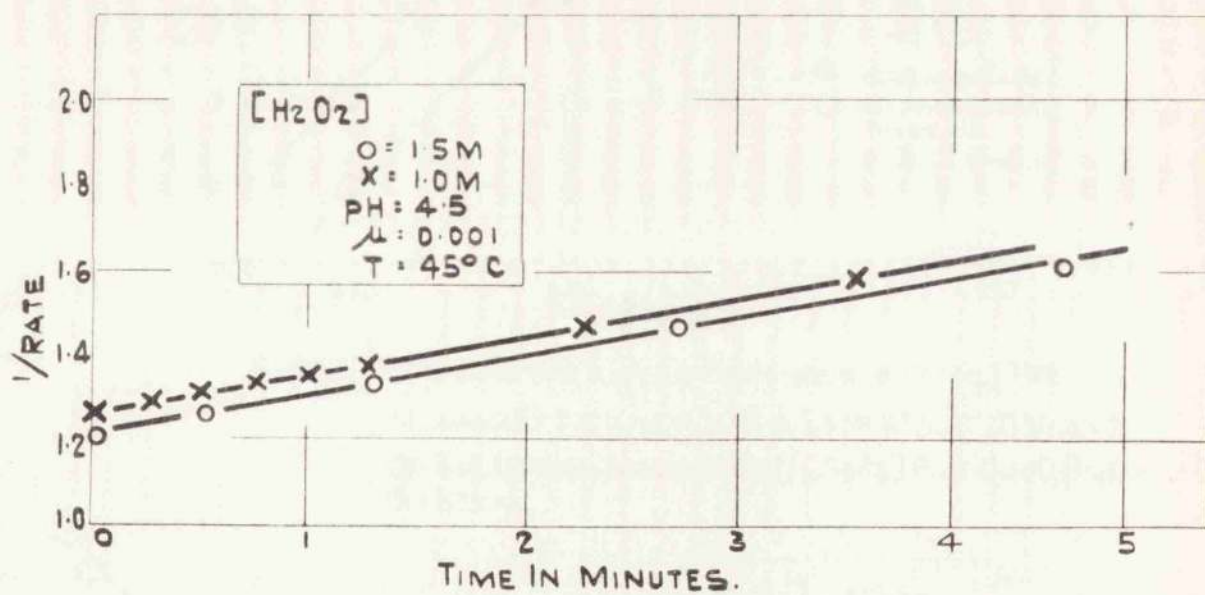


FIG. 56. SHOWING THE LINEAR VARIATIONS OF $1/r$ WITH TIME DURING THE DECLINE FROM THE PEAK EFFICIENCY FOR $\text{Cu}_2\text{O}/\text{H}_2\text{O}_2$.

This suggests that the minimum is more complex than complete conversion to S-Y would explain i.e. a surface species is more likely to consist of a steady state between destruction and regeneration. This will be discussed later in regard to specific mechanisms.

5. Final increase in efficiency.

The final increase in efficiency has the following characteristics:-

- (i) It is very much slower than the preceding processes e.g. at 45°C and with 1 M H_2O_2 55 minutes are required for completion compared with 7 minutes for the decline.
- (ii) It is unaffected by $[\text{H}_2\text{O}_2]$. This statement is particularly true for the smooth efficiency/time curves but requires qualification in the case of the step-wise growth curves referred to in (iii) below.
- (iii) At high $[\text{H}_2\text{O}_2]$ one or more discontinuities are usually observed in the curve, giving the effect of an onset of fresh growth before the first process is complete (Fig.25). In such cases extrapolation of the earlier smooth growth indicates a lower final efficiency than is actually attained. The $[\text{H}_2\text{O}_2]$ dependence of the final steady value is for this reason not quite the same as that of the intermediate steady state (Fig.31). Referring to the expression

$$\text{efficiency} = k + \frac{k'}{[\text{H}_2\text{O}_2]}$$

for the intermediate steady state, the addition of a term $k' [\text{H}_2\text{O}_2]$ makes it applicable to the final state. This satisfies the results and fits in with the observation of renewed "steps" at the high $[\text{H}_2\text{O}_2]$ if it can be said that the increase of efficiency due to these steps is proportional to $[\text{H}_2\text{O}_2]$.

- (iv) The growth is very sensitive to temperature change. Taking the rate of decomposition at the time of half change as a comparative measure of the rate, an activation energy of 37.5 kcal. is obtained (Fig.58).
- (v) The growth rate is independent of pH.

All these characteristics accord very well with the identification of this stage with a solid reaction set off by the change in the surface condition brought about by the H_2O_2 . This will be discussed in greater detail below.

6. Final steady efficiency.

The final steady efficiency is related to $[\text{H}_2\text{O}_2]$ in the same way as the minimum steady state provided the growth curve is smooth and without steps. In Fig.57 the final efficiency values obtained by extrapolation of the initial sigmoid (Fig.31) are plotted against $\frac{1}{[\text{H}_2\text{O}_2]}$. The resulting straight line indicates that this efficiency value varies

according to

$$r = k + k' \cdot \frac{1}{[H_2O_2]}$$

Discontinuous steps occur at the higher $[H_2O_2]$ - 1.5 M and 2 M - and give an actual final rate somewhat greater than indicated by this equation.

The temperature coefficient of the final efficiency (true or extrapolated) is 26.5 kcal. (Fig.39).

(b) 0.25 M to 0.025 M

Below 0.25 M H_2O_2 the cyclic efficiency changes are no longer observed. An efficiency - which increases slightly during prolonged contact with H_2O_2 - without peak or minimum is rapidly attained and is directly proportional to $[H_2O_2]$ and independent of ionic strength. There is a very slight pH effect. The temperature coefficient is low giving an activation energy of 6 kcal. on initial exposure to H_2O_2 which increases on prolonged contact with H_2O_2 to 11.0 kcal.

(c) General Mechanistic Treatment of Results

The above characteristics will be discussed further in two aspects:-

- (i) the catalyst surface, the adsorbed species and their reactions

(ii) the response of the catalyst in depth to the surface situation

and an attempt will be made to show that the results justify this division.

Briefly the scheme is as follows:-

1. On first exposure the oxide surface enters into a cyclic reaction with H_2O_2 . The active surface sites may already exist or be created rapidly by H_2O_2 .
2. A poisoning of these active sites takes place by reaction with H_2O_2 leading to a relatively inactive site. This reaction has a much lower probability than the reaction leading to catalysis. The inactive site can regenerate itself. The poisoning does not take place with low $[H_2O_2]$.
3. The minimum is reached when the poisoning and recovery in 2. are balanced.
4. As a result of 1, 2 and 3, the oxide surface is thrown out of equilibrium with the bulk. A slow return to equilibrium involving a complex solid diffusion process frees more surface sites to participate in the whole process of catalysis.

Steps 1, 2 and 3 can be considered as coming under (i) without noticeable interference from 4. which is entirely responsible for the later efficiency growth at high $[H_2O_2]$. Furthermore

any new sites created at the surface by 4, can be regarded as passing immediately to the equilibrium state of 3.

3. Initial Efficiency Changes on Cu_2O considered as a Catalytic Surface Process.

(a) Characteristics

The reaction mechanism describing the surface process must fulfil the conditions summarised here

1. High $[\text{H}_2\text{O}_2]$ region

(i) an initial peak efficiency proportional to the $[\text{H}_2\text{O}_2]$

(ii) a relatively slow decline from the peak efficiency during which

$$\frac{-d(\text{rate of decomposition})}{dt} \propto [\text{H}_2\text{O}_2]^2 \text{ at the peak}$$

and

$$\frac{1}{\text{rate}} \propto \text{time} \quad \text{near the peak where}$$

regeneration is still small.

(iii) a minimum efficiency given by

$$\text{efficiency} = k + \frac{k'}{[\text{H}_2\text{O}_2]}$$

2. Low $[\text{H}_2\text{O}_2]$ region

An initial efficiency proportional to the $[\text{H}_2\text{O}_2]$ and which remains almost steady during contact

with H_2O_2 .

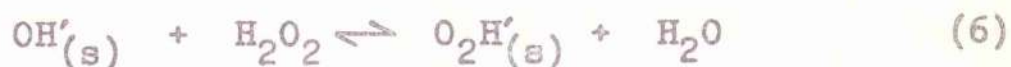
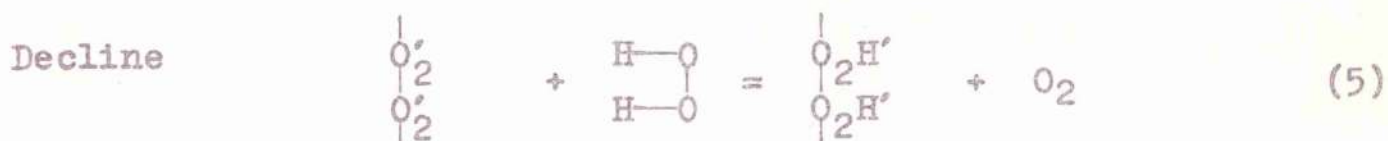
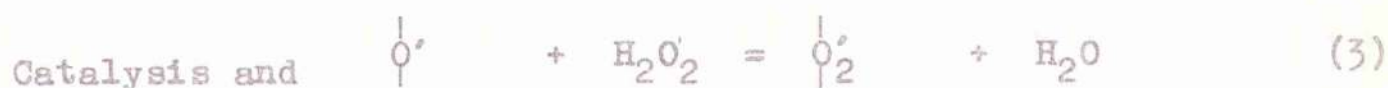
(b) Proposed Reaction Mechanism

The proposed reaction mechanism postulates the existence of three main processes which are at equilibrium when a steady catalysis is reached i.e.

(i) minimum efficiency in high $[\text{H}_2\text{O}_2]$ zone

(ii) initial efficiency in low $[\text{H}_2\text{O}_2]$ zone

The reaction mechanism is



where $\begin{array}{c} | \\ \text{O}' \\ | \end{array}$ and $\begin{array}{c} | \\ \text{O}'_2 \\ | \end{array}$ are surface anchored radical ions and

$\begin{array}{c} | \\ \text{HO}'_2 \\ | \end{array}$ and $\begin{array}{c} | \\ \text{OH}' \\ | \end{array}$ are regarded as surface hydroperoxide and

hydroxide ions rather more "active" than normal hydroxide or

hydroperoxide crystal ions would be.

As mentioned above the mechanism involves three processes viz:

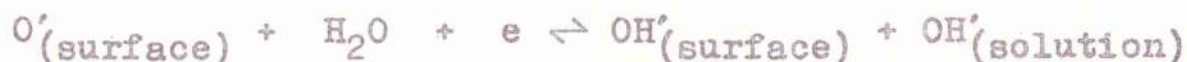
- (i) A decomposition cycle responsible for the initial peak efficiency - reactions (3) and (4).
- (ii) A poisoning reaction causing the slow decline in efficiency - reaction (5).
- (iii) A regeneration reaction re-activating the poisoned sites - reaction (7).

and reaction (6) involving the equilibrium between surface anchored OH' and HO'_2 ions and H_2O_2 . Studies on the decomposition of H_2O_2 on anion exchange resins (see Section II) have shown this equilibrium to be rapid and lying well over to the HO'_2 ($K = \frac{m_{\text{HO}'_2}}{c \times m_{\text{HO}'}} = 665$ for the resin where \underline{m} refers to the fraction of the surface covered by the particular species and \underline{c} is the $[\text{H}_2\text{O}_2]$.)

In the presence of water the surface is assumed to consist of a small but definite concentration of surface anchored radicals, viz: O' and O'_2 an assumption suggested by Garner and co-workers from results on the dry oxidation of Cu and the adsorption of O_2 on Cu_2O . The presence of O' on oxidised Cu, Ni and Co has recently been successfully applied by Zettlemyer, Yu, Chessick and Healey¹⁰⁸ and Yu, Chessick and Zettlemyer¹⁰⁹ to explain the oxidation and regeneration of reduced metal surfaces at high and low

temperatures. The above workers used the strong fields from the adsorbed O' to account for the strong physical adsorption of oxygen on oxidised samples of Cu, Ni and Co. When H_2O_2 comes in contact with the catalyst surface decomposition at these sites evolves O_2 at a high activity and it is possible that there is an immediate production of more catalyst sites of similar nature. The measured initial efficiency would be due to decomposition occurring on this induced concentration of active sites.

Potential measurements show that the change from H_2O to H_2O_2 is accompanied by a rapid increase in potential (Fig.49). The relationship between $m_{O'}$ and $m_{OH'}$ i.e. the surface fraction of the species O' and OH' respectively will be reflected in the potential of the surface and, without deciding what reaction actually controls the electrode reaction, it is reasonable to assume that the equilibrium



will hold. The potential will therefore be related to $m_{O'}$ and $m_{OH'}$ by

$$e = e_0 - \frac{RT}{F} \ln \frac{m_{OH'} \cdot [OH']}{m_{O'}}$$

where e is positive when the electrode is positively charged with respect to the solution, and the increase in active sites as demanded by the reaction mechanism will be followed by the above electrode reaction. Thus there is

evidence from an increase in the positiveness of the electrode for an increase in $m_{O'}$ relative to $m_{OH'}$.

At a certain $[H_2O_2]$ the production of active sites must reach a maximum depending as it does on a total available surface. Above this $[H_2O_2]$ the ratio $m_{OH'}/m_{O'}$ is constant and the potential under such conditions is given by

$$e = e_0 - \frac{RT}{F} \ln k[OH']$$

i.e. an $[H_2O_2]$ - independent e.m.f. Experiment verifies this (Fig.52) 0.25 M H_2O_2 being the limiting concentration. This effect is similar to that noted by Bockris and Oldfield¹⁰² who derived the expression

$$e = 0.87 - 0.059 \text{ pH}$$

for the e.m.f. of Pt and Au in the $[H_2O_2]$ range 5 M to 10^{-6} M.

Below 0.25 M H_2O_2 the e.m.f. is dependent on $[H_2O_2]$. If in this range $m_{O'}$ is proportional to the $[H_2O_2]$ and $m_{OH'}$ may be considered fixed, the potential will be proportional to $\log [H_2O_2]$ as found, (Fig.52).

As noted in the result section small e.m.f. changes (approximately 0.1 volts) occurred during catalysis. These variations were similar in form to the efficiency changes i.e. a rapid fall followed by a slower rise. According to the reaction mechanism the ratio $m_{OH'}/m_{O'}$ is considered large even at the peak rate. If a reasonable figure is

assumed for this ratio - say 100:1 - a change to 150:1 causes a drop in potential of 0.01 v. as given by

$$e = e_0 - \frac{RT}{F} \ln \frac{m_{OH'} \cdot [OH']}{m_{O'}}$$

at a given $[OH']$. This is of the order of the experimental swing in potential during catalysis.

(c) Kinetic Interpretation of Proposed Mechanism

Initially catalysis is due solely to the rapid cycle

(3) and (4) i.e.

$$\text{Rate} = 2k_4 \cdot m_{O'_2} [H_2O_2]$$

where as before $m_{O'_2}$ is the fraction of the surface covered by the designated species. This shows a peak efficiency dependent on the $[H_2O_2]$ at constant $m_{O'_2}$ which is the condition assumed present during the first stage of catalysis.

Experiment gives the peak efficiency as

$$\text{Efficiency} = k' + k'' [H_2O_2].$$

In this concentration zone the decline mechanism is rapid (increasing with $[H_2O_2]$) and it is to be expected that the true initial efficiency is rapidly poisoned. Although the efficiency readings are taken 30 seconds after the change from H_2O to H_2O_2 it is reasonable to expect that the decline is well developed and the measured efficiency lies below the 'true peak value'. Since readings are taken at constant time after the change to H_2O_2 the measured peak efficiency

shows first order dependence on $[H_2O_2]$ as would be expected.

Assuming steady state conditions at the minimum efficiency i.e. when equilibrium between decline and regeneration is attained, the reaction scheme gives

$$\text{For static } m_{O'_2} \quad r_4 + 2r_5 = r_3 \quad (8)$$

$$\text{" " } m_{O'} \quad r_3 = r_4 + 2r_7 \quad (9)$$

$$\text{" " } m_{HO'_2} \quad \overset{\rightarrow}{r_6} + 2r_5 = r_7 + \overset{\leftarrow}{r_6} \quad (10)$$

$$\text{" " } m_{OH'} \quad \overset{\leftarrow}{r_6} = \overset{\rightarrow}{r_6} + r_7 \quad (11)$$

where \underline{r} signifies the rate of the appropriate reaction.

$$\text{From (10) + (11) } r_5 = r_7 \quad (12)$$

$$\begin{aligned} \text{Overall rate} &= r_3 + r_4 + r_5 + \overset{\rightarrow}{r_6} - \overset{\leftarrow}{r_6} + r_7 \\ &= r_3 + r_4 \quad (\text{since } r_5 = r_7 \text{ and } \overset{\rightarrow}{r_6} = \overset{\leftarrow}{r_6}) \end{aligned}$$

$$\therefore \text{Overall rate} = k_3 m_{O'} [H_2O_2] + k_4 m_{O'_2} [H_2O_2] \quad (13)$$

$$\text{From (6) } K = \frac{m_{HO'_2}}{m_{OH'} [H_2O_2]} \quad (14)$$

Applying a Langmurian treatment to the surface species

$$m_{HO'_2} + m_{OH'} + m_{O'} + m_{O'_2} = 1$$

and if it is assumed that

$$m_{HO'_2} + m_{OH'} \gg m_{O'} + m_{O'_2}$$

$$\text{then } m_{HO'_2} + m_{OH'} = 1 \quad (15)$$

From (14) and (15)

$$m_{OH'} = \frac{1}{1 + K [H_2O_2]} \quad (16)$$

and

$$m_{HO'_2} = \frac{K [H_2O_2]}{1 + K [H_2O_2]} \quad (17)$$

From (12)

$$k_5 (m_{O'_2})^2 [H_2O_2] = k_7 m_{OH'} \cdot m_{HO'_2}$$

$$= k_7 \frac{K [H_2O_2]}{(1 + K [H_2O_2])^2}$$

$$\therefore (m_{O'_2})^2 = \frac{k_7}{k_5} \cdot K \cdot \frac{1}{(1 + K [H_2O_2])^2}$$

$$\therefore m_{O'_2} = \sqrt{\frac{k_7 \cdot K}{k_5}} \cdot \frac{1}{1 + K [H_2O_2]}$$

$$= \frac{\alpha}{1 + K [H_2O_2]} \quad (18)$$

$$\text{where } \alpha = \sqrt{\frac{k_7 \cdot K}{k_5}}$$

$$\text{From (8) } k_3 m_{O'_2} [H_2O_2] = k_4 \cdot \alpha \cdot \frac{[H_2O_2]}{1 + K [H_2O_2]} + \frac{2k_5 \cdot \alpha^2 [H_2O_2]}{(1 + K [H_2O_2])^2}$$

Substituting in (13)

$$\left. \begin{array}{l} \text{Overall rate at} \\ \text{steady state} \\ \text{conditions} \end{array} \right\} = \frac{k_4 \alpha [H_2O_2]}{1 + K [H_2O_2]} + \frac{2k_5 \alpha^2 [H_2O_2]}{(1 + K [H_2O_2])^2} + \frac{k_4 \alpha [H_2O_2]}{1 + K [H_2O_2]}$$

$$= \frac{2k_4 \alpha [H_2O_2]}{1 + K [H_2O_2]} + \frac{2k_5 \alpha^2 [H_2O_2]}{(1 + K [H_2O_2])^2}$$

$$= \frac{2\alpha [\text{H}_2\text{O}_2]}{1 + K [\text{H}_2\text{O}_2]} \left[k_4 + \frac{k_5 \alpha}{1 + K [\text{H}_2\text{O}_2]} \right] \quad (19)$$

Applying the above interpretation to the two concentration zones we have

1. High $[\text{H}_2\text{O}_2]$

(i) Initial catalysis due to reactions (3) and (4)

is given by

$$r_{\text{peak}} = 2 k_4 m_{\text{O}_2}' [\text{H}_2\text{O}_2]$$

i.e. efficiency at the true peak is proportional to $[\text{H}_2\text{O}_2]$ since m_{O_2}' can be considered constant.

(ii) The decline from the peak will be due to the fall-off of O_2' (or O'). Let $m_{\text{O}_2}' = m_{\text{O}'} = n$

$$r = n(k_3 + k_4) [\text{H}_2\text{O}_2] = kn [\text{H}_2\text{O}_2]$$

$$\text{then } \frac{-dr}{dt} = -k [\text{H}_2\text{O}_2] \cdot \frac{dn}{dt} \quad (20)$$

From (5)

$$\frac{-dn}{dt} = k_5 n^2 [\text{H}_2\text{O}_2] \quad (21)$$

which will be quite true only near the peak rate when recovery is yet a negligible factor.

From (20) and (21)

$$\begin{aligned} \frac{-dr}{dt} &= k [\text{H}_2\text{O}_2] \cdot k_5 n^2 [\text{H}_2\text{O}_2] \\ &= k k_5 n^2 [\text{H}_2\text{O}_2]^2 \end{aligned} \quad (22)$$

near the peak. At the limiting value of $\left(\frac{dr_{\text{peak}}}{dt}\right)$ at the peak

$$\left(\frac{d(r_{\text{peak}})}{dt}\right)_{\text{Limit}} \propto [\text{H}_2\text{O}_2]^2$$

since n will be a constant for high $[\text{H}_2\text{O}_2]$ before any poisoning sets in. (To support this claim reference may be made to the constancy of the electrode potential results at high $[\text{H}_2\text{O}_2]$.)

(iii) Near the peak rate

$$\begin{aligned} -\frac{d(r)}{dt} &= k k_5 n^2 [\text{H}_2\text{O}_2] \\ &= \frac{k k_5 r^2 [\text{H}_2\text{O}_2]^2}{k^2 [\text{H}_2\text{O}_2]^2} \\ &= \frac{k_5}{k} r^2 \end{aligned}$$

$$\text{i.e. } \frac{1}{r} = \frac{k_5}{k} t + \text{constant} \quad (23)$$

(iv) Assuming $K [\text{H}_2\text{O}_2] \gg 1$ in this $[\text{H}_2\text{O}_2]$ zone then for the steady state, equation (19) gives

$$\text{Overall Rate} = \frac{2\alpha [\text{H}_2\text{O}_2]}{K [\text{H}_2\text{O}_2]} \left[k_4 + \frac{k_5 \alpha}{K [\text{H}_2\text{O}_2]} \right] \quad (24)$$

$$= A + \frac{B}{[\text{H}_2\text{O}_2]} \quad (25)$$

$$\text{where } A = \frac{2k_4 \alpha}{K} \quad \text{and} \quad B = \frac{2k_5 \alpha^2}{K^2}$$

i.e. the steady state efficiency $\propto \frac{1}{[\text{H}_2\text{O}_2]}$ (26)

Comparison of the theoretical results obtained in (i), (ii) and (iii) with the experimental requirements (p.124) shows that the proposed mechanism fits in with the experimental results for the high $[\text{H}_2\text{O}_2]$ zone.

2. Low $[\text{H}_2\text{O}_2]$.

In this concentration region the decline is negligible and the peak efficiency and minimum efficiency are thus synonymous.

Assuming $K [\text{H}_2\text{O}_2] \ll 1$ in this $[\text{H}_2\text{O}_2]$ zone then from equation (19)

$$\left. \begin{array}{l} \text{Overall rate} \\ \text{at steady state} \\ \text{conditions} \end{array} \right\} = 2 \alpha [\text{H}_2\text{O}_2] (k_4 + k_5 \alpha) \\ = D \cdot [\text{H}_2\text{O}_2] \quad (27)$$

$$\text{where } D = 2 \alpha (k_4 + k_5 \alpha)$$

i.e. the steady rate is directly proportional to $[\text{H}_2\text{O}_2]$ which is of course an important experimental result.

(d) Evaluation of Constants in the Rate Equations.

The identification of the assumed plausible mechanism with the experimental results leads to the evaluation of the rate constants. This was done from experimental data at 45°C.

From the minimum steady state.--

(1) At low $[\text{H}_2\text{O}_2]$ the rate is given by

$$\begin{aligned} \text{Rate} &= \frac{2 \cdot k_7^{\frac{1}{2}} \cdot K^{\frac{1}{2}}}{k_5^{\frac{1}{2}}} [\text{H}_2\text{O}_2] \left[k_4 + \frac{k_7^{\frac{1}{2}} \cdot K^{\frac{1}{2}}}{k_5^{\frac{1}{2}}} k_5 \right] \\ &= [\text{H}_2\text{O}_2] \left[\frac{2 \cdot k_4 \cdot k_7^{\frac{1}{2}} \cdot K^{\frac{1}{2}}}{k_5^{\frac{1}{2}}} + 2 \cdot k_7 \cdot K \right] \end{aligned}$$

i.e. linear with $[\text{H}_2\text{O}_2]$ with a slope given by

$$\frac{2 \cdot k_4 \cdot k_7^{\frac{1}{2}} \cdot K^{\frac{1}{2}}}{k_5^{\frac{1}{2}}} + 2 \cdot k_7 \cdot K$$

From Fig.33 i.e. the experimental dependence of rate on $[\text{H}_2\text{O}_2]$

Slope = 1.9°C per mole per litre

Now 1 mole of H_2O_2 liberates 23000 calories when completely decomposed. In the efficiency apparatus 100 mls of H_2O_2 pass per minute. If this contained 1 mole it raises the temperature by 230°C when completely decomposed. Therefore 1.9°C can be written as $\frac{1.9}{230}$ moles per minute under the conditions of the experiment and

Slope = $\frac{1.9}{230}$ moles per minute per litre

$$\therefore \frac{1.9}{230} = \frac{2k_4 \cdot k_7^{\frac{1}{2}} \cdot K^{\frac{1}{2}}}{k_5^{\frac{1}{2}}} + 2 \cdot k_7 \cdot K \quad (28)$$

(ii) At high $[\text{H}_2\text{O}_2]$ the rate is given by

$$\begin{aligned}
 \text{Rate} &= \frac{2 \cdot k_4 \cdot k_7^{\frac{1}{2}} \cdot K^{\frac{1}{2}}}{K k_5^{\frac{1}{2}}} + \frac{2 \cdot k_5 \cdot k_7 \cdot K}{k_5 K^2} \cdot \frac{1}{[\text{H}_2\text{O}_2]} \\
 &= \frac{2 \cdot k_4 \cdot k_7^{\frac{1}{2}}}{K^{\frac{1}{2}} \cdot k_5^{\frac{1}{2}}} + \frac{2 \cdot k_7}{K} \cdot \frac{1}{[\text{H}_2\text{O}_2]} \quad (29)
 \end{aligned}$$

i.e. linear with

$$\text{slope} = \frac{2 \cdot k_7}{K} \quad \text{and Intercept} = \frac{2k_4 \cdot k_7^{\frac{1}{2}}}{K^{\frac{1}{2}} \cdot k_5^{\frac{1}{2}}}$$

$$\text{From Fig.57 i.e. Rate} = A + \frac{B}{[\text{H}_2\text{O}_2]}$$

$$\text{Slope} = B = \frac{0.05}{230} = \frac{2k_7}{K} \quad (30)$$

and

$$\text{Intercept} = A = \frac{0.355}{230} = \frac{2k_4 \cdot k_7^{\frac{1}{2}}}{K^{\frac{1}{2}} k_5^{\frac{1}{2}}} \quad (31)$$

$$\text{From (30)} \quad \frac{k_7^{\frac{1}{2}}}{K^{\frac{1}{2}}} = \left(\frac{0.05}{2 \cdot 230} \right)^{\frac{1}{2}}$$

Substituting in (31)

$$\frac{0.355}{230} = \frac{2k_4}{k_5^{\frac{1}{2}}} \cdot \left(\frac{0.05}{2 \cdot 230} \right)^{\frac{1}{2}}$$

$$\therefore \frac{k_4}{k_5^{\frac{1}{2}}} = \frac{0.355}{2 \cdot 230 \cdot 0.0142} = 0.074$$

Substituting this value of $\frac{k_4}{k_5^{\frac{1}{2}}}$ in (28)

$$\therefore \frac{1.9}{230} = 2 \cdot 0.074 \cdot k_7^{\frac{1}{2}} \cdot K^{\frac{1}{2}} + 2k_7 K$$

$$\text{Also from (30)} \quad K = \frac{2k_7 \cdot 230}{0.05}$$

$$\therefore \frac{1.9}{230} = 2 \cdot 0.074 \cdot k_7^{\frac{1}{2}} k_7^{\frac{1}{2}} \left(\frac{2 \cdot 230}{0.05} \right)^{\frac{1}{2}} + \frac{2k_7 \cdot 2k_7 \cdot 230}{0.05}$$

$$\therefore 920 k_7^2 + 6.93 k_7 - 0.00413 = 0$$

$$\text{from which} \quad k_7 = 5.5 \cdot 10^{-4} \quad (32)$$

Substituting for k_7 in (30)

$$\therefore K = 5.012 \quad (33)$$

Therefore from the above treatment the following relationships are obtained

$$k_7 = 5.5 \cdot 10^{-4}$$

$$K = 5.012$$

$$\frac{k_4}{k_5^{\frac{1}{2}}} = 0.074$$

In order to separate k_4 from k_5 data is required from the non-stationary state phase. The slope of the $\frac{1}{r}$ /time line for the decline from the peak (Fig.56) gives $\frac{k_5}{k_3 + k_4}$ i.e. from equation (23), after making the assumption that $m_{O_2}' = m_{O_2}''$ which is of course by no means justified. However with the same assumption the rate at any point can be put in the form

$$r = m_{O_2}'' \left[H_2O_2 \right] (k_3 + k_4) \quad (20)$$

This equation together with the slope from equation (23)

leads to an evaluation of k_3 , k_4 and k_5 separately if $m_{O_2'}$ can be assumed. To make an assumption here takes the work into the realm of conjecture. In fact it must be stated that there is a major weakness in the treatment already carried through in the assumption of equation (15).

An attempt to apply a more rigorous treatment to the non-stationary state so as to make use of equation (23) right up to the intermediate steady rate met with no success. In this the approach was to set up four non-linear simultaneous differential equations controlling the rate of appearance of the surface species O' , O_2' , OH' and O_2H' with the extra equation

$$m_{O'} + m_{O_2'} + m_{OH'} + m_{O_2H'} = 1$$

No simplifying assumptions could be made in the non-steady state so that a solution of the full set of equations had to be attempted. This proved too difficult without great elaboration or mechanical aid which the nature of the results did not seem to justify.

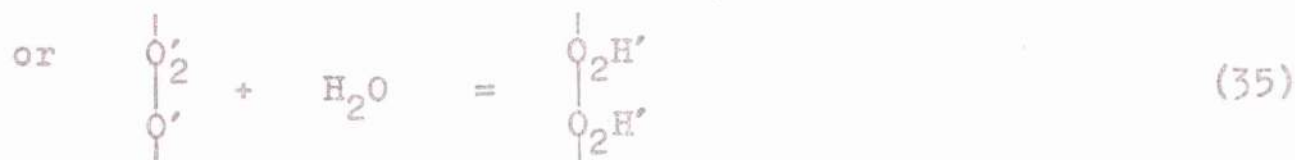
e. Discussion of Proposed Mechanism.

As outlined above the initial efficiency represented by reactions (3) and (4) assumes that since the radical ion surface activities are always small, a very rapid cycle takes place.

According to the work of Garner and co-workers the

occupants of these sites i.e. O' and O'_2 are always present in small amounts on Cu_2O . Potential results suggest a rapid increase in the sites on first contact with H_2O_2 . Below 0.25 M H_2O_2 the concentration of the active sites is proportional to $[H_2O_2]$ but above 0.25 M a maximum value is obtained. This agrees with an e.m.f. which is $[H_2O_2]$ dependent below 0.25 M.

The dependence of the decline of efficiency on $[H_2O_2]$ requires H_2O_2 as the poisoning species. H_2O is always present in large excess and possible poisoning steps viz:



can be excluded.

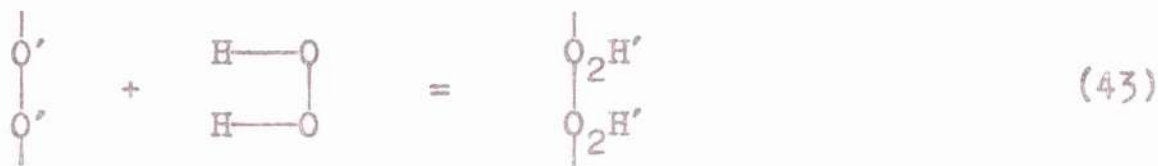
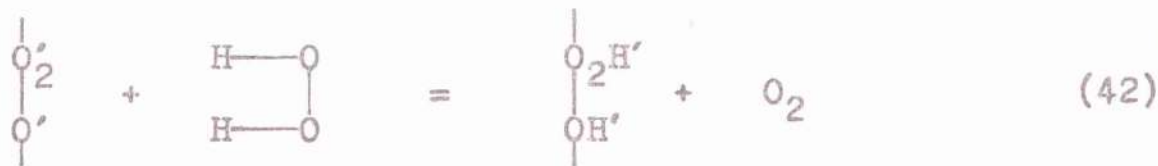
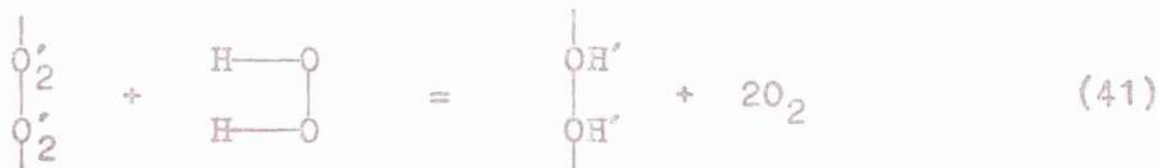
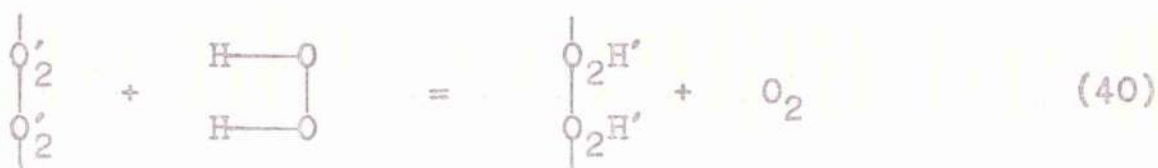
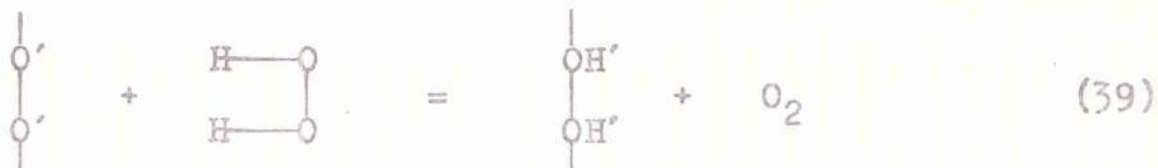
Poisoning steps involving single site destruction viz:



are considered unlikely because of the production of solution

phase free radicals.

Two-site poisoning can be accomplished through many possible routes all essentially the same kinetically. They are:-



each involving simple steric rearrangements. (39), (40), (41) and (42) are preferred to (43) since a poisoning step involving the liberation of O_2 seems energetically more favourable. Of the reactions (39), (40), (41) and (42), (40) alone is included in the reaction scheme although (39) and (42) could equally be used. (41) seems sterically a

little less likely. Reactions (39), (41) and (42) each involves the production of a surface OH' which according to the equilibrium reaction



is quickly brought to equilibrium with surface HO_2' so that (40) can be regarded as a summary process of the possible alternatives.

With regard to the recovery equation (7) is regarded as the sole contributor to regeneration.

A feature of the mechanism is the postulation of an intermediate peroxide i.e. HO_2' . Compounds of this type are already well established and their existence has been used on many occasions as a reactive intermediate in H_2O_2 reactions. A large number of inorganic derivatives of H_2O_2 are known including the peroxides which contain O_2 in the so-called active state. When H_2O_2 acts as an oxidising agent on inorganic compounds dissolved in water¹¹⁰ one of three reactions is possible i.e. (i) a change in valency, (ii) formation of an addition compound by dipole-dipole interaction in which no change of valency occurs (iii) formation of -O-O- bond with no change in valency. The formation of per-compounds containing the O-O bond is confined to cases (ii) and (iii) where no change in valency occurs and it has been shown that where an element possesses several valencies the formation of such a compound does not take place until

after the transition of the element to its highest valency state.

X-ray and diffraction studies have given the O-O interatomic distance in $\overset{\text{O}}{\text{H}_2\text{O}_2}$ as $1.49 \text{ \AA} \pm 0.01 \text{ \AA}$. The change in character of the -O-O- group caused by conversion to a peroxide has been shown to involve a degree of ionisation produced by variations in the relative electronegativity of the groups flanking the -O-O- group rather than an alteration in the character of the bond between the oxygen atoms.

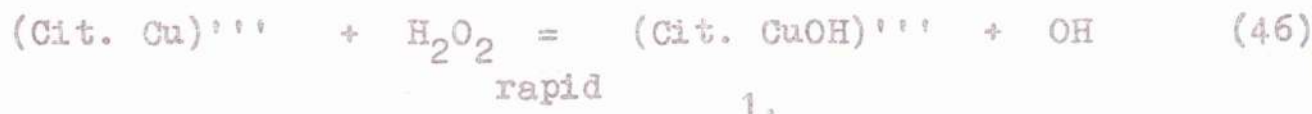
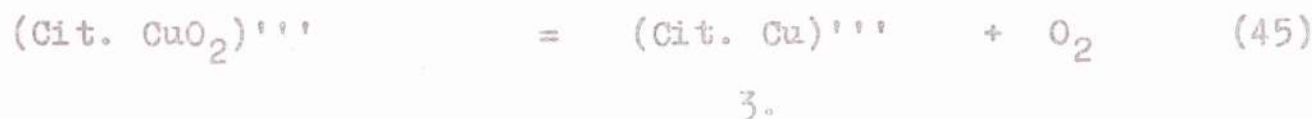
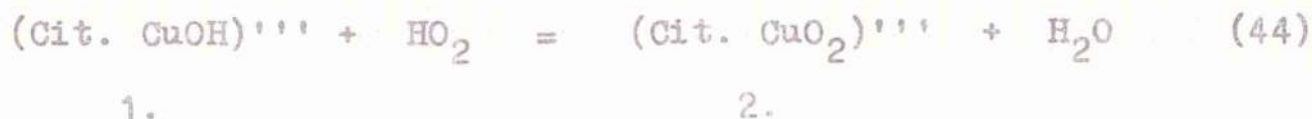
Bolland and Gee¹¹¹ noted that the strength of the O-O bond and therefore the stability of any compound containing this group varied according to the location of the group. Following this observation Walsh¹¹² explained the relative instability of peroxides as due to the proximity of the two strongly electronegative oxygen atoms causing an insufficiency of bonding electrons in the peroxide link. The variations in bond strength as noted above can therefore be understood in terms of charge transfer from the bonded group to the oxygen atoms i.e. the greater the transfer of negative charge to the oxygen atoms the greater the O-O bond strength.

Haïssinsky¹¹³, who arrived at similar conclusions, showed that the formation of a compound of the form Me-O-O- required that the electronegativity of the Me constituent should be smaller than or at the most equal to, 2.1 i.e. the reaction



requires that $x_{\text{Me}} < x_{\text{H}}$ where x is the electro-negativity and hydrogen has a value of 2.1 .

A peroxide intermediate has been proposed by Glasner¹¹⁴ for the homogeneous decomposition of H_2O_2 by dissolved Cu^{++} . The brown peroxide which was kept in solution with sodium citrate was given the structure $\text{CuO}\cdot\text{O}_2\text{H}$, formed by the simple addition of an HO_2 radical to the $\text{Cu}(\text{OH})_2$. Glasner's proposed mechanism is



Reaction (44) depends on the assumption that in all H_2O_2 solutions the following equilibria exist:-



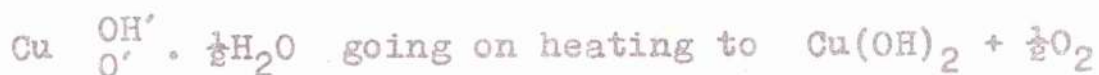
Compound 2. i.e. $\text{Cu}^{++}\text{O}_2'$ subsequently decomposes giving Cu^+ and liberating O_2 . Step (46) involves the addition of an OH radical which assumes the negative charge obtained by the Cu^{++} in step (45).

Although this scheme explains the experimental

results the mechanism, depending as it does on the existence in solution of the radicals OH and HO_2 , appears unlikely.

The proposed structure for the intermediate peroxide i.e.

$\text{Cu}^{++} \begin{matrix} \text{O}' \\ \text{HO}'_2 \end{matrix}$ does however fit in with the $\text{Cu}_2\text{O}/\text{H}_2\text{O}_2$ mechanism since the oxide surface is considered covered by the species O' and HO'_2 . In this connection a dark green compound was prepared by the addition of H_2O_2 to freshly precipitated $\text{Cu}(\text{OH})_2$. The compound which was formed and filtered at 0°C was found to be a peroxide and analysis indicated the proportions $\text{CuO}_{2.4}\text{H}_2$. This result could be accommodated by an equimolar mixture of the Glasner compound $\text{Cu}^{++} \begin{matrix} \text{O}_2\text{H}' \\ \text{O}' \end{matrix}$ and the hydroxide $\text{Cu}^{++} \begin{matrix} \text{OH}' \\ \text{OH}' \end{matrix}$ i.e. $\text{CuO}_{2.5}\text{H}_{1.5}$, but since 50% of the total O_2 is evolved on gentle heating, a compound of the form



seems more likely.

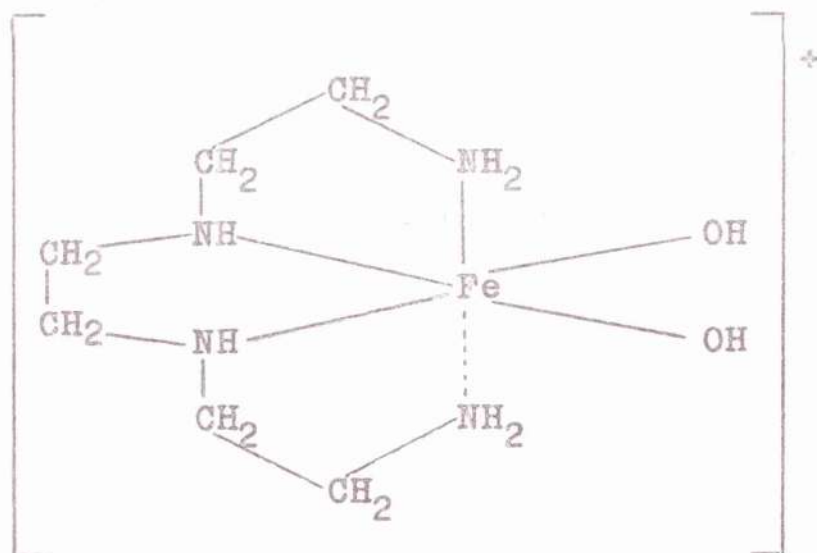
Although these results require further detailed investigation the results substantiate the suggestion that a relatively stable compound is formed with either $\text{O}_2\text{H}'$ or O' or even O'_2 .

A peroxide type intermediate has also been proposed by Wang^{115,116,117} to explain the decomposition of H_2O_2 on model enzyme catalyts. In addition to the postulation of this intermediate several points arise from this series of

papers which are relevant to a discussion of the $\text{Cu}_2\text{O}/\text{H}_2\text{O}_2$ mechanism proposed above.

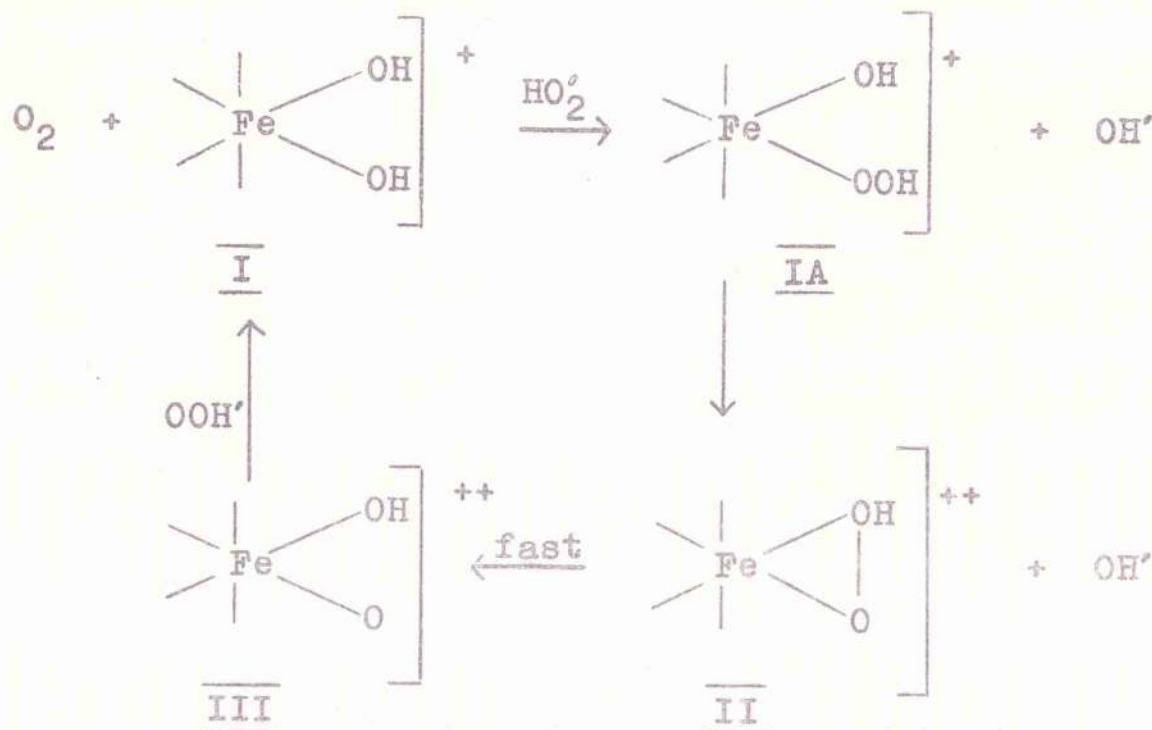
Since the structure of enzymes (the most active catalysts for H_2O_2 decomposition) is relatively unknown, Wang investigated the decomposition of H_2O_2 on small model molecules with catalase-like activity in an attempt to secure some analogy with H_2O_2 /enzyme reactions. The most successful model was formed from triethylenetetramine

(TETA) $\text{H}_2\text{NCH}_2\text{CH}_2\text{NHCH}_2\text{CH}_2\text{NHCH}_2\text{CH}_2\text{NH}_2$ and Fe^{+++} i.e. $(\text{TETA}) \text{Fe}(\text{OH})_2^+$



in which the primary amine nitrogen atoms are situated above and below the plane determined by the two secondary amine N atoms and the Fe^{+++} atom.

The proposed mechanism which involved the metathetical displacement of a bound OH' by a HOO' followed by a second displacement in which the other OH' was replaced by an O atom of the added OOH' is as follows

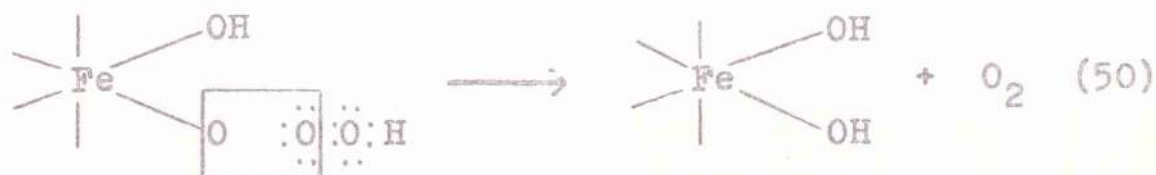


Several features of this mechanism are in agreement with certain postulates contained in the $\text{Cu}_2\text{O}/\text{H}_2\text{O}_2$ mechanism detailed above i.e.

1. The use of doubly O^{18} - labelled H_2O_2 showed unambiguously that the O_2 evolved from the decomposition of H_2O_2 by (TETA) $\text{Fe}(\text{OH})_2^+$, catalase, tris-(β -aminoethyl)-amine- Fe^{+++} and $\text{Fe}(\text{OH})_3$ originated from the same H_2O_2 molecule i.e. O_2 evolution was linked with intact O-O bonds. Step III to I takes the form therefore of

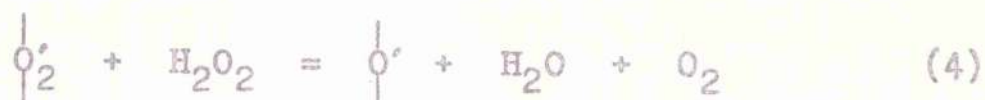


rather than

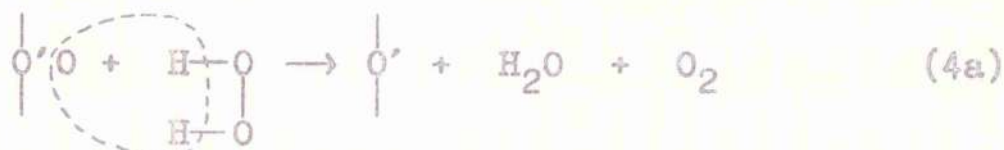


In the proposed mechanism for the $\text{Cu}_2\text{O}/\text{H}_2\text{O}_2$ reaction

O_2 is evolved according to



This seems sterically most probable to proceed by

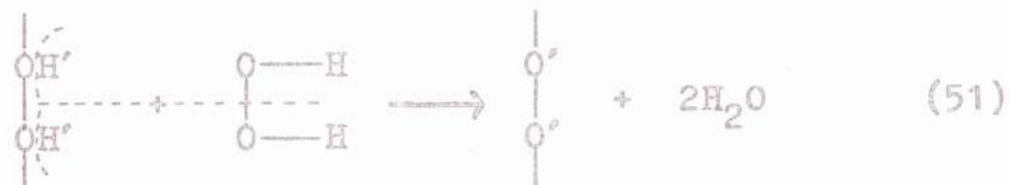


which does not involve rupture of the O-O bond.

2. Variation of the ligand showed (in order of decreasing efficiency for H_2O_2 decomposition) tetraethylenetetramine > diethyltriamine > ethylenediamine with tetraethylenepentamine practically inert. Wang explains this by the necessity of having adjacent sites for the formation of the active complex i.e. steps

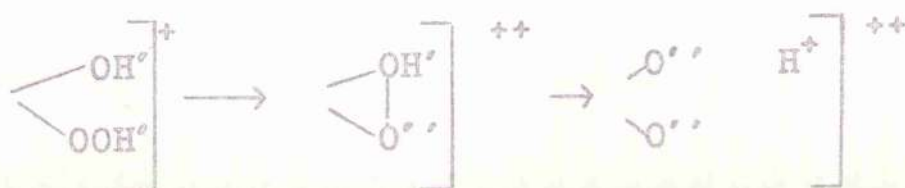


In the above mechanism for the Cu_2O/H_2O_2 reaction a two-site poisoning step is also considered necessary and a possible site creation step

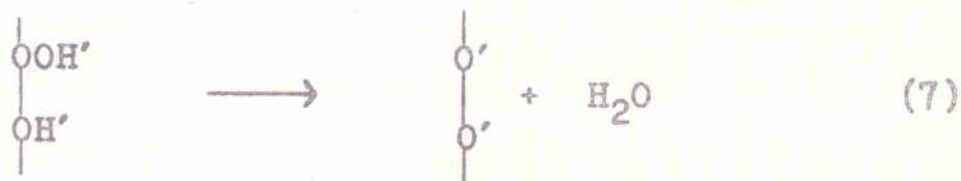


satisfies e.m.f. data and two-site requirements.

3. The production of compound III when written as



is not dissimilar to the recovery step in the $\text{Cu}_2\text{O}/\text{H}_2\text{O}_2$ mechanism i.e.



(f) Rejected Reaction Schemes.

In arriving at the $\text{Cu}_2\text{O}/\text{H}_2\text{O}_2$ reaction mechanism several alternative schemes were explored and rejected.

Many surface reactions may be explained kinetically on the basis of the simplest adsorption law i.e. the Langmuir-Hinshelwood treatment which assumes that adsorption takes place on an energetically uniform surface. According to this treatment the rate of chemisorption is given by

$$\frac{-dc}{dt} = kc(1 - \theta) - k'\theta \quad (52)$$

where $\frac{-dc}{dt}$ = rate of adsorption

c = [adsorbate]

θ = fraction of surface covered by adsorbate

$1 - \theta$ = fraction of surface bare.

Taylor¹¹⁸ following work by Pease¹¹⁹ and calorimetric studies by Garner¹²⁰ and Taylor¹²¹ showed that the heats of adsorption of gases varied with the surface covered. This he interpreted as due to a heterogeneous surface on which

adsorption first took place on sites involving favourable energetics followed as adsorption continued by those sites having greater heats of chemisorption and activation energies. On this basis Temkin and Pyzhev¹²² derived another adsorption rate expression on the assumption that the heat of chemisorption and the activation energy varied linearly with the surface covered i.e.

$$-\frac{dc}{dt} = k.c.e^{-\alpha\theta} - k'e^{\beta\theta} \quad (53)$$

where $-\frac{dc}{dt}$, c , θ and $(1 - \theta)$ are as above and $\alpha = \beta = 1$

Many reactions can be explained by a third adsorption law known as the Power Rate Law derived originally by Kwan¹²³ for the chemisorption of N_2 on promoted iron catalysts, i.e.

$$-\frac{dc}{dt} = k.c.\theta^{-\alpha} - k'\theta^{\beta} \quad (54)$$

where $-\frac{dc}{dt}$, c , θ , α and β are as above.

For adsorption far removed from equilibrium the three laws can be expressed as:-

$$-\frac{dc}{dt} = k.c.(1 - \theta) \quad (52a)$$

$$-\frac{dc}{dt} = k.c.e^{-\alpha\theta} \quad (53a)$$

$$-\frac{dc}{dt} = k.c.\theta^{-\alpha} \quad (54a)$$

In the $\text{Cu}_2\text{O}/\text{H}_2\text{O}_2$ mechanism the poisoning step (5) responsible for the decline in rate may be regarded as controlled by adsorption of H_2O_2 on the catalyst surface. This assumes that the rate at any time \underline{t} , \underline{r}_t , is proportional to the fraction of the active surface uncovered, i.e.

$$r_t = k_t(1 - \theta)$$

Now when $\theta = 0$

$$r_t = k_t = r_i$$

$$\therefore \frac{r_t}{r_i} = \frac{k_t(1 - \theta)}{k_t} = 1 - \theta$$

$$\therefore \theta = \frac{r_i - r_t}{r_i}$$

where r_t is the temperature difference at time \underline{t}
and r_i is the temperature difference at time $\underline{0}$

Since r_i is constant

$$\theta \propto r_t$$

i.e. the fraction covered is proportional to the temperature difference at that point.

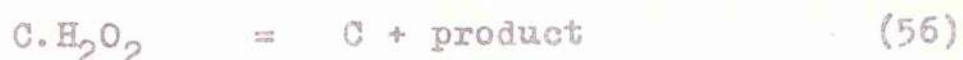
The validity of each adsorption rate law as applied to the present case is determined by plotting the rate of fall of the rate i.e. $-\frac{dc}{dt}$ against the coverage i.e. θ . In the case of the Langmuir-Hinshelwood treatment $-\frac{dc}{dt}$ is plotted against $(1 - \theta)$. For the Temkin or Elovich isotherm $\log \frac{dc}{dt}$ is plotted against θ and for the Power Rate Law $-\log \frac{dc}{dt}$ is plotted against $\log \theta$.

Since θ involves the fraction of the surface covered it is possible to test the validity of the Langmuir or Elovich adsorption laws but the Power Rate Law involving $\log \theta$ cannot be tested.

The validity of the Elovich and Langmuir adsorption laws were tested using experimental rate curves (Fig.59). As emphasised by Temkin¹²² and Brunaur¹²⁴ the Elovich isotherm was found to apply only to the middle coverage zone and since the simpler Langmuirian treatment held over the whole coverage range this isotherm was assumed to govern the rate of adsorption. The success of the final mechanism which yielded to a Langmuirian treatment supported this conclusion. As a result only the Langmuirian treatment of the rejected reaction schemes are detailed below.

1. Catalysis through the formation and decomposition of a hydroperoxidate.

The simplest catalytic cycle is given by



(where C is the catalyst) in which an intermediate surface hydroperoxidate forms and decomposes. Application of such a simple model to the experimental results is unsatisfactory as it fails to give successfully the dependence on $[H_2O_2]$, i.e.

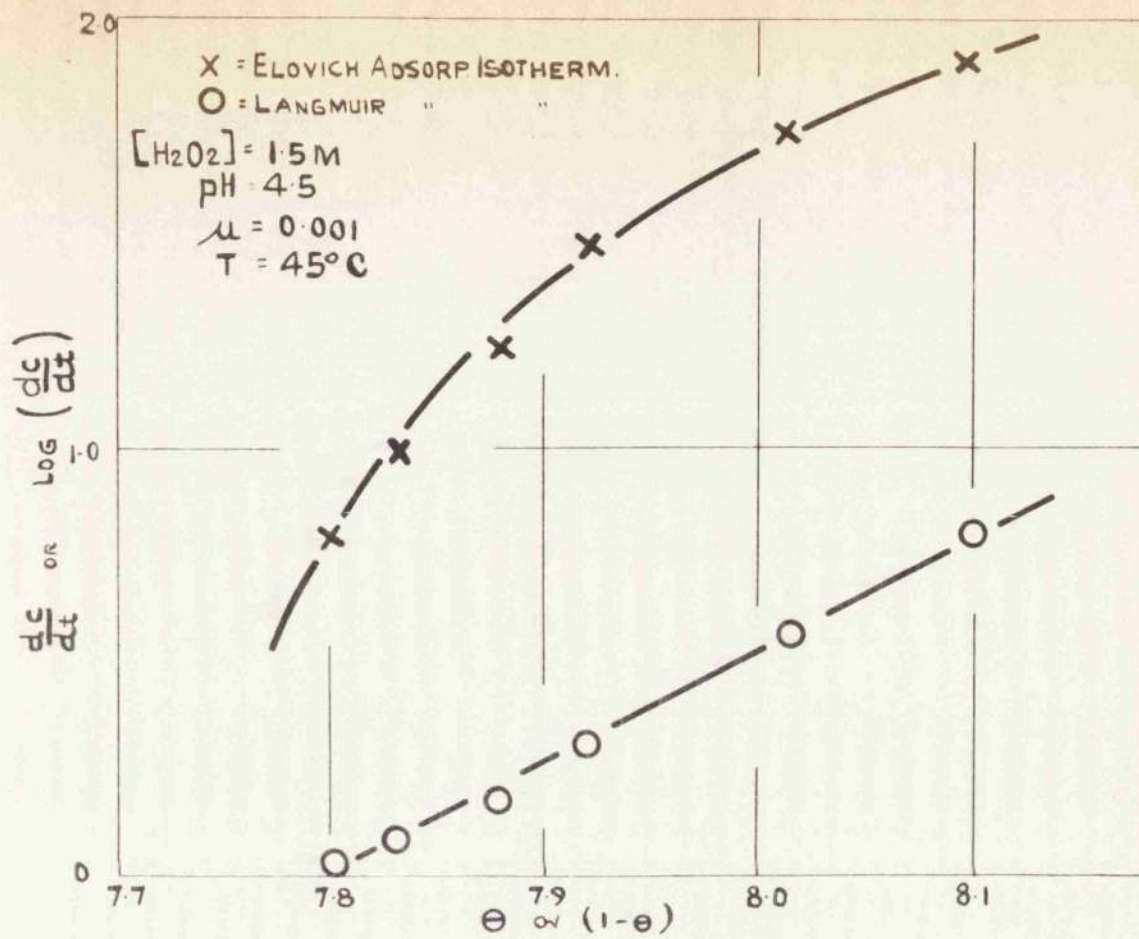


FIG. 59. SHOWING THE EFFICIENCY DECLINE CURVE IN Cu_2O/H_2O_2 TREATED AS (a) ON ELOVICH. (b) LANGMUIR, TYPE ADSORPTION.

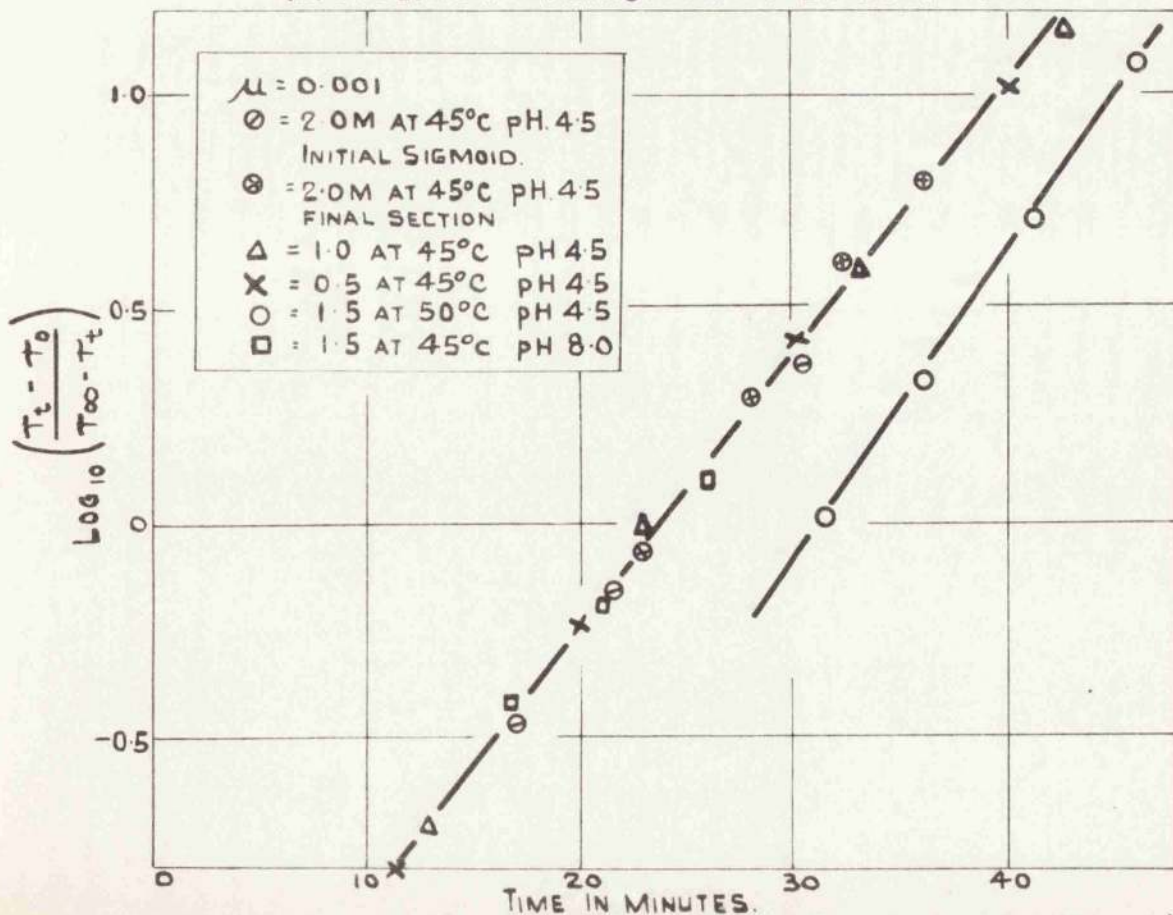


FIG. 60. SHOWING THE ADHERENCE OF THE FINAL RECOVERY IN Cu_2O/H_2O_2 TO THE FORM OF A SYMMETRICAL SIGMOID.

at high $[H_2O_2]$: Rate = $k_{56} [C.H_2O_2]$ i.e. H_2O_2 independent

at low $[H_2O_2]$: Rate = $k_{55} [C] [H_2O_2]$ i.e. proportional to $[H_2O_2]$

In addition the scheme fails to provide any mechanism for the decline in efficiency.

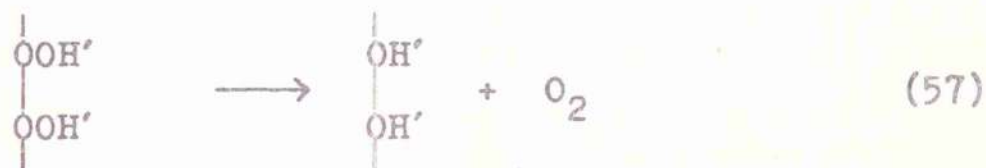
2. Catalysis solely involving ionic species.

In the present investigations the catalyst was allowed to remain in contact with H_2O between tests. The formation of surface OH' ions is therefore almost certain and two reactions involving OH' and H_2O_2 must be considered, viz:

(i) If OH' is the predominant surface species the equilibrium reaction



which favours HO_2' will produce a considerable concentration of HO_2' which can then react according to



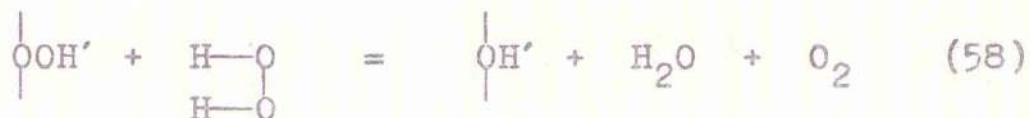
Reactions (6) and (57) produce a catalytic cycle with an equilibrium rate given by

$$\text{Rate} = \frac{k_{57} K_6^2 [H_2O_2]^2}{(1 + K_6 [H_2O_2])^2}$$

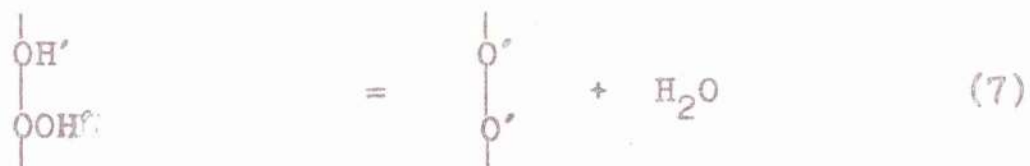
This gives zero order at high $[H_2O_2]$ and 2nd order

at low $[H_2O_2]$. As in 1. such a cycle does not agree with experimental observations. In addition reaction (57) is sterically awkward involving the rupture of the O-O bond for O_2 evolution.

(ii) As an alternative to (57) the reaction



could be combined with (6) to give a possible cycle. (58) once again involves a complex rearrangement which would be less likely than a step of the type



and the cycle does not give the experimental dependence on $[H_2O_2]$ i.e. at equilibrium

$$\text{Rate} = \frac{k_{58}K_6 [H_2O_2]^2}{1 + K_6 [H_2O_2]}$$

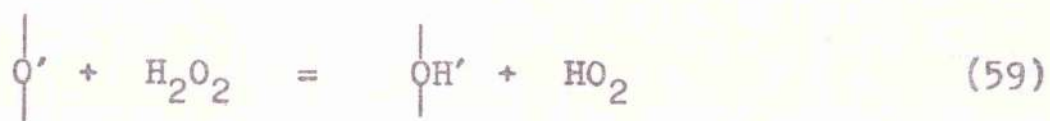
which gives 2nd order at low $[H_2O_2]$ and 1st order at high $[H_2O_2]$.

3. Catalysis involving single site poisoning.

Besides failing to give the correct kinetic result the main weakness in mechanisms 1 and 2 above is the absence of a possible rate decline step.

As already stated decline is linked to H_2O_2 so that

the simplest explanation for the decline involves single site poisoning by H_2O_2 . Several such steps are possible, viz:



each of which could be combined with (6)



Reactions (59), (60), (61) and (62) are improbable producing solution phase free radicals and (6) a feature of the final mechanism has been shown to be very fast. In addition a scheme of the form



with a destruction step



balanced at equilibrium by regeneration



(where X, Y and Z are some surface species) does not agree with experiment giving at equilibrium

$$\text{Rate} = \frac{k_{64}k_{65}k_{66} [\text{H}_2\text{O}_2]}{k_{64}k_{66} + k_{63}k_{66} + k_{64}k_{65} [\text{H}_2\text{O}_2]} \left[\frac{2k_{53}}{k_{65}} + 1 \right]$$

which is 1st order at low $[\text{H}_2\text{O}_2]$ going over to a simple zero order at high $[\text{H}_2\text{O}_2]$.

4. Catalysis involving twin-site poisoning.

Catalysis involving twin-site poisoning provides several alternatives as discussed above. Several mechanisms incorporating such steps were tried unsuccessfully before the final scheme was evolved.



where X, Y and Z are as above.

If X and Y cover the whole active surface i.e.

$[X] + [Y] = 1$, this scheme gives the following

rather complex rate equation

Rate =

$$\frac{2k_{63}k_{64}k_{68}^{\frac{1}{2}} [\text{H}_2\text{O}_2]}{\left(\frac{k_{68}^{\frac{1}{2}}}{k_{67}^{\frac{1}{2}}} + \frac{k_{63}k_{68}^{\frac{1}{2}}}{k_{64}k_{67}^{\frac{1}{2}}} + [\text{H}_2\text{O}_2] \right)^2} \left(\frac{k_{68}^{\frac{1}{2}}}{k_{67}^{\frac{1}{2}}} + \frac{k_{63}k_{68}^{\frac{1}{2}}}{k_{64}k_{67}^{\frac{1}{2}}} + \frac{1}{2} \frac{k_{67}^{\frac{1}{2}}k_{68}^{\frac{1}{2}}}{k_{63}} + [\text{H}_2\text{O}_2]^{\frac{1}{2}} \right)$$

which is of the form

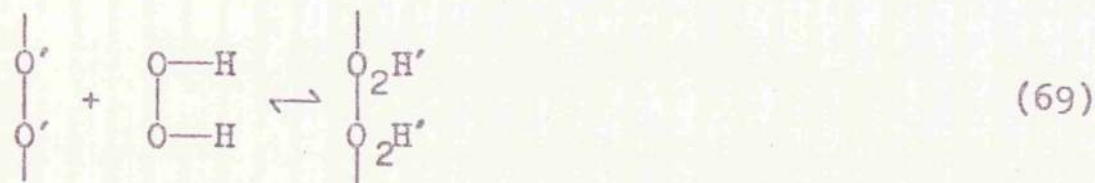
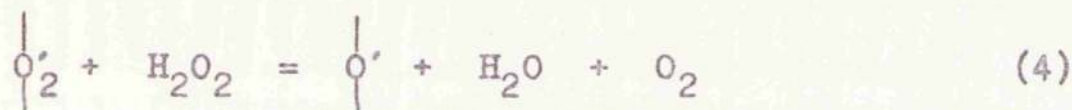
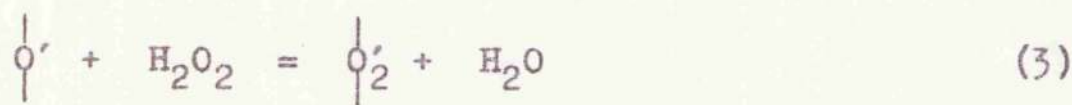
$$\text{Rate} = \frac{A [\text{H}_2\text{O}_2]}{(B + [\text{H}_2\text{O}_2]^{\frac{1}{2}})^2} (B + C + [\text{H}_2\text{O}_2]^{\frac{1}{2}})$$

This would give 1st order in $[H_2O_2]$ at low $[H_2O_2]$ but at high $[H_2O_2]$ the order would not be zero but according to the equation

$$\text{Rate} = A [H_2O_2]^{\frac{1}{2}} \quad \text{i.e. } \frac{1}{2} \text{ order}$$

This fails to satisfy the experimental data.

(ii) The scheme



suggests poisoning due to the slow attainment of equilibrium according to (69). This is unsatisfactory as the equilibrium rate is given by

$$\text{Rate} = \frac{2k_3 [H_2O_2]}{2 + K_{69}^{\frac{1}{2}} [H_2O_2]^{\frac{1}{2}}}$$

which gives first order kinetics at low $[H_2O_2]$ but half order at high $[H_2O_2]$ again failing to satisfy the experimental data.

4. The Final Efficiency Growth on Cu_2O Considered as a Bulk Solid Process.

The unmistakable sigmoid shape of the efficiency /

time curve developed from the minimum in the high $[H_2O_2]$ region suggests that the process involves a bulk solid change rather than a surface reaction. The slowness of the change also suggests a solid process perhaps involving the oxide to some depth below the surface.

A further feature is the occurrence of intermittent leaps in the curves at higher temperatures and higher $[H_2O_2]$ (Fig.25). This is most readily explained in terms of a simple film reaction in which cracking can occur when a certain thickness of film has reacted to the new form. The cracking discontinuously creates new surfaces and the process then goes on to a higher final rate than would be expected when the original growth started out. In Fig.25 it is possible to distinguish several steps which take the form of top portions of sigmoids, the lowest one of which can be extrapolated to a symmetrical maximum. It has to be borne in mind that the sudden onset of a step must affect simultaneously a large number of separate catalyst elements. This could be explained if it occurs at a certain degree of surface change or at some depth of change.

One difficulty about the assumption of cracking is that it implies an extension of the surface area. Yet in every case after removal of H_2O_2 a rapid return to pre-growth conditions takes place in a shorter time than is taken in growing. Even after many hundreds of cycles the original catalyst condition was maintained.

"Cracking" has therefore to be interpreted as meaning any sharply discontinuous breakdown of a pattern which is beginning to limit the growth of catalytic efficiency. It could refer to an internal movement of ions or ionic vacancies e.g. Cu^+ or vacant cation sites (v.c.s.) normally so small as to be negligible at these temperatures but able to move a few places under a high local potential gradient. This amounts to submerged crystal rearrangement and the effect of it would be lost once the H_2O_2 was removed.

The slow beginning of the growth process is the feature of the sigmoid which most limits the choice of mechanism. Suitable mechanisms are:-

- (i) A surface change involving nucleation like decomposition of a hydrate or other solid¹²⁵.
- (ii) A change in which each of the newly active sites is capable of activating an adjoining less active site. This can also be regarded as a surface nucleation or as a surface branching chain reaction.
- (iii) An electrical effect in the surface layers in which the space charge - at first concentrated - begins to spread out into the crystal depth thus permitting a greater capacity for catalysis in the surface. An analogous effect is that produced on a condenser plate when a high dielectric constant liquid is poured between the plates. The spread of charge

however must be accomplished by creation of electronic defects on an expanding front into the crystal until the potential gradient becomes too weak.

- (iv) A process in which the average binding energy of the active peroxide species i.e. O_2' , O' , OH , O_2H , is slowly decreased. This would result in a limited rise in the energy of activation of the overall process dependent on such active species. This change could come about through or be accompanied by, the slow increase in total surface coverage by the relevant species: it is well known that heats of adsorption fall as θ the fraction of coverage increases¹²⁶. It can therefore be suggested that the rate of increase of θ is a function of the area already covered and the area yet to cover. In terms of the change in activation energy when the rate increases from

$$r_0 \text{ at the minimum with } E_A = 19.5 \text{ kcal.}$$

$$\text{to } r_{\infty} \text{ at the final state with } E_A = 26.5 \text{ kcal.}$$

the number of sites increases by a factor of 10 or more (see below). Thus the number of sites at r_0 is very small and can easily account for the slow start of the growth.

Of the four suggested mechanisms only (ii) and (iv) are capable of similar simple kinetic analysis though it

might be said that all are to a first approximation capable of being fitted to an equation of the type:-

$$\frac{dr_t}{dt} = k_{70}(r_t - r_0)(r_{\infty} - r_t) \quad (70)$$

where r_0 = rate at the beginning of the process

r_{∞} = " " " end " " "

r_t = " " any time t during the process

This is not surprising since the processes suggested above were chosen with a sigmoidal shape in mind and equation (70) is the mathematical statement of such a shape. The derivation of equation (70) can however be explained from mechanism (ii) above:-

Let the fraction of the total rate r_t which is due to the increased efficiency at time t be a_t . Then the fraction of the surface capable of causing further growth will be a_t and that still able to be changed will be $(1-a_t)$.

$$\text{then } \frac{d(a_t)}{dt} = k_{71} a_t (1 - a_t) \quad (71)$$

when $a_t = 0$ rate = r_0

and when $a_t = 1$ rate = r_{∞}

$$\therefore a_t = \frac{r_t - r_0}{r_{\infty} - r_0} \quad \text{and} \quad 1 - a_t = \frac{r_{\infty} - r_t}{r_{\infty} - r_0}$$

$$\text{and } \frac{d(a_t)}{dt} = \frac{d(r_t)}{dt} \cdot \frac{1}{r_{\infty} - r_0}$$

Substituting in (71)

$$\frac{d(r_t)}{dt} = \frac{k_{71}}{(r_\infty - r_0)} \cdot (r_t - r_0)(r_\infty - r_0) \quad (72)$$

Integration by parts gives

$$\ln\left(\frac{r_t - r_0}{r_\infty - r_t}\right) = k_{71}t + \text{constant} \quad (73)$$

This is the equation of a symmetrical sigmoid which is shown by the results obtained in the lower regions of the high $[\text{H}_2\text{O}_2]$ zone: e.g. in Fig.60 (the 0.5 M series of points) where $\log_{10}\left(\frac{r_t - r_0}{r_\infty - r_t}\right)$ is plotted against time.

In some cases r_∞ must be estimated by trial and error since a stepwise increase occurs before the initial smooth curve has played itself out. This procedure is illustrated in Fig.61 where on an estimated r_∞ the initial sigmoid is plotted according to 73. Also in Fig.61 some of the higher steps are plotted to the same growth rate process by estimating r'_∞ - the new final rate - by visual extrapolation and using with it a new initial rate

$r'_0 = r_0 \cdot \frac{r'_\infty}{r_\infty}$. In addition the factor $\frac{r'_\infty}{r_\infty}$ must be introduced in the constant so that the new slope k' becomes $k_{71} \cdot \frac{r'_\infty}{r_\infty}$. Thus $\frac{r_\infty}{r'_\infty} \cdot \log_{10}\left(\frac{r_t - r'_0}{r'_\infty - r_t}\right)$ is plotted against time t and lines exactly parallel to the first are obtained.

Fig.60 shows the graphs for the initial sigmoid, of a number of different $[\text{H}_2\text{O}_2]$. They are substantially the same. Also in Fig.60 the extreme pH values 4.5 and 8.0 are

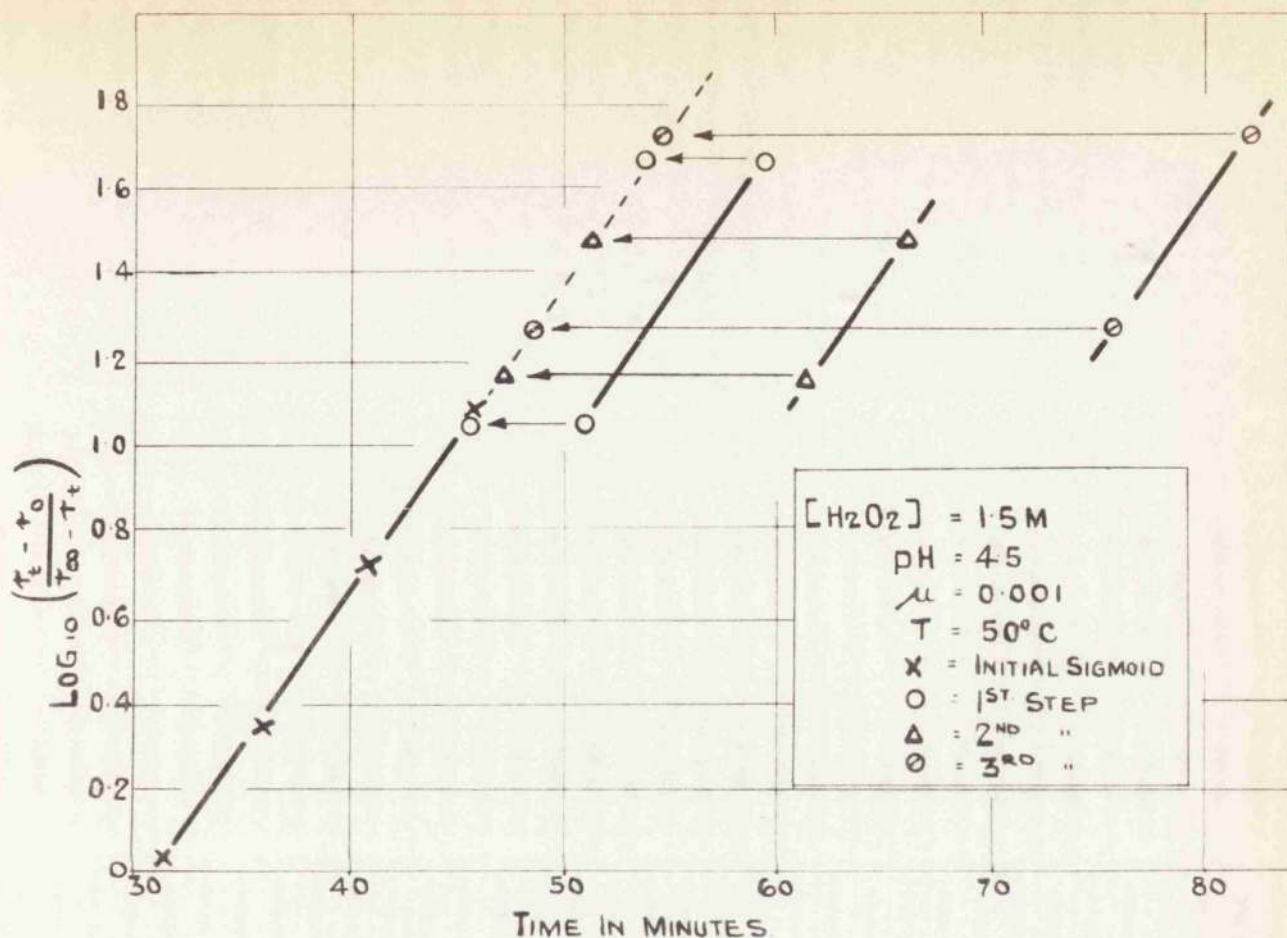


FIG. 61. SHOWING THE ADHERENCE OF THE INITIAL SIGMOID AND FINAL STEPS OF THE SLOW EFFICIENCY GROWTH IN $\text{Cu}_2\text{O}/\text{H}_2\text{O}_2$ TO THE FORM OF A SYMMETRICAL SIGMOID

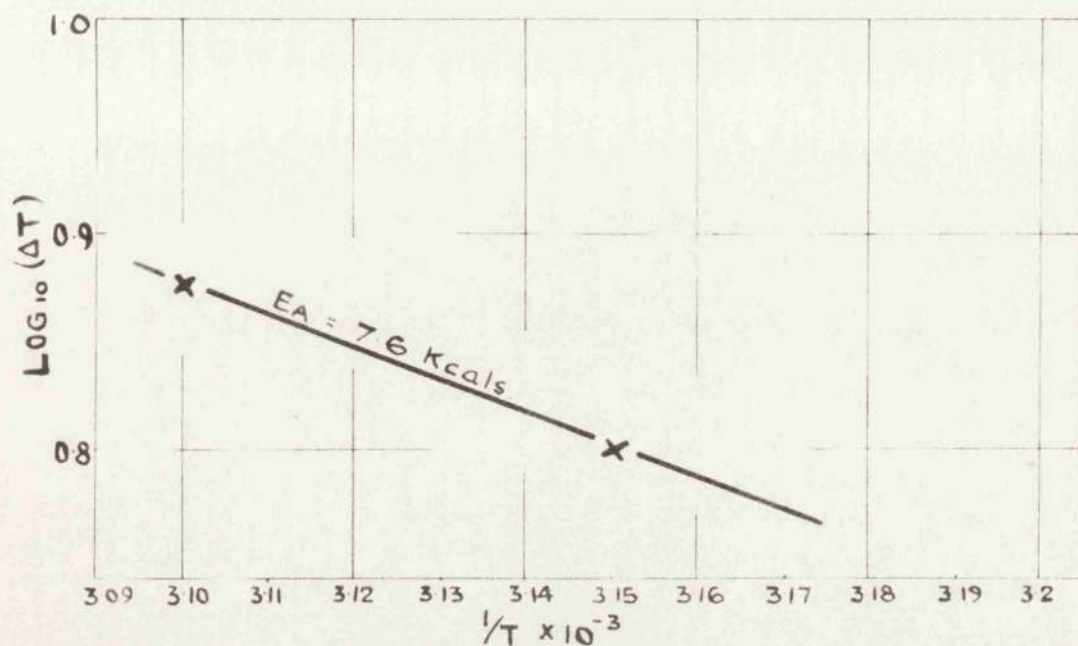


FIG. 62 SHOWING THE ACTIVATION ENERGY OF THE BULK PROCESS OCCURING ON Cu_2O .

compared and again no effect is observed.

The temperature coefficient is obtained from the slopes of the lines in Fig.60 for 45°C and 50°C as 7.6 kcal. (Fig.62). It is of some interest to note that this is of the same order as the energy of activation of surface diffusion of conducting species in Cu_2O , found from the temperature coefficient of electrical conductivity as 7 to 10 kcal.^{127,128}. It may also be noted that the value obtained agrees approximately with the temperature coefficient of the growth slope at the point of inflection which gives 37.5 kcal. (i.e. including 26.5 kcal. the activation energy of the maximum final rate).

The rôle of $[\text{H}_2\text{O}_2]$ in the growth process is clearly to make the change possible but not to control its rate. Thus H_2O_2 could create a potential difference between the surface and the bulk which decides the extent to which the diffusional rearrangement can proceed. If the final efficiencies of the growth process are taken as the extrapolated maxima of the first sigmoid the values naturally differ considerably from those of the measured maxima which exhibit an almost zero order dependence on $[\text{H}_2\text{O}_2]$ - Fig.31. They are in fact proportional to $\frac{1}{[\text{H}_2\text{O}_2]}$ - Fig.57 - i.e. similar to the initial state which suggests that the two states, initial and final, do not differ basically.

If the minimum and final rate processes are essentially the same as the kinetic analysis seems to suggest,

it is necessary to explain the difference in temperature coefficients i.e. 19.5 kcal. for the minimum and 26.5 kcal. for the maximum. Clearly the higher E_A at the maximum together with the higher rate suggests a greater number of active sites. The question arises, do the sites responsible for the minimum rate continue to work or are they now obliterated, having their work done by the larger number of sites of higher E_A ? The kinetics of the growth process have been explained earlier as being controlled by a diffusion of current carrying species in the oxide, under the influence of a potential difference. It could be supposed that these species come up out of the bulk of the oxide and flow into the surface layer each creating there a new active centre. In the same process the original centres of low E_A could be pulled back into line so that the new surface is homogeneous. Quantitatively however the question is unimportant.

5. Potential Measurements from Cu_2O during Reaction.

The main potentials correspond readily with those expected under the conditions. Thus a fresh Cu_2O electrode in water (no H_2O_2) at pH 4.5 gave $e = 0.174$ v. This potential is referred to the standard H_2 electrode at 298°K - as are all the other potentials in this section - by adding 0.230 v. (the value of the S.C.E. reference electrode at 45°C on this scale) to the measured potentials. A "used" Cu_2O electrode i.e. one which had been exposed to an H_2O_2 containing solution, gave the value of 0.267 v. in H_2O .

This higher oxidised value was permanent i.e. it did not decay even on heating and reimmersion.

Now the potential of a Cu/Cu₂O, OH' electrode under these conditions can be calculated as 0.222 v. The calculation derives from data reported in Latimer¹²⁹ and is carried out as follows.

The standard electrode potential of the electrode, for which the reaction is



and the e.m.f. at 45°C is given by

$$e = e_o^{45^\circ\text{C}} - 0.063 \log_{10} a_{\text{OH}'}$$

is -0.358 at 298°A. The entropy change again from Latimer's tables is

$$\Delta S = -17.2 = \frac{-d(\Delta G)}{dT} = J.F. \frac{de}{dt}$$

Thus the temperature coefficient is -0.00089 v./degree which gives $e_o^{45^\circ\text{C}} = -0.376$ v. and hence the expected e.m.f. of such an electrode at pH 4.5 becomes

$$-0.376 + 0.598 = 0.222 \text{ v.}$$

These results suggest at first sight that an unused Cu₂O electrode is in a somewhat reduced state since the potential is 0.048 v. below that corresponding to the Cu₂O/OH' electrode. On the other hand a once used electrode remains in an oxidised state relative to pure Cu₂O, to an

extent indicated by the displacement of 0.045 v.

The potential, on immersion in H_2O_2 solution at the same pH, is displaced to 0.56 ± 0.02 v. where the spread refers to different electrodes. This corresponds closely to the potential of the $\text{Cu}_2\text{O}/\text{Cu}(\text{OH})_2/\text{OH}'$ electrode, the reaction at which is



From Latimer's data ($e_o^{298} = -0.050$ v., $\Delta S = -1.2$ units) $e_o^{318} = -0.048$ v. and the calculated potential in a solution of pH 4.5 is 0.551 v. Thus H_2O_2 oxidises the Cu_2O surface to the $\text{Cu}(\text{OH})_2$ state. This is somewhat like the process which occurs during the anodic treatment of Cu in alkaline solution. A good summary of work on Cu anodisation is given by Halliday¹³⁰ who identifies three stages viz: (i) formation of Cu_2O (ii) formation of a mixed $\text{Cu}(\text{OH})_2$, CuO layer (iii) passivation of the copper. In the case of treatment by H_2O_2 inhibition of dissolution by high $[\text{H}_2\text{O}_2]$ can be regarded as passivation. The passivated surface was shown by Halliday to be either $\text{Cu}(\text{OH})_2$ or CuO the latter being responsible in stirred solution. Since the solutions in the present work were always well stirred (by flow and bubbling) it can be taken that the potential results are in keeping with the explanation that during catalysis the more concentrated H_2O_2 solutions give rise to CuO . The actual surface however may possibly still be thought of as $\text{Cu}(\text{OH})_2$.

The actual potential during catalysis is almost certainly not controlled by the $\text{Cu}_2\text{O}/\text{Cu}(\text{OH})_2$ potential. It has the same value as would be expected from the results of Bockris and Oldfield¹⁰² on Pt and Au and from the detailed work of Hart, Aitken and Beaton¹⁰³ where the potentials were given (irrespective of metal) in the range of pH and $[\text{H}_2\text{O}_2]$ by the expression

$$e = 0.84 - 0.059 \text{ pH} \quad (76)$$

at 25°C. This would give 0.56 v. at 45°C and pH 4.5

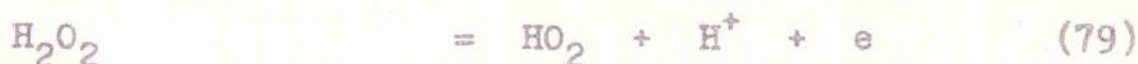
Since the same identical potential is found on Pt, Au, Ag, Cu and Ni it is clear that the H_2O_2 is the determining factor and the nature of the underlying oxide or metal negligibly so. Thus it is probably only accidental that the potential of 0.56 v. \pm 0.02 (obtained in the present work) agrees so closely with 0.551 v., the potential expected if $\text{Cu}(\text{OH})_2$ and Cu_2O exist together at the used pH. It is also impossible to explain the steady H_2O_2 potential in terms of $\text{Cu}(\text{HO}_2)$ or $\text{Cu}(\text{HO}_2)_2$ layers since such an explanation extended to other metals would surely give a wide range of e_0 values.

Bockris and Oldfield¹⁰² suggested that these steady potentials are due to the equilibrium



This would give the relation (76) with the value of e_0 decided by the particular state of adsorption of the OH

radical on the surface in question. Gerischer and Gerischer¹³¹ suggested that the potential is controlled by the cyclic process



which gives the required e/pH relation.

In both cases radicals are formed. It is these which are regarded as responsible for catalysis in chain processes. The electrode potential thus reflects the production of a steady surface concentration of radicals during catalysis.

The oxidation-reduction potential set up during catalysis will of course decide the nature of the underlying surface of the metal or oxide. In the present case it is clear that a surface consisting of Cu_2O and $\text{Cu}(\text{OH})_2$ will be in equilibrium with decomposing H_2O_2 . The full equation for the electrode potential given by reaction (75) is

$$e = -0.048 - \frac{RT}{F} \ln \left(\frac{a_{\text{Cu}_2\text{O}}^{\frac{1}{2}} \cdot a_{\text{OH}^-}}{a_{\text{Cu}(\text{OH})_2}^{\frac{1}{2}}} \right)$$

The value of -0.048 v. or 0.551 v. in pH 4.5 will only be given when the activities of the two solids are the same or when each is unity as in the case of mixing the bulk solids. It can be seen now however that the slightly more positive value of the measured potentials compared with their e_0

value corresponds with a value of the ratio $\frac{a_{\text{Cu}_2\text{O}}}{a_{\text{Cu}(\text{OH})_2}}$ somewhat greater than unity, viz:

$$0.560 - 0.551 = 0.031 \cdot \log_{10} \left(\frac{a_{\text{Cu}(\text{OH})_2}}{a_{\text{Cu}_2\text{O}}} \right)$$

$$\text{Whence } \frac{a_{\text{Cu}(\text{OH})_2}}{a_{\text{Cu}_2\text{O}}} = 2.0$$

If the whole surface is supposed covered with OH' ions, the ratio of Cu^{++} to Cu^+ will be about unity at the peak conditions. The value of the final steady potential changes only slightly in this $[\text{H}_2\text{O}_2]$ range with $[\text{H}_2\text{O}_2]$. However this change seems significant and to tie up with the catalysis. Thus from 0.5 M to 2 M there is a small fall in the peak potential of 0.003 v. and a small fall in the steady catalysis. This would be in keeping with a fall in the surface fraction of Cu^{++} (see below for calculation) from 0.50 to 0.33 .

The small changes of potential during catalysis were reproducible, uniform and coincided in time with the marked changes of catalytic efficiency occurring under the same conditions of $[\text{H}_2\text{O}_2]$ and pH - inset Fig.49 illustrates these effects clearly. The movement from peak to minimum is 0.013 v. to 0.015 v. taking about 10 minutes with a slower recovery to a constant value at almost exactly the same potential as the peak.

In one case using 1.5 M H_2O_2 the peak and final

potentials were 0.560 v. and the minimum 0.547 v. Considering the surface to consist of Cu ions fixed in position but with possible charge variation i.e. either Cu^{++} or Cu^+ , these potentials can be used to calculate the charge distribution. For this purpose the single charged ions will be used in the hypothetical surface form CuOH .



$$\text{so that } a_{\text{Cu}_2\text{O}} = \text{constant} \cdot a_{\text{CuOH}}^2$$

At the peak (as given above)

$$\frac{a_{\text{Cu}(\text{OH})_2}}{a_{\text{Cu}_2\text{O}}} = 2.0$$

$$\text{i.e. } \frac{a_{\text{Cu}(\text{OH})_2}}{a_{\text{CuOH}}^2} = 2 = \frac{a_{\text{Cu}^{++}}}{a_{\text{Cu}^+}^2}$$

where a is the fraction of surface Cu ions in the given form. At the minimum

$$\frac{a_{\text{Cu}^{++}}}{a_{\text{Cu}^+}^2} = 0.75$$

If $a_{\text{Cu}^{++}} + a_{\text{Cu}^+} = 1$ it can be calculated that the variation of the fraction of Cu^{++} from peak to minimum is 0.5 to 0.33. Such a change is entirely in keeping with the change in catalysis if the surface concentration of catalytically active species e.g. O^- ions, is proportional to $a_{\text{Cu}^{++}}$.

In the first order zone of $[H_2O_2]$ i.e. below 0.25 M the potentials rise to a value below the "peak" value measured above this concentration. There is no cycle thereafter. This again resembles the catalytic efficiency behaviour in the low $[H_2O_2]$ zone. The actual potential values suggest a very low $a_{Cu^{++}}$ e.g. at 0.1 M H_2O_2 the above calculation gives $a_{Cu^{++}} = 0.001$. The relationship between the measured potential and $[H_2O_2]$ in this concentration zone is very sensitive. It can be represented by a logarithmic dependence of potential on $[H_2O_2]$ but no special significance can be attached to this.

On removal of H_2O_2 the elevated, oxidised potential decays to a value only slightly above the Cu_2O/OH' equilibrium value. This decay is extremely rapid and suggests that only the surface is converted during catalysis to the oxidised state responsible for the high potential. Otherwise a slow decay would occur while the oxide was reducing itself in depth. It will be necessary to answer the question: why does the catalyst not undergo deep oxidation to bring it into equilibrium with the surface as would be the case if anodisation were the cause of the surface oxidation? For the present this question must be left unanswered with perhaps the tentative suggestion that a passivation of the surface layers, induced by the H_2O_2 itself, prevents extension of the reaction to any depth in the oxide.

6. Comparison of the NiO/H₂O₂ and CoO/H₂O₂ Systems
with the Cu₂O/H₂O₂ System.

The experimental investigations carried out on the Cu₂O/H₂O₂ system were extended to NiO/H₂O₂ and CoO/H₂O₂ in order to:-

- (i) compare the relative catalytic activities of the three systems
- (ii) to examine any efficiency changes taking place and to test the general applicability of the mechanism proposed for Cu₂O/H₂O₂.

(a) Results.

- (i) Relative catalytic efficiency.

The efficiency changes taking place on Cu₂O, NiO and CoO in 0.5 M H₂O₂ at pH 4.5 and 45°C are shown in Fig.63. Since almost twice as much (by weight) Cu₂O as CoO and NiO was used the results show clearly that in order of decreasing catalytic activity



In addition it is likely that the surface area in the Cu₂O was much greater than in CoO and NiO since it was subject to a greater number of oxidation and reduction cycles.

- (ii) Changes in catalyst efficiency taking place during

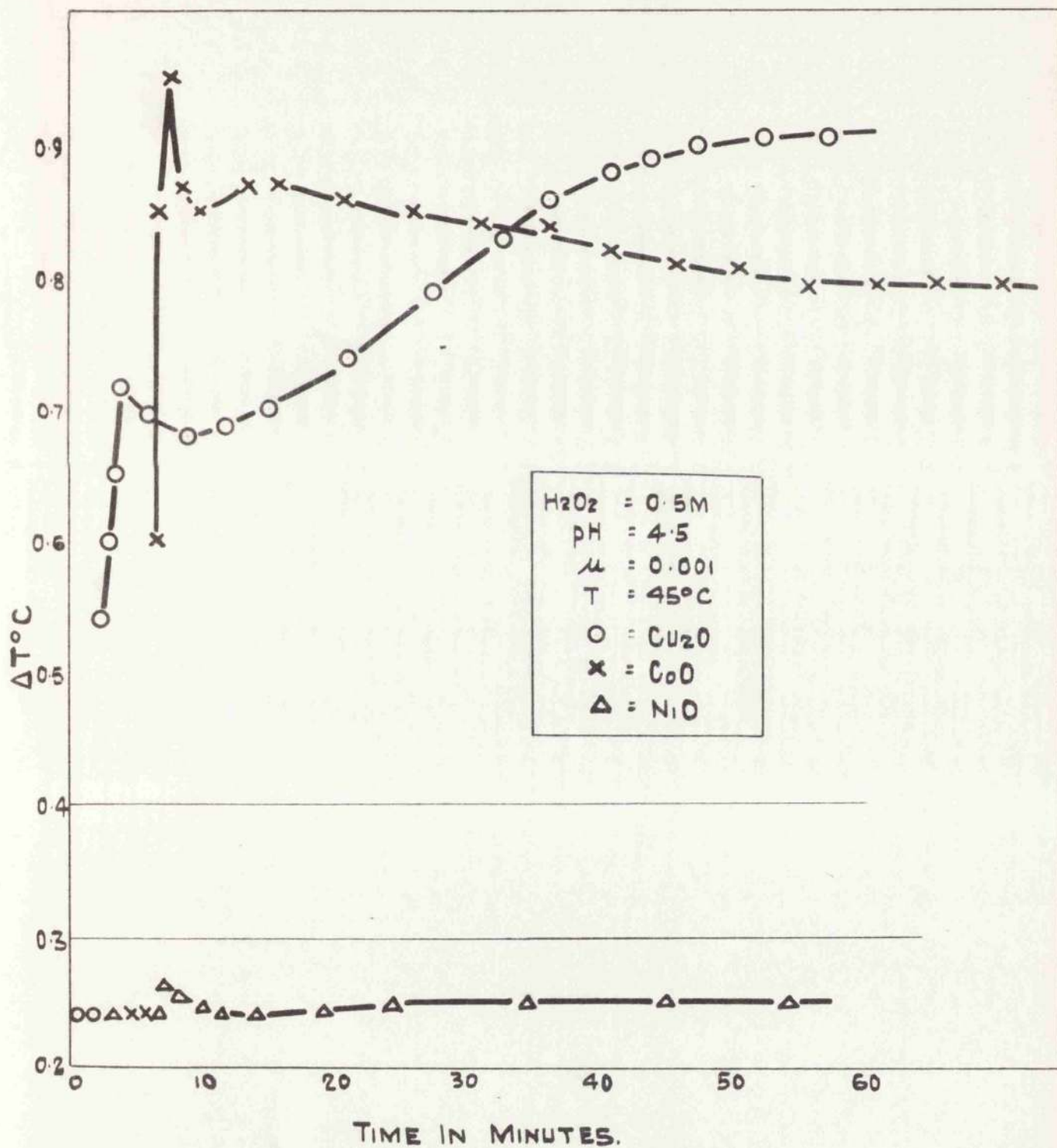


FIG. 63. COMPARISON OF EFFICIENCY CHANGES TAKING PLACE ON Cu_2O , CoO , NiO , UNDER THE ABOVE CONDITIONS.

catalysis.

In the case of NiO no measurable rates of decomposition were obtained in the concentration range 5 M H_2O_2 - 1 M H_2O_2 and it is concluded that NiO is inactive in this aqueous H_2O_2 concentration zone.

For CoO the changes in efficiency taking place during decomposition for the concentration zone 1 M H_2O_2 to 0.12 M H_2O_2 are shown in Fig.64. As in Cu_2O a good degree of reproducibility was obtained using the same sample of catalyst which was kept immersed in distilled water between tests.

As in Cu_2O , efficiency changes take place during decomposition and like Cu_2O fall into two main $[H_2O_2]$ zones, i.e. a high $[H_2O_2]$ zone lying above 0.5 M H_2O_2 and a low $[H_2O_2]$ zone below 0.5 M H_2O_2 .

In the high concentration region four stages are obtained

1. an initial rapid increase to a peak value
2. a peak efficiency
3. a relatively slow fall from the peak efficiency
4. a minimum efficiency.

In the low concentration zone a steady efficiency is obtained immediately the reaction commences. This is followed by a small fall after some time.

The effect of $[H_2O_2]$ on the above changes was

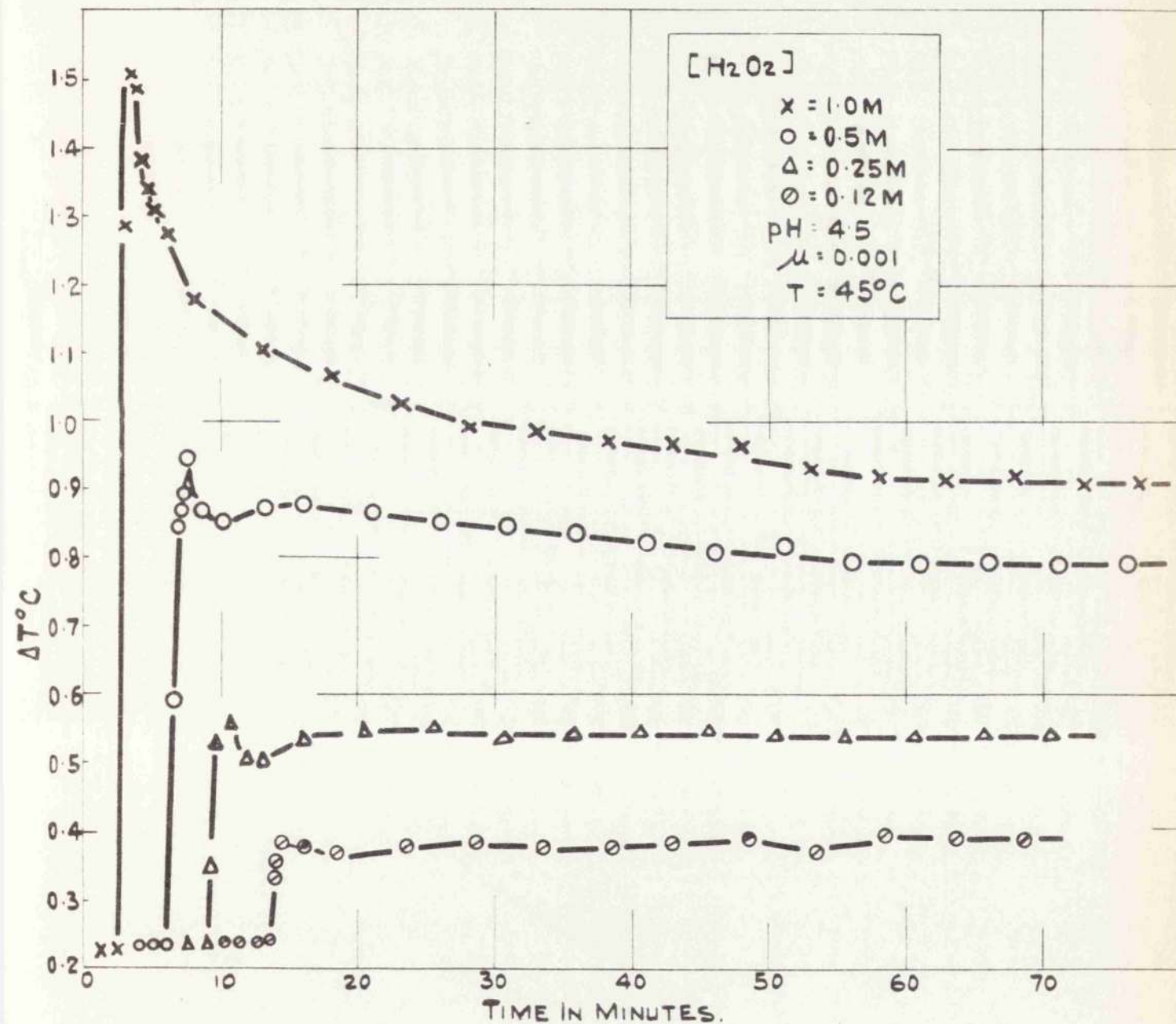


FIG. 64. SHOWING THE VARIATION WITH [H₂O₂] OF THE EFFICIENCY AND ALSO THE EFFICIENCY CHANGES OF THE CoO/H₂O₂ SYSTEM.

studied at pH 4.5 ionic strength 0.001 and 45°C.

A. High $[H_2O_2]$ zone.

1. Initial increase in efficiency.

Due to the high efficiency of CoO for the decomposition of H_2O_2 it was not possible to go above 1 M H_2O_2 in the present apparatus. Results obtained at 1.0 M and 0.5 M combined with those in the low $[H_2O_2]$ zone show that $[H_2O_2]$ has no measurable effect on the initial increase in efficiency.

2. Peak efficiency.

The peak efficiency is directly proportional to the $[H_2O_2]$ (Fig.65).

3. Decline from peak efficiency.

The transformation from high to low $[H_2O_2]$ behaviour is not so sharp as in Cu_2O , but the results shown in Fig.66 indicate that the decline in efficiency varies inversely with $[H_2O_2]$. The half-life period for the decline at 1 M and 0.5 M H_2O_2 is 4.5 minutes and 10 minutes respectively.

4. Minimum efficiency.

As above a full examination could not be carried out on this stage due to the high activity of the CoO. From the results obtained however (Fig.65) it appears that the change from low $[H_2O_2]$ to high $[H_2O_2]$ is

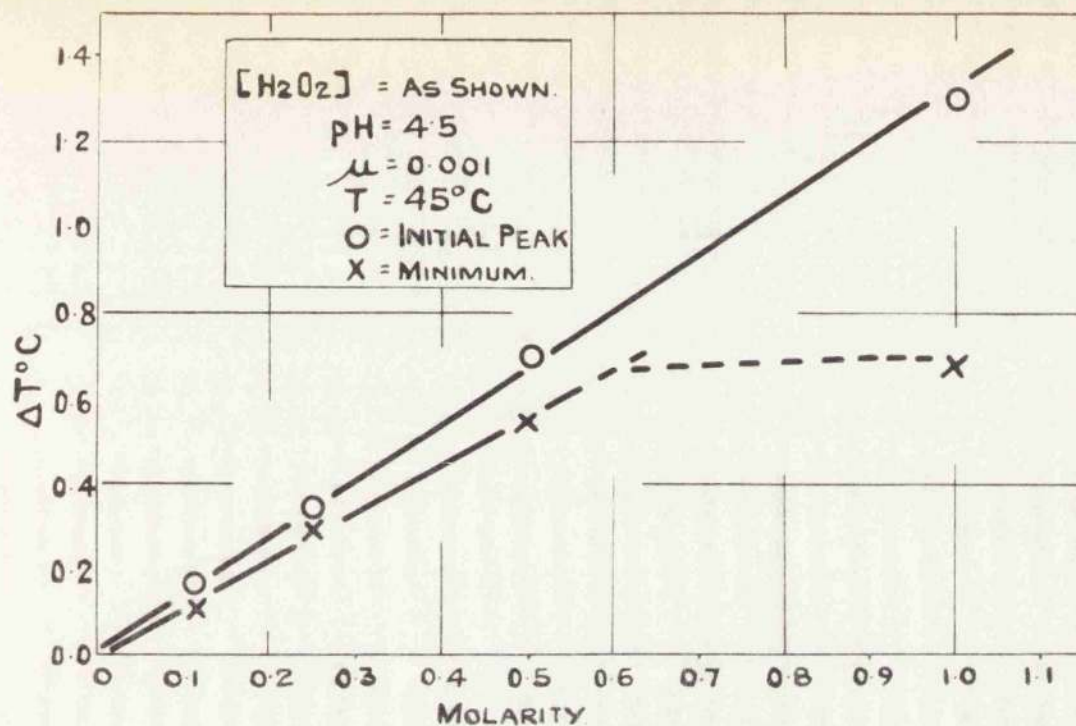


FIG. 65. SHOWING THE EFFECT OF $[H_2O_2]$ ON (a) THE INITIAL PEAK EFFICIENCY (b) FINAL OR MINIMUM EFFICIENCY FOR CoO .

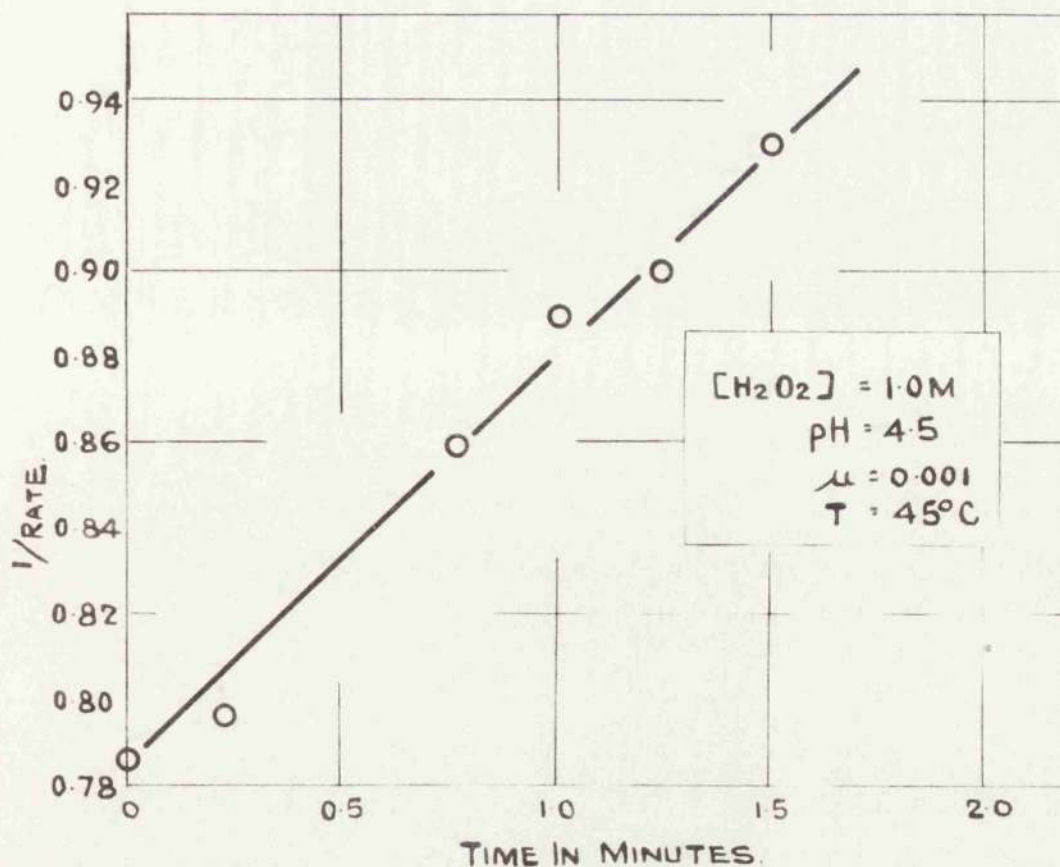


FIG. 66. SHOWING THE VARIATION WITH TIME OF $1/\text{RATE}$ DURING THE DECLINE FROM THE PEAK EFFICIENCY IN CoO .

accompanied by a change in the $[H_2O_2]$ dependence of of this stage similar to that taking place on Cu_2O .

B. Low $[H_2O_2]$ zone.

Fig.65 shows that the efficiency is directly proportional to $[H_2O_2]$.

(b) Discussion.

The cyclic efficiency changes taking place on Cu_2O involve as proposed above two processes, viz:

- (i) a surface reaction
- (ii) a bulk reaction

each of which exhibits different behaviour in the two concentration zones.

The form of the initial efficiency changes taking place on CoO suggests a surface reaction similar to that taking place on Cu_2O . In addition the experimental results follow closely the conditions required to fulfil the proposed mechanism i.e.

A. High $[H_2O_2]$ zone.

1. Initial increase in efficiency.

The initial rapid increase in efficiency is unaffected by $[H_2O_2]$ and as in Cu_2O can only be considered as due to an equilibrium attainment effect in the system.

2. Peak efficiency.

Although only two peak efficiencies were measured in this concentration zone the values when combined with the initial efficiencies in the low concentration zone show that

$$\text{Peak efficiency} = k [\text{H}_2\text{O}_2]$$

over the studied $[\text{H}_2\text{O}_2]$ range 0.1 M to 1.0 M. This regards the initial steady efficiency in the low $[\text{H}_2\text{O}_2]$ zone as a peak value. At higher concentrations than those studied it is likely that the true peak efficiencies will not be measured and as in Cu_2O the peak efficiency will obey the relationship

$$\text{Peak efficiency} = k' + k'' [\text{H}_2\text{O}_2]$$

It is interesting to note that the rate of decline at 1.0 M in CoO is slower than the similar stage in Cu_2O at this concentration. This is in agreement with the results of Yu, Chessick and Zettlemyer¹⁰⁹ who concluded that the proportion of O' was greater in CoO than in Cu_2O . On this basis it is to be expected that the catalytic efficiency of NiO for the decomposition should lie between CoO and Cu_2O . This is indeed the case in the vapour phase decomposition of H_2O_2 as shown by Ross⁴⁹ but as is stated above NiO is relatively inactive in aqueous H_2O_2 . Experiments have shown that $\text{Ni}(\text{OH})_2$ is very much more stable than either $\text{Cu}(\text{OH})_2$ or $\text{Co}(\text{OH})_2$ and it is therefore concluded

that the inactivity of NiO for the decomposition is due to the stability of the hydroxide.

3. Decline of efficiency.

The proposed mechanism for $\text{Cu}_2\text{O}/\text{H}_2\text{O}_2$ requires that the decline from the peak efficiency has the following characteristics

$$(i) \text{ near the true peak } \frac{-d(\text{efficiency})}{dt} = k [\text{H}_2\text{O}_2]^2$$

(ii) at constant $[\text{H}_2\text{O}_2]$ the efficiency fall from the peak value gives

$$\frac{1}{\text{rate}} \propto \text{time} + \text{constant}$$

Since the efficiency curve obtained at 0.5 M appears to lie on the border between high and low $[\text{H}_2\text{O}_2]$ behaviour, only one characteristic curve is available i.e. for 1.0 M. Relationship (i) cannot be tested but for the 1.0 M decline curve, $\frac{1}{\text{rate}}$ is proportional to the time (Fig.66).

4. Minimum efficiency

Although there are insufficient results to determine the $[\text{H}_2\text{O}_2]$ dependence of the minimum the effects noted are similar to those for Cu_2O , when the results obtained at 1.0 M and 0.5 M are combined with those measured in the low concentration zone (i.e. Fig.65). In the case of $\text{Cu}_2\text{O}/\text{H}_2\text{O}_2$ the minimum (or non poisoned peak in the low $[\text{H}_2\text{O}_2]$ zone) is directly proportional

to the $[H_2O_2]$ in the low $[H_2O_2]$ zone. At the change over concentration (0.25 M H_2O_2) the linear relationship flattens out and the minimum efficiency becomes dependent on $\frac{1}{[H_2O_2]}$. A similar pattern is obtained for CoO and although the high concentration range was not covered the results so far obtained appear analogous.

B. Low $[H_2O_2]$ zone.

The behaviour in this zone is exactly similar to that in Cu_2O . The initial efficiency, which can be considered a non-poisoned peak, and the final efficiency which is analogous to the minimum steady state at high $[H_2O_2]$ both obey the relationship

$$\text{Rate} = k [H_2O_2]$$

From the close similarity between the results obtained in the Cu_2O/H_2O_2 and CoO/H_2O_2 systems, it appears reasonable to propose that the surface reaction mechanism derived for Cu_2O/H_2O_2 not only holds for CoO/H_2O_2 but is of general applicability for all P-type semiconducting oxide/ H_2O_2 systems.

The main difference in behaviour of the Cu_2O and CoO systems is the absence in CoO of the final recovery or bulk effect so prominent in Cu_2O . It must be concluded that in CoO the surface conductivity is such as to prevent diffusion of ionic or electronic vacancies at the temperature of the

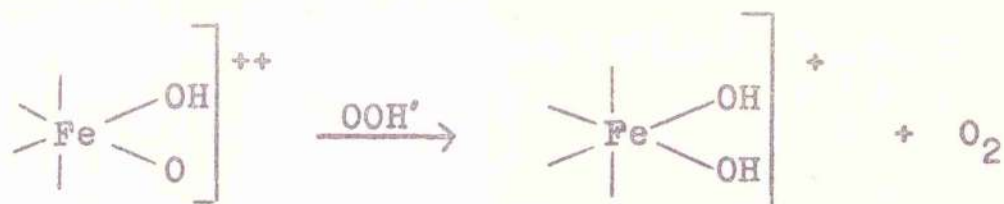
experiment.

7. The Importance of Isotopic Tracer Studies.

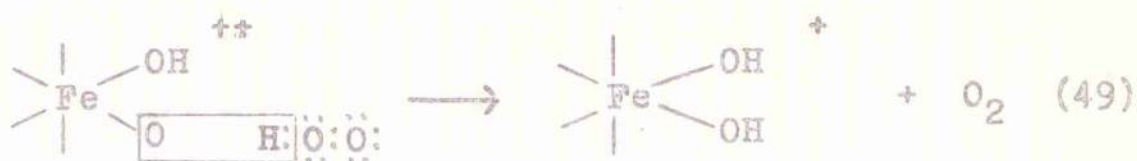
Results from the use of O^{18} as a tracer in the decomposition of H_2O_2 on various catalysts have come to have an important bearing on proposed mechanisms.

Winter and Briscoe¹³² and Dole et al.¹³³ using H_2O_2 dissolved in H_2O bearing a slight enrichment of O^{18} showed that in reactions catalysed by inorganic catalysts and catalase the evolved O_2 came exclusively from the H_2O_2 . In addition Dole and co-workers found that the enrichment which occurred in the decomposition catalysed by inorganic compounds did not occur with catalase catalysed reactions.

Similar results were obtained by Wang¹¹⁶ whose explanation was in accord with that proposed by Dole i.e. for the inorganic catalysed reaction the relatively weak nature of the attachment of H_2O_2 to the surface favoured the splitting of the weaker $O^{16} - O^{16}$ and $O^{16} - O^{18}$ bonds in preference to the $O^{18} - O^{18}$ bond (therefore causing enrichment) whilst the more active catalase did not differentiate, breaking the O-O bond irrespective of the proportions of O^{16} or O^{18} . The mechanism proposed by Wang for the decomposition did not differentiate between O_2 evolution from a single H_2O_2 molecule or O_2 evolution from two H_2O_2 molecules, i.e. for catalysis by (TETA) $Fe(OH)_2^+$ (see above, p.145) the exact mechanism for the step



was not postulated. Later work by Wang¹¹⁷ did make this differentiation claiming to prove conclusively that O_2 was produced from a single H_2O_2 molecule i.e.



rather than

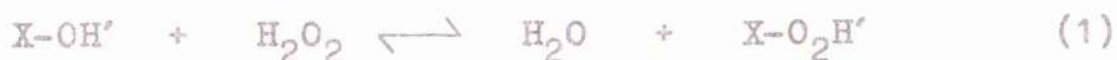


In general therefore the conclusions from these tracer experiments accord with the mechanism proposed above for the semiconducting metal oxide/ H_2O_2 catalytic reaction

SECTION II

I N T R O D U C T I O N

An important feature of the mechanism proposed in Section I for the decomposition of H_2O_2 on Cu_2O (and p-type semiconductor oxides in general) was the assumption that the active surface species consisted of the radical ions, O_2' or O' , which were linked by a cyclic reaction to the inactive OH' , and O_2H' ions. An essential detail in the scheme was the maintenance of equilibrium between these last two surface ions, thus:



where X is a surface site. From the kinetic analysis the equilibrium constant for this process was calculated as:-

$$K = \frac{m_{O_2H'}}{m_{OH'} [H_2O_2]} = 5.6 \quad (2)$$

In an attempt to examine this equilibrium in an independent system, an investigation was undertaken of the behaviour of an anion exchange resin in the OH' form in the presence of H_2O_2 . These resins are markedly catalytic to H_2O_2 but at low $[H_2O_2]$ it was felt to be possible to study the exchange equilibrium



while allowing for the small amount of catalysis going on.

At the same time, a brief study was made, in a static system,

of the kinetics of decomposition of H_2O_2 on the resin in the hope that it would be possible to match the results to a mechanism which would have an appropriate relation, (bearing in mind the differences between the two solids) to that derived for oxide catalysis.

EXPERIMENTAL

1. Exchange Material

The resin-exchange materials now available consist of synthetic polymers, e.g. substituted polystyrene, cross-linked by copolymerisation with divinylbenzene, which act as a matrix for exchangeable groups. The strongly basic¹ substituted type in which quaternary ammonium groups are the anion binding species, was used in the present work and B.D.H. Amberlite IRA 400 was chosen. It was obtained in the form of 50-100 mesh particles as the chloride substituted resin which was inert to H_2O_2 . It had first to be converted to the OH form.

2. Preparation of Resin in OH form.

About 25 gm. of resin were placed in a 2.5 cm. diameter chromatographic column. It was allowed to settle after shaking up with water; it gave a 12 cm. deep uniform bed. Air above the resin was blown out with N_2 and 2 N carbonate free NaOH passed down the column until no chloride was detected in the effluent (about 12 hr.). The resin was then shaken up and allowed to settle to a new bed. Further NaOH solution was percolated: this was to check for channelling in the first run. Finally ion free distilled water was passed down the column until pH 7 was recorded in

the effluent. The water was prepared in an "Elgastat" ion exchange apparatus (to a specific conductivity of 8×10^{-6} reciprocal ohms) from once distilled water. When the resin was free from excess NaOH it was kept under CO_2 -free water until required.

All the experiments described below were carried out at the natural pH of the solution i.e. pH 5.8 - 6.0 .

3. Sampling and Estimation of Resin.

It was necessary to devise a method for measuring out the damp resin since drying and weighing seemed to introduce difficulties due to loss of water and carbonate contamination. A simple volumetric procedure was used, pouring a mobile slurry to a mark in a 5 mm. tube resting on a pad of filter paper. The tube had a capacity of 3 mls. to the mark. The slug of resin, which lost adherent moisture to the pad but did not meanwhile alter its dimensions in the tube was extruded into the apparatus in which it was to be used.

The accuracy of the sampling was tested in two ways.

(i) Weighing after a standard drying procedure.

The weights of four samples were 1.04 ± 0.02 g.

(ii) By wet assay.

This was done by estimating the OH' liberated on conversion of the sample completely to the chloride form. The measured slug was warmed at 40°C with

100 mls. N KCl in bubbling N_2 for 1 hour. The solution was filtered, the resin washed, and the combined washings and filtrate immediately titrated with 0.01 N HCl. The resin was later treated with more N KCl but no appreciable further exchange took place. The total exchangeable OH' initially present on the resin was calculated. The result of three experiments, 2.525×10^{-3} , 2.510×10^{-3} and 2.480×10^{-3} moles OH' demonstrate a satisfactory degree of reproducibility in the sampling and permit the use of the value of 2.5×10^{-3} as the amount of resin (expressed in moles of exchangeable OH') used in all further experiments.

4. Resin-Peroxide Equilibrium.

Careful determinations of oxygen evolution with time were carried out at $25^\circ C$ in preliminary experiments so that allowance could be made for this in calculating the equilibrium constants. These experiments are described in the following section. The resin was introduced into a measured quantity (40 or 100 mls. in most experiments) of 0.07, 0.0525, or 0.035 M H_2O_2 , which had been brought to temperature equilibrium at $25^\circ C$. It was stirred, in the apparatus described below, and after short periods of time (2-5 minutes) a 10 ml. sample of the solution removed for analysis by

titration with 0.01 N KMnO_4 solution. It was clear from the results that the equilibrium was reached very rapidly. It was not convenient to determine the oxygen loss in the same experiment as was used to measure the exchange equilibrium. This was calculated from a knowledge of the time of sampling and the rate of catalysis from a parallel experiment under the same conditions. Table 1 gives the results of these experiments. The final column gives

$$K = \frac{\theta}{(1 - \theta) [\text{H}_2\text{O}_2]} \quad (4)$$

where θ is the fraction of resin covered by H_2O_2 i.e. $\frac{m_R}{0.0025}$. This is a form of equation (2) and is the application of the Law of Mass Action to equation (1).

m_R is the moles of H_2O_2 adsorbed on the resin at equilibrium:
 $1 - \theta = \frac{(0.0025 - m_R)}{0.0025}$. $[\text{H}_2\text{O}_2]$ refers to the solution at equilibrium.

Initial Concn. H_2O_2 Mole/litre	Volume of Solution ml.	K
0.07	40	668
0.0525	40	676
0.035	40	644
0.035	40	640
0.035	100	660
0.035	120	653

Table 1. Equilibrium of 1 g. (0.025 moles) resin with H_2O_2 solution.

The average value of $K = 657$ is subject to satisfactorily little deviation in these experiments. The constancy of the value obtained under these different conditions was taken to substantiate the assumption that true equilibrium was attained in all cases and that the exchange is very rapid.

5. Decomposition Rate Experiments.

(a) Decomposition Apparatus

The apparatus is shown in Fig. 1. It consisted of a three-necked pyrex flat-bottomed flask. Stirring was by a magnetic stirrer, the agitator being a short length of iron encased in polythene. Evolving oxygen was metered by a soap-film movement in a horizontal tube of 3-5 mm. diameter. The tube was calibrated with water. In a run the clean dry vessel was clamped in position with its base 0.5 cm. from the glass bottom of the thermostat tank. The flask was flushed out with N_2 and the resin introduced. A measured volume of the H_2O_2 stock solution (which had been brought to $25^\circ C$) was measured in from a fast delivery pipette. The flask was stoppered, the stirrer started and the flow meter connected without delay. The addition of solution and establishment of equilibria conditions in the flask could be achieved in about 15 seconds.

Stirring was fast enough to lift the particles of

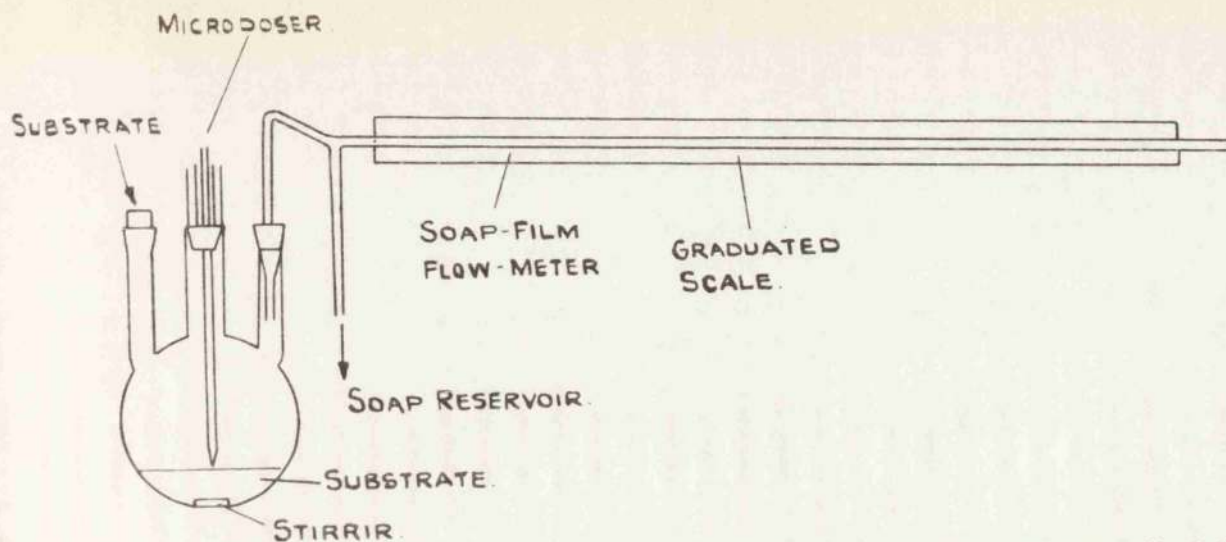


FIG. 1. APPARATUS FOR THE MEASUREMENT OF RATE OF DECOMPOSITION OF H_2O_2 BY ANION EXCHANGE RESIN.

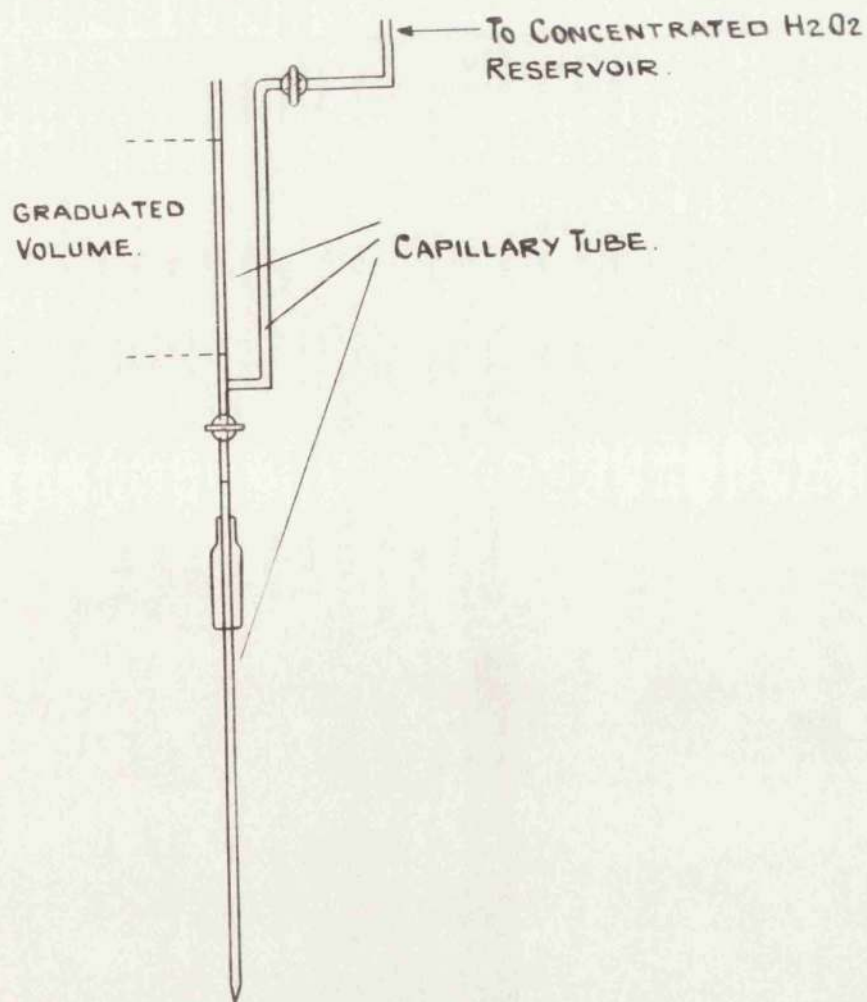


FIG. 2. MICRODOSER FOR MAINTAINING CONSTANT H_2O_2 CONCENTRATION.

resin from the bottom but not so as to cause unbalance in the flask. If this mean range was adhered to, the actual rate of stirring had no effect on the rate of evolution of gas.

(b) Steady $[H_2O_2]$ Procedure

In some experiments an attempt was made to measure the catalyst efficiency under conditions of steady $[H_2O_2]$. The object of this was to show whether the resin changed its efficiency with time as with oxides. This could have been better achieved by a flow method but there was no time to solve the problem of the use of the particulate material in a flow apparatus.

The procedure adopted was to replenish the H_2O_2 lost by catalysis in a number of small steps by a microdoser as shown in Fig.2. The doser was filled with 8 M H_2O_2 . It consisted of 0.5 mm. true-bore capillary ending in a very fine nozzle immersed in the solution. The concentrated solution was added in microamounts to correspond with the loss of O_2 . The volume change in the solution was, of course, quite negligible, a fact which simplified the calculation of the amount to add. The results of these experiments are illustrated in Fig.3 where it is seen that the efficiency remained perfectly constant for up to 20 mins. when the $[H_2O_2]$ was maintained

constant.

(c) Reproducibility of Rate Measurements.

Fig.3 also gives three rate/time curves obtained without "makeup" of $[H_2O_2]$ with three different resin samples. A satisfactory degree of reproducibility was found. Table 2 demonstrates this with reference to the peak rate.

Resin Sample	Rate in mls. O_2 /min.
1	3.60
2	3.65
3	3.60

Table 2.

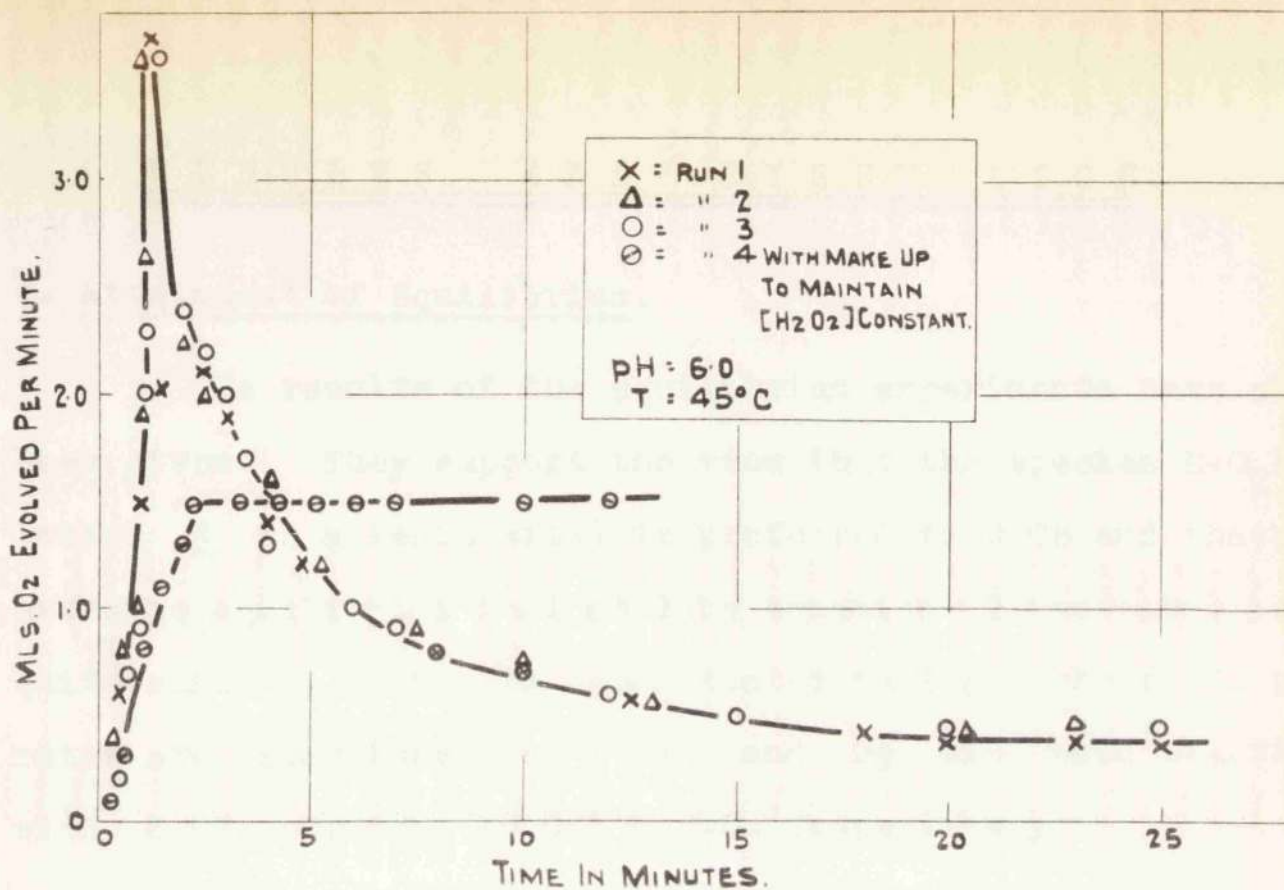


FIG. 3. X, Δ, O. SHOWING REPRODUCIBILITY OF A RATE/TIME CURVE FOR THREE DIFFERENT RESIN SAMPLES.
 ⊙ SHOWING STEADY RATE WHEN [H₂O₂] IS KEPT CONSTANT BY MAKE-UP WITH MICRO-DOSER.

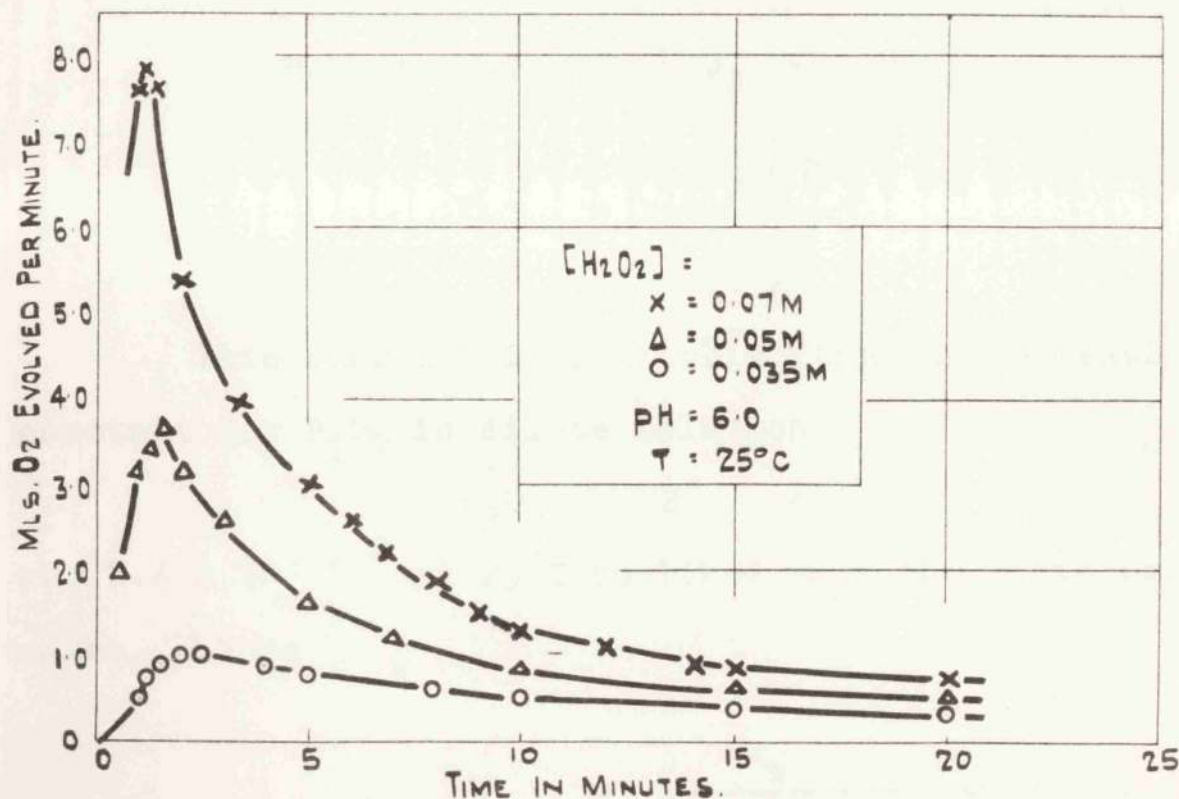


FIG. 4. VARIATION IN RATE OF DECOMPOSITION OF H₂O₂ BY THE OH FORM OF AN ANION EXCHANGE RESIN. SHOWING ALSO THE VARIATION OF THE RATE/TIME CURVE WITH INITIAL [H₂O₂]

RESULTS AND DISCUSSION

1. Attainment of Equilibrium.

The results of the equilibrium experiments have already been given. They support the view that the species $R-O_2H$ (where R is a resin site) is preferred to $R-OH$ and that the exchange equilibrium indicated by equation (2) is established quite quickly. This is demonstrated in Fig.4 where the peak rates are established in 1, $1\frac{1}{2}$ and $2\frac{1}{2}$ min. when starting with 0.07, 0.0525, 0.035 M H_2O_2 respectively.

It may be noted that the equilibrium constant for reaction (3) is numerically quite close to the reciprocal of the hydrolysis constant K_h for the HO_2' ion i.e.



$$K_h = \frac{[H_2O_2][HO']}{[HO_2']}$$

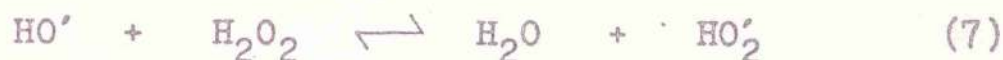
This constant is available from the ionisation constant for H_2O_2 in dilute solution



of 2.4×10^{-12} at $25^\circ C$ combined with the ionic product of water. Thus

$$K_h = \frac{K_w}{2.4 \cdot 10^{-12}} = 4.2 \times 10^{-3}$$

The equilibrium constant for the reaction .



is thus $\frac{1}{K_h} = 239$. Comparison of this with the value of 657 obtained for (3) indicates that the resin bond favours HO'_2 considerably more than does a proton, so that if α_s is the ratio $\frac{[\text{O}_2\text{H}']}{[\text{OH}]}$ in solution and α_r is the ratio of the fractions of resin surface covered at given $[\text{H}_2\text{O}_2]$ in dilute solution,

$$\frac{\alpha_r}{\alpha_s} = \frac{657}{239} = 2.75$$

It seems valid to regard the equilibrium as established throughout the process of catalysis at least for volumes of 40 ml. Use of larger volumes of 120 ml. gave a larger delay in reaching the peak rate and so these larger volume results have not been used in the kinetic analysis.

2. Efficiency of Exchanged Resin as a Catalyst.

An interesting result of these measurements is the demonstration of the anion exchange resin as an efficient remover of H_2O_2 from solution. Thus 40 mls. of a 0.05 M solution is cleared by 1 g. of resin of H_2O_2 down to a concentration of 0.004 M in 3 mins. Decomposition reduces this to 0.001 in 20 mins.

The efficiency of these $-\text{HO}_2$ exchange surfaces as catalysts was surprisingly high and what began as a brief investigation of the exchange equilibria continued as a

kinetic study. On the question of the efficiency we may note that the peak rates referred to in Table 2 i.e. 2.60 mls. O_2 per minute or $2.3 \cdot 10^{-4}$ moles. H_2O_2 decomposed per minute, represent one mole. of H_2O_2 decomposed per second for every ten adsorbing sites (0.0025 moles. of the resin as R-OH (RO_2H) was used). This is a calculation which cannot be made for Cu_2O as a catalyst, owing to the uncertainty about the effective surface area exposed to the catalyst and even if that were known to the lack of knowledge of the proportion of that area providing catalytically active sites. It might be said of course that some or even the majority of the 0.0025 equivalents of R-OH (or RO_2H) provided by the resin consists of sites deep in the pores of the resin and not able to take a fair share of catalysis owing to (a) delay in penetration by H_2O_2 or (b) delay in escape of O_2 . (b) is likely to be a more serious factor than (a). The fact that the establishment of the exchange equilibria is fast however, strongly suggests that unimpeded penetration of the H_2O_2 to the whole of the effective resin surface may be assumed in the experiments. If this is so, it seems fair to suggest that R- HO_2 is not itself responsible for catalysis but some other species present on the surface to only a very much smaller extent.

The possible influence of occlusion of some of the more deep-lying sites by O_2 on the kinetic analysis will however have to be borne in mind. It would result in the

catalyst having a greater apparent effectiveness at very low rates of catalysis than at high rates.

3. Rate and $[H_2O_2]$

Only a cursory examination of the change of rate of catalysis with $[H_2O_2]$ has so far been made. In the dilute solutions of the equilibrium measurements ($\theta = 0.13$ to 0.87) a vigorous catalysis is observed. This increases with $[H_2O_2]$ until at about 3 M the rate becomes independent of $[H_2O_2]$ and then commences to fall as $[H_2O_2]$ rises above 10 M. If the OH resin is immersed in 80% H_2O_2 catalysis is almost negligible. At raised temperatures catalysis can become self-heating and as vigorous as on an active oxide.

The present results refer only to the dilute solutions used for the equilibrium measurements. The static method was used, calculating the $[H_2O_2]$ at various times by allowing for decomposition and adsorption.

The change of rate with time is shown in Fig.3 and Fig.4. In the latter the results with three initial $[H_2O_2]$ of 0.07 , 0.0525 and 0.035 M are shown. From a knowledge of the amount of O_2 evolved up to a given time and the equilibrium in reaction (1) it was possible to calculate $[H_2O_2]$ at that time and furthermore to calculate precisely the fraction of the total resin surface covered with $R-O_2H$ or $R-OH$. It is convenient for the calculation to express

Θ in terms of C_R which is the reduction in concentration in the volume (40 mls.) of solution used, when this amount of H_2O_2 is adsorbed on the resin.

If n_R is the number of moles of H_2O_2 on the resin

$$\Theta = \frac{n_R}{0.0025}$$

and expressed as concentration alteration (C_R)

$$\begin{aligned} n_R &= C_R \cdot \frac{40}{1000} \\ \text{so } \Theta &= \frac{C_R \cdot 40}{1000 \cdot 0.0025} = 16 C_R \end{aligned}$$

Rearrangement of equation (4) in the form

$$\Theta = \frac{K \cdot [H_2O_2]}{1 + K \cdot [H_2O_2]}$$

or in the more convenient form

$$\frac{1}{\Theta} = \frac{1}{K \cdot [H_2O_2]} + 1$$

and substituting for Θ from above, relates C_R to $[H_2O_2]$ which is now denoted as C_t i.e. the concentration in the solution at time t ,

$$\frac{1}{C_R} = 16 + \frac{16}{657} \cdot \frac{1}{C_t} \quad (5)$$

and if ΔC is the loss of H_2O_2 due to catalysis up to the time t and C_i is the original $[H_2O_2]$ we define

$$C_t = C_i - \Delta C \quad (6)$$

$$\text{and } C_o = C_R + C_t \quad (7)$$

where C_0 is the total H_2O_2 expressed as a concentration. Solving (5), (6), and (7) gives C_R and C_t at any time for which ΔC is known. This is best done graphically and curves were constructed giving C_R and C_t from various values of C_0 . Table 3 collects results for θ and C_t , and the rates of oxygen evolution \underline{r} expressed in mls./minute, found in a number of different experiments. Fig.5 plots \underline{r} against C_t and \underline{r} against $C_t^{\frac{1}{2}}$. It is clear that all the points from different initial concentrations lie reasonably well on the same curve.

C_i Moles/litre	r mls. O_2 /min.	C_t moles/litre	θ
0.07	4.62	0.00875	0.827
	3.30	0.00650	0.806
	2.64	0.00520	0.774
	2.00	0.00340	0.700
	1.33	0.00220	0.590
	0.87	0.00146	0.456
	0.33	0.0004	0.217
0.0525	2.38	0.00420	0.720
	1.60	0.00256	0.621
	0.925	0.00160	0.521
	0.528	0.00110	0.415
0.0350	0.66	0.00130	0.462
	0.27	0.00076	0.355
	0.13	0.00036	0.132

Table 3.

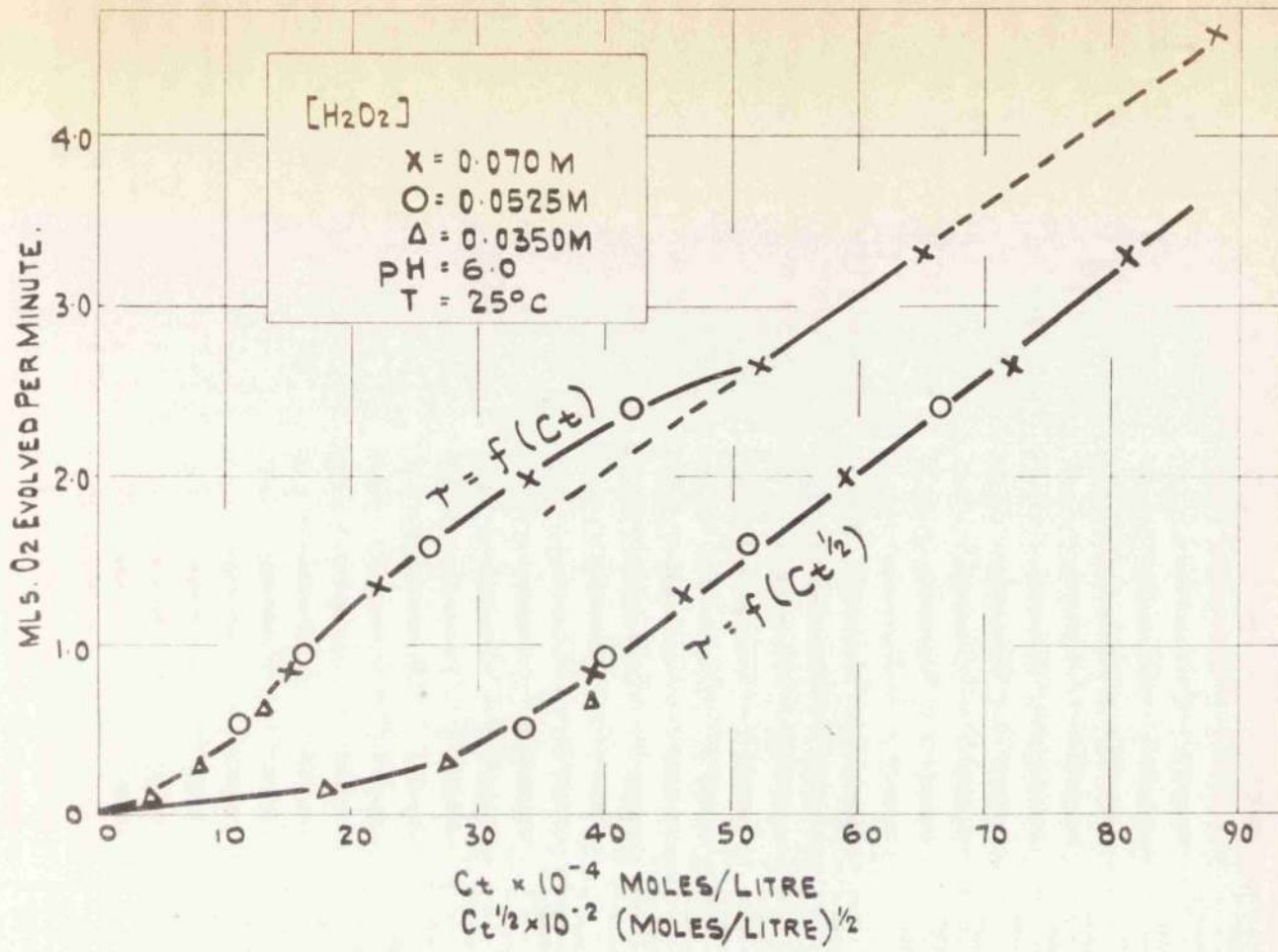


FIG. 5 SHOWING THE FAILURE OF DATA TO CONFORM TO KINETIC LAWS OF (i) 1ST. ORDER AS REQUIRED BY SIMPLE SITE ADSORPTION RATE CONTROL (ii) 1/2 ORDER AS REQUIRED BY DUAL SITE ADSORPTION RATE CONTROL.

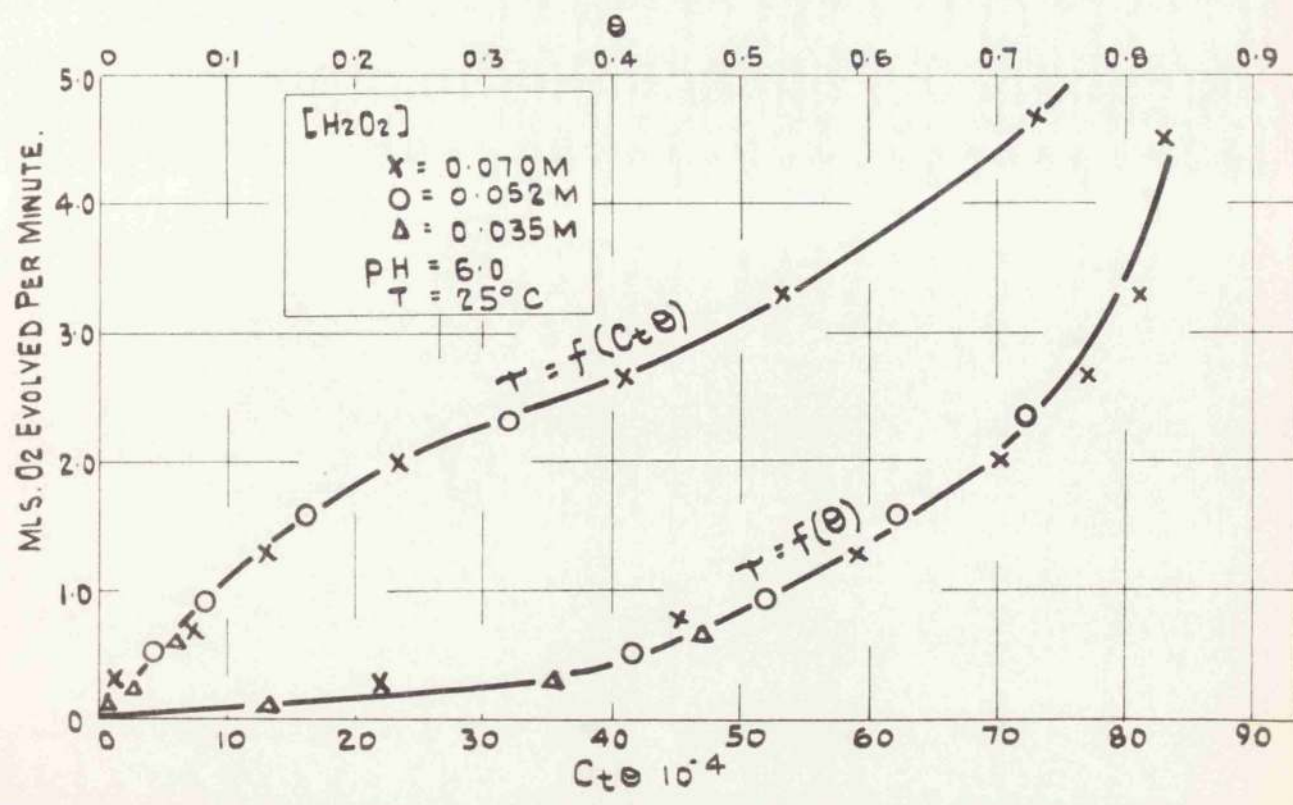


FIG. 6 SHOWING THE FAILURE OF THE RESULTS TO FIT IN WITH THE REQUIREMENTS OF THE MECHANISMS (i) RATE CONTROLLED BY DECOMPOSITION OF R-HO₂ i.e. $\tau = f(\theta)$ (ii) RATE CONTROLLED BY THE REACTION R-HO₂ + H₂O₂ i.e. $\tau = f(C_t \theta)$.

At high values of C_t the rate seems to vary linearly with C_t according to

$$r = k_1 C_t + \text{constant} \quad (8)$$

There is no evidence of any onset of a zero order process at high concentration but it is known from separate qualitative tests that this occurs at greater than 3 M H_2O_2 and indeed at > 10 M H_2O_2 the catalysis is extinguished. On the other hand at lower concentrations the rate falls off from the value given by equation (8).

To understand these relationships a mechanism for the catalysis must first be proposed. Certain simple general schemes can be excluded.

The suggestion can first be made that the rate depends entirely on the HO_2 attached to the resin.

$$\text{i.e. } r = k'\theta$$

This must be rejected since it would require that when $\theta \rightarrow 1$ the rate would become independent of C_t . Furthermore it can be calculated that this independence of C_t should begin when C_t has the value of about 0.0004. Clearly \underline{r} continues to increase with C_t at values of C_t well above this. Fig.6 demonstrates the relationship between r and θ when θ is nearly 1. $r = k_1 C_t \theta$ must also be rejected i.e. that the rate is controlled by a reaction between dissolved H_2O_2 and the adsorbed HO_2 . \underline{r} is also plotted against $C_t \theta$ in Fig.6.

4. Mechanism.

In order to make further progress in the interpretation of these results it is necessary to consider some plausible mechanisms. It has already been seen that it is necessary to reject a simple bimolecular reaction between a resin-linked HO_2' and solution H_2O_2 e.g.



because in the range of concentration chosen, where both $[\text{R.HO}_2] = \theta$ and $[\text{H}_2\text{O}_2] = C_t$ are varying substantially, the relationship $r = k_1 C_t \theta$ is unable to satisfy the results. Such a step could however be built into a more complex process. A parallel reaction could be proposed directly proportional to C_t in the lower part of the range but becoming practically constant at $C_t = 30-40 \cdot 10^{-4}$ moles/litre (or $\theta = 0.7 - 0.75$). Such a process would be of the form

$$r = k_1 C_t \theta + k_2 \theta \quad (10)$$

and could be explained by adding a step such as



to (9). (11) would be followed by recombination of O atoms in such a manner as not to affect the rate.

Both (9) and (11) seem inherently to lack plausibility since unlikely rearrangements of atoms are involved in each of them.

A more acceptable process would involve HO_2 sites in

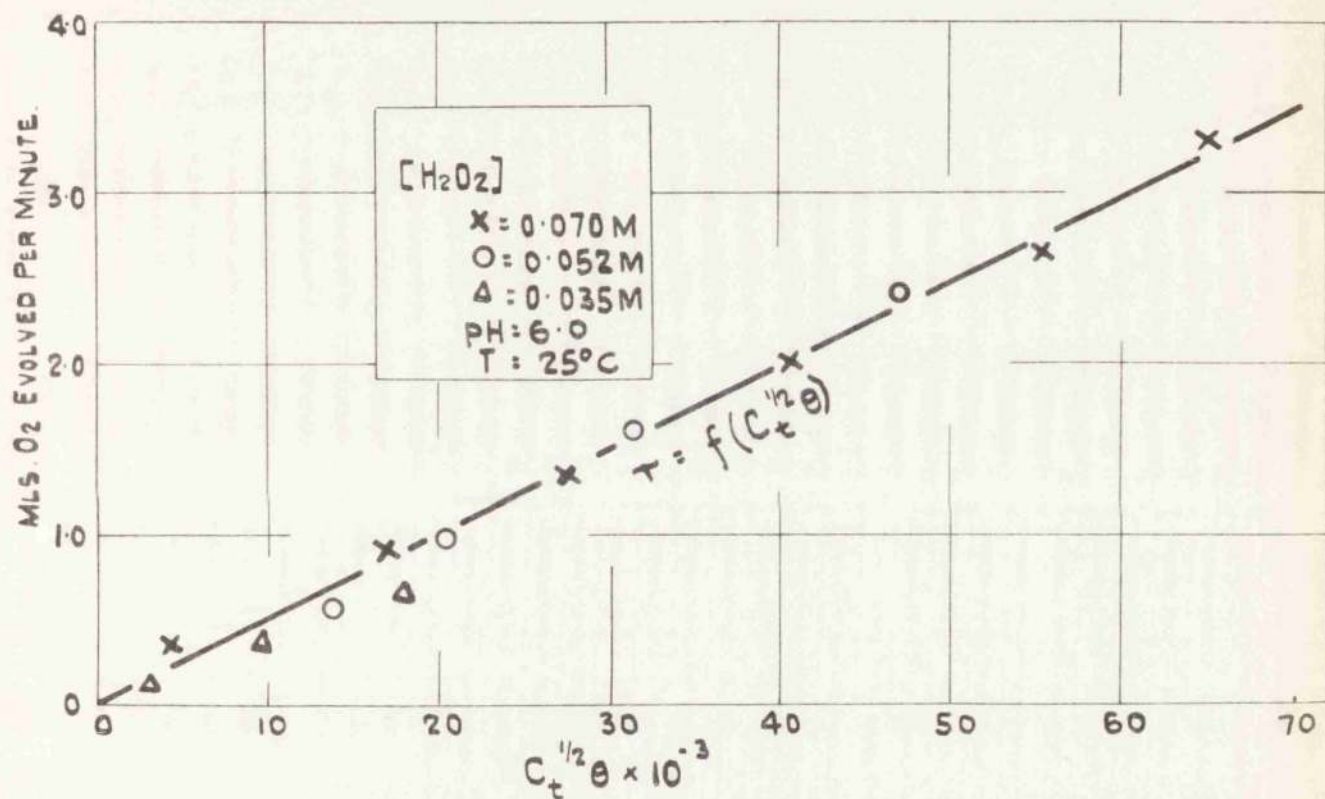
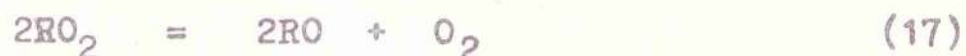


FIG. 7. SHOWING GOOD FIT OF RESULTS WITH PROPOSAL THAT RATE IS CONTROLLED BY DECOMPOSITION OF R-O₂ WHICH IS FORMED IN THE EQUILIBRIUM
 $2 RO_2H + H_2O_2 \leftrightarrow 2 RO_2 + 2 H_2O$

this scheme is not in disagreement with the results.

Selection of (14) as the catalytic rate controlling step rather than another double site step such as



was dictated by the need to obtain a rate equation like (16).

Equation (16) has the form

$$r = \frac{kK' \cdot 657C_t^{3/2}}{1 + 657C_t}$$

It fails entirely to predict extinction of catalysis at high $[\text{H}_2\text{O}_2]$. It does however predict zero order kinetics when ϕ becomes appreciable. Then the equation has to be modified to give

$$r = \frac{kK' \cdot 657C_t^{3/2}}{1 + 657C_t + 657K'C_t^{3/2}}$$

r is independent of C_t when $K'C_t^{1/2} > 1$ or when $C_t > \frac{1}{K'} \cdot 2$

It must be stated that the limited range of results here available does not permit any scheme to be put forward at this stage with any finality. A wide range of concentrations and in particular a range of flow measurements would be desirable. The latter would eliminate uncertainty about the extent to which the whole of the exchangeable surface is available for catalysis. It would also be desirable to make measurements at higher pH values. There is evidence,

indicated on Fig.7 , that a smaller active surface is in use in the case of the smallest of the three initial concentrations used. The constant in (16) from the slope of the graph is markedly smaller in this case. It is suggested that the exchange particles maybe penetrated to a standard depth (perhaps completely) only in the case of the two higher concentrations but less deeply with the smaller one. This is a point which would require work with different particle sizes to clarify.

C O N C L U S I O N S

Anion exchange resins in the OH form come to equilibrium with H_2O_2 forming what is considered to be a relatively stable $R-O_2H$ surface. In this form the resin is catalytically active but the kinetics in a narrow range of $[H_2O_2]$ cannot be described in terms of a simple cyclic reaction with H_2O_2 e.g.



or by a simple decomposition of the adsorbed HO_2 ions. It is necessary to invoke a different active species in equilibrium with the peroxide exchanged surface.

It is felt that further study of this system will yield information with a bearing on decomposition of H_2O_2 at solid catalysts in general and also about the mechanism of decomposition of solid hydroperoxides $R-O_2H$.

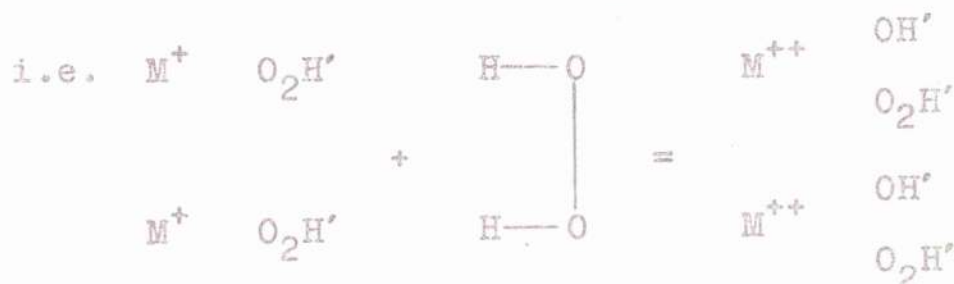
GENERAL CONCLUSIONS FROM SECTIONS I AND II

General Conclusions

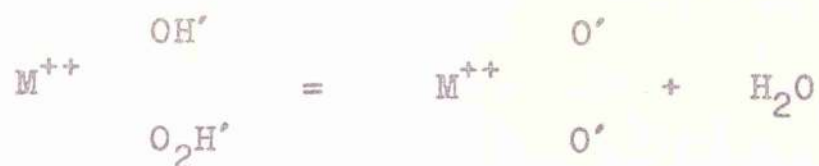
From the above studies the following general conclusions are drawn concerning the catalytic decomposition of aqueous H_2O_2 by P-type semiconducting metal oxides and anion exchange resins.

1. In the case of Cu_2O , CoO and anion resin catalysis, there is evidence that the surface, which can be regarded as consisting initially of OH' ions, is covered with adsorbed HO_2' ions during catalysis.
2. Catalysis does not occur at the HO_2' sites but takes place on a small concentration of O' or O_2' sites present on the surface. In the case of P-type oxides these sites may be present to a small extent on the surface previous to treatment with H_2O_2 (resulting from oxidative adsorption at p-holes) but a considerable number more are formed by:-

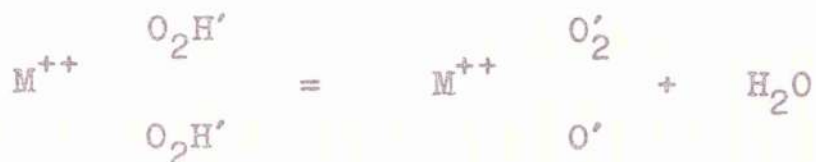
(a) oxidative adsorption of H_2O_2 .



followed by dehydration



or after further exchange with H_2O_2



(b) by dehydration



where M^{++} may be regarded as a p-hole in the $(M^+)_2 O''$ lattice. Potential measurements suggest that a Cu_2O (or $CuOH$) surface is 50% converted to $Cu(OH)_2$ in the presence of H_2O_2 .

In the case of the resin it is suggested that catalysis similarly depends on decomposition of the hydroperoxide surface to yield an active surface site.

3. No free radicals are believed to occur in any of the cases studied. All kinetics are adequately explained in terms of adsorbed radical ions which do not move into the solution - not even into the Van der Waals layer.
4. There is no evidence that dissolved metal plays any part in catalysis except perhaps as mentioned in 5. Participation of dissolved ions in a homogeneous-heterogeneous

cycle seems to be ruled out.

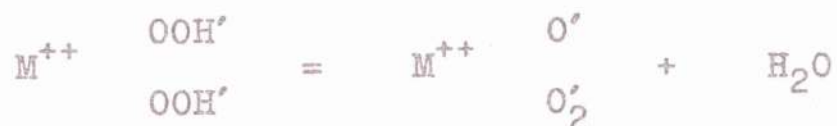
5. The kinetics require a poisoning step in the case of oxides and possibly also in the case of the resin. With oxides the dual-site poisoning implied is required unambiguously by the kinetics and measurement of the rate of this poisoning contributes to an analysis of the overall kinetics. A reverse of the formation of O_2' or O' is suggested for poisoning i.e. the reversion to inactive OH' or O_2H' ions. A factor in deciding the relative catalytic power of oxides will be the relation between formation and poisoning of these active sites. The dissolution of the hydroperoxide layer (when it occurs) may be a factor in ameliorating the poisoning tendency.

Studies comparable with those on the oxides involving a flow system are not yet available with the resin.

6. The active ions are adsorbed on the oxides at p-holes, i.e. at Cu^{++} in the Cu_2O case or Co^{+++} in CoO . Potential studies lead to the conclusion that every other Cu ion in the surface is in the Cu^{++} state during catalysis with H_2O_2 greater than 0.25 M. This tends to suggest that the valency change is what favours the formation of the active ions. On the other hand no such valency change can occur on the resin and it therefore appears preferable to think of the effect being geometric - the O_2H' attached to the higher valency ions or p-holes being brought into closer

contact than at the lower valency ions. The condition in the resin is then seen to depend on some of the O_2H' being in this close position, favourable for conversion by dehydration to O'_2 and O' .

7. The relative activity of the oxides, $CoO > Cu_2O > NiO$ is paralleled by the stability of the hydroxides $Co(OH)_2$, $Cu(OH)_2$ and $Ni(OH)_2$. The tendency for the freshly precipitated hydroxides to pass on standing from the coloured form to the black hydrated oxide, is greatest for $Co(OH)_2$ and least for $Ni(OH)_2$. This is taken to reflect on the tendency for the step



to occur i.e. the recovery process.

8. The slow growth of catalysis on Cu_2O was not observed with CoO . This is taken to reflect on the relative ease of diffusion of ionic and electronic species in the two oxides which will affect the concentration of p-holes at the surface and thus the number and reactivity of the active sites. Such slow processes do not occur on resins where there would be no likelihood of such solid interaction, the surface +ve charge remaining isolated.
9. The detailed kinetic analysis of the slow growth accords adequately with the assumption of a solid reaction and

indeed there is quantitative correlation with the energy of activation for p-hole diffusion in Cu_2O .

10. This work is closely linked to the studies on catalase and the catalase model $(\text{TETA}) \text{Fe}(\text{OH})_2^+$ by the similarity of the overall kinetics which require a similar mechanism. Just as single radical producing electron transfer mechanisms have been increasingly excluded by results in the enzyme field, so it is now found that these inorganic catalysts require two-electron steps to explain the kinetics.

FUTURE LINES OF RESEARCH

As a continuation of the above investigations the following suggestions are made for future lines of research which appear likely to clarify further the detailed mechanism of heterogeneous catalytic decomposition:-

1. the studies carried out on the $\text{CoO}/\text{H}_2\text{O}_2$ and $\text{NiO}/\text{H}_2\text{O}_2$ systems require further detailed investigations on lines similar to those followed for the examination of the $\text{Cu}_2\text{O}/\text{H}_2\text{O}_2$ system.
2. extension of the Cu_2O , NiO , $\text{CoO}/\text{H}_2\text{O}_2$ investigations to include other p-type semiconducting metal oxide / H_2O_2 systems is necessary.
3. the preliminary studies completed on the resin/ H_2O_2 system suggest:-
 - (a) extension of the static condition studies described above to cover a wider field of $[\text{H}_2\text{O}_2]$, pH, ionic strength and temperature
 - (b) application of flow system techniques to resin studies.
4. the application of isotopic tracer techniques to elucidate further the reactions occurring in oxide / H_2O_2 and resin/ H_2O_2 systems.

REFERENCESSECTION I

1. Thenard, Ann.chim.et phys., 1818, 8, 306.
2. Schumb, Satterfield and Wentworth, Hydrogen Peroxide, Monograph Series 128, 1955.
3. Giguère, Can.J.Res.B, 1950, 28, 485.
4. Evans, Hush and Uri, Quart.Revs., 1952, 6, 186.
5. Hydrogen Peroxide (reference 2 above), references 5,6, 7,8,9 p.28.
6. Thenard, Ann.chim.et phys., 1818, 9, 94 and 314.
7. Schönbein, Phil.Mag., 1858, 16, 178.
8. Brodie, Phil.Trans., 1850, 2, 759.
9. Brodie, Proc.Roy.Soc.London, 1860, 11, 442.
10. Bredig and Müller von Berneck, Zeit.phys.Chem., 1899, 31, 258
 Bredig and Ikeda, *ibid.* 1901, 37, 1.
 Bredig and Reinders *ibid.* 1901, 37, 323
 Bredig and Weinmayer *ibid.* 1903, 42, 601
 Bredig and Fortner, Ber., 1904, 37, 798.
11. Teletof and Gritsan, CA, 37, 3659.
12. Haber and Weiss, Proc.Roy.Soc.London, A, 1934, 147, 332.
13. Haber and Willstätter, Ber., 1931, 64, 2844.
14. Baxendale, Evans and Parks, Trans.Far.Soc., 1946, 42, 155.
15. Dainton and Rowbottom, Trans.Far.Soc., 1953, 49, 1160.
16. Weiss, Far.Soc.Disc., 1947, 2, 212.
17. Barb, Baxendale, George and Hargrave, Nature, 1949, 163, 692.
18. *idem.* Trans.Far.Soc., 1951, 47, 462.
19. Weiss and Humphrey, Nature, 1949, 163, 691.
20. Lea, Trans.Far.Soc., 1949, 45, 81.
21. Weiss, Nature, 1944, 153, 748.
22. Evans, Hush and Uri, Quart.Revs., 1952, 6, 186.
23. Bray and Gorin, J.Amer.Chem.Soc., 1932, 54, 2124.

24. Griffith, Recent Advances in Catalysis, Vol.1., Acad. Press.Inc.,N.Y. 1948, p.91.
25. Russell, Nature, 1926, 117, 47.
26. Langmuir, J.Amer.Chem.Soc., 1916, 38, 2221.
27. idem. ibid. 1918, 40, 1361.
28. idem. , Trans.Far.Soc., 1921, 17, 607.
29. Burk, J.Phys.Chem., 1926, 30, 1134.
30. Beeck, Smith and Wheeler, Proc.Roy.Soc.London, A, 1940, 177, 62.
31. Beeck Rev.Mod.Phys., 1945, 17, 61.
32. Twigg and Rideal, Trans.Far.Soc., 1940, 36, 533.
33. idem., Proc.Roy.Soc.London, A, 1939, 171, 55.
34. Twigg, Trans.Far.Soc., 1939, 35, 934.
35. Balandin, Z.phys.Chem., B, 1929, 2, 289.
idem., ibid., 1929, 3, 167.
36. Schwab, Trans.Far.Soc., 1946, 42, 689.
37. Dowden and Reynolds, Nature, 1949, 164, 50.
38. Couper and Eley, Nature, 1949, 164, 578.
39. Dowden and Reynolds, Far.Soc.Disc., 1950, 8, 184.
40. Blench and Garner, J.Chem.Soc., 1924, 125, 1288.
Garner and McKie, ibid., 1927, 2451.
Bull, Garner and Hall ibid., 1931, 837.
41. Beebe and Taylor, J.Amer.Chem.Soc., 1924, 46, 43.
Kistiakowsky, Flosdorf and Taylor, ibid., 1927, 49, 2200.
42. Taylor, Proc.Roy.Soc.London, A, 1925, 108, 105.
43. Gray and Darby, J.Phys.Chem., 1956, 60, 201.
44. Volkenshtein, Zhur.Fiz.Khim., 1949, 23, 931.
45. Boudart, J.Amer.Chem.Soc., 1952, 74, 1531.
46. Taylor and Thon, ibid., 1953, 75, 2747.
47. Weiss, Trans.Far.Soc., 1935, 31, 1547.
48. Garney, Proc.Roy.Soc.London,A, 1931, 134, 137.
49. Ross, Ph.D. thesis, Glasgow University, 1958.
50. Cabrera and Mott, Rep.Prog.Phys., 1949, 12, 163.
51. Garner, Gray and Stone, Proc.Roy.Soc.London,A,1949,197,294
52. Garner, Stone and Tiley, ibid., 1952,211,472

53. Wagner, J. of Chem.Phys., 1950, 18, 69.
54. Stone, Summer School on Heterogeneous Catalysis,
Bristol, 1953.
55. Giguère, Can.J.Res., B, 1947, 25, 135.
56. Dell, Stone and Tiley, Trans.Far.Soc., 1953, 49, 201.
57. Schmid and Keller, Naturwiss, 1950, 37, 42.
58. Broughton and Wentworth, J.Amer.Chem.Soc., 1947, 69, 741.
59. Broughton, Wentworth and Laing, *ibid.*, 1947, 69, 744.
60. Mooi and Selwood, *ibid.*, 1952, 74, 1750.
61. Dubois, Compt.rend., 1933, 196, 1401.
62. *idem.*, *ibid.*, 1934, 199, 1310.
63. Voltz and Weller, J.Amer.Chem.Soc., 1954, 76, 1586.
64. Schwab, La Chimica e Industria, 1953, 35, 810.
65. Uri, Far.Soc.Disc., 1950, 8, 207.
66. Hart and McFadyen, In course of publication, Roy.
Coll. of Sci. and Tech., Glasgow, 1958.
67. Hart and Ross, *ibid.*
68. Schumb, Satterfield and Wentworth, Hydrogen Peroxide,
Monograph Series 128, p.248.
69. Bengough and Melville, Proc.Roy.Soc.London,A, 1954, 225, 330.
70. *idem.*, *ibid.*, 1955, 230, 429.
71. Miyama, J.Chem.Soc.Japan, 1956, 77, 196.
72. Fujii and Tanaka, J.Polymer Sci., 1956, 20, 409.
73. Becker, Green and Pearson, Elect.Eng., 1946, 65,
transaction 711.
74. Mott and Gurney, Electronic Processes in Ionic Crystals,
Oxford U.P., London, 1948.
75. Zeffert and Hormats, Anal.Chem., 1949, 21, 1420.
76. Richards and Campbell, Soil Science, 1948, 65, 429.
77. Müller and Stolten, Anal.Chem., 1953, 25, 1103.
78. Beck, J.Sci.Instr., 1956, 33, 16.
79. Brady, Huff and McBain, J. of Phys. and Colloid. Chem.,
1951, 55, 304.
80. Duncan, Trans.Far.Soc., 1949, 45, 879.

81. Wooten and Callaway-Brown, J.Amer.Chem.Soc., 1943, 65, 113.
82. Organic Reagents for Metals, Hopkin and Williams Ltd., London, 1943.
83. Grendel, Pharm.Weekly, 1930, 67, 913.
84. Ovenston and Parker, Analytica Chemica Acta., 1950, 4, 135.
85. Moseley, Rohwer and Moore, Science, 1934, 79, 507.
86. Zinzadze, Ind. and Eng.Chem.Anal.Ed., 1935, 7, 227.
87. Heyrovsky, Trans.Far.Soc., 1924, 19, 785.
88. Lingane, Ind.Eng.Chem.Anal.Ed., 1943, 15, 583.
89. Lingane and Kolthoff, "Polarograph" Interscience Pub. Inc., N.Y., 1941.
90. Lingane, J.Amer.Chem.Soc., 1945, 67, 919.
91. Niggli, Z.Kristall, 1922, 57, 253.
92. Hinshelwood, Proc.Roy.Soc.London, A, 1922, 102, 318.
93. Constable, *ibid.*, 1927, 115, 570.
94. Thomson, *ibid.*, 1930, 128, 654.
95. Marison, Phil.Mag., 1934, 17, 96.
96. Darbyshire, Trans.Far.Soc., 1931, 27, 675.
97. Evans and Stockdale, J.Chem.Soc., 1929, 2651.
98. Preston and Bircumshaw, Phil.Mag., 1935, 20, 706.
99. Briggs, Jones and Wynne-Jones, Trans.Far.Soc., 1955, 51, 1433
100. Joyner, Z.anorg.chem., 1912, 77, 103.
101. Kargin, *ibid.*, 1929, 183, 77.
102. Bockris and Oldfield, Trans.Far.Soc., 1955, 51, 249.
103. Hart, Aitken and Beaton, In course of publication, Roy.Coll.of Sci. and Tech., Glasgow, 1958.
104. Brunauer, Emmett and Teller, J.Amer.Chem.Soc., 1938, 60, 309.
105. Wooten and Callaway-Brown, *ibid.*, 1943, 65, 113.
106. Zwietering and Roukens, Trans.Far.Soc., 1954, 50, 178.
107. Roginskii and Tselinskaya, Zhur.Fiz.Khim., 1948, 22, 1360.
108. Zettlemyer, Yu, Chessick and Healey, J.Phys.Chem., 1957, 61, 1319.
109. Yu, Chessick and Zettlemyer, Advances in Catalysis, 1957, 9, 415.
110. Haissinsky, Far.Soc.Disc., 1947, 1, 254.

111. Bolland and Gee, Trans.Far.Soc., 1946, 42, 244.
112. Walsh, Trans.Far.Soc., 1946, 42, 264.
113. Haïssinsky, J. of Chem.Phys., 1947, 15, 152.
114. Glasner, J.Chem.Soc., 1951, 904.
idem., ibid., 1950, 2795.
115. Wang, J.Amer.Chem.Soc., 1955, 77, 822.
116. idem., ibid., 1955, 77, 4715.
117. Jarnagin and Wang, ibid., 1958, 80, 786.
118. Taylor, Proc.Roy.Soc.London,A, 1925, 108, 105.
119. Pease, J.Amer.Chem.Soc., 1923, 45, 2235.
120. Blench and Garner, J.Chem.Soc., 1924, 125, 1288.
Garner and McKie, ibid., 1927, 2451.
Bull, Garner and Hall,ibid., 1931, 837.
121. Beebe and Taylor, J.Amer.Chem.Soc., 1924, 46, 43.
122. Temkin and Pyzhev, Acta Physicochim., 1940, 12, 327.
123. Kwan, J. of Phys.Chem., 1956, 60, 1033.
124. Brunaur, J.Amer.Chem.Soc., 1942, 64, 751.
125. Jacobs and Tompkins, "Chemistry of the Solid State",
ed., Garner, 1955, p.184.
126. Structure and Chemical Properties of Surfaces, Gomer
and Smith, p.402.
127. Dubar, Compts.Rend., 1936, 202, 1330.
128. Rideal and Wilkins, Proc.Roy.Soc., London, A, 1930,128,394
129. Latimer, Oxidation States of the Elements and their
Potentials in Aqueous Solutions, Prentice-Hall,
Inc. 1952.
130. Halliday, Trans.Far.Soc., 1954, 50, 171.
131. Gerischer and Gerischer, Zeit.phys.Chem., 1956, 6, 178.
132. Winter and Briscoe, J.Amer.Chem.Soc., 1951, 73, 496.
133. Dole, Rudd, Muchow and Compte, J. of Chem.Phys., 1952,
20, 961.

